EXPERIMENTAL MEASUREMENTS AND MODELING OF VOID FRACTION AND PRESSURE DROP IN UPWARD AND DOWNWARD INCLINED NON-BOILING GAS-LIQUID TWO PHASE FLOW

By

SWANAND MADHAV BHAGWAT

Bachelor of Engineering in Mechanical Engineering
Amravati University
Maharashtra, India
2008

Master of Science in Mechanical Engineering
Oklahoma State University
Stillwater, Oklahoma
2011

Submitted to the Faculty of the
Graduate College of the
Oklahoma State University
in partial fulfillment of
the requirements for
the Degree of
DOCTOR OF PHILOSOPHY
JULY, 2015

EXPERIMENTAL MEASUREMENTS AND MODELING OF VOID FRACTION AND PRESSURE DROP IN UPWARD AND DOWNWARD INCLINED NON-BOILING GAS-LIQUID TWO PHASE FLOW

Dissertation Approved:

Dr. Afshin Ghajar

Dissertation Adviser

Dr. Khaled Sallam

Dr. Lorenzo Cremaschi

Dr. Clint Aichele

ACKNOWLEDGMENTS

I take this opportunity to express my most sincere gratitude and thank my adviser Dr. Afshin Ghajar for his continual support and motivation throughout this study. His invaluable guidance, technical insights and timely suggestions have been pivotal in shaping this dissertation and making it a success.

I would also like to express appreciation and thank my committee members Dr. Khaled Sallam, Dr. Lorenzo Cremaschi and Dr. Clint Aichele for taking out their valuable time and providing useful suggestions and constructive criticism in this work. The financial assistance provided by School of Mechanical and Aerospace Engineering during the entire tenure of doctoral studies is highly acknowledged. Special thanks are due to Dr. Clement Tang who as a senior provided me initial guidance and trained me to work on the two phase flow setup.

Finally, I am also thankful to my wife, Charuta, for her unwavering love, patience and faith in me. I would like to express my profound regards and gratitude towards my mother, Madhuri Bhagwat, and my in-laws for their support and encouragement to pursue the degree of Doctor of Philosophy.

I dedicate this document to my late father, Madhav Bhagwat, whom I lost during the tenure of my doctoral studies.

Acknowledgments reflect the views of the author and are not endorsed by committee members or Oklahoma State University.

Name: SWANAND MADHAV BHAGWAT

Date of Degree: JULY, 2015

Title of Study: EXPERIMENTAL MEASUREMENTS AND MODELING OF VOID FRACTION AND PRESSURE DROP IN UPWARD AND DOWNWARD INCLINED NON-BOILING GAS-LIQUID TWO PHASE FLOW

Major Field: MECHANICAL AND AEROSPACE ENGINEERING

Abstract: The prime objective of this research is to contribute to the fundamental understanding of the effect of upward and downward pipe inclinations on flow patterns, void fraction and pressure drop in non-boiling gas-liquid two phase flow. To accomplish the proposed objective, 2970 experimental measurements are carried out using air-water fluid combination in a 0.5" I.D. polycarbonate (smooth) and stainless steel (rough) pipes mounted on a variable inclination frame. Based on flow visualization, flow pattern maps are developed for each pipe orientation and a significant effect of change in pipe orientation is found on the transition between stratified-slug and stratified-intermittent flow patterns. The physical structure as well as the transition between intermittent-annular flow patterns is found to be virtually independent of the pipe orientation. Based on this flow visualization data and that collected from literature, an empirical model is developed to predict occurrence of stratified flow in horizontal and downward inclined pipes. Experimental measurements show that the effect of change in pipe orientation on the void fraction as well as two phase pressure drop is significant at low liquid and gas flow rates. This effect is essentially due to the change in flow pattern and the relative dominance between buoyancy and inertia forces. It is observed that the increase in pipe surface roughness increases the frictional pressure drop with increase in gas and liquid flow rates. Effect of pipe roughness on the frictional pressure drop is found to be independent of the pipe orientation. A comprehensive data bank is generated using the experimental data collected in this study and that available in the open literature and is used to develop flow pattern independent models to predict void fraction and frictional pressure drop. Void fraction correlation applicable for micro to macro scale two phase flow is developed based on drift flux modeling technique. Frictional pressure drop correlation also applicable for micro macro scale two phase flow is based on separated flow model and provides an expression to predict two phase frictional multiplier as a function of several two phase flow variables. Both of these correlations are valid for non-stratified two phase flows.

TABLE OF CONTENTS

LIST OF TABLES

LIST OF FIGURES

NOMENCLATURE

Symbol	Description	Units
a	variable in Cioncolini and Thome (2012) correlation	[-]
A	cross sectional area	[m^2]
A_F	variable in Friedel (1979), Friedel (1985) correlations	[-]
A_{Lim}	parameter used in Lim and Fujita (2002) correlation	[-]
b	variable used in Lombardi and Carsana (1992)	[-]
B_r	variable in Chisholm (1973) correlation for rough pipe	[-]
B_s	variable in Chisholm (1973) correlation for smooth pipe	[-]
B_1	variable used in Eq. (6.2) for Φ^2_{LO}	[-]
B_2	variable used in Eq. (6.2) for Φ^2_{LO}	[-]
B_3	variable used in Eq. (6.2) for Φ^2_{LO}	[-]
Bo	Bond number	[-]
c_1	constant in Lau and Rezkallah (1995) correlation	[-]
c_2	constant used in Zhang et al. (2010) correlation	[-]
C	Chisholm (1967) constant	[-]
C_o	distribution parameter	[-]
$C_{o,1}$	parameter defined by Bhagwat and Ghajar (2014)	[-]
C_1	constant used in Bhagwat and Ghajar (2014) correlation	[-]
C_2	variable used in Bhagwat and Ghajar (2014) correlation	[-]
C_3	variable used in Bhagwat and Ghajar (2014) correlation	[-]
C_4	constant used in Bhagwat and Ghajar (2014) correlation	[-]

Ca	Capillary number	[-]
Ce	non-dimensional variable in Lombardi and Carsana (1992)	[-]
C_w	variable used by Wang et al. (1997)	[-]
C_G	constant in Lockhart and Martinelli (1949) correlation	[-]
C_L	constant in Lockhart and Martinelli (1949) correlation	[-]
d	Local pipe diameter	[m]
dP/dL	pressure gradient	[Pa/m]
$(dP/dL)^+$	non-dimensional pressure gradient	[-]
D	pipe diameter	[m]
D_h^*	non-dimensional pipe diameter by Kataoka and Ishii (1987)	[-]
D_h	hydraulic pipe diameter	[m]
D_{ref}	reference pipe diameter in Bhagwat and Ghajar (2015) model	[m]
E	liquid entrainment fraction	[-]
f	friction factor	[-]
f_i	interface friction factor	[-]
F	any two phase flow parameter	[-]
F_1	variable in Smith (1969) correlation	[-]
Fr	Froude number	[-]
F_w	variable in Wang et al. (2001) correlation	[-]
g	acceleration due to gravity	[m/s^2]
G	mixture mass flux	[kg/m^{2}s]
G_{eq}	equivalent mass flux defined by Akers et al. (1959)	[kg/m^{2}s]
G_{max}	maximum mass flux at which stratified flow can exist	[kg/m^{2}s]
h	variable in Cioncolini and Thome (2012) correlation	[-]
h_L	liquid height in stratified flow	[m]
k	multiplying factor to homogeneous void fraction (β)	[-]
L	pipe length	[m]

La	Laplace number	[-]
Lo	variable in Lombardi and Carsana (1992) correlation	[-]
m	exponent in radial velocity profile	[-]
$\dot{m}$	mass flow rate	[kg/s]
m_1	exponent in Lau and Rezkallah (1995) correlation	[-]
m_2	exponent in Lau and Rezkallah (1995) correlation	[-]
MARD	mean absolute relative deviation	[-]
MRD	mean relative deviation	[-]
n	exponent in radial void fraction profile	[-]
N	number of data points	[-]
N_{conf}	confinement number	[-]
$N_{\mu L}$	viscosity number	[-]
o	exponent used in Eq. (2.95)	[-]
p	perimeter	[m]
p_1	exponent in Awad and Muzychka (2004) correlation	[-]
P	pressure	[Pa]
P_r	reduced pressure	[-]
q	exponent used in separated flow model Eq. (2.95)	[-]
Q	volumetric flow rate	[m^3/s]
r	exponent used in separated flow model Eq. (2.95)	[-]
r^+	radial distance measured from pipe centerline	[m]
R	pipe radius	[m]
Re	Reynolds number	[-]
s	exponent used in separated flow model Eq. (2.95)	[-]
S	slip ratio	[-]
Su	Suratman number	[-]
U	velocity	[m/s]

U_{GM}	drift velocity	[m/s]
U_i	gas-liquid interface velocity	[m/s]
U_S	slip velocity	[m/s]
v	specific volume	[m^3/kg]
We	Weber number	[-]
x	two phase flow quality	[-]
X	Lockhart and Martinelli (1949) parameter	[-]
Y	ratio of gas only to liquid only pressure drop	[-]
z	exponent in Yamazaki and Yamaguchi (1979) correlation	[-]
Z_1	constant used in Bhagwat and Ghajar(2015) correlation	[-]
Z_2	constant used in Bhagwat and Ghajar(2015) correlation	[-]
Z_3	constant used in Bhagwat and Ghajar(2015) correlation	[-]
Z_4	constant used in Bhagwat and Ghajar(2015) correlation	[-]

Greek symbols

α	void fraction	[-]
β	gas volumetric flow fraction	[-]
δ	film thickness	[m]
ΔP	pressure drop	[Pa]
$\Delta\rho$	density difference	[kg/m^3]
ϵ	pipe wall surface roughness	[m]
γ	variable in Bankoff (1960) correlation	[-]
Γ	variable in Tu and Hrnjak (2002) correlation	[-]
μ	phase dynamic viscosity	[Pa·s]
Ω	variable in Chen et al. (2001) correlation	[-]
Φ	two phase friction multiplier	[-]

Ψ	variable in Tu and Hrnjak (2002) correlation	[-]
ρ	phase density	[kg/m^3]
σ	surface tension	[N/m]
θ	pipe orientation	[deg.]
τ	shear stress	[N/m^2]
ξ	fluid property group Eq. (6.13)	[-]
λ	pipe geometry aspect ratio	[-]
Π_1	non-dimensional variable defined by Eq. (6.10)	[-]
Π_2	constant defined by Eq. (6.11)	[-]
Π_3	non-dimensional variable defined by Eq. (6.12)	[-]
$\langle\rangle$	cross section averaged	[-]
$\langle\langle\rangle\rangle$	cross section and void weighted averaged	[-]
$\sim$	non-dimensionalising term in Taitel and Dukler (1976) model	[-]

Subscripts

a	accelerational	[-]
ATM	atmospheric	[-]
c	core	[-]
cal	calibrated	[-]
$CRIT$	critical	[-]
exp	experimentally measured value	[-]
f	frictional	[-]
Fr	parameter based on Froude number	[-]
G	gas phase	[-]
GO	gas only	[-]
h	hydrostatic	[-]
i	pipe inlet	[-]

j	phase (gas, liquid or mixture)	[-]
ll	laminar-laminar	[-]
lt	laminar-turbulent	[-]
L	liquid phase	[-]
LF	liquid film	[-]
LO	liquid only	[-]
M	two phase mixture	[-]
o	pipe outlet	[-]
$pred$	predicted value	[-]
ref	reference	[-]
S	superficial	[-]
SP	single phase	[-]
SYS	system	[-]
t	total	[-]
tl	turbulent-laminar	[-]
tt	turbulent-turbulent	[-]
TP	two phase	[-]
w	pipe wall	[-]

CHAPTER I

INTRODUCTION

1.1 Background

The term two phase flow designates a flow situation where two distinct phases flow simultaneously usually through a pipe. The two phases can be a combination of any two phases viz. gas-liquid, liquid-solid, gas-solid or even two immiscible liquids; however, the main focus of this research is the simultaneous flow of gas-liquid two phase flow in round pipes. The two phase flow of gas and liquid can be further classified as one component and two component two phase flow. The one component two phase flow is due to phase change process and consists of gas and liquid phase of same substance such as steam-water or liquid refrigerants and their vapors whereas two component two phase flow essentially consists of gas and liquid phase of two chemically different substances such as air-water. The prime scope of this work is to study the two component two phase flow.

Depending upon the mass flow rates of individual phases, pipe orientation and pipe diameter; the two phases align themselves in a particular fashion across the pipe cross section identified as a flow pattern. The principal problem associated with the gas-liquid two phase flow is its flow pattern dependent complex structure due to turbulent mixing, compressibility nature of the gas phase, significantly different thermo physical properties of the two phases, phase flow rates and the pipe orientation

that renders the analytical relationships for void fraction, two phase pressure drop and heat transfer difficult. Thus, it is necessary to study the gas-liquid two phase flow phenomenon experimentally and device a systematic method to correctly predict the two phase flow parameters such as void fraction, pressure drop and heat transfer.

Gas-liquid two phase flow finds its existence in a wide range of industrial applications including energy, petroleum and chemical engineering operations. The gas-liquid two phase flow occurring in energy industry, typically in heat exchangers, water tube boilers and cooling of nuclear reactor rods is essentially one component two phase flow of steam and water. The correct prediction of two phase heat transfer coefficient and the total pressure drop is pivotal in nuclear industry to avoid loss of coolant accident (LOCA) while the exact knowledge of two phase pressure drop is required in designing of the pumping system and sizing the condenser and evaporator systems in refrigeration units. Additionally, the correct knowledge of the void fraction is also required in estimation of the refrigerant charge inventory in the refrigeration loops. The gas-liquid two phase flow is also incorporated in chemical processes for enhanced mixing of two chemical species as in case of ozonification of water. The phenomenon of gas-liquid two phase flow is inevitable during the production and simultaneous transportation of oil and natural gas through pipes. Due to offshore exploration of the oil and gas, the long pipe lines that connect the remote oil wells to the processing stations are usually undulated and are laid with upward and downward inclinations and hence its always desired to have additional information on the effect of pipe orientation on the two phase flow parameters. In general for any industrial application that handles a specific throughput of two phase flow, accurate estimation of void fraction and pressure drop is essential for optimized design and performance, improved efficiency, sizing and reduction in the material costs of industrial equipment that involve two phase flow.

1.2 Need of Two Phase Flow Study in Inclined Systems

The research in the field of gas-liquid two phase flow can be classified in terms of its relevance to flow patterns, void fraction, two phase pressure drop and heat transfer. The accurate prediction of void fraction is very important in correct estimation of two phase mixture density and hence the two phase hydrostatic pressure drop and the convective heat transfer coefficient. The two phase pressure drop essentially varies from that of its single phase counterpart due to the significant density difference and hence the slippage between the two phases. Although, the two phase flow literature reports a number of void fraction and pressure drop correlations, however, they are found to be inadequate in their range of application in terms of flow patterns, pipe orientation and the fluid physical properties. Most of these correlations are of empirical form and are developed based on limited experimental data and hence perform well only over the certain range of two phase flow conditions.

In comparison to the horizontal and vertical pipe orientations, the two phase flow literature is devoid of flow patterns, void fraction and two phase pressure drop data in upward and downward inclined pipes. Consequently, the accuracy and performance of the existing two phase flow correlations for the the case of upward and downward inclined two phase flow is unknown and uncertain. Moreover, due to lack of experimental initiatives, the two phase flow literature lacks sound understanding of the effect of pipe orientation on two phase flow parameters. This uncertainty and lack of sound understanding of the inclined two phase flow phenomenon posses a challenge in the selection procedure of the most appropriate correlation to be used for upward or downward inclined two phase flow situations.

Thus, this creates a room for further experimental investigation of two phase flow parameters for upward and downward inclined pipe orientations and contribution

to the fundamental understanding of the two phase flow mechanism. Additionally, due to wide industrial applications of two phase flow and high uncertainty in correct prediction of flow patterns; it is strongly desired to have unified two phase flow models that can predict two phase flow parameters such as void fraction and two phase pressure drop independent of flow patterns, pipe orientation and thermo-physical properties of gas and liquid phases.

1.3 Basic Definitions and Concepts in Gas-Liquid Two Phase Flow

The gas-liquid two phase flow is realistically a three dimensional flow with flow conditions and fluid properties varying with respect to the pipe cross section, length and time. Moreover, the simultaneous gas-liquid two phase flow is marked by the continuous interaction between the two phases with a dynamic interface along the pipe length and cross section and thus making it difficult to model two phase flow phenomenon mathematically. Thus this complexity limits the application of conventional equations designed for single phase flow to the two phase flow situations. In order to have an understanding of the two phase flow parameters and its deviation from single phase flow, basic definitions of two phase flow are presented here assuming a steady state one-dimensional flow followed by general description of flow patterns in different pipe orientations.

The mass flow rates of individual phases through the pipe can be measured directly by mass flow meters. Based on these mass flow rates, the total or mixture mass flow rates is as defined by Eq. (1.1),

$$\dot{m} = \dot{m}_G + \dot{m}_L \tag{1.1}$$

Based on the mass flow rate of each phase, the two phase flow quality is defined as

the ratio of mass flow ate of the gas phase to the two phase mixture mass flow rate as given by Eq. (1.2).

$$x = \frac{\dot{m}_G}{\dot{m}_G + \dot{m}_L} \tag{1.2}$$

One of the important two phase flow variables is the void fraction and can be defined in different ways based upon its measurement technique. For example, if the void fraction is measured using conductance/capacitance probe technique then it is defined as the ratio of pipe cross sectional area occupied by the gas phase to the total cross sectional area.

$$\alpha = \frac{A_G}{A} \tag{1.3}$$

Whereas, in case of volumetric void fraction measurement using quick closing valves, the void fraction is defined as the ratio of volume of the pipe occupied by the gas phase to the total volume of test section. The cross sectional and volumetric definition of void fraction is expressed as shown in Eqs. (1.3) and (1.4), respectively.

$$\alpha = \frac{V_G}{V} \tag{1.4}$$

Another important two phase flow parameter that is usually used in the analysis of two phase flow is the gas volumetric flow fraction. Gas volumetric flow fraction also known as homogeneous void fraction and is defined as the ratio of the volumetric flow of gas phase (or superficial gas velocity) to the total volumetric flow rate of mixture (or mixture velocity) assuming no slip between the two phases as shown in Eq. (1.5)

$$\beta = \frac{Q_{SG}}{Q_{SG} + Q_{SG}} = \frac{U_{SG}}{U_{SG} + U_{SL}} \tag{1.5}$$

Velocity of liquid and gas phase assuming that phase is flowing alone through the pipe occupying the entire cross section is called as phase superficial velocity. In terms of mass flux (G) and two phase flow quality (x) or the volumetric flow rate, the

superficial gas velocity is as defined by Eq. (1.6)

$$U_{SG} = \frac{Gx}{\rho_G} = \frac{Q_{SG}}{A} \tag{1.6}$$

Similarly, the superficial liquid velocity is defined by Eq. (1.7),

$$U_{SL} = \frac{G(1-x)}{\rho_L} = \frac{Q_{SL}}{A} \tag{1.7}$$

The actual phase velocity is quite higher than that of the superficial phase velocity due to the reduced pipe cross sectional area available for each phase. The actual phase velocity is expressed in terms of the void fraction in conjunction with the superficial phase velocity. The actual gas and liquid velocity is expressed by Eqs. (1.8) and (1.9), respectively.

$$U_G = \frac{U_{SG}}{\alpha} \tag{1.8}$$

$$U_L = \frac{U_{SL}}{(1-\alpha)} \tag{1.9}$$

Slip ratio is defined as the ratio of actual gas velocity to the actual liquid velocity averaged across the pipe cross section. Mathematically it is expressed as,

$$S = \frac{U_G}{U_L} = \left(\frac{x}{1-x}\right)\left(\frac{1-\alpha}{\alpha}\right)\left(\frac{\rho_L}{\rho_G}\right) \tag{1.10}$$

The Reynolds number in context of two phase flow is usually defined in terms of the phase superficial velocity and the fluid properties of individual phases. The gas and liquid Reynolds numbers are thus defined by Eqs. (1.11) and (1.12).

$$Re_{SG} = \frac{\rho_G U_{SG} D}{\mu_G} \tag{1.11}$$

$$Re_{SL} = \frac{\rho_L U_{SL} D}{\mu_L} \tag{1.12}$$

1.4 Two Phase Flow Patterns

Flow patterns observed in gas-liquid two phase flow are essentially due to alignment of one phase with respect to the other phase across the pipe cross section. The physical structure and appearance of the flow patterns is a function of several two phase flow variables such as pipe orientation, pipe diameter, fluid properties and system pressure. In two phase flow literature, the identification of a flow pattern is usually carried out by visual observation and hence the definition, description and tagging of a certain flow pattern depends on an individual's perception to a great extent. The knowledge of the general appearance of the flow patterns and its dependency on other two phase flow variables is important since flow patterns directly affect the hydrodynamics of two phase flow and hence influence two phase flow parameters such as void fraction, two phase pressure drop and heat transfer coefficient.

1.4.1 Flow Patterns in Horizontal Two Phase Flow

The main flow patterns that are typically observed in horizontal two phase flow are shown in Figure 1.1. The description of flow patterns are as follows:

Bubbly flow: Bubbly flow is featured by the flow of small discrete bubbles distributed in the continuous liquid medium. Because of the buoyancy force acting on the lighter phase, the gas bubbles are always seen to be in contact with the pipe top wall.

Plug flow: Plug flow is formed by the agglomeration of small bubbles to form a large bubble that flows in the vicinity of pipe top wall.

Slug flow: Slug flow is characterized by the alternate flow of elongated gas bubble and a liquid plug. The length and frequency of the gas slugs is typically

determined by the flow rates of individual phases.

Stratified flow: Stratified flow is typically observed at low liquid and gas flow rates. The gas phase flows on the top and parallel to the liquid layer.

Wavy flow: Wavy flow occurs when the gas flow rate is increased in the stratified flow regime. The gas-liquid interface becomes wavy and unstable with occasional splashing of the liquid phase on the pipe top wall.

Annular flow: Annular flow is characterized by the flow of liquid phase in contact with the pipe wall that surrounds the central fast moving gas core.

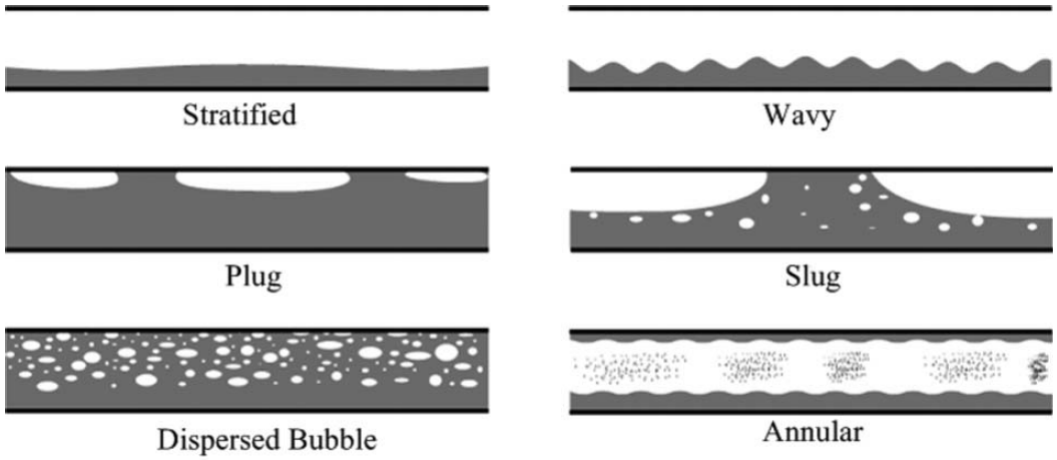

Figure 1.1: Flow patterns in horizontal two phase flow (adapted from Cheng et al. (2008)).

1.4.2 Flow Patterns in Vertical Two Phase Flow

The main flow patterns observed in vertical upward two phase flow are shown in Fig. 1.2. Unlike horizontal flow, stratified flow does not exist in vertical flow and the flow patterns are found to be symmetric about the pipe axis. The description of main flow patterns in vertical flow is as follows:

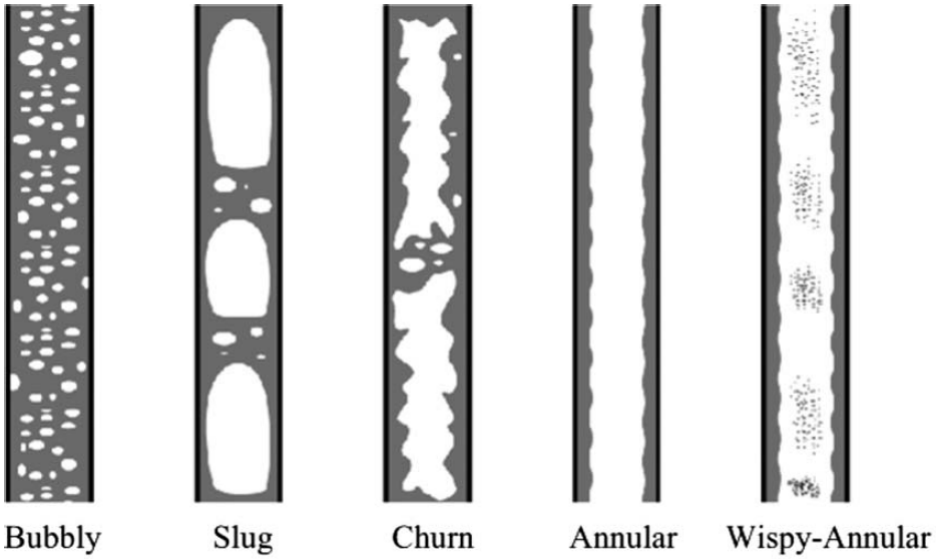

Figure 1.2: Flow patterns in vertical upward two phase flow (adapted from Cheng et al. (2008)).

Bubbly flow: Gas phase is dispersed in continuous liquid medium and is approximately uniformly distributed across the pipe cross section.

Slug flow: Elongated bullet shaped gas bubbles with tiny gas bubbles near the slug nose and slug tail.

Churn flow: Chaotic and pulsating two phase flow that appears to be oscillating up and down.

Annular flow: Liquid film flowing in contact with the pipe wall in form of film that surrounds the central fast moving gas core. In comparison to horizontal flow, the liquid film thickness in vertical annular flow is symmetric about the pipe axis.

Wispy-Annular flow: Wispy annular flow is essentially an annular flow characterized by significant entrainment of liquid droplets to the central gas core.

All flow patterns listed for vertical upward flow also appear in vertical downward flow. In addition to this, a new flow pattern identified as falling film flow and a physically modified version of bubbly flow known as coring bubbly flow appears in vertical downward flow. Moreover, all key flow patterns observed in horizontal two phase flow also appear in upward and downward pipe inclinations. However, their physical structure (cross sectional phase distribution) and characteristics (in terms of relative magnitudes of buoyancy and inertia forces) are significantly affected by the change in pipe orientation. More details and the photographic evidences of some of these flow patterns identified in this work will be presented later in Chapter IV.

1.5 Research Objectives

The main objective of this research is to explore and understand the effect of change in upward and downward pipe orientation on the physical structure of flow pattern, flow pattern transition, void fraction and pressure drop in non-boiling gas-liquid two phase flow. This objective can be accomplished by carrying out systematic experimental measurements of two phase pressure drop and the supplemental data of flow patterns and void fraction that govern and significantly influence two phase pressure drop both qualitatively and quantitatively. Once the necessary experimental data is collected and the nexus and inter-dependencies between flow patterns, void fraction and two phase pressure drop are established, the next major move to accurately quantify the void fraction and two phase pressure drop is the development of the two phase flow models. Two separate models, one for the void fraction and other for the frictional component of two phase pressure drop are required that can predict these quantities independent of flow patterns, pipe orientation and fluid physical properties. In order to have a sound understanding of the effect of pipe orientation on two phase flow phenomenon, following issues need to be addressed.

1. What is the qualitative and quantitative effect of pipe orientation on the physical structure of flow patterns and their transition boundaries?

2. What is the relationship between flow patterns and void fraction as a function of pipe orientation?

3. How sensitive is the two phase pressure drop to the void fraction for different flow patterns at any given pipe orientation?

4. What is the effect of flow pattern structure and their transition from one to other on the frictional component of the two phase pressure drop?

5. What is the effect of pipe surface roughness on the frictional component of two phase pressure drop for different flow patterns at any given pipe orientation?

6. What is the most reliable and accurate method to predict void fraction and pressure drop in upward and downward inclined gas-liquid two phase flow.

Following is a list of tasks required to answer these questions.

Task 1: A thorough review of literature relevant to flow patterns, void fraction and two phase pressure drop and their modeling techniques in upward and downward inclined pipe orientations. One of the important tasks while doing literature review is to generate a data bank of void fraction and two phase pressure drop for a wide range of two phase flow conditions.

Task 2: Collect experimental data of void fraction and pressure drop for different flow patterns and pipe orientations ($-90^o \leq \theta \leq +90^o$). Study the effect of pipe surface roughness by repeating experiments in rough pipe.

Task 3: Analyze the experimental data and that available in the literature to get a good qualitative and quantitative understanding of the different two phase flow

variables that affect void fraction and two phase pressure drop.

Task 4: Develop flow pattern and pipe orientation independent two phase flow models that can correctly predict void fraction and two phase pressure drop in upward and downward inclined gas-liquid two phase flow.

Task 5: Validate the accuracy of developed correlations against the experimental data collected in the present study and that available in the literature.

Task 6: Document and present the research findings in the form of published papers and doctoral dissertation as deliverable.

1.6 Brief Outline of this Study

The contents of this work are distributed in six main chapters provide details of the research background, experimental work and modeling techniques adopted and developed in this work. Chapter II presents a brief review of previous research work, flow pattern maps and a thorough review of the void fraction and two phase pressure drop models available in the literature. Chapter III describes details of the experimental setup and the experiment procedure followed for flow visualization, void fraction and pressure drop measurements carried out in this work. Next, Chapter IV presents the experimental results of flow patterns and flow pattern maps and measured values of void fraction and two phase pressure drop. Based on the conclusions of Chapters II and IV, a flow pattern independent void fraction model for a wide range of two phase conditions is presented and validated against a comprehensive data bank in Chapter V. This is followed by Chapter VI that proposes a frictional pressure drop model applicable for micro to macro scale two phase flow in horizontal and upward inclined pipes. Finally, in Chapter VII, the conclusions of this work and recommendations for the future work are discussed.

CHAPTER II

LITERATURE REVIEW

The initial literature on pressure drop in gas-liquid two phase flow dates back to 1960's. Since then several investigators have contributed to the general understanding of the pressure drop phenomenon in two phase flow by carrying out experimentation and developing models for different two phase flow situations. The initial research related to the pressure drop in two phase flow was focused on air-water and steam-water fluid combinations. However, in past few decades, fluid combinations such as refrigerants and their vapors, air-oil, air-kerosene and other miscellaneous fluid combinations have been included in the domain of the two phase flow research. In this chapter, the literature review is essentially organized in four sections. Section 2.1 gives a brief summary of some of the past studies focused on experimental measurements of void fraction and pressure drop done in upward and downward inclined two phase flows. Section 2.2 presents some of the existing flow pattern maps available in two phase flow literature. Section 2.3 presents two phase frictional pressure drop correlations available in the literature. Finally, Section 2.4 is a presentation of some of the top performing void fraction correlations available in the literature based on two different modeling techniques.

2.1 Experimental Work in Inclined Two Phase Flow

As mentioned earlier, majority of the research done in the field of two phase flow is for vertical and horizontal pipe orientations while little attention is paid to the two phase flow phenomenon in inclined pipe orientations. Some of the comprehensive experimental investigation of two phase flow phenomenon in inclined systems available in the literature is that of Beggs (1972), Nguyen (1975), Mukherjee (1979), Lips and Meyer (2012a) and Lips and Meyer (2012c).

Beggs (1972) investigated the two phase flow phenomenon for $+90^o \leq \theta \leq -90^o$ in a 25.4 mm and 38.1 mm I.D. transparent pipe using air-water fluid combination. He covered the wide range of void fraction and identified the dispersed, intermittent and segregated flow types as the key flow patterns and concluded that the pipe orientation affects the two phase flow parameter in most of the two phase flow cases. He developed flow pattern specific empirical void fraction (liquid holdup) and two phase frictional pressure drop correlations based on his own data. However, the experimental data collected in this study is found to be limited due to limited number of data points ($\approx$ 25 points) collected in each pipe orientation and unequal distribution of these data points for different flow patterns. Beggs (1972) concluded that since his work was carried out in smooth pipe, the effect of pipe surface roughness on two phase frictional pressure drop should be studied and insisted on the additional experimental investigation of inclined two phase flow for a better understanding of this phenomenon at different operating conditions.

Nguyen (1975) conducted experimental measurements (1900 data points) of void fraction and two phase pressure drop in a 45.5 mm I.D. transparent perspex pipe for $+90^o \leq \theta \leq -90^o$ using air-water fluid combination. The void fraction and two phase pressure drop measurements were carried out at a distance of 50D from mixer using

manually operated simultaneously closing valves and inclined manometers. Since any delay more than 0.1 seconds in closing of valves (to trap two phase mixture in the test section) is known to affect the measured void fraction, the accuracy and reliability of his data measured using manually operated valves is open to further verification. He concluded that the two phase flow pattern transition boundaries are sensitive to the pipe orientations and the pipe orientation affects both the void fraction and two phase pressure drop. Similar to Beggs (1972) and Mukherjee (1979), Nguyen (1975) also insisted on the further investigation of inclined two phase flow phenomenon in different pipe diameters and fluid combinations.

Mukherjee (1979) experimentally investigated the two phase flow in upward and downward inclined systems ($+90^o \leq \theta \leq -90^o$) in a 38.1 mm I.D. steel pipe using air-kerosene and air-oil fluid combinations. The void fraction was measured using capacitance sensor while the two phase pressure drop was measured using Validyne pressure transducer after allowing a calming length of 170 D. He identified the four major flow patterns that exist in all pipe orientations as bubbly, slug, stratified and annular-mist flow patterns and proposed empirical (curve fitting using non-linear regression) void fraction and two phase pressure drop correlations for each of these flow patterns. They measured around 1000 data points using air-kerosene and air-oil fluid (only for $\theta = 0^o, \pm 90^o$) combinations with majority of the data taken for high values of void fraction typically $\alpha \geq 0.6$. Mukherjee (1979) concluded that the flow pattern structure and void fraction are significantly affected by the near horizontal pipe inclination ($+30^o \leq \theta - 30^o$). He further recommended a need of additional experimental investigation of two phase flow phenomenon for different pipe diameters and fluids with different thermo-physical properties.

Although, this study is aimed at the investigation of non-boiling two phase flow phenomenon in inclined pipes, it is worthwhile to mention the comprehensive work

of Lips and Meyer (2012a) and Lips and Meyer (2012c) for the condensing flow of R134a in a 8.4 mm I.D. copper pipe with a calming length of 60D. They observed flow patterns using a high speed camera (200 fps) and measured two phase pressure drop and heat transfer coefficient in upward and downward inclined pipe orientations. They found the void fraction and two phase pressure drop to be very sensitive to the pipe orientation especially at low two phase flow qualities typically $x \leq 0.3$. Lips and Meyer (2012a) compared the performance of the two phase pressure drop correlations against the experimental data and found that the existing correlations poorly predict the pressure drop data in downward inclined two phase flows.

There are some other studies reported in the two phase literature which focused on a specific and narrow aspect of the inclined two phase flows. For instance, the Bonnecaze et al. (1971), Kokal and Stanislav (1989a) andKokal and Stanislav (1989b) investigated the void fraction and two phase pressure drop for slug flow in near horizontal upward and downward pipe orientations ($+10^o \leq \theta \leq -10^o$) using air-water and air-oil fluid combinations, respectively. Bonnecaze et al. (1971) proposed a void fraction and two phase pressure drop model for slug flow based on field data of 154 points. They concluded that the velocity profile of a slug flow is a function of pipe orientation however, the void fraction in inclined pipes can be predicted using flow pattern independent parameters with a reasonable accuracy. Kokal and Stanislav (1989b) in their experimental work in a 25.8 mm I.D. pipe found that the slug and stratified flow in downward inclinations were associated with considerable higher values of void fraction compared to the intermittent flow in upward inclinations. They found that the downward inclined flow is associated with the pressure recovery phenomenon due to negative hydrostatic pressure gradient. Additionally, they observed that the effect of pipe orientation on void fraction and pressure drop is predominant only for the small values of gas and liquid flow rates and any dependency on the pipe

orientation was vanished for increasing gas and liquid flow rates.

Spedding et al. (1998) did flow visualization and void fraction and two phase pressure drop measurements at near horizontal pipe inclinations ($+5^o \leq \theta \leq -5^o$) in 50.8 mm I.D. pipe using air-water fluid combination. In addition to main flow patterns such as bubbly, slug, intermittent and annular they identified several flow patterns such as stratified, stratified-ripple, roll wave, film-stratified and droplet-stratified. Similar to the studies of Beggs (1972), Mukherjee (1979) and Kokal and Stanislav (1989b), Spedding et al. (1998) found that the void fraction in downward inclinations is consistently higher than that in upward pipe inclinations and the void fraction is found to be sensitive to flow patterns and pipe orientations. They found that the two phase pressure drop in upward inclined flows was higher compared to that in horizontal flows up to $U_{SL} = 10$ m/s. However, for liquid flow rates corresponding to $U_{SL} \geq 10$ m/s, a pressure drop minimum is observed that renders pressure drop in horizontal flow higher than that in upward inclined flow. This effect was thought of as a consequence of the two phase flow structure in 'blow through slug' flow pattern that resembles the phenomenon of flow reversal and hence results in lower values of pressure drop.

Wongwises and Pipathttakul (2006) performed experimental investigation of air-water two phase flow phenomenon in a 4.5 mm narrow concentric annular pipe at 0^o, $+30^o$ and $+60^o$, respectively. Similar to a circular pipe geometry all major flow patterns such as bubbly, slug, intermittent and annular were observed in the annular channel. Their experimental results suggested that the pipe inclination angle has a significant effect on the flow pattern transition, void fraction and pressure drop especially in the buoyancy driven flows such as slug and some region of intermittent flows. The void fraction was found to decrease with increasing upward inclined pipe orientations whereas the effect of pipe orientation on two phase pressure drop was

noticed at low liquid and gas flow rates.

In summary, it can be concluded that there are very few studies available in the literature that investigate the combined effect of flow patterns, pipe diameter and pipe orientation on the void fraction and two phase pressure drop. Almost all of the existing experimental work for non-boiling gas liquid two phase flow in inclined systems (except that of Wongwises and Pipathttakul (2006)) is for $D \geq 25$ mm. None of these studies analyzed the effect of pipe surface roughness on frictional component of the two phase pressure drop. Moreover, these studies did not explore the phenomenon on flow reversal and its relationship with pipe orientation and surface roughness and hence creates a room for further investigation in comparatively smaller pipe diameters ($D < 25$ mm).

2.2 Two Phase Flow Pattern Maps

The flow pattern maps or flow maps reported in two phase flow literature serve as a tool to estimate the span and sequence of appearance of different flow patterns with change in gas and liquid flow rates for a given set of flow conditions. The flow patterns and their transition are defined qualitatively based on visual observations and hence the accurate mapping of the transition between different flow patterns is highly subjective and totally depends upon the observer's perception. Moreover, the transition between different flow patterns is gradual and sensitive to several parameters such as pipe diameter, pipe orientation and fluid properties making it is extremely difficult to have a universal flow pattern map that can correctly predict the existence of different flow patterns covering a wide range of two phase flow conditions.

Despite lack of universal flow pattern map, it is important to consider some of the existing most referred flow pattern maps to get an idea about the sequence,

extend and transitions between different flow patterns. Some of the most referred flow pattern maps available in the two phase flow literature are those of Mandhane et al. (1974) and Taitel and Dukler (1976). The flow pattern map of Mandhane et al. (1974) shown in Fig. 2.1 is developed based on the following two phase flow parameters: $12.7 \leq D \leq 165$ mm, $705 \leq \rho_L \leq 1009$ kg/m^3, $0.8 \leq \rho_G \leq 51$ kg/m^3, $0.0003 \leq \mu_L \leq 0.09$ Pa-s, $10^{-5} \leq \mu_G \leq 2.2 \times 10^{-5}$ Pa-s and $0.024 \leq \sigma \leq 0.1$ N/m.

It is evident that the Mandhane et al. (1974) flow map considers the existence of bubbly/dispersed bubbly flow to be insensitive to the change in gas flow rate. Moreover, their flow pattern map shows a common transition boundary between slug and annular flow patterns. Although, Mandhane et al. (1974) flow pattern map is based on data consisting of wide range of fluid properties, their flow pattern map is claimed to be more accurate for air-water two phase flow and is limited to horizontal pipe orientation.

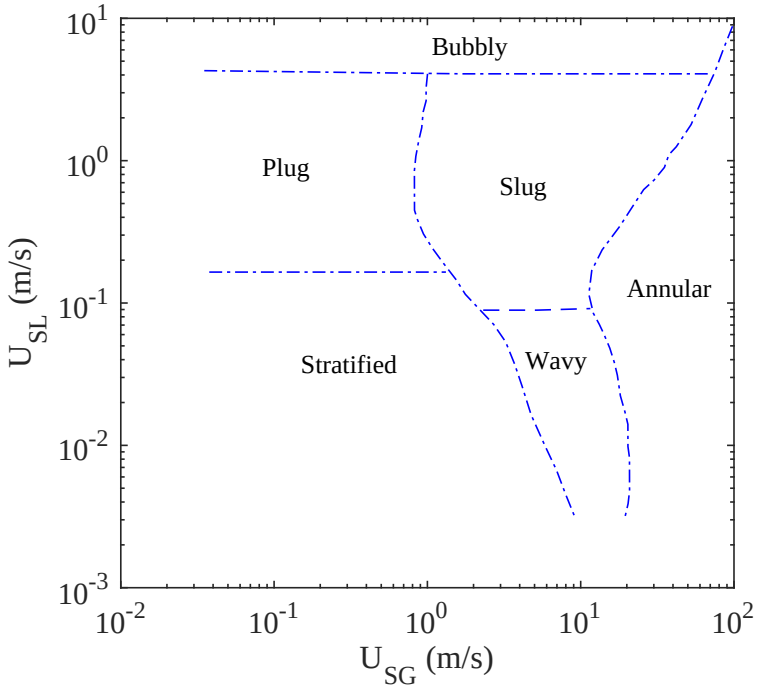

Figure 2.1: Flow pattern map for horizontal flow (adapted from Mandhane et al. (1974)).

The flow pattern map for Taitel and Dukler (1976) shown in Fig. 2.2 is based on mechanistic modeling of two phase flow patterns and is presented in non-dimensional form using Lockhart and Martinelli (1949) parameter X and parameters F and T given by Eqs. (2.1) to (2.3). Parameters $F - X$ are used to determine annular, stratified and intermittent flows while $T - X$ are used to determine existence of dispersed bubbly flow. Unlike Mandhane et al. (1974) flow map, Taitel and Dukler (1976) classify plug/slug/wavy flow patterns as intermittent flow. For other pipe orientations, these transition lines could be generated using the transition theories proposed by Taitel and Dukler (1976).

$$X = \sqrt{\frac{(dP/dL)_L}{(dP/dL)_G}} \tag{2.1}$$

$$F = \sqrt{\frac{\rho_G}{\rho_L - \rho_G}} \frac{U_{SG}}{\sqrt{gD}\cos\theta} \tag{2.2}$$

$$T = \sqrt{\frac{(dP/dL)_L}{(\rho_L - \rho_G)g\cos\theta}} \tag{2.3}$$

In case of vertical upward two phase flow, the flow pattern map of Hewitt and Roberts (1969) developed for air-water two phase flow and pipe diameters within the range of $10 \leq D \leq 30$ mm. Hewitt and Roberts (1969) flow map shown in Fig 2.3. is plotted using momentum flux of each phase. This flow map is also verified against the high pressure steam-water data and is found to give satisfactory prediction of the flow patterns.

Considering the several different forms of the flow pattern maps, it appears that it is difficult to have an exact agreement between the shape and trends of transition lines between specific flow patterns represented in different flow maps. This is partly because of the different coordinate systems adopted to generate flow maps and variations inconsistencies in the definition of flow patterns adopted by different

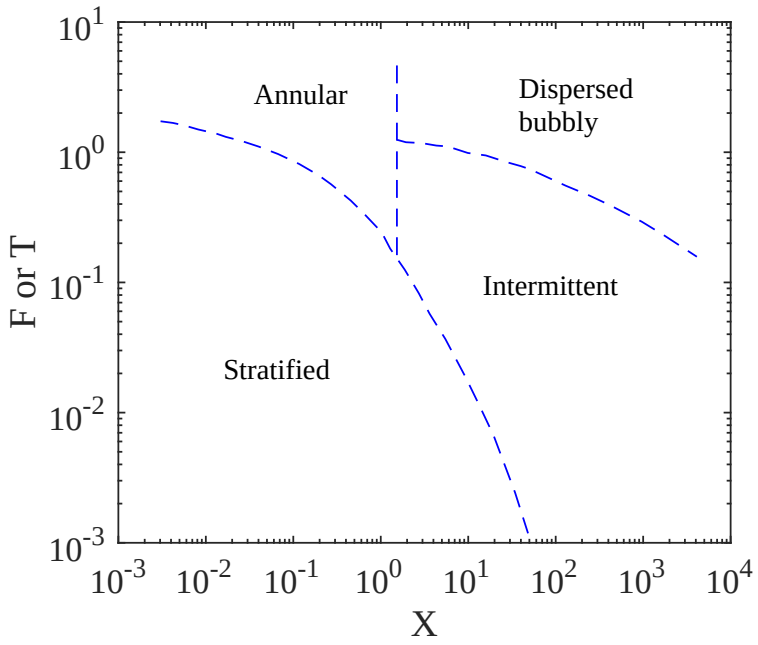

Figure 2.2: Flow pattern map of horizontal flow (adapted from Taitel and Dukler (1976)).

researchers. However, in a broad sense these flow maps show agreement between the qualitative range (low, moderate, high) of gas and liquid flow rates that represent certain flow patterns. Another important issue that must be considered here is the 'gradual' transition between different flow patterns. For the purpose of clarity, the transition boundaries between different flow patterns are shown as thin lines. However, in reality, the transition region may be spread over a range of gas and liquid flow rates. in general, keeping in mind the uncertainty, sensitivity and qualitative identification of flow patterns, following facts and limitations about the flow pattern maps must be perceived:

1. It is difficult to have a universal flow pattern map that can accurately predict the transition of one flow pattern to other for a wide range of two phase flow conditions.

2. Unlike represented in most flow pattern maps, the transition from one flow

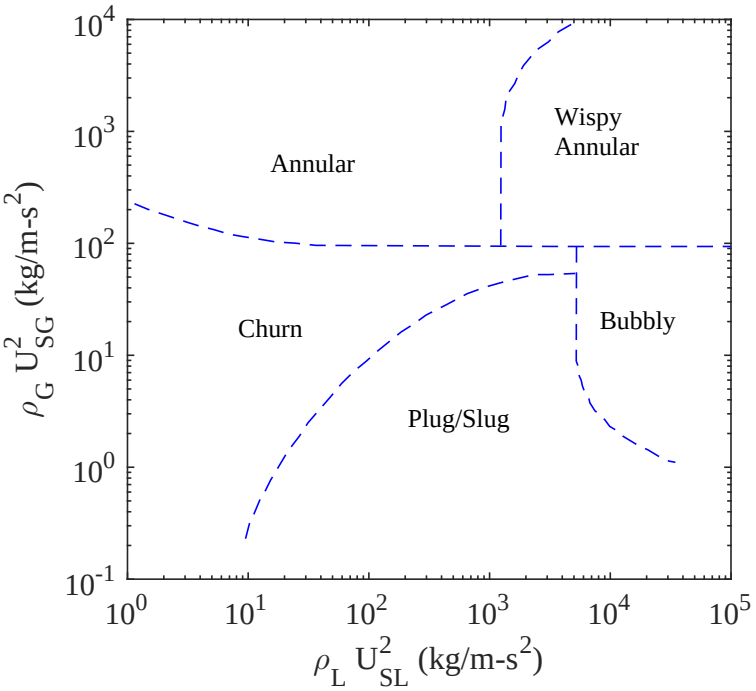

Figure 2.3: Flow pattern map for vertical upward flow (adapted from Hewitt and Roberts (1969)).

pattern to other is always gradual and cannot be presented in form of a thin continuous line.

3. Correct identification of a flow pattern in the vicinity of the transition line depends on the judgment of an individual.

2.3 Gas-Liquid Two Phase Pressure Drop

The pressure drop in gas-liquid two phase flow consists of three main components: hydrostatic pressure drop (due to pipe elevation), pressure drop due to acceleration (due to change in specific volume of the two phase mixture) and pressure drop due to friction at pipe wall and gas-liquid interface. The contribution of each of these components to the total pressure drop depends upon the flow patterns, fluid properties, pipe orientation and the pipe diameter. For example, in case of bubbly flow in

vertical upward orientation, the hydrostatic pressure drop component can be dominant in comparison to the frictional pressure drop depending upon the pipe diameter. While, for annular flow regime the frictional pressure drop has a prominent share in the total pressure drop and the hydrostatic pressure drop component is negligible. Moreover, the contribution of the frictional pressure drop to the total pressure drop is observed to increase with decreasing pipe diameter. The total two phase pressure drop per unit pipe length is the summation of its three components and is expressed by Eq. (2.4).

$$\left(\frac{dP}{dL}\right)_t = \left(\frac{dP}{dL}\right)_h + \left(\frac{dP}{dL}\right)_a + \left(\frac{dP}{dL}\right)_f \tag{2.4}$$

The right hand side of Eq. (2.4) is typically modeled using homogeneous and separated flow models. Thus, the formulation for hydrostatic, accelerational and frictional components of two phase pressure drop depends upon the simplifying assumptions such as time averaged or space averaged equations and the selection of homogeneous or separated flow model. Following is the elaborated description of each of the two phase pressure drop components using homogeneous and separated flow models.

2.3.1 Homogeneous Flow Model (HFM)

The homogeneous flow model (HFM) is based on the assumption that the two phases are well mixed with each other and move with identical velocity i.e., there is no slip between the gas and liquid phase. Additionally, HFM assumes that there exists thermodynamic equilibrium between the two phases. Thus, in the homogeneous flow model the underlying idea is to represent the two phase mixture to behave as a pseudo single phase fluid that has thermo-physical properties as that of two phase mixture. Thus, the use of homogeneous flow model is appropriate when there is no rapid change

in the flow variables and when there is negligible slip and thermodynamic equilibrium between gas liquid interface. Typically the bubbly and dispersed bubbly flow are the most suitable flow patterns to be modeled using homogeneous flow model. Using the concept of homogeneous flow model, the two phase mixture density is calculated using Eq. (2.5) and then the hydrostatic component of the two phase pressure drop is calculated from Eq. (2.6).

$$\rho_M = \left(\frac{x}{\rho_G} + \frac{1-x}{\rho_L} \right)^{-1} \tag{2.5}$$

$$\left(\frac{dP}{dL} \right)_h = \rho_M g \sin\theta = \left(\frac{x}{\rho_G} + \frac{1-x}{\rho_L} \right)^{-1} g \sin\theta \tag{2.6}$$

The accelerational component of the two phase pressure drop is due to the change in specific volume of the two phase mixture and neglecting the compressibility of the liquid phase it can be expressed by Eq. (2.7). In case of non-boiling two phase flow, the two phase pressure drop due to change in specific volume of the two phase mixture is negligible and hence is ignored.

$$\left(\frac{dP}{dL} \right)_a = G^2 \frac{dv_M}{dL} = G^2 \left[v_{LG} \frac{dx}{dL} + x \frac{dv_G}{dP} \frac{dP}{dL} \right] \tag{2.7}$$

Finally, the frictional component of the two phase pressure drop is expressed in terms of the two phase friction factor as expressed by Eq. (2.8). Combining these different components of pressure drop and with some rearrangement of equations, the total component of two phase pressure drop is calculated from Eq. (2.9).

$$\left(\frac{dP}{dL} \right)_f = \frac{2 f_{TP} G^2}{D \rho_M} \tag{2.8}$$

$$\left(\frac{dP}{dL}\right)_t = \frac{\frac{2f_{TP}G^2}{D}\left(\frac{x}{\rho_G}+\frac{1-x}{\rho_L}\right)+G^2 v_M\left(\frac{v_{LG}}{v_L}\right)\frac{dx}{dL}+\left(\frac{x}{\rho_G}+\frac{1-x}{\rho_L}\right)^{-1} g\sin\theta}{1+G^2 x\left(\frac{dv_G}{dP}\right)} \tag{2.9}$$

For the case of non-boiling two phase flow, the change of two phase quality with respect to pipe length is negligible ($dx/dL \approx 0$) and the two phase flow literature reports that even at high system pressure for a relatively short length of pipe, $|G^2 x(d\nu_G/dP)| << 1$. Thus, the Eq. (2.9) for total component of two phase pressure drop can be simplified to Eq. (2.10).

$$\left(\frac{\Delta P}{L}\right)_t = \frac{2f_{TP}G^2}{D\rho_M} + \rho_M g\sin\theta \tag{2.10}$$

Correlations based on Homogeneous Flow Model

As mentioned earlier, the homogeneous flow model (HFM) can be used with sufficient accuracy only when there is no rapid change in the flow variables and when there is negligible slip and there exists thermodynamic equilibrium between gas liquid interface. The frictional pressure drop using homogeneous flow model is calculated with conventional equations used for single phase flow that uses pseudo two phase mixture properties as given by Eq. (2.8). This general form of the frictional pressure drop equation can be used to calculate two phase frictional pressure drop using two phase friction factor based on the two phase Reynolds number and the two phase mixture density.

Most of the homogeneous flow model based two phase frictional pressure drop correlations recommend use of Blasius (1913) correlation to determine the fanning friction factor. Eqs. (2.11) and (2.12) are the Blasius (1913) friction factor (fanning)

equations for laminar and turbulent single phase flows, respectively.

$$f_{TP} = \frac{16}{Re_{TP}} \tag{2.11}$$

$$f_{TP} = \frac{0.079}{Re_{TP}^{0.25}} \tag{2.12}$$

The two phase Reynolds number is based on the two phase dynamic viscosity and is defined by Eq. (2.13).

$$Re_{TP} = \frac{GD}{\mu_{TP}} \tag{2.13}$$

Thus to predict the two phase frictional pressure drop correctly, an appropriate estimate of two phase Reynolds number and hence the two phase dynamic viscosity is obviously required. Literature reports several models to calculate the two phase dynamic viscosity as listed in Table 2.1. It should be noted that the two phase viscosity model of Akers et al. (1959) uses equivalent two phase mixture mass flux defined by Eq. (2.14).

$$G_{eq} = G\left((1-x) + x\sqrt{\rho_L/\rho_G}\right) \tag{2.14}$$

Thus, it is evident that the accuracy of homogeneous flow model depends upon the correct selection of the two phase dynamic viscosity model that governs the values of two phase mixture Reynolds number and hence the two phase friction factor. The variation of different two phase dynamic viscosity models with change in the two phase quality is shown in Figures 2.4 and 2.5. It is evident that the two phase dynamic viscosity models significantly differ from each other and hence it is expected that there is a considerable variation in the two phase frictional pressure drop predicted by these homogeneous flow models. The two phase dynamic viscosity models of Awad and Muzychka (2008) is based on the analogy of two phase viscosity with the thermal conductivity of the porous media and is essentially based on the data of refrigerants

(R12, R22, R740, R717, R134a, R410A and R290) consisting of pipe diameters in a range of 1.4 to 10 mm in horizontal orientation.

Table 2.1: Two phase dynamic viscosity models.

Source	Correlation
Akers et al. (1959)	$\mu_{TP} = \dfrac{\mu_L}{(1-x)+x\sqrt{\rho_L/\rho_G}}$
McAdams et al. (1942)	$\mu_{TP} = \left(x/\mu_G + (1-x)/\mu_L\right)^{-1}$
Ciccihitti et al. (1960)	$\mu_{TP} = x\mu_G + (1-x)\mu_L$
Beattie and Whalley (1982) [a]	$\mu_{TP} = \mu_L(1-\beta)(1+2.5\beta) + \mu_G\beta$
Dukler et al. (1964)	$\mu_{TP} = \rho_m\left[x(\mu_G/\rho_G) + (1-x)(\mu_L/\rho_L)\right]$
Lin et al. (1991)	$\mu_{TP} = \dfrac{\mu_L\mu_G}{\mu_G + x^{1.4}(\mu_L-\mu_G)}$
Fourar and Boris (1995)	$\mu_{TP} = \rho_M\left(\sqrt{x\mu_G/\rho_G} + \sqrt{(1-x)\mu_L/\rho_L}\right)^2$
Davidson et al. (1943)	$\mu_{TP} = \mu_L(1 + x(\rho_L/\rho_G) - 1)$
Owens (1961)	$\mu_{TP} = \mu_L$
Garcia et al. (2003)	$\mu_{TP} = \dfrac{\mu_L\rho_G}{x\rho_L + (1-x)\rho_G}$
Awad and Muzychka (2008) Model 1 [b]	$\mu_{TP} = \mu_L\left[\dfrac{2\mu_L + \mu_G - 2(\mu_L-\mu_G)x}{2\mu_L + \mu_G + 2(\mu_L-\mu_G)x}\right]$
Awad and Muzychka (2008) Model 2 [b]	$\mu_{TP} = \mu_G\left[\dfrac{2\mu_G + \mu_L - 2(\mu_G-\mu_L)(1-x)}{2\mu_G + \mu_L + 2(\mu_G-\mu_L)(1-x)}\right]$
Awad and Muzychka (2008) Model 3 [b]	Arithmetic mean of Model 1 and Model 2
Awad and Muzychka (2008) Model 4 [b]	$\mu_{TP} = 0.25([(3x-1)\mu_G + [3(1-x)-1]\mu_L] + \sqrt{[(3x-1)\mu_G + [3(1-x)-1]\mu_L]^2 + 8\mu_L\mu_G}$

[a] Use Colebrook (1939) correlation to calculate two phase friction factor
[b] Use Churchill (1977) correlation to calculate two phase friction factor

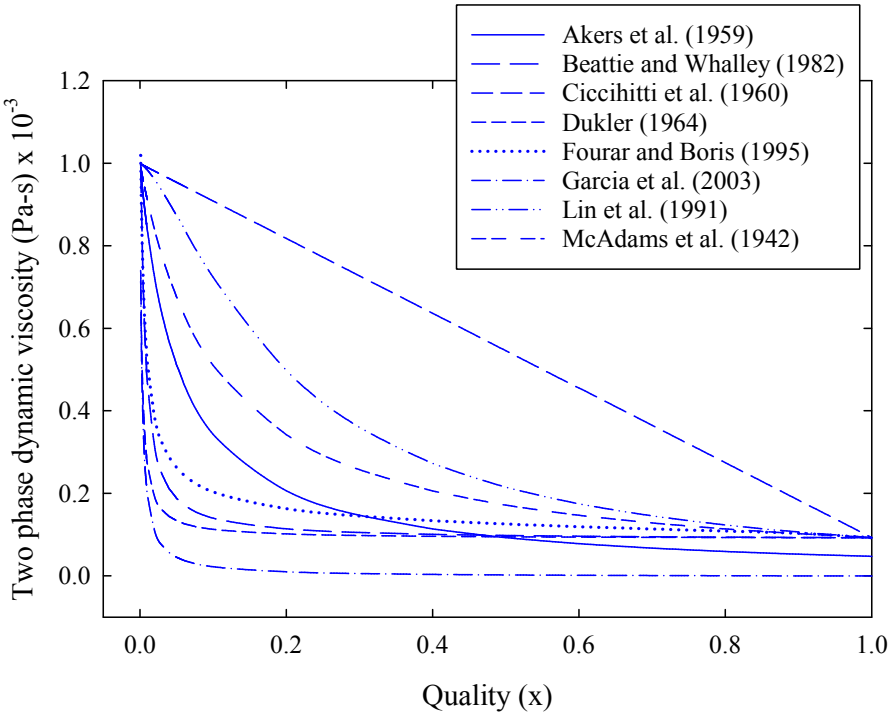

Figure 2.4: Two phase dynamic viscosity vs. quality for eight correlations listed in Table 2.1 .

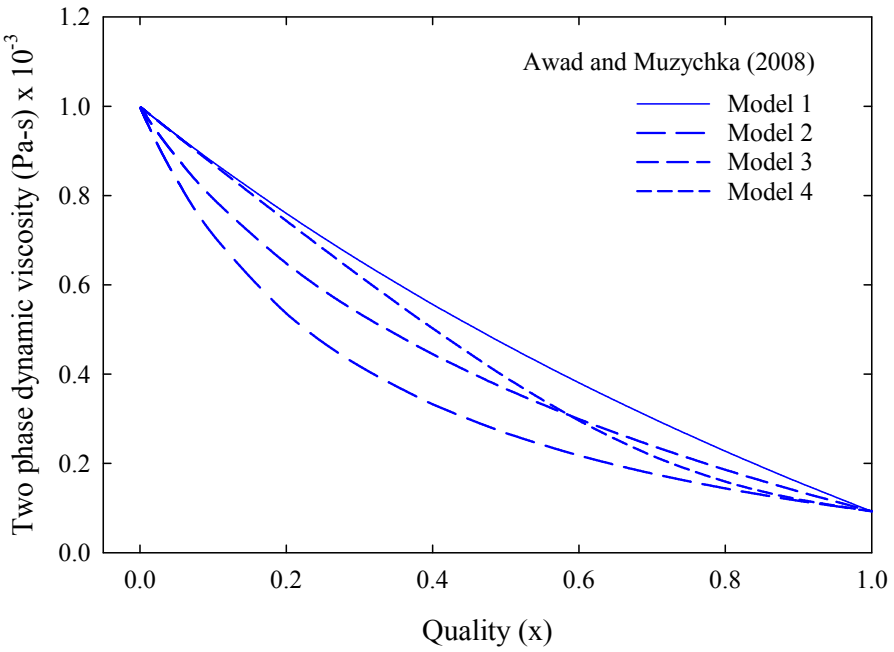

Figure 2.5: Two phase dynamic viscosity vs. quality for Awad and Muzychka (2008) correlations listed in Table 2.1.

2.3.2 Separated Flow Model (SFM)

Separated flow model (SFM) accounts for the two phases flowing separately with constant but not necessarily same velocities and having a definite gas-liquid interface. Similar to homogeneous flow model, separated flow model is based on the assumption that thermodynamic equilibrium exists between the gas and liquid phase. Typically, stratified and annular flow patterns are appropriate for the use of separated flow model. The weighted averaged two phase mixture density is calculated as a function of the void fraction defined by Eq. (2.15) and the the hydrostatic component of the two phase pressure drop is calculated from Eq.(2.16).

$$\rho_M = \rho_G \alpha + \rho_L (1 - \alpha) \tag{2.15}$$

$$\left(\frac{dP}{dL}\right)_h = \rho_M g \sin\theta = (\rho_G \alpha + \rho_L (1 - \alpha)) g \sin\theta \tag{2.16}$$

Comparison between Eqs. (2.6) and (2.16) shows that the hydrostatic component of the two phase pressure drop will agree with each other when there is an agreement between the two phase mixture densities calculated using Eqs. (2.5) and (2.15). The accelerational component of the two phase pressure drop is expressed as a function of the two phase flow quality, void fraction, mass flux and the density of gas and liquid phase as defined by Eq. (2.17)

$$\left(\frac{dP}{dL}\right)_a = G^2 \frac{d}{dL}\left[\frac{x^2}{\alpha \rho_G} + \frac{(1-x)^2}{(1-\alpha)^2 \rho_L}\right] \tag{2.17}$$

Finally, the frictional component of the two phase pressure drop is calculated using the concept of two phase multiplier as shown in Eq. (2.18).

$$\left(\frac{dP}{dL}\right)_f = \Phi^2 \left(\frac{dP}{dL}\right)_{f,SP} \tag{2.18}$$

Thus combining the three components of pressure drop, the total two phase pressure drop using SFM for a linear change of two phase quality over the pipe length (saturated liquid at inlet) can be expressed by Eq. (2.19).

$$\left(\frac{\Delta P}{L}\right)_t = \Phi^2 \left(\frac{dP}{dL}\right)_{f,SP} + \frac{G^2}{L}\left[\left(\frac{x^2}{\alpha\rho_G} + \frac{(1-x)^2}{(1-\alpha)\rho_L}\right)_o - \left(\frac{x^2}{\alpha\rho_G} + \frac{(1-x)^2}{(1-\alpha)\rho_L}\right)_i\right] + \left(\rho_G\alpha + \rho_L(1-\alpha)\right) g \ \sin\theta \tag{2.19}$$

The change in two phase quality and the void fraction with respect to pipe length is negligible for the case of non-boiling two phase flow and hence the accelerational component of two phase pressure drop can be neglected. Moreover, the the two phase mixture density defined in terms of the void fraction is assumed to stay constant for a negligible change in two phase quality over a short length of pipe. Hence, the Eq. (2.19) can be simplified to Eq. (2.20) for the case of non-boiling two phase flow.

$$\left(\frac{\Delta P}{L}\right)_t = \Phi^2 \left(\frac{dP}{dL}\right)_{f,SP} + \left(\rho_G\alpha + \rho_L(1-\alpha)\right) g \sin\theta \tag{2.20}$$

The term Φ^2 and the single phase pressure gradient on the right hand side (first term) can have several forms depending upon the assumption of flow of gas or liquid phase through the pipe and is discussed later in the next section. The calculation of the hydrostatic pressure gradient (second term on right side) would require accurate knowledge of the void fraction which is covered in Section 2.4.

Correlations based on Separated Flow Model

Analytical solution to the separated flow model requires in all six equations; mass, momentum and energy conservation equations for each phase. Additional information such as velocity and temperature profile and other hydrodynamic parameters are also

required to solve these equations thus making it complex and difficult. An easy and a quick approach listed in the literature is to use empirical methods based on extensive experimental data.

The empirical model based on the concept of separated flow was first conceived by Lockhart and Martinelli (1949) and since then several investigators have proposed different correlations by modifying the correlation of Lockhart and Martinelli (1949). They suggested that the separated flow model can be expressed in four different ways in terms of the two phase friction multiplier (Φ^2) that accounts for the pressure drop due to the flow of single phase liquid or gas. The subscripts 'LO' and 'GO' correspond to frictional pressure drop when the single phase liquid or gas flow rate is assumed to be equivalent to the entire two phase mixture flow rate (G). Whereas, the subscripts 'L' and 'G' indicate the frictional pressure drop when single phase liquid or gas is flowing at a rate of $G(1-x)$ and Gx, respectively. The understanding of these four approaches that can be used in separated flow model becomes more apparent from their mathematical definitions presented by Eqs. (2.21) to (2.24).

$$\left(\frac{dP}{dL}\right)_{f,TP} = \Phi_L^2 \left(\frac{dP}{dL}\right)_L = \Phi_L^2 \left[\frac{2f_L G^2 (1-x)^2}{D\rho_L}\right] \tag{2.21}$$

$$\left(\frac{dP}{dL}\right)_{f,TP} = \Phi_G^2 \left(\frac{dP}{dL}\right)_G = \Phi_G^2 \left[\frac{2f_G G^2 x^2}{D\rho_G}\right] \tag{2.22}$$

$$\left(\frac{dP}{dL}\right)_{f,TP} = \Phi_{LO}^2 \left(\frac{dP}{dL}\right)_{LO} = \Phi_{LO}^2 \left[\frac{2f_{LO} G^2}{D\rho_L}\right] \tag{2.23}$$

$$\left(\frac{dP}{dL}\right)_{f,TP} = \Phi_{GO}^2 \left(\frac{dP}{dL}\right)_{GO} = \Phi_{GO}^2 \left[\frac{2f_{GO} G^2}{D\rho_G}\right] \tag{2.24}$$

The single phase friction factor used in above equations may be determined using existing correlations such as Blasius (1913), Colebrook (1939) and Churchill (1977). Following is a brief documentation of the separated flow model based two

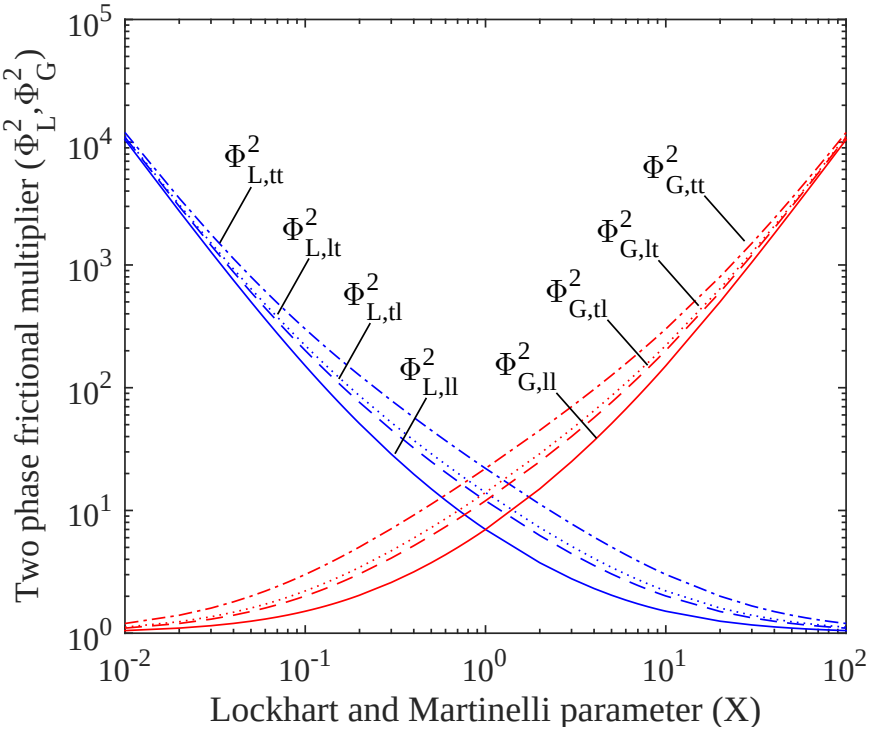

Figure 2.6: Variation of Φ^2 with change in Lockhart and Martinelli (1949) parameter.

phase pressure drop correlations available in the literature.

As mentioned earlier, Lockhart and Martinelli (1949) were the first to propose an empirical form of the separated flow model to predict two phase pressure drop in smooth horizontal pipe of pipe diameters between 12.6 and 25.4 mm I.D. and for a maximum system pressure of 400 kPa. They classified the two phase flow essentially in four flow regimes based on the flow nature of gas and liquid phase as, turbulent-turbulent, turbulent-laminar, laminar-turbulent and laminar-laminar, respectively. The calculation method of two phase pressure drop using Lockhart and Martinelli (1949) is represented as shown in Eq. (2.21). The variation of two phase friction multiplier with respect to change in Lockhart and Martinelli (1949) parameter for different flow regimes (tt,ll,tl and lt) is illustrated in Fig. 2.6. The two phase frictional multiplier is expressed by Eq. (2.25). The parameter X is defined for four different

flow regimes as shown in Table 2.2.

$$\Phi_L^2 = 1 + \frac{C}{X} + \frac{1}{X^2} \tag{2.25}$$

Table 2.2: Expressions to calculate Lockhart and Martinelli (1949) parameter X.

Liquid	Gas	X	C_L	C_G
Laminar	Laminar	$\left[\left(\frac{\dot{m}_L}{\dot{m}_G}\right)\left(\frac{\rho_G}{\rho_L}\right)\left(\frac{\mu_L}{\mu_G}\right)\right]^{0.5}$	0.046	0.046
Laminar	Turbulent	$\left[Re_{SL}^{-0.8}\left(\frac{C_L}{C_G}\right)\left(\frac{\dot{m}_L}{\dot{m}_G}\right)\left(\frac{\rho_G}{\rho_L}\right)\left(\frac{\mu_L}{\mu_G}\right)\right]^{0.5}$	16	0.046
Turbulent	Laminar	$\left[Re_{SL}^{0.8}\left(\frac{C_L}{C_G}\right)\left(\frac{\dot{m}_L}{\dot{m}_G}\right)\left(\frac{\rho_G}{\rho_L}\right)\left(\frac{\mu_L}{\mu_G}\right)\right]^{0.5}$	0.046	16
Turbulent	Turbulent	$\left[\left(\frac{\dot{m}_L}{\dot{m}_G}\right)^{1.8}\left(\frac{\rho_G}{\rho_L}\right)\left(\frac{\mu_L}{\mu_G}\right)^{0.2}\right]^{0.5}$	16	16

The value of constant C in Eq. (2.25) simplified by Chisholm (1967) that change with change in single phase flow regime is presented in Table 2.3.

Table 2.3: Values of constant C for different single phase flow regimes.

Liquid phase	Gas phase	C
Turbulent	Turbulent	20
Laminar	Turbulent	12
Turbulent	Laminar	10
Laminar	Laminar	5

Friedel (1979) and Friedel (1985) proposed a separated flow model based correlation to predict two phase frictional pressure drop in horizontal, vertical upward and vertical downward two phase flow. The expressions for two phase frictional multiplier as reported by Friedel (1979) and Friedel (1985) for vertical upward, horizontal and

vertical downward are given by Eqs. (2.26) and (2.27), respectively.

$$\Phi_{LO}^2 = A_F + 3.24x^{0.78}(1-x)^{0.24}\left(\frac{\rho_L}{\rho_G}\right)^{0.91}\left(\frac{\mu_G}{\mu_L}\right)^{0.19}\left(1-\frac{\mu_G}{\mu_L}\right)^{0.7}\frac{Fr^{-0.0454}}{We^{0.035}} \quad (2.26)$$

$$\Phi_{LO}^2 = A_F + 5.7x^{0.7}(1-x)^{0.14}\left(\frac{\rho_L}{\rho_G}\right)^{0.85}\left(\frac{\mu_G}{\mu_L}\right)^{0.36}\left(1-\frac{\mu_G}{\mu_L}\right)^{0.2}\frac{Fr^{0.09}}{We^{-0.007}} \quad (2.27)$$

These equations account for the effect of gravity, pipe diameter and mass flow rate through the Froude number ($Fr = G^2/gD\rho_M^2$) and the surface tension, pipe diameter and mass flow rate through the Weber number ($We = G^2D/\rho_M\sigma$). The two phase mixture density used in definitions of Froude number and Weber number is the homogeneous flow density as defined by Eq. (2.5). The parameter A_F is defined as shown in (2.28).

$$A_F = (1-x)^2 + x^2\frac{\rho_L f_G}{\rho_G f_L} \quad (2.28)$$

The single phase friction factors f_L and f_G are calculated based on the superficial Reynolds number (Re_j) for j^{th} phase. For laminar flows, the single phase friction factors are calculated using Blasius (1913) correlation while for turbulent flows ($Re_{SL} > 1000$) and ($Re_{SG} > 1000$), the single phase friction factor is defined by Eq. (2.29),

$$f_j = 0.25\left[0.86859\ln\left(\frac{Re_j}{1.964\ln(Re_j) - 3.8215}\right)\right] \quad (2.29)$$

Friedel (1979) verified his correlation for horizontal and vertical upward flow against the air-water and refrigerant data base consisting of 16000 data points while the correlation for vertical downward flow was verified against 1800 data points. The data consisted of pipe diameters in a range of 5 to 51 mm I.D. and the correlations were claimed to give an accuracy within $\pm 38\%$ standard deviation. It should be noted that the two phase frictional multiplier used by Friedel (1979) and Friedel (1985) is

different than that of Lockhart and Martinelli (1949) and hence single phase pressure drop expression given in Eq. (2.23) must be used instead of Eq. (2.21).

Chen et al. (2001) proposed a modified form of Friedel (1979) correlation to account for the pipe diameter effect ($D \leq 9$mm) by correlating two phase multiplying factor in terms of the phase superficial Reynolds number, Weber number and Bond number. The correlation is claimed to be applicable for air water flows and R-410a and its vapor in small diameter ($1 \leq D \leq 9\,$mm) horizontal pipes. However, since the non-dimensional numbers used in this form of correlation incorporate fluid physical properties and diameter effect, this correlation should be tested against the pressure drop data in comparatively large diameter pipes and different fluid combinations. The correlation for two phase frictional pressure drop defined by Eq. (2.30) takes the following form where Ω is defined by Eq. (2.31).

$$\left(\frac{dP}{dL}\right)_f = \Omega \left(\frac{dP}{dL}\right)_{Friedel} \tag{2.30}$$

$$\Omega = \begin{cases} \dfrac{0.0333 Re_{SL}^{0.45}}{Re_{SG}^{0.09}\left(1 + 0.4\exp(-Bo)\right)}, & Bo < 2.5 \\ \dfrac{We^{0.2}}{(2.5 + 0.06Bo)}, & Bo \geq 2.5 \end{cases} \tag{2.31}$$

The Weber number is defined on the basis of two phase density similar to that of Friedel (1979) correlation and the Bond number is defined as, $Bo = g\left(\rho_L - \rho_G\right)\left(\dfrac{0.25D^2}{\sigma}\right)$.

Bankoff (1960) proposed a correlation to predict frictional pressure drop in one component two phase flow (steam-water) as a function of two phase mixture quality and two phase density applicable for $0 < x < 1$. The correlation is expressed in the

following form by Eq. (2.32) where γ is defined by Eq. (2.33).

$$\Phi_{LO}^2 = \left(\frac{1}{1-x} \left[1 - \gamma \left(1 - \frac{\rho_G}{\rho_L} \right) \right]^{3/7} \left[1 + x \left(\frac{\rho_L}{\rho_G} - 1 \right) \right] \right)^{4/7} \tag{2.32}$$

$$\gamma = \frac{0.71 + 2.35\,(\rho_G/\rho_L)}{1 + (1/(1-x))\,(\rho_G/\rho_L)} \tag{2.33}$$

He concluded that the two phase frictional pressure drop is also a function of system pressure and hence captured the effect of system pressure by inclusion of the density ratio in his correlation. Bankoff (1960) verified his correlation against the data for system pressures ranging from 0.6 to 17 MPa and void fraction range of $0 < \alpha < 0.85$; however, the accuracy and statistical performance of his correlation is not reported.

Chisholm (1973) proposed a method to calculate two phase frictional pressure drop in evaporating flow conditions based on the concept of separated flow model and applicable for vapor qualities $0 \leq x \leq 1$. The two phase friction multiplier was expressed as shown in Eq. (2.34) where Y is defined by Eq. (2.35).

$$\Phi_{LO}^2 = 1 + (Y^2 - 1) \left(B_s x^{0.875} (1-x)^{0.875} + x^{1.75} \right) \tag{2.34}$$

$$Y = \sqrt{\frac{(dP/dL)_{f,GO}}{(dP/dL)_{f,LO}}} \tag{2.35}$$

The frictional pressure gradients for single phase liquid and gas phase are calculated using Eqs.(2.23) and (2.24), respectively. His correlation is essentially a transformation of graphical solution of Barcozy (1966) to predict the two phase frictional pressure drop. The correlation is claimed to be applicable for a pressure range of 0.6 to 4 MPa. He proposed a set of different conditional equations to predict parameter B_s for different values of Y and mixture mass flux (G) as shown in Table 2.4.

Table 2.4: Values of parameter B_s used in Chisholm (1973) correlation.

Y	G [kg/m^{2}s]	Equation for B_s
$0 < Y < 9.5$	$G \geq 1900$	$B_s = 55/\sqrt{G}$
	$500 < G < 1900$	$B_s = 2400/G$
	$500 > G$	$B_s = 4.8$
$9.5 < Y < 28$	$G \leq 600$	$B_s = 520/(Y\sqrt{G})$
	$G \geq 600$	$B_s = 21/Y$
$Y > 28$		$B_s = 15000/(Y^2\sqrt{G})$

He further modified his equation for two phase friction multiplier by replacing B_s by B_r to predict the frictional pressure drop in rough pipes.

$$B_r = B_s \left[0.5 \left\{ 1 + \left(\frac{\mu_G}{\mu_L} \right)^2 + 10^{\frac{-600\epsilon}{D}} \right\} \right]^4 \tag{2.36}$$

He reported that the effect of surface roughness on two phase frictional pressure drop is noticeable for ($\epsilon/D > 0.004$).The Eq. (2.36) is claimed to be applicable for ϵ/D upto 0.068.

Awad and Muzychka (2004) proposed a correlation based on a separated flow model for both gas and liquid phase in turbulent - turbulent regime and applicable for two phase flow through smooth horizontal pipes. They devised a method to determine two phase frictional multiplier to be used in conjunction with Lockhart and Martinelli (1949) correlation. The two phase frictional multiplier is expressed as shown in Eq. (2.37) where $p_1 = 0.307$ and X_{tt}^2 is taken from Lockhart and Martinelli (1949) correlation.

$$\Phi_L^2 = \left[1 + \left(\frac{1}{X_{tt}^2} \right)^{p_1} \right]^{(1/p_1)} \tag{2.37}$$

The correlation is claimed to work well for large diameter pipes and both phases in turbulent regime. However, the authors did not report the criteria to separate large diameter pipes from small diameter pipes. More details can be obtained from Awad

and Muzychka (2004).

Lau and Rezkallah (1995) developed a two phase frictional pressure drop correlation based on the data of air-water two phase flow in a 9.53 mm I.D. vertical upward and downward pipe. The frictional component of two phase pressure drop was found to be consistently higher in downward flow compared to vertical upward flow. They concluded that the two phase frictional multiplier for all flow patterns other than annular flow regime ($0.1 \leq \alpha \leq 0.9$) could be expressed as a function of void fraction as shown in Eq. (2.38) where n is the empirical constant and is equal to 1.51 and 1.14 for vertical upward and downward flow, respectively.

$$\Phi_L^2 = \begin{cases} \dfrac{1}{(1-\alpha)^{m_2}}, & (0.1 \leq \alpha \leq 0.9) \\ c_1 Re_{SL}^{m_1} \left(\dfrac{U_{SG}}{U_{SL}}\right)^{m_2}, & (\alpha > 0.9) \end{cases} \tag{2.38}$$

The constants c_1, m_1 and m_2 for vertical upward and downward flows are 0.000123, 1.04, 1.64 and 0.0042, 0.52, 1.26, respectively. This correlation was compared against the data of other investigators with an overall RMS deviation of 19.2% for vertical upward flow and 42% for vertical downward flow.

Yamazaki and Yamaguchi (1979) carried out experimental investigation of two phase pressure drop in a 25.4 mm I.D. pipe using air-water fluid combination. Based on a data of 350 measurements they proposed a correlation to predict frictional pressure drop in vertical upward and downward two phase flow. The correlation based on the concept of separated flow model expressed two phase frictional multiplier as a function of void fraction as shown by Eq. (2.39) where the z value was obtained by curve fitting the data to this equation and was found to be 0.875 and 0.9 for vertical upward and downward flows, respectively. The correlation was claimed to predict the two phase frictional pressure drop data within ±30% of experimentally measured

data as long as the gas volumetric flow fraction (β) stayed below 0.3.

$$\Phi_L^2 = (1-\alpha)^{-z} \tag{2.39}$$

Mishima and Hibiki (1996) developed a two phase frictional pressure drop correlation for turbulent-turbulent flow regime applicable for horizontal and vertical upward flow. The correlation is essentially a modification of Lockhart and Martinelli (1949) where the Chisholm (1973) parameter C in Eq. (2.25) is expressed as a function of pipe diameter as given by Eq. (2.40).

$$C = 21(1 - \exp(-0.319 D_h/1000)) \tag{2.40}$$

The correlation is claimed to be applicable for pipe diameters in a range of 0.7 to 10 mm I.D. (circular and rectangular cross sections) and is tested against the experimental data consisting of air-water and ammonia vapor fluid combination. Except for the data of liquid and ammonia vapor, the air-water data was predicted within $\pm 15\%$ of the measured values of small diameter pipes.

Gronnerud (1979) proposed a two phase frictional pressure drop correlation especially for refrigerants in horizontal pipe orientation based on a separated flow model. The two phase frictional pressure drop is represented in terms of the two phase multiplier as shown in Eq. (2.41). The frictional pressure gradient based on the Froude number is calculated from Eq. (2.42).

$$\Phi_{LO}^2 = 1 + \left(\frac{dP}{dL}\right)_{FR} \left[\frac{(\rho_L/\rho_G)}{(\mu_L/\mu_G)^{0.25}} - 1\right] \tag{2.41}$$

$$\left(\frac{dP}{dL}\right)_{FR} = f_{FR}\left[x + 4\left(x^{1.8} - x^{0.1}\sqrt{f_{FR}}\right)\right] \tag{2.42}$$

The variable f_{FR} used in Eq. (2.42) is calculated from Eq. (2.43).

$$f_{FR} = \begin{cases} 1, & Fr_L \geq 1 \\ Fr_L^{0.3} + 0.0055 \ln\left(\frac{1}{Fr_L}\right)^2, & Fr_L \leq 1 \end{cases} \tag{2.43}$$

The correlation is claimed to be applicable for all vapor qualities i.e., $0 \leq x \leq 1$ or alternatively all flow patterns including the limiting case of single phase liquid and gas flow.

Muller-Steinhagen and Heck (1986) developed a correlation to extrapolate between single phase liquid and single phase gas flow. The physical form of the correlation is as shown in Eq. (2.44). The parameter Y is same as that defined by Chisholm (1973) in Eq. (2.35). The correlation is verified against 9300 measurements including data of air-oil, air-water, and steam-water fluid combinations and pipe diameters ranging from 4 to 39 mm I.D.

$$\Phi_{LO}^2 = Y^2 x^3 + (1-x)^{0.33}(1 + 2x(Y^2 - 1)) \tag{2.44}$$

The application of Eq. (2.44) is restricted to $Re_{LO} > 100$ and $Re_{GO} > Re_{LO}$. Muller-Steinhagen and Heck (1986) claimed their correlation to predict the two phase frictional pressure drop data with an average error of 41.7% with only 49.5% of the data points predicted within ±30% error bands.

Jung and Radermacher (1989) developed a correlation for turbulent-turbulent flow regime of boiling refrigerants (pure and mixed) and their vapors (R12, R22, R114, R152a) in a horizontal pipe. Their correlation is a modification of Martinelli and Nelson (1948) and is applicable for system pressure (reduced pressure) in a range

of 0.2 to 0.8 MPa (0.08-0.16) and mixture mass flux in a range of 230 to 720 kg/m^{2}s.

$$\Phi_{LO}^2 = 30.78x^{1.323}(1-x)^{0.477}P_r^{-0.7232} \tag{2.45}$$

Jung and Radermacher (1989) found that there is no significant difference between the two phase pressure drop of pure and mixed refrigerants and hence concluded that the correlations developed for pure refrigerants can be used to predict two phase frictional pressure drop of mixed refrigerants. Eq. (2.45) is applicable for annular flow regime in horizontal pipe and is claimed to predict the two phase frictional pressure drop with 8.4% average error.

Sun and Mishima (2009) developed a correlation for two phase frictional multiplier for horizontal flow based on more than 2000 data points consisting of nine refrigerants and air-water fluid combinations. The physical form of the two phase frictional multiplier as shown in Eq. (2.46) is similar to that of Lockhart and Martinelli (1949). The parameter C is redefined by Eq. (2.47).

$$\Phi_L^2 = 1 + \frac{C}{X_{tt}^{1.19}} + \frac{1}{X_{tt}^2} \tag{2.46}$$

$$C = 1.79\left(\frac{Re_G}{Re_L}\right)^{0.4}\left(\frac{1-x}{x}\right)^{0.5} \tag{2.47}$$

The experimental data used for development of this correlation consisted of $0.5 \leq D_h \leq 12$ mm, $10 \leq Re_L \leq 37000$ and $10 \leq Re_G \leq 4 \times 10^5$ and the correlation is to predict the two phase frictional pressure drop with mean error of 29%.

Wang et al. (1997) proposed a correlation based on two phase frictional multiplier of Lockhart and Martinelli (1949). The correlation of Wang et al. (1997) is based on the flow of refrigerant data (R22, R134a and R407C) in a 6.5 mm horizontal pipe. The correlation is applicable for $50 < G < 700$ kg/m^{2}s. The parameter C to be used

in Eq. (2.25) is redefined by Wang et al. (1997) for $G < 200$ kg/m^{2}s as C_w as shown in Eq. (2.48). In case of $G \leq 200$ kg/m^{2}s, the two phase friction multiplier is defined in terms of single phase gas defined by Eq. (2.49). Wang et al. (1997) claimed that use of Eqs. (2.48) and (2.49) can predict 85% and 90% of data points within ±20% error bands, respectively.

$$C_w = \frac{4.566}{10^6} X_{tt}^{0.128} Re_{LO}^{0.938} \left(\frac{\rho_G}{\rho_L}\right)^{2.15} \left(\frac{\mu_G}{\mu_L}\right)^{5.1} \tag{2.48}$$

$$\Phi_G^2 = 1 + 9.4X^{0.62} + 0.564X^{2.45} \tag{2.49}$$

Wang et al. (2001) proposed a modified form of the Lockhart and Martinelli (1949) correlation to predict frictional pressure drop in horizontal two phase flow of R22, R410A and R407C refrigerants in small pipe diameters ranging from 3 to 9 mm.The general form of the correlation in terms of two phase liquid multiplier is expressed similar to that of the Lockhart and Martinelli (1949) correlation wheere the Chisholm (1967) parameter is modified as given by Eq. (2.50).

$$C = \begin{cases} 1.08 \left(\dfrac{\mu_L}{\mu_G}\right)^{0.5 Fr_L^{0.05}}, & F_w \leq 1 \\ \dfrac{0.68487 + 4.0156\ Bo^{-0.21812}\ We^{\left(0.01(\rho_L/\rho_G)^{0.73}\right)}}{(X - 0.02)^{0.27}}, & F_w > 1 \end{cases} \tag{2.50}$$

The variable F_w is defined using Eq. (2.51) where $La = \dfrac{\sqrt{\sigma/(g(\rho_L - \rho_G))}}{D}$.

$$F_w = 0.074 \left(\frac{1}{La}\right)^{0.67} \left[\frac{U_{SG}^2 \rho_G}{\Delta\rho G D}\right] + 8 \left[1 - \left(\frac{\rho_G}{\rho_L}\right)^{0.1}\right]^2 \left[\frac{U_{SL}^2 \rho_L}{\Delta\rho G D}\right] \tag{2.51}$$

The correlation is reported to predict two phase frictional pressure drop within ±50% of the experimental data and with 17% mean deviation.

Souza and Pimenta (1995) developed correlation based on experimental data of R12, R22, R134a and R32/R125 in horizontal pipe of diameter less than 10 mm. Their correlation was developed for turbulent-turbulent region and considered the density and dynamic viscosity of the gas and liquid phase as shown in Eq. (2.52) where Γ is defined as, $\Gamma = (\rho_L/\rho_G)^{0.5}(\mu_G/\mu_L)^{0.125}$.

$$\Phi_{LO}^2 = 1 + (\Gamma^2 - 1)x^{1.75}(1 + 0.952 \times \Gamma\, X_{tt}^{0.4126}) \tag{2.52}$$

Recently, Xu and Fang (2012) proposed a two phase frictional pressure drop correlation for evaporating two phase flow of refrigerants in horizontal pipe. Their correlation is based on 2622 data points of 14 refrigerants (R11, R12, R22, R134a, R32, R407C, R507, R507A, R410A, CO_2, R404A, R32/R125, R123 and Ammonia) for $0.8 < D_h < 19$ mm (circular and rectangular pipe geometries) and $25 < G < 1150$ kg/m^{2}s. They found that the pipe hydraulic diameter and gas-liquid interface surface tension affect the two phase frictional pressure drop significantly than any other two phase flow parameter and hence their correlation accounts for these two variable through the inclusion of non-dimensional Laplace number. The physical form of the correlation is as expressed in Eq. (2.53).

$$\Phi_{LO}^2 = \left[Y^2x^3 + (1-x)^{0.33}\left(1 + 2x(Y^2 - 1)\right)\right]\left(1 + 1.54(1-x)^{0.5}La\right) \tag{2.53}$$

In above equation Y is calculated from Eq. (2.35) while La is the Laplace number similar to that used by Wang et al. (2001). Their correlation is claimed to predict the two phase frictional pressure drop data with a mean absolute relative deviation of 25.2%. It should be noted that Xu and Fang (2012) recommends use of Fang et al. (2011) correlation to calculate single phase friction factor and hence the single phase liquid pressure drop required in Eq. (2.23). The correlation of Fang et al. (2011) for

single phase pressure drop is reported in Eq. (2.54).

$$f_{LO} = 0.25 \left[\log \left(\frac{150.39}{Re_{LO}^{0.98865}} - \frac{152.66}{Re_{LO}} \right) \right]^{-2} \tag{2.54}$$

Lim and Fujita (2002) developed a two phase frictional pressure drop correlation for the boiling two phase flow of refrigerants R123, R134a an their binary mixtures in a 10 mm I.D. stainless steel horizontal pipe. The empirical form of the correlation is shown in Eq. (2.55). The variable A_{Lim} is defined based on the two phase mixture mass flux as given in Eq. (2.56).

$$\Phi_{LO}^2 = \frac{0.36(0.6 + A_{Lim} Fr_{TP})^{1.3}}{Fr_{TP}^{0.51} We_{TP}^{-0.031}} X_{tt}^{0.15} \tag{2.55}$$

$$A_{Lim} = \begin{cases} -1.06 \log(G) + 7.04, & G \leq 300 \text{ kg/m}^2 s \\ 1260\ G^{-1.24}, & G > 300 \text{ kg/m}^2 s \end{cases} \tag{2.56}$$

The $Fr_{TP} = G^2/(gD\rho_{TP}^2)$ and $We_{TP} = (G^2 D)/(\sigma \rho_{TP})$ are the two phase Froude and Weber number, respectively. The two phase mixture density used in Fr_{TP} and We_{TP} is found from Eq. (2.5). The proposed correlation of Lim and Fujita (2002) is valid for both adiabatic and diabatic turbulent-turbulent two phase flows in horizontal pipe and is claimed to predict the two phase frictional pressure drop with a mean deviation of 20%. In case of diabatic flows, the two phase frictional multiplier may be integrated over the pipe length for given change in two phase flow quality. They also found that in case of diabatic two phase flow, the accelerational component of two phase pressure drop contributes up to 30% of the total pressure drop and hence cannot be neglected.

Yoon et al. (2004) presented a modified form of Chisholm (1973) correlation for two phase frictional multiplier. Their correlation was developed for boiling two phase flow of CO_2 in a 7.5 mm horizontal pipe and for $200 < G < 600$ kg/m^{2}s. In order to avoid dry spots on the pipe wall during boiling, in their experiments, the two phase flow quality was maintained below 0.7. They suggested that two phase frictional pressure drop is significantly affected by the gas-liquid interface surface tension and hence recommended use of Weber and Bond numbers. The correlation reported in Eq.(2.57) is claimed to predict the two phase frictional pressure drop data within $\pm 20\%$ error bands with an average error of 16.2%.

$$\Phi_{LO}^2 = 1 + 4.2(Y^2 - 1)\left(\frac{Bo}{We}x^{0.875}(1-x)^{0.875} + x^{1.75}\right) \tag{2.57}$$

The Weber number used in (2.57) is based on two phase mixture velocity and the gas phase density defined as $We = (\rho_g U_M^2 D)/\sigma$. The Bond number is to account for the balance between gravity and surface tension forces and is defined as $Bo = (g\Delta\rho D^2)/\sigma$.

Tran et al. (2000) proposed a two phase frictional multiplier pressure drop developed based on the data for R12, R134a and R113 in smooth tubes. The correlation is claimed to be applicable for system pressures less than 860 kPa. The physical structure of the correlation is as shown in Eq. (2.58) where Y is same as that defined by (2.35) and La is the Laplace number. This correlation is applicable for smooth tubes and R-12, R-113 and R-134a refrigerants and the system pressure, two phase quality and mass flux in a range of 130 to 900 kPa, 0 to 0.95 and 30 to 850 kg/m^{2}s, respectively. It should be noted that the correlation of Tran et al. (2000) is developed for boiling flow of refrigerants and pipe diameter of 2.4 and 2.92 mm, respectively.

$$\Phi_{LO}^2 = 1 + (4.3Y^2 - 1)\left(La \times x^{0.875}(1-x)^{0.875} + x^{1.75}\right) \tag{2.58}$$

Zhang et al. (2010) proposed a two phase frictional pressure drop correlation based on the experimental data for refrigerants, air-water, air-ethanol and air-water in horizontal and vertical upward mini and micro channels consisting of circular and rectangular pipe geometries with hydraulic diameter in a range of $0.4 \leq D_h \leq 4$ mm. They found that the HFM two phase frictional pressure drop correlations tend to fail and give poor accuracy for pipe diameters of mini and micro scale. The correlation of Zhang et al. (2010) is essentially a separated flow model and is similar to that of the Lockhart and Martinelli (1949) except that the variable is expressed as shown in Eq. (2.59). Using artificial neural network (ANN), they found that the two phase frictional pressure drop in small diameter pipes can be best correlated using non-dimensional Laplace constant.

$$C = 21(1 - \exp(-c_2/La)) \tag{2.59}$$

The constant c_2 is 0.142 and 0.674 for adiabatic vapor-liquid (one component two phase) and gas-liquid (two component two phase) flow, respectively. The Laplace number used in this equation is inverse of the Laplace number used by Xu and Fang (2012). Their correlation predicted the data of gas-liquid and vapor-liquid with an average mean deviation of 17.9% and 21.7%, respectively.

For horizontal two phase flow through non-circular (rectangular) channels, Lee and Lee (2001) proposed a set of variables to replace Chisholm (1967) constant used in Lockhart and Martinelli (1949) correlation. Their correlation is based on 305 data points with hydraulic diameters in a range of 0.4 to 5.5 mm, $0.3 < X < 80$ and $170 < Re_{LO} < 17700$. The set of equations each for laminar-laminar, laminar-turbulent, turbulent-laminar and turbulent-turbulent flows to calculate C value are as shown in Table 2.5.

Hwang and Kim (2006) developed a correlation for micro scale two phase flow of R134a with pipe diameters in a range of 0.2 to 0.8 mm. Their correlation given

Table 2.5: Lee and Lee (2001) correlation for different flow regimes.

Flow regime		C
Liquid	Gas	
Laminar	Laminar	$6.833 \times 10^{-8} Su_{LO}^{1.317} Ca^{0.719} Re_{LO}^{0.557}$
Laminar	Turbulent	$6.185 \times 10^{-2} Re_{LO}^{0.726}$
Turbulent	Laminar	$3.627 \times Re_{LO}^{0.174}$
Turbulent	Turbulent	$0.408 \times Re_{LO}^{0.451}$

by Eq. (2.60) provides an expression to replace Chisholm (1967) parameter used in Lockhart and Martinelli (1949) correlation and is claimed to predict the two phase frictional pressure drop with an absolute average deviation of 8.9%. The Confinement number used in Eq. (2.60) is essentially equivalent to the Bond number such that $N_{conf} = 1/\sqrt{Bo}$.

$$C = 0.227 Re_{LO}^{0.452} X^{-0.32} N_{conf}^{-0.82} \tag{2.60}$$

Recently, Kim and Mudawar (2012) proposed a correlation for mini-micro scale adiabatic and condensing two phase flow. Their correlation provides an expression to model the Chisholm (1967) correlation used in Lockhart and Martinelli (1949) correlation. The correlation of Kim and Mudawar (2012) for C parameter is in terms of Reynolds number, Suratman number and the phase density ratio as shown in Table 2.6. The Suratman number used in Kim and Mudawar (2012) correlation is the ratio of square of gas only Reynolds number to Weber number defined as $Su = Re_{GO}^2/We = (\rho_G \sigma D_h)/\mu_G^2$.

Table 2.6: Constants used in Kim and Mudawar (2012) correlation.

Flow regime		C
Liquid	Gas	
Laminar	Laminar	$3.5 \times 10^{-5} Su_{GO}^{0.5}\ Re_{LO}^{0.44}\ (\rho_L/\rho_G)^{0.48}$
Laminar	Turbulent	$0.0015 \times Su_{GO}^{0.19}\ Re_{LO}^{0.59}\ (\rho_L/\rho_G)^{0.36}$
Turbulent	Laminar	$8.7 \times 10^{-4} Su_{GO}^{0.5}\ Re_{LO}^{0.17}\ (\rho_L/\rho_G)^{0.14}$
Turbulent	Turbulent	$0.39 \times Su_{GO}^{0.1}\ Re_{LO}^{0.03}\ (\rho_L/\rho_G)^{0.35}$

2.3.3 Correlations based on Two Phase Friction Factor

These types of correlations provide an expression for two phase friction factor which can be used to find the frictional component of the two phase pressure drop. In comparison to HFM and SFM types of correlations, there are very few two phase friction factor correlations available in the literature.

Wisman (1975) developed a correlation to predict two phase friction factor and hence the frictional pressure drop. He used the Dukler et al. (1964) correlation for two phase friction factor of the form shown in Eq. (2.61).

$$f_{TP} = 0.00560 + \frac{0.5}{Re_{TP}^{0.32}} \tag{2.61}$$

The two phase mixture Reynolds number used in Eq. (2.61) is defined by Eq. (2.62).

$$Re_{TP} = \frac{\rho_L U_{SL} D}{\mu_L}(1-\alpha)(1-\sqrt{\alpha})\left[1 + \frac{\alpha}{1-\alpha}\frac{\rho_G}{\rho_L}\left(\frac{U_G}{U_L}\right)^2\right] \tag{2.62}$$

Finally, the two phase frictional pressure drop is found using Eq. (2.63).

$$\left(\frac{dP}{dL}\right)_{f,TP} = \frac{f_{TP}}{1-0.5\alpha f_{TP}}\frac{(1-\alpha)\rho_L U_L^2}{2D}\left[1 + \frac{\alpha}{1-\alpha}\frac{\rho_G}{\rho_L}\left(\frac{U_G}{U_L}\right)^2 + \alpha\frac{\Delta\rho g D}{\rho_L U_L^2}\right] \tag{2.63}$$

Wisman (1975) verified his correlation against 236 experimental data points consisting of pipe diameters in a range of 25.4 to 115 mm and found his correlation to predict 68% of the frictional pressure drop data within 28.2% error band and with a mean deviation of 1.7%. He suggested that this correlation may not be used for $\alpha > 0.9$ since in this region the pressure drop is strongly influenced by the gas shear and the flow patterns enter the annular-mist flow regime.

Lombardi and Carsana (1992) proposed an empirical correlation to predict two phase friction factor expressed by Eq. (2.64) where f_L and f_G are determined using Blasius (1913) for laminar flow based on the phase superficial Reynolds number. For $Re_{SL} > 2400$ and $Re_{SG} > 2400$ the friction factor for individual phase is expressed by Eq. (2.65).

$$f_{TP} = (f_G b_G + f_L b_L + f_M b_M) \tag{2.64}$$

$$f_j = \frac{1}{\left(3.8 \ln\left(\frac{10}{Re_j} + 0.2\frac{\epsilon}{D}\right)\right)^2} \tag{2.65}$$

To calculate f_M, Lombardi and Carsana (1992) proposed the following equations. The variable Ce is defined as a function of pipe diameter, phase dynamic viscosity, liquid density and gas-liquid interface surface tension expressed by Eq. (2.66).

$$Ce = \rho_L g \frac{(D - 0.001)^2}{\sigma}\left(\frac{\mu_G}{\mu_L}\right) \tag{2.66}$$

It is evident from this equation that for $D = 0.001$ m, $Ce = 0$. They proposed that for all $D \leq 0.001$ m, $Ce = 0$. The next constraint is applied on f_m in terms of a variable Lo as shown in Eq. (2.67).

$$f_M = \begin{cases} 0.046 Lo^{-0.25}, & Lo > 30Ce \\ 0.046 Ce Lo^{-0.25}, & Lo \leq 30Ce \end{cases} \tag{2.67}$$

The dimensionless variable Lo is defined as $Lo = \left((G^2 D)/(\rho_M \sigma)\right)\sqrt{\mu_G/\mu_L}$. The terms b_G, b_L and b_M are defined by Eqs. (2.68) to (2.70).

$$b_G = x^{[600(\rho_G/\rho_L)]} \tag{2.68}$$

$$b_L = (1 - x)^{[2(\rho_L/\rho_G)]} \tag{2.69}$$

$$b_M = 1 - b_L - b_G \tag{2.70}$$

The correlation is developed for vertical upward flow accounting for both adiabatic and diabetic flow conditions and its performance is verified against a data set of 10,971 data points consisting of the pipe diameters in a range of 0.005 to 0.5 m I.D., pressure range of 2 to 90 bars and set of different fluid combinations.

Shannak (2008) proposed a correlation for two phase friction factor (Darcy) based on the experimental data for both boiling and non-boiling flows and for varying pipe roughness. His correlation is based on modified definition of two phase Reynolds number expressed in terms of two phase density and two phase dynamic viscosity. The two phase Reynolds number is defined by Eq. (2.71).

$$Re_{TP} = \frac{GD\left(x^2 + (1-x^2)\frac{\rho_G}{\rho_L}\right)}{\mu_G x + \mu_L(1-x)\frac{\rho_G}{\rho_L}} \tag{2.71}$$

The two phase friction factor given by Chen (1979) is redefined in terms of two phase mixture Reynolds number as shown in Eq. (2.72).

$$\frac{1}{\sqrt{f_{TP}}} = -2\log\left[\frac{1}{3.7065}\frac{\epsilon}{D} - \frac{5.0452}{Re_{TP}}\log\left(\frac{1}{2.2857}\left(\frac{\epsilon}{D}\right)^{1.1098} + \frac{5.8506}{Re_{TP}^{0.8981}}\right)\right] \tag{2.72}$$

This correlation is claimed to have been tested against a comprehensive data set of 16000 data points and is valid for $0 < x < 1$ and system pressure of upto 14 bars. The correlation is valid for a mass flux range of 200 to 1500 kg/m^{2}s and is claimed to predict 80% of data with a standard deviation of $\pm 35\%$.

Recently, Cioncolini et al. (2009) developed a two phase friction factor (Fanning) correlation exclusively applicable for annular flow and pipe diameters covering both micro and macro channels. They found that the two phase friction factor in annular flow regime is a function of core Weber number and the liquid phase Reynolds number.

The two phase friction factor of Cioncolini et al. (2009) is expressed by Eq. (2.73).

$$f_{TP} = \begin{cases} 0.172We_c^{-0.372}, & D > 3 \text{ mm (Macro channels)} \\ 0.0196We_c^{-0.372}Re_L^{0.318}, & D \leq 3 \text{ mm (Micro channels)} \end{cases} \tag{2.73}$$

The core Weber number (We_c) and the liquid phase Reynolds number (Re_L) are defined by accounting for the liquid entrainment fraction (E) from the liquid film to the gas core and are expressed as $We_c = (G_c^2 D_c)/(\sigma\rho_c)$ and $Re_L = (1-E)(1-x)GD/\mu_L$. The core mass flux and the core diameter required in definition of We_c is defined by Eqs. (2.74) and (2.75). The droplet laden gas core density is define as $\rho_c = (1-\alpha_c)\rho_L + \alpha_c\rho_G$ where the droplet laden gas core void fraction is defined by Eq. (2.76).

$$G_c = \frac{4}{\pi}\frac{[x + E(1-x)]\,\dot{m}}{D_c^2} \tag{2.74}$$

$$D_c = D\sqrt{\alpha + E\left(\frac{\alpha}{1-\alpha}\frac{1-x}{x}\frac{\rho_G}{\rho_L}\right) - \alpha\left(E\frac{\alpha}{1-\alpha}\frac{1-x}{x}\frac{\rho_G}{\rho_L}\right)} \tag{2.75}$$

$$\alpha_c = \frac{\alpha}{\alpha + (1-\alpha)\left(E\frac{\alpha}{1-\alpha}\frac{1-x}{x}\frac{\rho_G}{\rho_L}\right)} \tag{2.76}$$

The void fraction and liquid entrainment fraction (E) required in Eq. (2.75) is found using Woldesemayat and Ghajar (2007) and Oliemans et al. (1986) correlations, respectively. The performance of Cioncolini et al. (2009) correlation is verified against a data bank of 3908 points consisting of different fluid combinations such as air-water, steam-water, argon-water, nitrogen-water, argon-alcohol, R134a and R245fa, twenty two pipe diameters ($0.51 \leq D \leq 31.7$ mm) and system pressure in a range of 0.1 to 9.4 MPa.

2.4 Void Fraction Models

As seen in Eqs. (2.15) and (2.20), the accurate knowledge of void fraction is required in calculation of two phase mixture density and hence the hydrostatic component of two phase pressure drop. Thus, it is required to take a look at the void fraction correlations available in the two phase flow literature. Two phase literature provides a large number of void fraction correlations essentially based on the concept of drift flux model (DFM) and separated flow model (SFM).

2.4.1 Drift Flux Model (DFM)

The drift flux model (DFM) correlations assumes one phase dispersed in other continuous phase and requires the determination of distribution parameter and drift velocity as variables to calculate void fraction. The flow patterns such as bubbly flow, slug flow and mist flow are the preferred flow patterns to be modeled using the concept of drift flux. The general form of drift flux model to calculate void fraction is presented by Eq. (2.77) where, C_o and U_{GM} are the distribution parameter and drift velocity, respectively. The concept of drift flux model will be revisited in detail in Chapter V. Following is the brief summary of some of the top performing void fraction correlations based on the concept of drift flux model (DFM).

$$\alpha = \frac{U_{SG}}{C_o U_M + U_{GM}} \tag{2.77}$$

One of the most widely used DFM void fraction correlation in the refrigeration industry is that of Rouhani and Axelsson (1970). Their correlation proposes two different forms of distribution parameter for vertical and horizontal two phase flows.

For vertical two phase flow, the distribution parameter is expressed by Eq. (2.78).

$$C_o = \begin{cases} 1 + 0.2(1-x)(gD\rho_L^2/G^2)^{0.25} & \alpha \leq 0.1 \\ 1 + 0.2(1-x), & \alpha > 0.1 \end{cases} \tag{2.78}$$

For horizontal flow, the distribution parameter of Rouhani and Axelsson (1970) correlation is presented by Eq. (2.79) while the drift velocity using Rouhani and Axelsson (1970) correlation is calculated from Eq. (2.80) for both vertical and horizontal pipe orientations.

$$C_o = 1 + 0.12(1-x) \tag{2.79}$$

$$U_{GM} = 1.18 \left(g\sigma\Delta\rho/\rho_L^2\right)^{0.25} \tag{2.80}$$

The correlation of Rouhani and Axelsson (1970) is essentially developed for steam-water two phase flow having system pressure in a range of 2 to 14 MPa and circular, rectangular, annular and rod bundle pipe geometries. The accuracy and statistical performance of their correlation is not reported by authors.

Shipley (1982) developed a void fraction model for large diameter pipes by using a constant of 1.2 for distribution parameter. The drift velocity is defined as a function of pipe diameter, void fraction and phase superficial velocities as shown in Eq. (2.81).

$$U_{GM} = 0.24 + 0.35(U_{SG}/U_M)^2\sqrt{gD\alpha} \tag{2.81}$$

The correlation of Shipley (1982) is specific to bubbly flow pattern and is developed based on the air-war water fluid combination data in a 457 mm I.D. vertical pipe and is also verified against the data of Hills (1976) for 150 mm I.D. vertical pipe. However, the author has not reported the accuracy and statistical performance of his correlation.

Clark and Flemmer (1985) proposed a correlation to predict void fraction in vertical upward flow typically in bubbly flow regime ($0 < \alpha \leq 0.3$). Their correlation was developed based on the air-water data in large diameter pipe typically $D \geq 50\,\text{mm}$. The physical form of distribution parameter and drift velocity is reported in Eqs. (2.82) and (2.83).

$$C_o = 0.942(1 + 1.42\alpha) \tag{2.82}$$

$$U_{GM} = 1.53\left(g\sigma\Delta\rho/\rho_L^2\right)^{0.25} \tag{2.83}$$

Mishima and Hibiki (1996) proposed a void fraction correlation for two phase flow of air-water through pipe diameters in a range of $1 \leq D \leq 4$mm. They suggested that for small diameter pipes, the drift velocity is very small and hence can be neglected. They further recommended that the distribution parameter be modeled as function of pipe diameter only as shown in Eq. (2.84). The accuracy and statistical performance of this correlation for the large diameter pipes is not reported by the authors.

$$C_o = 1.2 + 0.51\ \exp(-0.691(D/1000)) \tag{2.84}$$

Zhang et al. (2010) modified the correlation of Mishima and Hibiki (1996) for the data of air-water and pipe diameters in a range of 0.2 to 4.9 mm and system pressure close to atmospheric pressure. Their correlation is as shown in Eq. (2.85) where La is the Laplace variable. Their correlation is claimed to be applicable for $Re_{SL} \leq 1000$ and $Re_{SG} \leq 1000$ for air-water two phase flow.

$$C_o = 1.2 + 0.38\exp(-1.39/La) \tag{2.85}$$

Similar to Mishima and Hibiki (1996), Zhang et al. (2010) assumed that the drift velocity in small diameter pipes typically D< 4mm is negligible.

Kataoka and Ishii (1987) proposed a void fraction correlation for large diameter pipes and different values of liquid phase dynamic viscosity. The equation for distribution parameter is same as that of Hibiki and Ishii (2003) for slug flow. Whereas, the drift velocity is expressed by Eq. (2.86) for two different ranges of viscosity number ($N_{\mu L}$).

$$U_{GM} = \begin{cases} 0.03 \left(\frac{\rho_L}{\rho_G}\right)^{0.157} \left(\frac{g\sigma\Delta\rho}{\rho_L^2}\right)^{0.25} N_{\mu L}^{-0.562}, & \text{for } N_{\mu L} \leq 0.00225 \\ 0.92 \left(\frac{\rho_L}{\rho_G}\right)^{0.157} \left(\frac{g\sigma\Delta\rho}{\rho_L^2}\right)^{0.25}, & \text{for } N_{\mu L} > 0.00225 \end{cases} \tag{2.86}$$

The viscosity number is defined as $N_{\mu L} = \dfrac{\mu_L}{(\rho_L \sigma \sqrt{(\sigma/g\Delta\rho)})^{0.5}}$. Their correlation is developed based on air-water and steam-water two phase flow data and is claimed to predict void fraction within ±20% error bands for pipe diameters in a range of 10 to 600 mm and system pressure in a range of 0.1 to 18.2 MPa.

Gomez et al. (2000) developed a void fraction model for bubbly flow in horizontal to vertical upward inclined pipe orientations. The distribution parameter was assigned a constant value of 1.15 ($C_o = 1.15$) while the drift velocity was defined as shown in Eq. (2.87). The accuracy of this correlation was validated against limited data of air-kerosene, air-water and natural gas-oil with pipe diameters in a range of 50 to 100 mm. The correlation is claimed to predict void fraction with an absolute average error of 2.7%.

$$U_{GM} = 1.53 \left(g\sigma\Delta\rho/\rho_L^2\right)^{0.25} \sqrt{1-\alpha} \sin\theta \tag{2.87}$$

Hibiki and Ishii (2003) presented a flow pattern specific DFM void fraction correlation for bubbly, slug and annular flow regimes. The distribution parameter and drift velocity expressions for Hibiki and Ishii (2003) are shown in Eqs. (2.88) and

(2.89).

$$C_o = \begin{cases} 1.2 - 0.2\sqrt{\rho_G/\rho_L}(1 - exp(-18\alpha)), & \text{Bubbly flow} \\ 1.2 - 0.2\sqrt{\rho_G/\rho_L}, & \text{Slug flow} \\ 1 + (1-\alpha)/(\alpha + 4\sqrt{\rho_G/\rho_L}, & \text{Annular flow} \end{cases} \tag{2.88}$$

$$U_{GM} = \begin{cases} 1.41(g\sigma\Delta\rho/\rho_L^2)^{0.25}(1-\alpha)^{1.75}, & \text{Bubbly flow} \\ 0.35\sqrt{gD\Delta\rho/\rho_L}, & \text{Slug flow} \\ (1-\alpha)/\left(\alpha + 4\dfrac{\sqrt{\rho_G/\rho_L}(\sqrt{gD\Delta\rho(1-\alpha)})}{0.015\rho_G}\right), & \text{Annular flow} \end{cases} \tag{2.89}$$

Instead of the comparison between predicted and measured values of void fraction, the authors verified the performance of these correlations by comparing the predicted and measured values of C_o and U_{GM} for data measured in 24.4 and 50.8 mm I.D. vertical pipes using air-water fluid combination. They found the predicted values of drift velocity to be within ±30% error bands.

Sun et al. (1981) proposed a DFM void fraction correlation and expressed the distribution parameter as a function of system pressure and critical pressure of the given liquid phase as shown in Eq. (2.90). The drift velocity is expressed using Eq. (2.89) for bubbly flow.

$$C_o = (0.82 + 0.18P_{SYS}/P_{CRIT})^{-1} \tag{2.90}$$

Woldesemayat and Ghajar (2007) analyzed 68 void fraction correlations for the void fraction data in horizontal and upward inclined two phase flow. They proposed a flow pattern independent void fraction correlation based on drift flux model. The

distribution parameter is defined as a function of phase superficial velocities and the phase densities as shown in Eq. (2.91) while the drift velocity is expressed as a function of fluid thermo-physical properties, pipe orientation, pipe diameter and the system pressure as expressed by Eq. (2.92). Please note that the multiplier of 2.9 in Eq. (2.92) carries units of $\mathrm{m}^{-0.25}$.

$$C_o = \frac{U_{SG}}{U_M}\left[1 + \left(\frac{U_{SL}}{U_{SG}}\right)\left(\frac{\rho_G}{\rho_L}\right)^{0.1}\right] \tag{2.91}$$

$$U_{GM} = 2.9\left(\frac{gD\sigma(1+\cos\theta)(\rho_L-\rho_G)}{\rho_L^2}\right)^{0.25}(1.22+1.22\sin\theta)^{P_{ATM}/P_{SYS}} \tag{2.92}$$

The correlation of Woldesemayat and Ghajar (2007) is essentially a modification of Dix (1971) correlation and is based on 2845 data points comprising of air-water and air-kerosene fluid combinations. Woldesemayat and Ghajar (2007) correlation is claimed to predict 85.6% of data points within ±15% error bands.

Choi et al. (2012) proposed a DFM based correlation to predict void fraction in inclined two phase flows. The distribution parameter defined by Eq. (2.93) is expressed in terms of two phase Reynolds number and by including the distribution parameter equation of Hibiki and Ishii (2003) for bubbly flow.

$$C_o = \frac{2}{1+(Re_{TP}/1000)^2} + \frac{1.2-0.2\sqrt{\rho_G/\rho_L}(1-\exp(-18\alpha))}{1+(1000/Re_{TP})^2} \tag{2.93}$$

$$U_{GM} = 0.0246\ \cos\theta + 1.606\left(\frac{g\sigma(\rho_L-\rho_G)}{\rho_L^2}\right)^{0.25}\sin\theta \tag{2.94}$$

The correlation of Choi et al. (2012) given by Eqs. (2.93) and (2.94) is verified against 779 data points consisting of pipe diameters in a range of 20 to 150 mm, the liquid dynamic viscosity in a range of 0.001 to 0.6 Pa-s and pipe orientations in a range of $-30^o \leq \theta \leq 90^o$. Their correlation is claimed to predict the void fraction with mean

absolute error of 0.096 and standard deviation of 0.057. Another comprehensive drift flux model based void fraction correlation available in the literature is that of Chexal et al. (1992) that models the distribution parameter and the drift velocity as a function of several two phase flow variables. Their correlation consists of several empirical curve fitted parameters for each fluid combination and hence is very complex for practical applications. Although this correlation is independent of flow patterns, it needs the fluid combination as input to the computer program. The correlation of Chexal et al. (1992) is designed to accept fluid combinations of air-water, steam-water and refrigerants as input and hence may not be used for other fluid combinations. Moreover, their correlation does not show any evidence of its application for high viscosity liquids. The physical form of Chexal et al. (1992) correlation is intricate and hence it is advised to refer to the original paper of Chexal et al. (1992) for more details.

2.4.2 Separated Flow Model (SFM)

The separated flow model is based on the assumption that the two phases flow separately with different velocities and share a definite interface. The flow patterns such as stratified and annular flow behave as a separated flow and can be effectively modeled using these types of correlations. The SFM based correlations are mostly preferred in refrigeration industry due to the stratified and annular flow pattern dominated two phase flow in evaporators and condensers. The general form of separated flow model is reported in Eq. (2.95). Some of the top performing void fraction correlations based on separated flow model are listed in Table 2.7.

$$\alpha = \left[1 + s\left(\frac{1-x}{x}\right)^{o}\left(\frac{\rho_G}{\rho_L}\right)^{q}\left(\frac{\mu_L}{\mu_G}\right)^{r}\right]^{-1} \tag{2.95}$$

The homogeneous flow model listed in Table 2.7 assumes no slip between the two

Table 2.7: Parameters used in separated flow model for different void fraction correlations.

Correlation	s	o	q	r
Homogeneous model	1	1	1	0
Lockhart and Martinelli (1949)	0.28	0.64	0.36	0.07
Zivi (1964)	1	1	0.67	0
Thom (1964)	1	1	0.89	0.18
Turner and Wallis (1965)	1	0.72	0.40	0.08
Barcozy (1966)	1	0.74	0.65	0.13
Smith (1969)	Eq. (2.96)	1	1	0
Permoli et al. (1971)	Eq. (2.97)	1	1	0
Chen (1986)	0.18	0.6	0.33	0.07
Xu and Fang (2014)	Eq. (2.98)	1	1	0

phases and do not consider the effect of liquid and gas dynamic viscosity on the void fraction. After some rearrangement of the terms in homogeneous flow model it can be easily shown that the void fraction calculated assuming no slip between the two phases is essentially equal to the gas volumetric flow fraction. Eq. (2.96) for s by

Smith (1969) captures the effect of phase density ratio and the two phase quality while Eq. (2.97) considers the effect of phase density ratio, liquid phase Reynolds number (Re_{LO}) and liquid phase Weber number (We_{LO}) on the value of s where $y = ((1/x - 1)(\rho_G/\rho_L))^{-1}$ and $F_1 = 0.0273 We_{LO} Re_{LO}^{-0.51} (\rho_L/\rho_G)^{-0.08}$.

$$s = 0.4 + 0.6\sqrt{\frac{(\rho_L/\rho_G) + 0.4(1/x - 1)}{1 + 0.4(1/x - 1)}} \tag{2.96}$$

$$s = 1 + 1.578 Re_{LO}^{-0.19} \left(\frac{\rho_L}{\rho_G}\right)^{0.22} \left[\frac{y}{1 + yF_1} - yF_1\right] \tag{2.97}$$

The liquid phase Reynolds number and Weber numbers are based on the two phase mixture mass flux and single phase liquid thermo-physical properties defined as $Re_{LO} = GD/\mu_L$ and $We_{LO} = (G^2 D/\sigma\rho_L)$. Eq. (2.98) for '$s$' proposed by Xu and Fang (2014) is based on the liquid phase Froude number (Fr_{LO}) and the gas volumetric flow fraction (β).

$$s = 1 + 2 Fr_{LO}^{-0.2} \beta^{3.5} \tag{2.98}$$

The correlation of Chen (1986) is based on the experimental data of air-water and steam-water for annular flow regime consisting of the system pressure in a range of 0.1 to 6 MPa. He illustrated the performance of his correlation graphically without reporting any statistical performance. Smith (1969) correlation is based on the experimental data base of air-water (D = 11 mm) and steam-water ($6 \leq D \leq$38 mm) fluid combinations and is claimed to be valid for system pressures in a range of 0.1 to 5.9 MPa and mass flux in a range of 50 to 2050 kg/m^{2}s. Smith (1969) reported the validity of the value of 0.4 used in Eq. (2.96) for circular pipes and recommended further investigation for its accuracy in case of rectangular and annular pipe geometries. The recent correlation of Xu and Fang (2014) is based on 1574 data

of refrigerants and hydraulic pipe diameters in a range of 0.5 to 10 mm. The authors reported that their correlation can be used for $0 \leq x \leq 1$, $0.02 \leq Fr_{LO} \leq 145$ and $0.004 \leq \rho_G/\rho_L \leq 0.153$.

In addition to DFM and SFM types of correlation, the correlation of Cioncolini and Thome (2012a) based on Hill (1910) function is also considered in this study. The correlation of Cioncolini and Thome (2012a) is presented in Eq. (2.99) where $h = -2.129 + 3.129(\rho_G/\rho_L)^{-0.2186}$ and $a = 0.3487 + 0.6513(\rho_G/\rho_L)^{0.515}$.

$$\alpha = \frac{hx^a}{1 + (h-1)x^a} \tag{2.99}$$

Their correlation is developed for annular flow and is based on a comprehensive data base of 2673 data points consisting of 8 different fluid combinations and pipe diameters in a range of 1 to 45 mm. The performance of Cioncolini and Thome (2012a) correlation is validated against data consisting of system pressure in a range of 0.1 to 9 MPa and is valid for $\alpha \geq 0.7$. Their correlation is claimed to predict about 98% of data points in annular flow regime within $\pm 10\%$ error bands.

2.5 Chapter Summary

A review of previous experimental work, flow pattern maps and different methods of calculation of two phase frictional pressure drop i.e., homogeneous and separated flow models is presented in this chapter. Likewise, the void fraction correlations based on drift flux and separated flow models are discussed. It is found that the there are very limited void fraction correlations available in the literature applicable for a wide range of two phase flow conditions. It is found that most of the two phase pressure drop correlations available in the literature are developed for the flow of air-water data and refrigerants in horizontal two phase flow. Thus, there is room for further development of flow pattern independent void fraction and two phase frictional pressure drop correlations applicable for a wide range of two phase flow conditions.

CHAPTER III

EXPERIMENTAL SETUP

As mentioned earlier in Chapter I, a plethora of experimental data on void fraction and two phase pressure drop is available in the literature. However, it is found that majority of this data is limited to certain pipe orientations e.g., vertical upward and horizontal and certain flow patterns e.g., the annular flow regime. In order to understand the phenomenon and physics of void fraction and pressure drop in two phase flow and study its dependency on various flow parameters it is necessary to experimentally measure void fraction and pressure drop for different flow patterns and pipe orientations. The experimental work in this study intends to complement the two phase flow data available in the literature and aid to analyze the behavior of void fraction and two phase pressure drop with varying flow patterns and pipe orientations.

3.1 Details of Experimental Setup

The experimental setup (0.5" I.D.) used in the present study consists of two test sections; a 12.7 mm I.D. polycarbonate transparent pipe section and a 12.5 mm I.D. stainless steel pipe. This experimental setup constructed by Cook (2008), is capable of flow visualization and measurement of void fraction, phase pressure drop and heat transfer in non-boiling two phase flow. The experimental setup is mounted on a variable inclination frame (made up of rectangular steel tubings) with the help

of pulleys and bolts and thus making it flexible to be rotated from $+90^o$ to -90^o including the horizontal orientation. The test section of 12.7 mm I.D. transparent polycarbonate pipe is used for flow visualization, void fraction and pressure drop measurements while 12.5 mm I.D. stainless steel pipe having a surface roughness of 0.02 mm is used for pressure drop and heat transfer measurements. The experimental setup and variable inclination frame is shown in Figs. 3.1 and 3.2.

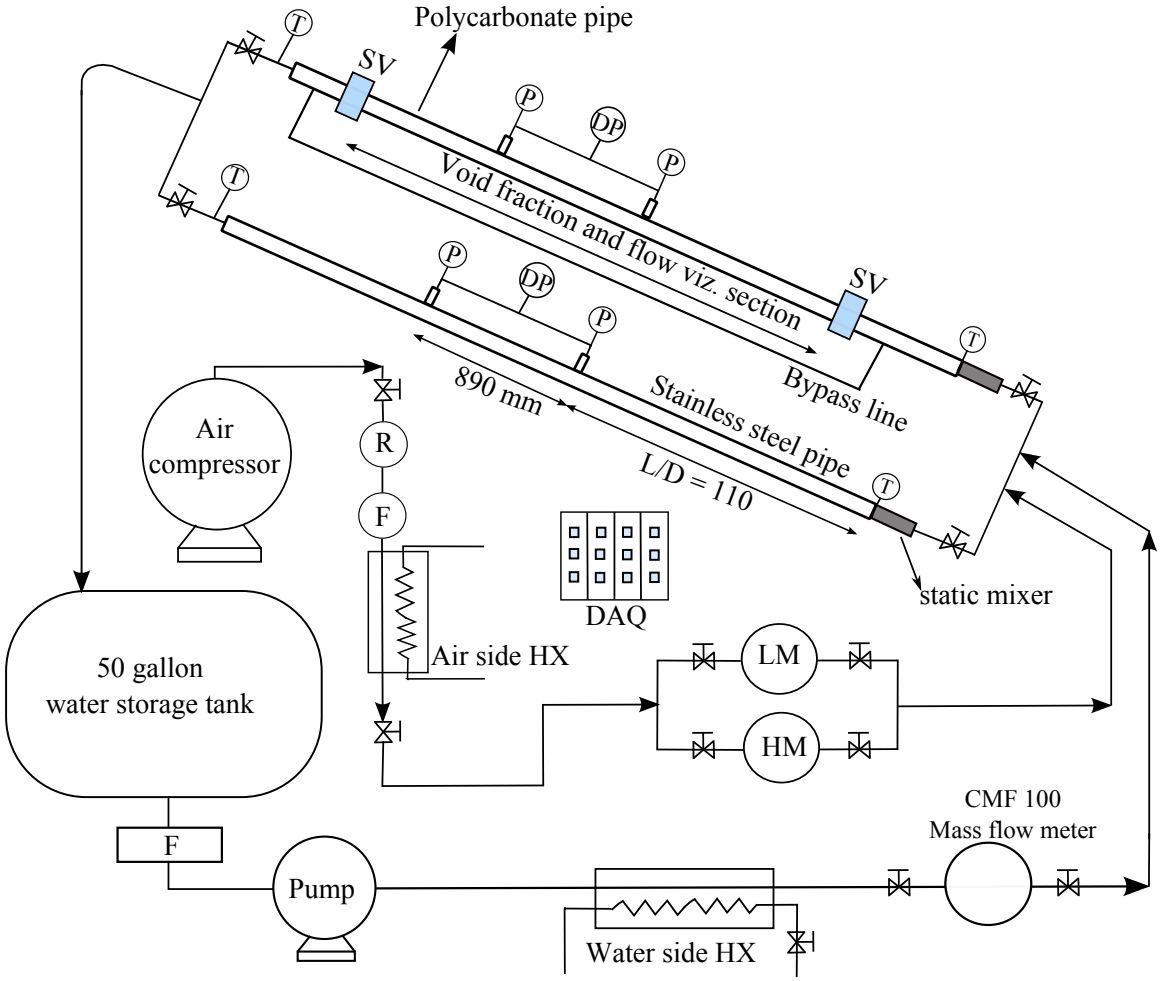

P: Pressure gauge	F: Air filter, Water filter
DP: Differential pressure transducer	LM: Low mass flow meter (air side)
T: Thermocouple probe	HM: High mass flow meter (air side)
SV: Solenoid valve	DAQ: Data acquisition system
R: Pressure regulator	HX: Heat exchanger

Figure 3.1: Schematic of the experimental setup used for flow visualization and void fraction and pressure drop measurements.

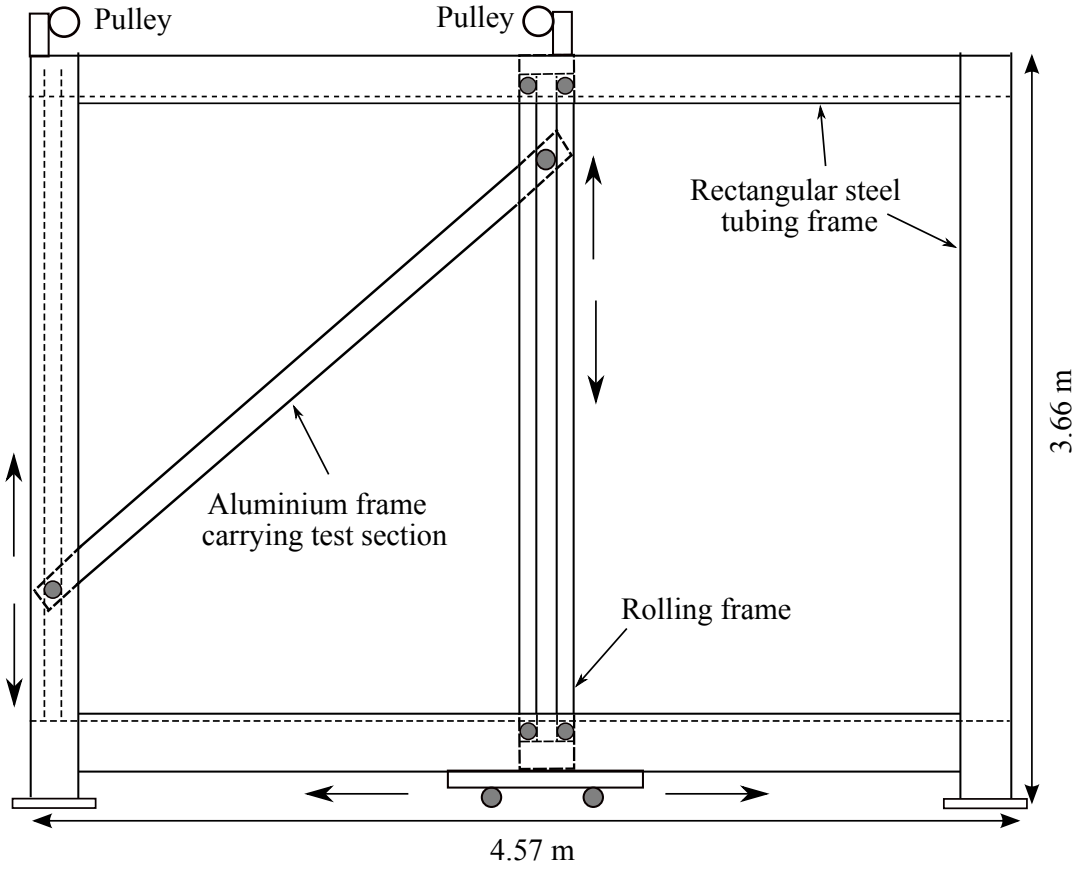

Figure 3.2: Schematic of variable inclination frame carrying test section.

Water Flow Circuit: The liquid phase used in this study is distilled water supplied by ATRC lab at Oklahoma State University. The water stored in a 55 gallon (208 liter) polyethylene tank is pumped by a centrifugal pump of Bell and Gosset (series 1535, model number 3445 D10) and filtered through an Aqua-Pure AP12-T purifier before it is passed through an ITT model BCF 4063 one shell and two tube pass heat exchanger. The heat exchanger is necessary to remove heat generated due to pipe wall friction and maintain a constant liquid inlet temperature during the experiment. The water then flows through an Emerson (Micro Motion Elite Series model number CMF 100) Coriolis mass flow meter and then allowed to mix with air in a static mixer. The CMF 100 mass flow meter along with a gate control valve allows to regulate the mass flow rate in a range of 0.25 kg/min to 40 kg/min. The water then mixes with air as it passes through one of the test sections and then returned

to the storage tank.

Air Flow Circuit: Compressed air supplied by Ingersoll-Rand T-30 Model 2545 industrial air compressor is used as gas phase in this two phase flow experimentation. The maximum pressure attained by this compressor is around 125 psi (850 kPa). The compressed air is then passed through a 200 psi pressure Speedaire (model 4ZM22) regulator and Speedaire filter/drier unit (model 4ZL49) and fetched to the submerged copper coil heat exchanger to maintain the compressed air at room temperature. The filter/drier unit serves to remove any dust/foreign particles present in air and also controls the unwanted condensation developed in the compressed air. The cooling fluid used for submerged copper coil is same as that used for water side heat exchanger and hence it is ensured that inlet air is at the same temperature as that of liquid. It is then again passed through air filter/drier unit and then through the Emerson flow meter (Mocro Motion Elite Series Model number LMF 3M and CMF 025) using a Parker (24NS 82(A)-8LN-SS) needle valve. The needle valve provides precise control over the mass flow rate necessary for generation of certain flow patterns. The Corilois mass flow meters give an accuracy of up to $\pm 0.05\%$ and $\pm 0.2\%$ of measured liquid and gas flow rates, respectively. On air side LMF 3M is the low mass flow meter capable of generating a minimum and maximum mass flow rate of 0.001 kg/min and 0.007 kg/min, respectively. Whereas, CMF 025 mass flow meter can handle air flow rates in a range of 0.01 kg/min to 0.25 kg/min. The air is finally directed to the mixing section where it is thoroughly mixed with distilled water using a Koflo model 3/8-40C-4-3V-23/8 static spiral mixer before entering the test section.

Test Section: As mentioned earlier the two test sections constructed for this experimental setup consists of 12.7 mm I.D. and 12.5 mm I.D. pipes made up of polycarbonate and 40 IPS alloy 304 stainless steel material ($\epsilon = 0.02$ mm), respectively.

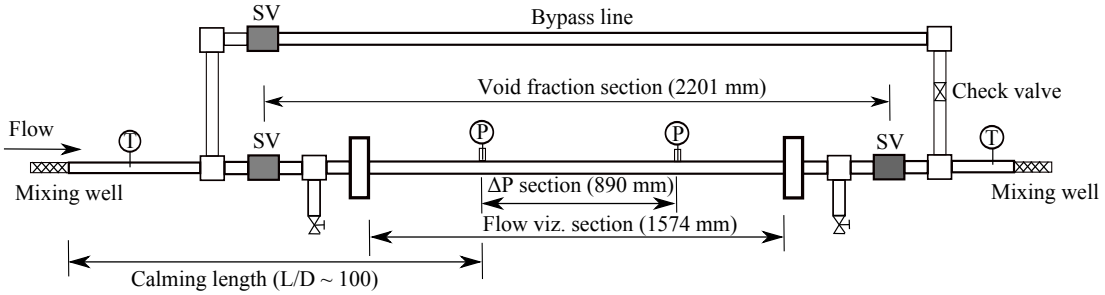

Figure 3.3: Dimensional details for flow visualization and void fraction sections.

A Kolflo Model 3/8-40C-4-3-3V-2 3 vane static mixer is placed at the beginning of the test section to ensure enhanced mixing of the two phases. The static mixer is immediately followed by a TMQSS-062U-6 thermocouple probe with an accuracy of $\pm 0.1^oC$ inserted from the pipe wall to measure the inlet and exit bulk temperature. The thermocouple probes are inserted such that it almost touches the other end of pipe to ensure that the probe is always in contact with two phase mixture. As shown in Fig. 3.3, the 1574 mm long transparent polycarbonate pipe is used for flow visualization and 2201 mm long section for void fraction measurements. Additionally, a 890 mm long test section in the void fraction section is used for pressure drop measurement. A bypass line is also connected to this section to redirect the two phase flow during void fraction measurement. The void fraction measurement technique and procedure is documented in next section. Similar to polycarbonate test section, the upstream and downstream pressure taps in stainless steel section are located at a distance of 890 mm. The system pressure is measured by using Omega PX242-060G absolute pressure transducer connected at the upstream and downstream pressure taps. The average of these two absolute pressures is taken as a representative of the system pressure. The distance between the two phase mixture inlet and the first pressure tap, also known as calming length is $\approx 100D$ for polycarbonate test section and $\approx 110D$ for stainless steel test section. A calming length in two phase flow experiments is required for the flow to attend fully developed conditions. The term fully developed flow in context to two phase flow refers to a flow situation in which the physical

alignment of one phase with respect to other do no change appreciably along the downstream direction. Two phase flow literature do no report any consensus over the exact calming length for different flow patterns, however, the calming length reported in the literature is anywhere between L = 40D to L = 300D. The calming length used in this experimental work is compared with some of the experimental setups reported in the literature and is documented in Table 3.1.

Table 3.1: Calming lengths reported in two phase flow literature.

Source	Pipe orientation	Diameter (mm)	L/D
Present work	H, I, V	12.7 and 12. 5	100 (S), 110 (R)
Oshinowo (1971)	V	25.4	60
Gibson (1981)	H, I	25 and 54	60
Laurinat (1982)	H	25 and 54	75
Yijun and Rezkallah (1993)	V	9.5	120
Sujumnong (1997)	V	12.5	120
Wolf et al. (2001)	V	31.8	300
Goda et al. (2003)	V	25 and 54	100
Han et al. (2006)	V	9.5	76
Sawant et al. (2008)	V	9.5	270
Hazuku et al. (2008)	V	11	250
Schubring (2009)	V	23.4	150
Ashwood (2010)	H, V	23.4	150

H = Horizontal, V = Vertical, I = Inclined, (S) = Smooth, (R) = Rough

Data Acquisition System: A national instrument data acquisition system is used for recording and storing of the data measured during the experiment. The graphic user interface (GUI) used for data acquisition is developed using Lab View program developed by National Instruments. The AC powered 4 slots SCXI 1000 chassis is used to house SCXI 1102 and SCXI 1125 modules. The modules serve as signal conditioning device and are connected to terminal blocks. Terminal blocks are directly connected to the sensors/transducers attached to the test section to acquire the data. The data such as inlet and outlet temperature and pressure, mass flow rate

of air and water, differential pressure drop signal in form of voltage is acquired by the data acquisition system. More details about the data acquisition system can be found in Cook (2008).

Flow Visualization: The flow visualization of different flow patterns was carried out in transparent polycarbonate section using Nikon D3100 digital camera having a resolution of 14.2 mega pixels and a shutter speed of 1/4000 s. This camera is used along with Nikon VR 55-200 mm, f/5.6 focal length lens for the desired zoom and focus on the test section. The camera is positioned perpendicular to the test section and precaution is taken to prevent shadows and reflections of camera. By trial and error it was found that the backlighting improved the picture quality significantly compared to the front lighting. The uniform backlight required for the flow visualization is provided by a 500 LED panel light source with adjustable light intensity. A white polycarbonate translucent sheet was placed between the light source and test section that acted as a light diffuser. Still pictures were taken in burst mode and about 20 pictures were taken for each fixed liquid and gas flow rates to confirm the existence of a certain flow pattern. Since, the purpose of taking still pictures was merely for flow pattern identification without making any physical measurements, the correction of any possible image distortion due to the pipe wall curvature was not deemed necessary.

3.2 Experimental Procedure

This section briefly describes the measurement technique and the experimental procedure followed for the measurement of void fraction and two phase pressure drop.

3.2.1 Void Fraction Measurements

The void fraction measurements are carried out in 12.7 mm I.D. transparent polycarbonate pipe using pneumatically operated quick closing valves. These valves use W. E. Anderson Model ABV1DA101 pneumatic ball valve having a closing time of 0.03 seconds. The pneumatic ball valves are operated at a pressure of 690 kPa (100 psi) using solenoid controllers from Dynaquip Controls. The three pneumatic closed valves are placed along the transparent test section (polycarbonate pipes) and the by pass line such that in normal two phase flow through the test section, the upstream and downstream valves are open and the bypass line valve is closed. After actuating these valves for void fraction measurement, the bypass line valve is in open position while the inline valves are closed and thus traps the two phase mixture in the test section. The two phase mixture trapped inside the test section is then evacuated by pushing high pressure air and is collected in a tank. The mass of the total liquid that can be trapped in the test section is calculated from the known volume of the test section (277.5 cc). Assuming constant specific volume of the liquid water, the total mass of the liquid water (m_{tot}) that can be trapped in the test section is found to be 279.6 g. The two phase liquid holdup i.e., (1 - α) is calculated by taking the ratio of amount of liquid water (m_{liq}) trapped in the test section + amount of water trapped in pipe fittings (m_{cal}) during the two phase flow to the maximum amount of water that can be trapped in the test section (m_{tot}). Finally, subtracting this liquid holdup

from unity gives the measured value of void fraction as shown in Eq. (3.1).

$$\alpha = 1 - \frac{(m_{liq} + m_{cal})}{m_{tot}} \tag{3.1}$$

It was observed that while evacuating liquid water from the test section, a little amount of water gets trapped in the solenoid valves fittings. To overcome this loss of evacuated water, the void fraction test section is calibrated to measure the amount of liquid trapped in the valve fittings. By measuring the mass of the water drained from the completely filled (by liquid water) void fraction section and comparing that mass with the mass that would be drained from the section ideally (276.9 g), it was possible to estimate the amount of liquid water that would be trapped in the void fraction section. This calibrated mass of liquid water (m_{cal}) is then added to the measured values of the evacuated mass of liquid water to calculate final value of the void fraction. The calibrated liquid mass for different pipe orientations (horizontal, inclined and vertical) is reported in Table 3.2.

Table 3.2: Calibrated mass for void fraction measurement at different pipe orientations.

Pipe orientation (θ)	m_{cal} (gram)	% error
0^o	14.5	5.4
$\pm 45^o$	15.9	5.7
$\pm 90^o$	17.8	6.4

The void fraction measurements for each combination of gas and liquid flow rate is repeated for 4-5 times to obtain consistent values of void fraction. The number of measurements required for each flow rate also depends on the physical structure of the flow pattern. In case of slug flow at low gas and liquid flow rates, its was quite possible to have trapped very long or short slugs that directly influences the

measured void fraction. For the slug flow regime in particular occurring at low gas and liquid flow rates, the void fraction measurements were repeated for 7-8 times until consistent values were obtained. Finally, the average value of the repeated measurements was taken as a representative value of void fraction for the gas and liquid flow rate under consideration. The uncertainty associated with measurement of void fraction is reported in Section 3.3.

3.2.2 Pressure drop measurements

Two phase pressure drop measurements are carried out in both polycarbonate and stainless steel sections. In this study, the two phase pressure drop data is measured in both polycarbonate (smooth) and stainless steel (rough) pipes at varying gas and liquid mass flow rates. The two phase pressure drop between the pressure taps at a distance of 890 mm is measured using DP-15 Validyne differential pressure transducer that is capable of accommodating pressure diaphragms of different ranges. Based on the range of two phase pressure drop encountered in this study, a DP 15-26 0.5 psi (3.5 kPa) and DP 15-32 2 psi (14 kPa) diaphragm was used for low and high values of two phase pressure drop, respectively. The pressure drop measured using Validyne pressure transducer is the total pressure drop and hence hydrostatic component of two phase pressure drop is subtracted or added (depending upon the pipe orientation) from the measured pressure drop to obtain frictional component of two phase pressure drop. The value measured by the differential pressure transducer is the pressure difference across the two sides of pressure diaphragm and not the pressure difference between two pressure taps. In order to find the pressure differential across the pressure taps, the values read by differential pressure transducer are corrected by adding or subtracting (depending upon the pipe orientation) the hydrostatic head due to single phase liquid in the connecting lines. Before putting the transducer to

use, it is first calibrated for the range of pressure diaphragm against air using portable digital manometer. The air pressure generated by Ametek T-970 hand pump is gradually increased from 0 to the maximum allowable pressure of the inserted pressure diaphragm and the corresponding voltage is recorded using the data acquisition program. The curve fitted equation as shown in Fig. 3.4 is then entered into the main data acquisition program that converts the voltage recorded by transducer to the analog pressure signal in psi.

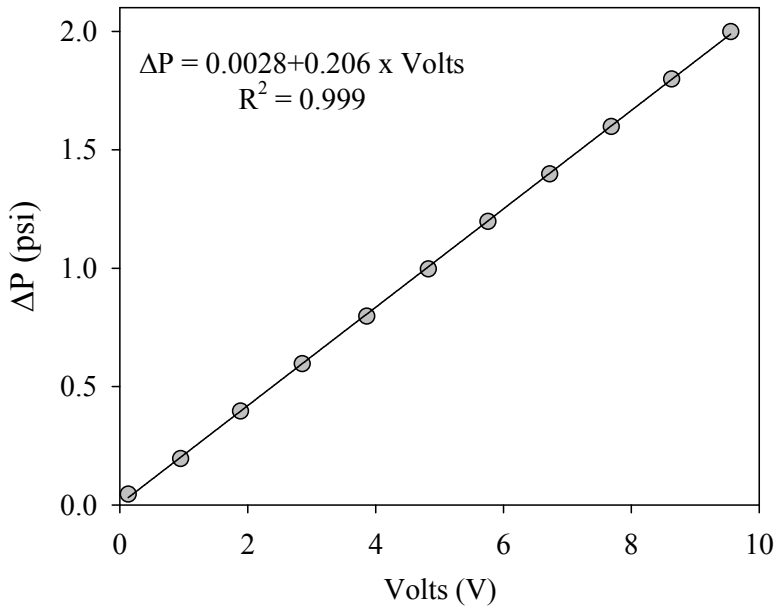

Figure 3.4: Calibration curve for DP 15-32 (2 psi) pressure diaphragm.

In order to ensure that the data obtained from the experimental setup is accurate and is of high repeatability, it is necessary to incorporate a systematic method to measure two phase pressure drop. As discussed earlier different pressure diaphragms are available to be used with the Validyne differential pressure transducer and the selection of the right diaphragm is of utmost importance for better accuracy. The experimental procedure followed for pressure drop measurements comprised of four major steps; checks, system warm up, data acquisition and finally the safe shut down of the setup.

1. The first step before starting pressure drop measurements is to ensure that the pressure regulator and valves for water line are working correctly. The single phase liquid is allowed to flow through the pipe and connecting lines of pressure transducer to remove air pockets trapped inside. This process also allows detecting any leakage in the connecting lines and the joints.

2. After the system check, the air compressor is turned ON and in order to stabilize the system the two phase mixture is allowed to flow through the test section for 3-5 minutes before actual readings are taken.

3. After allowing the system to stabilize, the data acquisition program is turned ON. The data acquired through different channels of data acquisition system includes mass flow rates, inlet and outlet temperature and pressure, the differential pressure between the pressure taps and calculates the superficial Reynolds number and the fluid physical properties of individual phases. The data is collected for 5-6 minutes (3000 samples) so as to have significant number of samples to nullify any errors in the reading due to flow fluctuation. In case of flow patterns such as intermittent and annular flows; significant fluctuations are observed in the pressure drop signal and hence the sampling time is increased to 10 minutes (6000 samples) to ensure accuracy in the measured data.

4. The average values of these samples for every parameter are considered to be representatives of the measured values.

The two phase pressure drop measurements are carried out over a range of gas and liquid mass flow rates and the test matrix used for experimental purpose is listed in Table 3.3. These experimental conditions are selected such that the experimental data covers the entire range of void fraction and all the flow patterns observed in two phase flow. In addition to these gas and liquid flow rates, in particular for upward

inclined flows, additional data at low liquid flow rates of 0.25 kg/min, 0.5 kg/min, 0.75 kg/min and 1.6 kg/min and gas flow rates of 0.01 kg/min, 0.03 kg/min and 0.05 kg/min is also measured. This additional data was required in upward inclinations to study the phenomenon of flow reversal.

Table 3.3: Test matrix of the flow conditions used for experimental measurements.

	Liquid mass flow rate, $\dot{m}_L$ (kg/min)								
Gas mass flow rate, $\dot{m}_G$ (kg/min)	**1.1**	**2.3**	**3.4**	**4.5**	**5.7**	**6.8**	**7.9**	**9.1**	**10.2**
	0.002	0.002	0.002	0.002	0.002	0.002	0.002	0.002	0.002
	0.004	0.004	0.004	0.004	0.004	0.004	0.004	0.004	0.004
	0.006	0.006	0.006	0.006	0.006	0.006	0.006	0.006	0.006
	0.015	0.015	0.015	0.015	0.015	0.015	0.015	0.015	0.015
	0.04	0.04	0.04	0.04	0.04	0.04	0.04	0.04	0.04
	0.07	0.07	0.07	0.07	0.07	0.07	0.07	0.07	0.07
	0.09	0.09	0.09	0.09	0.09	0.09	0.09	0.09	–
	0.12	0.12	0.12	0.12	0.12	0.12	0.12	0.12	–
	0.15	0.15	0.15	0.15	0.15	0.15	–	–	–
	0.17	0.17	0.17	0.17	–	–	–	–	–
	0.18	0.18	0.18	0.18	–	–	–	–	–
	0.19	0.19	0.19	0.19	–	–	–	–	–
	0.2	0.2	0.2	0.2	–	–	–	–	–

3.3 Uncertainty in Void Fraction and Pressure Drop Measurements

The uncertainty estimation in measurements of void fraction and two phase pressure drop is important to gauge the accuracy of experimental setup and confirm its credibility to measure data consistently over a range of gas and liquid mass flow rates. The experimental uncertainty in the measured void fraction and pressure drop is calculated using Engineering Equation Solver (EES) and is verified against the results obtained by the method proposed by Kline and McClintock (1953).

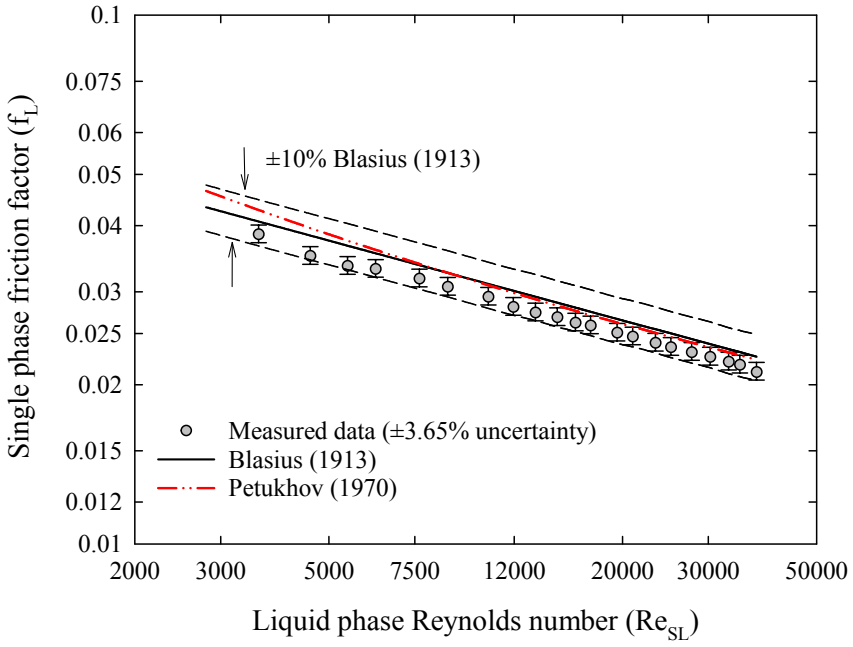

(a) Smooth pipe

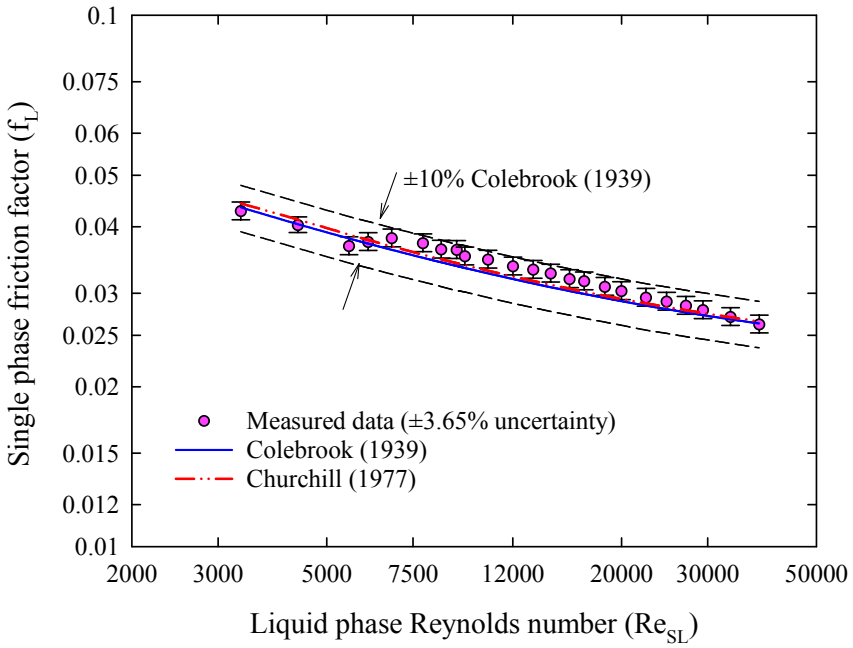

(b) Rough pipe

Figure 3.5: Comparison between measured and calculated single phase liquid friction factor.

The accuracy and reliability of the experimental setup is confirmed as shown in Fig. 3.5 by direct comparison of the measured single phase pressure drop and hence the single phase friction factor against the correlations. Single phase friction factor for liquid phase in smooth pipe is compared against the prediction of Blasius (1913) and Petukhov (1970) while the single phase friction factor in rough pipe is compared against the prediction of Colebrook (1939) and Churchill (1977). It is seen from Fig. 3.5(a)-(b) that the single phase friction factor (f_L) in both smooth and rough pipes is within $\pm 10\%$ of the prediction of Blasius (1913) and Colebrook (1939) correlations, respectively. The maximum uncertainty in measurement of single phase friction factor is found to be $\pm 3.65\%$.

The two phase pressure drop measured by the differential pressure transducer is the pressure difference between the two sides of diaphragm and not the pressure difference between the upstream and downstream pressure taps. To get the differential pressure across the pressure taps, the measured two phase pressure drop is corrected by the pressure drop due to single phase liquid present in the connecting lines as shown in Eq. (3.2). Further, the frictional component of two phase pressure drop can be deduced from Eq. (3.3).

$$\left(\frac{dP}{dL}\right)_t = \left[\frac{(dP)_{meas} + \rho_L g L \sin\theta}{L}\right] \tag{3.2}$$

$$\left(\frac{dP}{dL}\right)_f = \left(\frac{dP}{dL}\right)_t - [\rho_L(1-\alpha) + \rho_G \alpha] g \sin\theta \tag{3.3}$$

The uncertainty in measured values of total pressure drop, frictional pressure drop and void fraction in two phase flow using method of Kline and McClintock (1953) is documented below in Eqs. (3.4) to (3.7).

$$u(\Delta P)_f = \left[\left(\frac{\partial(\Delta P)_f}{\partial(\Delta P)_m} u(\Delta P)_m \right)^2 + \left(\frac{\partial(\Delta P)_f}{\partial \rho_L} u(\rho_L) \right)^2 + \left(\frac{\partial(\Delta P)_f}{\partial \rho_G} u(\rho_G) \right)^2 + \left(\frac{\partial(\Delta P)_f}{\partial L} u(L) \right)^2 + \left(\frac{\partial(\Delta P)_f}{\partial \alpha} u(\alpha) \right)^2 + \left(\frac{\partial(\Delta P)_f}{\partial g} u(g) \right)^2 + \left(\frac{\partial(\Delta P)_f}{\partial \theta} u(\theta) \right)^2 \right]^{0.5} \tag{3.4}$$

$$u(\Delta P)_f = \Big[[u(\Delta P)_m]^2 + [\Delta \rho L \alpha \sin\theta u(g)]^2 + [\Delta \rho g L \sin\theta u(\alpha)]^2 + [\Delta \rho \alpha g \sin\theta u(L)]^2 + [\alpha g L \sin\theta u(\rho_L)]^2 + [(-\alpha g L \sin\theta u(\rho_G)]^2 + [\Delta \rho \alpha g L \cos\theta u(\theta)]^2 \Big]^{0.5} \tag{3.5}$$

The uncertainty in measurement of void fraction based on Eq. (3.1) is calculated as,

$$u(\alpha) = \sqrt{\left(\frac{\partial \alpha}{\partial m_{liq}} u(m_{liq}) \right)^2 + \left(\frac{\partial \alpha}{\partial m_{cal}} u(m_{cal}) \right)^2 + \left(\frac{\partial \alpha}{\partial m_{tot}} u(m_{tot}) \right)^2} \tag{3.6}$$

$$u(\alpha) = \sqrt{\left(\frac{-1}{m_{tot}} u(m_{liq}) \right)^2 + \left(\frac{-1}{m_{tot}} u(m_{cal}) \right)^2 + \left(\frac{m_{liq} + m_{cal}}{m_{tot}} \right)} \tag{3.7}$$

Uncertainty in calculation of gas and liquid phase density is taken to be 0.06% of its absolute value. Maximum uncertainty in determination of m_{tot}, m_{liq} and m_{cal} is taken to be $\pm$2gm each. The pipe orientation was measured using Johnson magnetic angle locator having an accuracy of 0.5 degree. The uncertainty of the measured and calculated variables for a sample run is documented in Table 3.4. Similar procedure of uncertainty calculation is followed for all data points measured at different pipe orientations. For a case of two phase flow through upward inclined pipe at $+60^o$ as shown in Table 3.4, the minimum and maximum uncertainty in measurement of void fraction was found to be $\pm$0.0102 and $\pm$0.012, respectively. Similarly, the minimum

and maximum uncertainty in measurement of two phase frictional pressure drop was found to be ±90 (Pa/m) and ±127 (Pa/m), respectively.

Table 3.4: Uncertainty of measured and calculated variables for a sample run.

Parameter	Value	Uncertainty	% Uncertainty
ρ_L (kg/m^3)	997.2	±0.598	±0.06
ρ_G (kg/m^3)	1.631	±0.0095	±0.06
m_{tot} (gm)	276.9	±2	±0.72%
m_{liq} (gm)	140	±2	±1.14%
m_{cal} (gm)	14.5	±2	±13.7%
α	0.319	±0.0113	±3.54%
L (m)	0.89	± 0.000127	±0.14%
θ (deg.)	60	±0.5	±0.8%
$(\Delta P/L)_{meas}$ (Pa/m)	-880.4	±2.21	±0.25%
$(\Delta P/L)_f$ (Pa/m)	2737	±98.5	±3.6%

3.4 Chapter Summary

This chapter presents details of variable inclination experimental setup used for flow visualization and measurements of void fraction and two phase pressure drop. A step by step procedure followed during measurements of void fraction and two phase pressure drop is reported. Furthermore, the calculation of uncertainty involved in measurements of void fraction and two phase pressure drop is discussed and uncertainty calculation for a sample run is presented.

CHAPTER IV

EXPERIMENTAL RESULTS AND DISCUSSION

In this chapter, the results of the flow visualization and experimental measurements of void fraction and two phase pressure drop measured at different pipe orientations are presented. The chapter is divided into three main parts where the first part highlights flow visualization and presents flow pattern maps for upward and downward pipe inclinations with reference to horizontal two phase flow. The second and third part of this chapter presents parametric studies of the void fraction and two phase pressure drop, respectively. The parametric study illustrates the effect of phase flow rates (or alternatively the flow patterns), pipe orientation, pipe diameter and pipe wall surface roughness on void fraction and two phase pressure drop.

4.1 Flow Patterns and Flow Pattern Maps

The flow patterns in gas-liquid two phase flow are essentially generated due to the significant density difference between the two phases and depend on the alignment of one phase with respect to the other phase across the pipe cross section. In the present study, the existence of a certain flow pattern is acknowledged based on the visual observations and the still photographs captured by the camera for different flow rates. The key flow patterns that appear at all pipe orientations are bubbly, slug, intermittent, stratified and annular flow regime. In addition to this, the falling film flow, a special type of stratified flow is also observed for vertical downward and

near vertical downward pipe inclinations. The stratified flow pattern exists only in horizontal and downward inclined pipe orientations. The physical description of flow patterns and their span on the 2-D plot of gas and liquid flow rates is discussed next in this chapter.

4.1.1 Flow Patterns

The flow visualization is carried out over the entire range of mass flow rates permitted by the mass flow meter used in this experimental work. The gas and liquid mass flow rates (superficial Reynolds number) are varied in a range of 0.001 to 0.2 kg/min (90 to 20000) and 1 to 12 kg/min (800 to 19000), respectively.

Bubbly flow: Bubbly flow is characterized by the flow of small size discrete gas bubbles dispersed in the continuous liquid phase. For horizontal and inclined two phase flow, the gas bubbles are always located near the pipe upper wall region (asymmetric flow). While for vertical flows (both upward and downward) the gas bubbles are evenly distributed across the pipe cross section (symmetric flow). It is observed that the gas and liquid flow rates significantly affect the size, shape and distribution of the gas bubbles dispersed in the liquid medium.As shown in Fig. 4.1 at fixed gas flow rate, increase in the liquid flow rate results in the shearing of gas bubbles that reduces its size, and consequently increase the number of bubbles that try to penetrate the single phase liquid and enter the near pipe axis region. This change in shape, size and distribution of bubbles may not affect time and space averaged two phase flow parameters however, it can definitely influence the local characteristics of the two phase flow field.

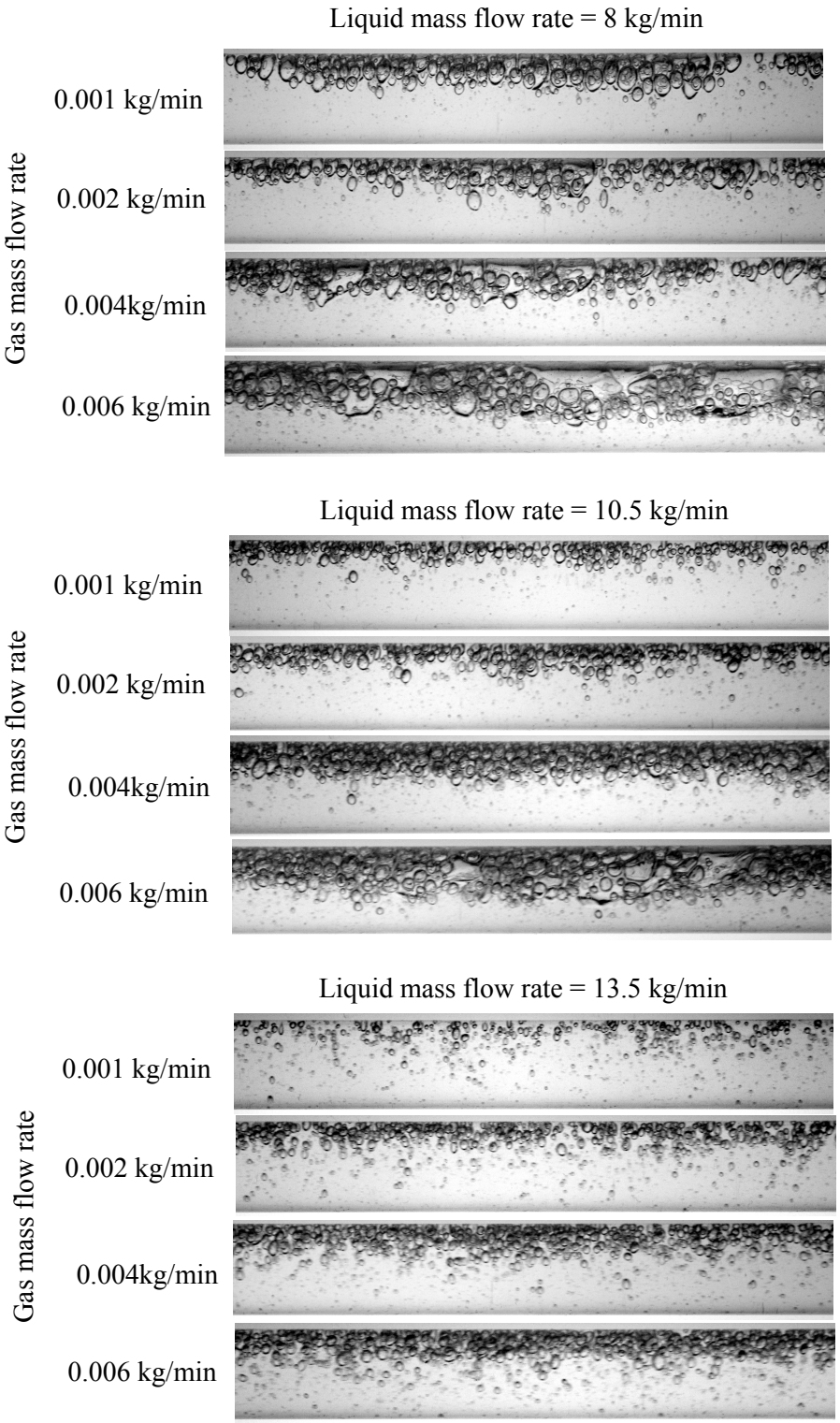

Figure 4.1: Bubbly flow at varying gas and liquid flow rates in horizontal pipe orientation.

In case of vertical downward flow, at low gas flow rates, the gas bubbles appear

to be distributed only in the central region of pipe with single phase liquid occupying the near wall region. This appearance of bubbly flow in vertical downward flow is essentially due to the 'coring phenomenon' characterized by the repulsive force exerted by the pipe wall on the liquid phase. The coring phenomenon is a consequence of interaction between buoyancy and inertia forces and is conceptually similar to the lift force exerted on the golf ball due to Magnus effect. As shown in Fig. 4.2, the buoyancy and lift force (due to the pressure gradient present on the two sides of gas bubble) act on the gas bubble that causes the bubble to move towards the pipe centerline or the pipe wall depending upon the pipe orientation. In case of vertical upward flow, the buoyancy is in direction of the mean flow and lift force acts on the gas bubble towards the pipe wall. However, for vertical downward flow, the opposite direction of the buoyancy force to that of the mean flow exerts a shear lift on the bubble away from the pipe wall. This causes the gas bubble to migrate near the pipe axis region. It is found that with increase in the gas and liquid flow rates, the gas bubbles tend to coalesce and the inertia forces supersede the buoyancy effects and hence also supersedes the repulsion (lift) force exerted by the pipe wall. Consequently, bubbles start to move towards pipe wall and get more evenly distributed throughout the pipe cross section and finally the physical appearance of the bubbly flow is similar in both vertical upward and downward flow directions. The coring effect observed in vertical downward bubbly flow is illustrated in Fig. 4.3 for different gas and liquid flow rates.

Usui and Sato (1989), Oshinowo and Charles (1974) and Nguyen (1975) observed similar type of observations for the coring phenomenon in 19 mm, 25 mm and 45 mm I.D. vertical downward pipes, respectively. It should be noted that the coring phenomenon occurs only in vertical downward and near vertical downward pipe orientations and is prominent for large diameter pipes. It is anticipated that the coring phenomenon vanishes with decrease in the pipe diameter since two phase flow

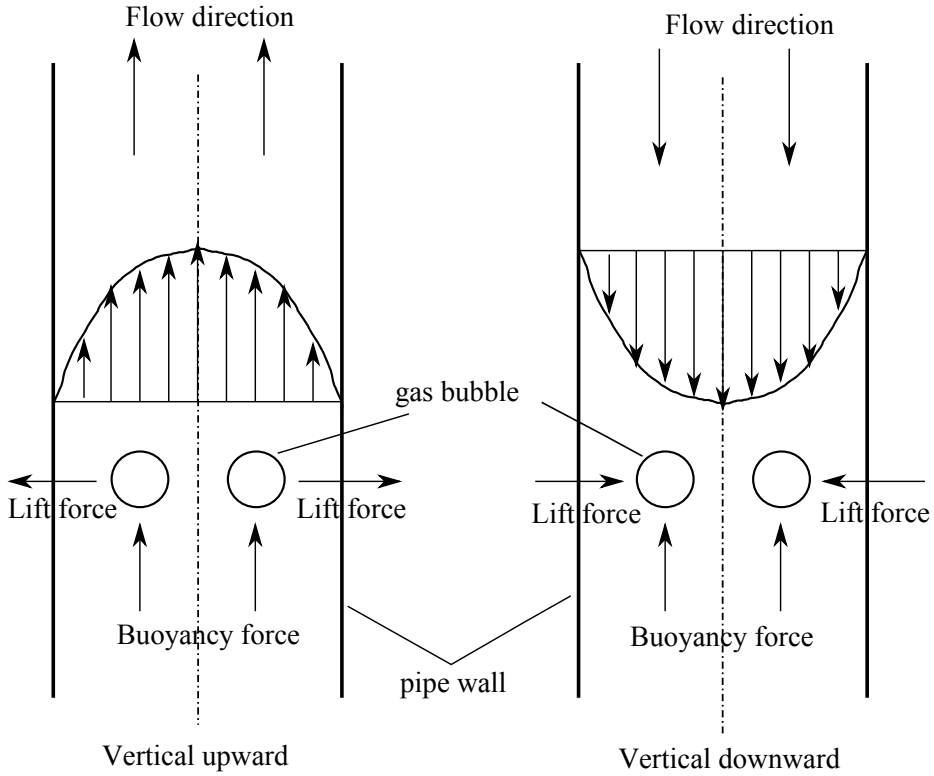

Figure 4.2: Buoyancy, inertia and lift force interaction in vertical upward and downward bubbly flow.

literature doesn't provide any evidence of its existence for pipe diameters typically $D < 12$ mm. Bhagwat et al. (2012a) and Bhagwat et al. (2012b) reported that the coring phenomenon affects the frictional pressure drop and heat transfer trends in two phase bubbly flow essentially due to the wall repulsion forces acting towards pipe centerline.

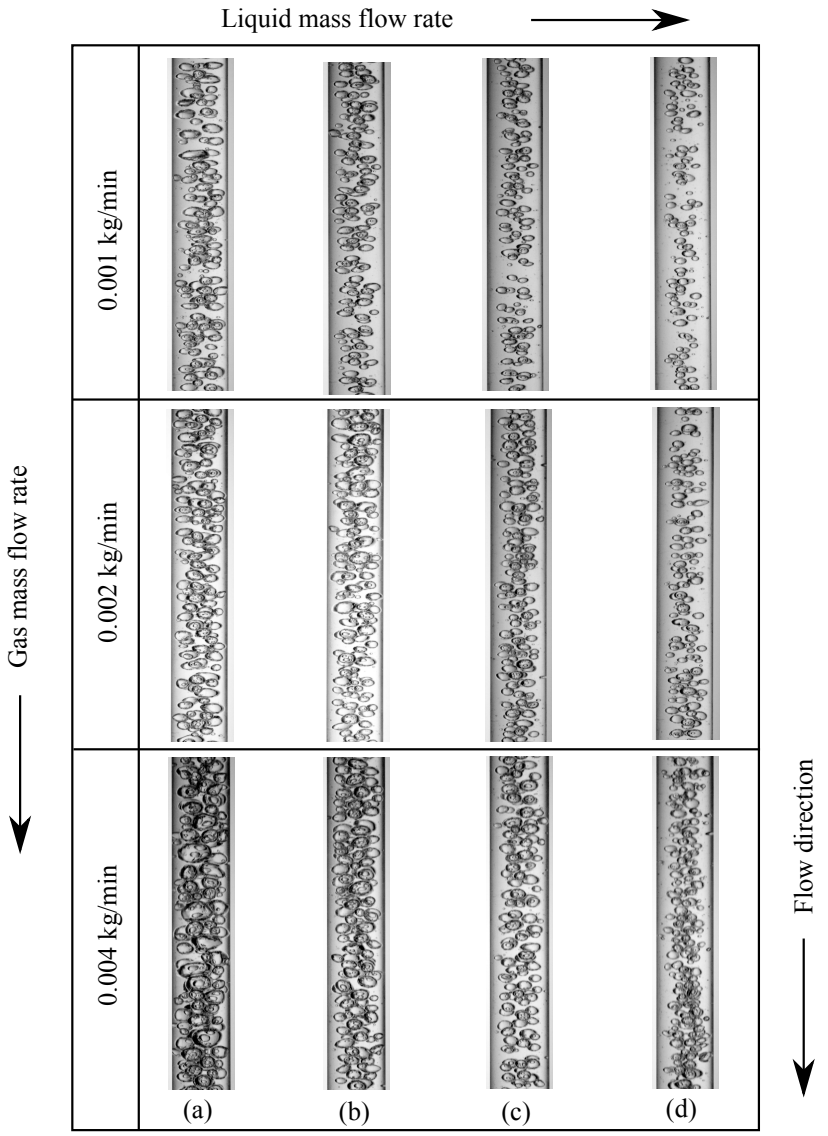

Figure 4.3: Coring phenomenon in vertical downward bubbly flow for varying $\dot{m}_L$ (a) 7 kg/min, (b) 8 kg/min, (c) 10 kg/min and (d) = 12 kg/min.

Slug flow: Slug flow typically appears at low to moderate gas and liquid flow rates and is characterized by the alternate flow of elongated gas bubble and a liquid slug. For horizontal and inclined pipe orientations, the elongated gas bubble (gas slug) is asymmetric to the pipe axis and is in the vicinity of the pipe upper wall. Whereas, for vertical upward flow, the gas slug is symmetric about the pipe centerline and has a bullet shaped nose and a flat trailing edge. The gas slug in vertical upward flow is also recognized as 'Taylor Bubble' and its schematic is shown in Fig. 4.4. It important to

mention that for the vertical upward and all upward pipe inclinations, as the gas slug moves through a given pipe cross section, it accelerates the liquid phase right ahead of the slug nose. To maintain the continuity, the liquid phase decelerates and falls back in the downward direction along the pipe wall in form of film. This trailing liquid film is found to affect the frictional pressure drop in inclined systems giving a pressure drop minimum even with increasing gas flow rates. The nexus between pressure drop minimum and trailing liquid film in upward inclined slug flow is established later in this chapter.

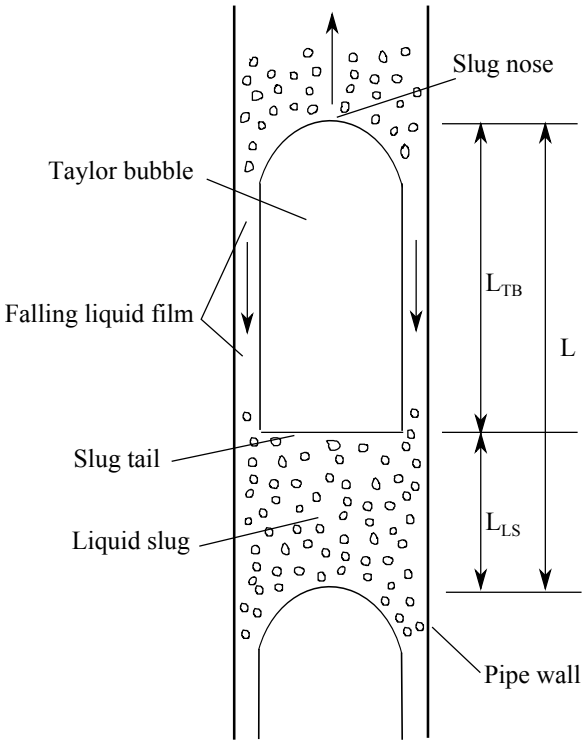

Figure 4.4: Schematic of a slug flow unit cell.

The physical structure, length and frequency of the gas bubble is found to be sensitive to gas and liquid flow rates and pipe orientation. Based on the flow visualization, it is found that at low gas and liquid flow rates, the length of gas bubbles (slug) is up to 70D and it moves quiescently through the pipe. With increase in the gas and liquid flow rates, the gas bubble length reduces and is found to move through the pipe at increased frequency and more vigorously. The change in physical struc-

ture of the slug in horizontal pipe orientation is evident from Fig. 4.5. At a fixed liquid flow rate, the increase in gas flow rate increases the slug length. The physical structure of the gas slug i.e., the nose (upstream region) and the tail (downstream region) is found to be significantly different for upward and downward inclined pipe orientations. In case of upward pipe inclinations, the buoyancy force acting on the gas phases aids the motion of gas slug and the slug nose points in the direction of two phase flow. Whereas, for downward inclined two phase flow, the buoyancy force acting on the gas phase in a direction opposite to that of the two phase flow that causes distortion of the slug nose and a tail pointing in the direction opposite to that of the flow direction is observed. Moreover, the slug length in downward pipe inclinations is observed to be greater than the upward pipe inclinations. Due to the influence of buoyancy force on the gas phase, the frequency of slugs in downward pipe inclinations is considerably smaller than that in upward pipe inclinations. The difference between the nose and tail structure of a slug observed in upward and downward inclinations is evident from Fig. 4.6. It is also worthwhile to mention that the shape of the slug nose in vertical downward orientation is found to change with chnage in the phase flow rates depending upon the interaction between buoyant and inertia forces. In case of vertical downward flow, at low liquid and gas flow rates, the elongated slug bubble appears very similar to that of the vertical upward flow i.e., the slug tail appears to be pointed in the upward direction and remains undistorted. As shown in Fig. 4.6 with increase in the gas and liquid flow rates, the slug nose and tail (both ends of slug) becomes flat and at further increased phase flow rates, the slug nose points in the direction of the mean flow. These different types of slug nose in vertical downward flow are an indication of the different residence times of the gas phase in the test section (different magnitudes of interaction between buoyant and inertial forces) which is further expected to influence the void fraction, pressure drop and heat transfer characteristics of two phase flow.

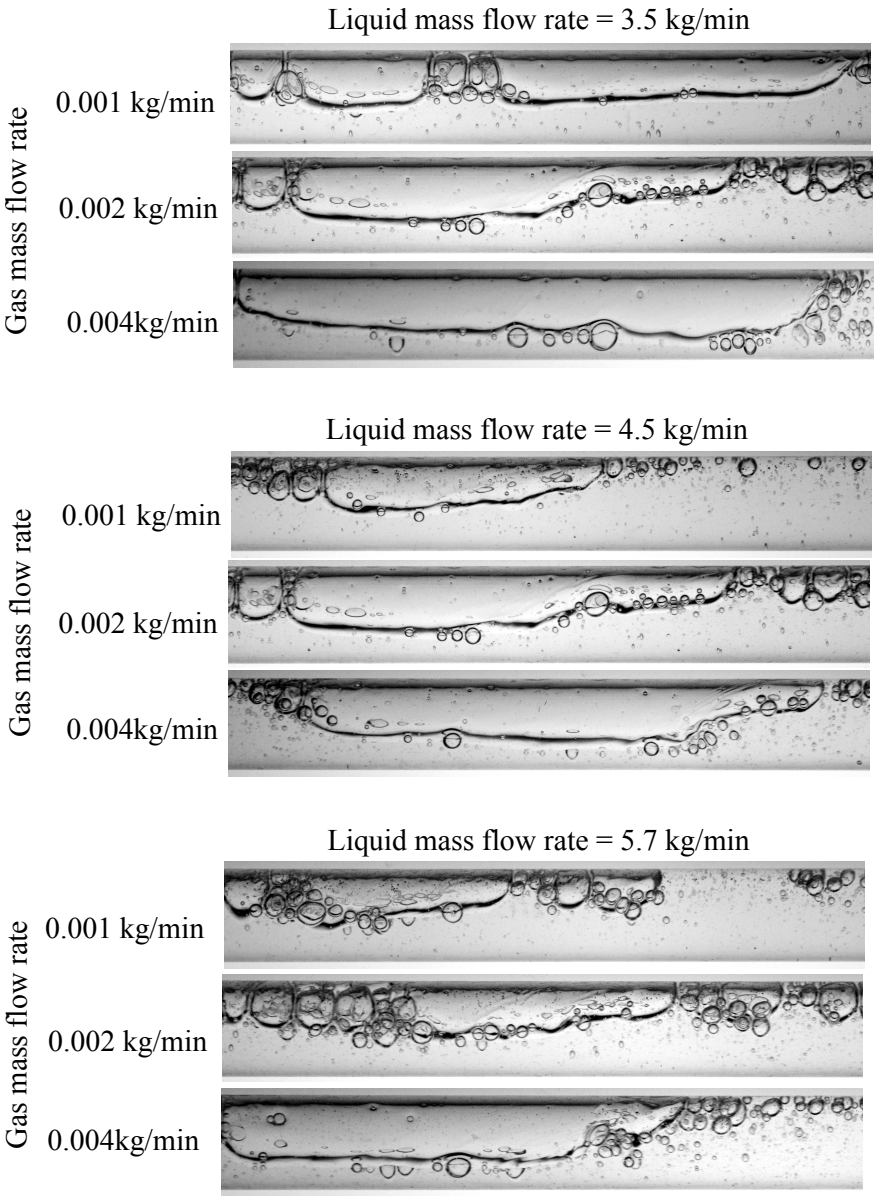

Figure 4.5: Slug flow at varying gas and liquid flow rates in horizontal pipe orientation.

Intermittent flow: The intermittent flow exists for moderate gas and liquid flow rates and is a representation of a two phase flow having chaotic, pulsating and indefinite phase alignment characteristics. Different sub flow patterns such as slug wavy flow, wavy flow and annular wavy flow which exhibit these characteristics can be tagged as intermittent flow pattern as shown in Fig. 4.7. Similar type of flow pattern classification has been adopted by Barnea (1987). The main purpose of

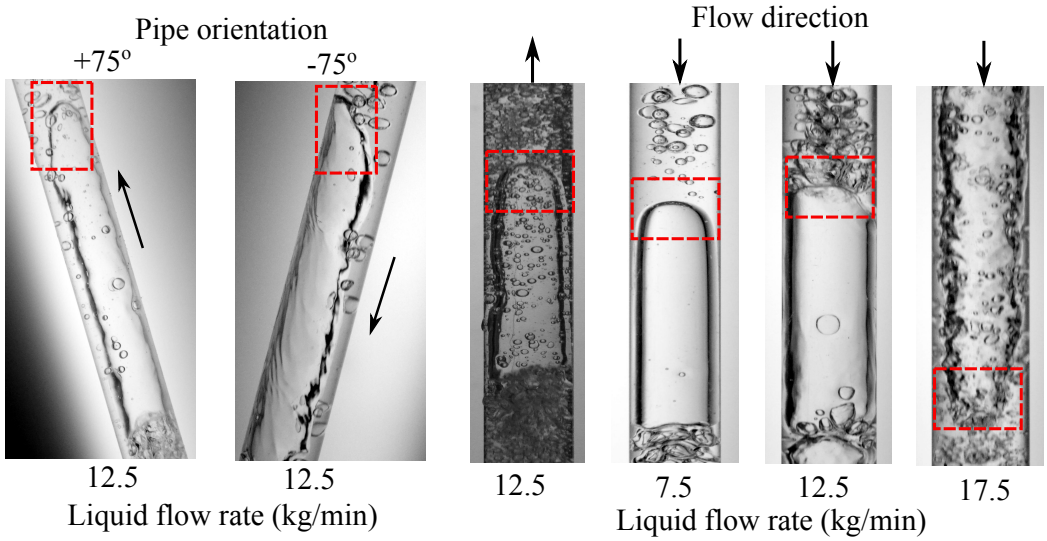

Figure 4.6: Slug geometry in near vertical upward, vertical downward and near vertical downward two phase flow at $\dot{m}_G = 0.01$ kg/min.

combining these sub flow patterns into one in this study referred to as intermittent is to reduce any difficulty and uncertainty in identifying the transition boundaries between them. The slug wavy flow as a subcategory of intermittent flow can be defined as the flow of gas pockets that flow in a wavy and aerated liquid phase. In comparison to slug flow, slug wavy flow exhibit enhanced level of mixing, disorderliness and significant aeration (in form of tiny gas bubbles) in the liquid phase. With increase in the gas flow rate, the slug wavy pattern is switched to wavy flow regime. In near horizontal orientations, wavy flow is featured by a flow of gas over unstable liquid layer that creates disturbance waves on the liquid surface. Increase in the gas flow rate causes the surface waves to grow due to well known Kelvin-Helmholtz instability phenomenon, touch the pipe top wall and then fall back again giving a vibrating string like appearance. Furthermore, at high gas flow rates typically 0.12 to 0.15 kg/min, the flow pattern features a thick wavy liquid film at the pipe bottom wall and a discontinuous thin liquid film at the pipe top wall and is identified as wavy annular flow. The common features that these three flow patterns share are the chaotic and wavy nature of the two phase flow and hence it is considered appropriate to categorize these three flow patterns together and call them as intermittent two phase flow.

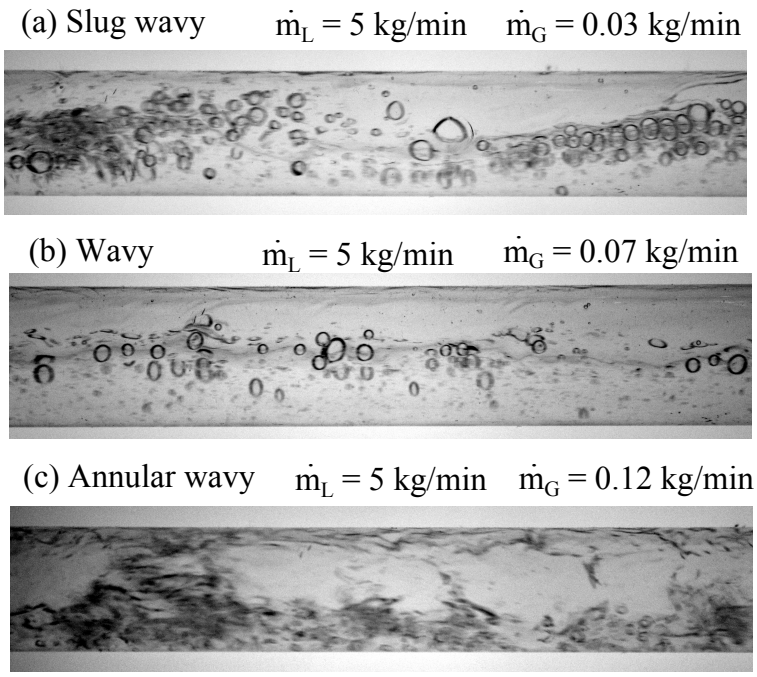

Figure 4.7: Sub types of intermittent flow.

Stratified flow: Stratified flow is characterized by the flow of liquid layer at the pipe bottom wall that flows parallel to the gas phase on top of it. The stratified flow is a separated type of flow that has a definite, dynamic and continuous interface. Typically the two phase flow literature classifies stratified flow as smooth stratified and wavy stratified flows. The smooth stratified flow usually appears for very low liquid and gas flow rates with a smooth interface between the gas and liquid phase. The wavy stratified flow is characterized by an unstable and dynamic gas liquid interface which is a consequence of Kelvin-Helmholtz instability. Without acknowledging the difference between smooth and wavy stratified flows, this study refers to this flow of gas and liquid parallel to each other as stratified flow. In the present study, stratified flow is observed at horizontal and all downward pipe inclinations. The physical appearance of stratified flow in -45^o from horizontal is shown in Fig. 4.8.

The stratified flow is observed by reducing the liquid flow rate in slug flow thereby reducing the tendency of liquid phase to bridge the entire pipe cross section. Two phase flow literature reports that the most complex part in modeling of a stratified

flow is the determination of liquid height and hence the wetted perimeter. It is noticed in this study that the height of stratified liquid layer is an increasing function of pipe orientation and liquid flow rate. Whereas, any increase in gas flow rate will cause the liquid layer height to decrease accompanied by the entrainment of liquid droplets into the gas core. Based on the physical structure of stratified flow shown in Fig. 4.8, it is anticipated that the void fraction and pressure drop stay virtually independent of the gas flow rate and are a function of only liquid height (or liquid flow rate) and pipe orientation.

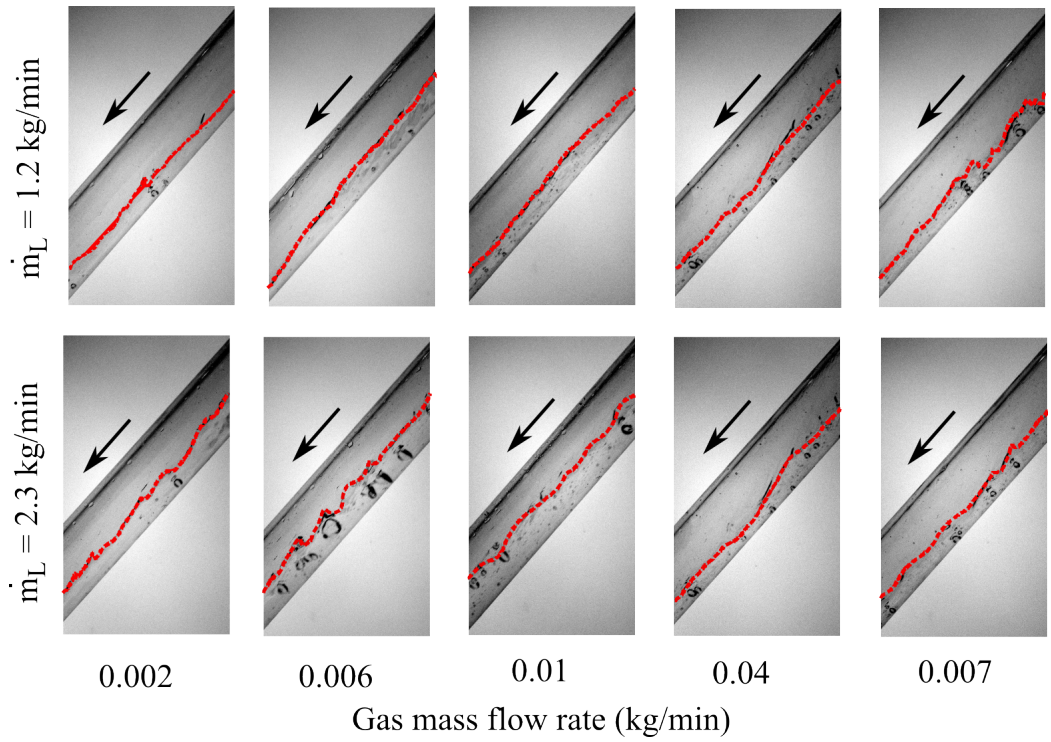

Figure 4.8: Stratified flow in downward inclined two phase flow ($\theta = -45^o$).

Falling film flow: Falling film flow is characterized by the flow of thin liquid film flowing quiescently along the pipe wall while the gas phase flows through the central region. The falling film flow that exists at low liquid and low to moderate gas flow rates may be regarded as a special case of stratified flow in vertical downward and near vertical downward pipe orientations. Falling film flow has a strong tendency

of creating dry spots on the pipe wall and hence may be regarded as undesirable flow pattern for the two phase flow involving high heat flux at the pipe wall. The physical form of falling film for various gas and liquid flow rates is depicted in Fig. 4.9. The dry spots on the pipe wall surface for gas flow rates ($\dot{m}_G \leq 0.01$ kg/min) are quite evident and with increase in the gas flow rate typically $\dot{m}_G > 0.01$ kg/min, liquid droplets are seen to entrain the gas core.

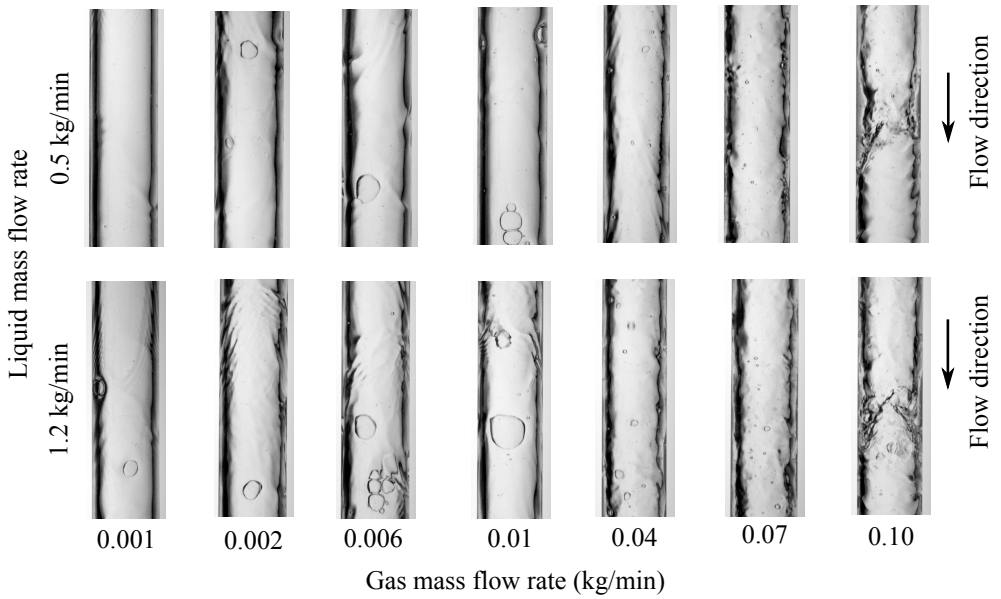

Figure 4.9: Falling film flow in vertical downward flow for different liquid flow rates.

Another striking feature of falling film flow is the membrane like structure shown in Fig. 4.10 that appears for a small range of gas and liquid flow rates. In the present study this membrane like structure was observed only for liquid mass flow rates of 0.5 kg/min and 1.2 kg/min and the gas mass flow rate in a range of 0.005 to 0.01 kg/min. Due to limitations of the flow meters used in this work, additional flow visualization to detect the existence of the membrane like structure in falling film flow could not be done.

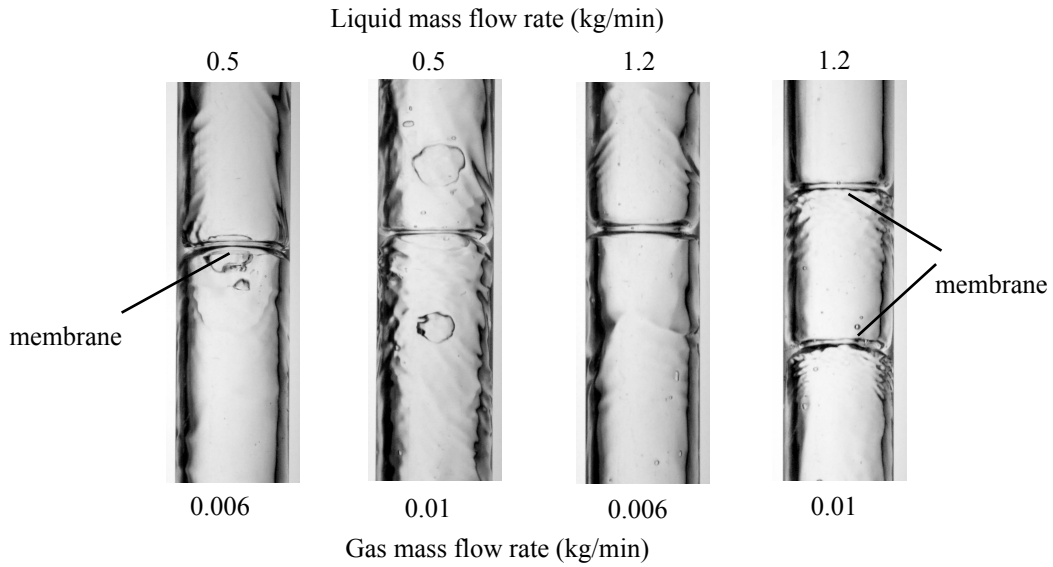

Figure 4.10: Membrane like structure in vertical downward falling film flow.

Similar type of membrane like structure is also reported in the recent work of Milan et al. (2014). They observed the membrane motion using a high speed video camera and concluded that the formation of membrane is due to the deformation of the thin liquid film by the gas phase in the core region and speculated that the occurrence of these membrane like structure may depend on the inlet mixing device. A preliminary analysis of experimental data collected in this study shows that the membrane like structures in falling film do not have an appreciable effect on void fraction and pressure drop and hence an in-depth study of this membrane like structure in falling film flow is considered beyond the scope of this work.

Annular flow: Annular flow can be described as the flow of liquid film in contact with the pipe wall that surrounds the central gas core. The annular flow pattern typically appears for low liquid and high gas flow rates and possess a definite, continuous and dynamic interface between gas and liquid phase. For horizontal and near horizontal inclined systems, the liquid film thickness at the pipe bottom wall is always thicker than that at the pipe top wall. Based on the visual evidence the distribution of film thickness around the pipe circumference (or pipe top and bottom

wall for a 2-D flow visualization) is found to depend on the gas and liquid phase flow rates and the pipe orientation.

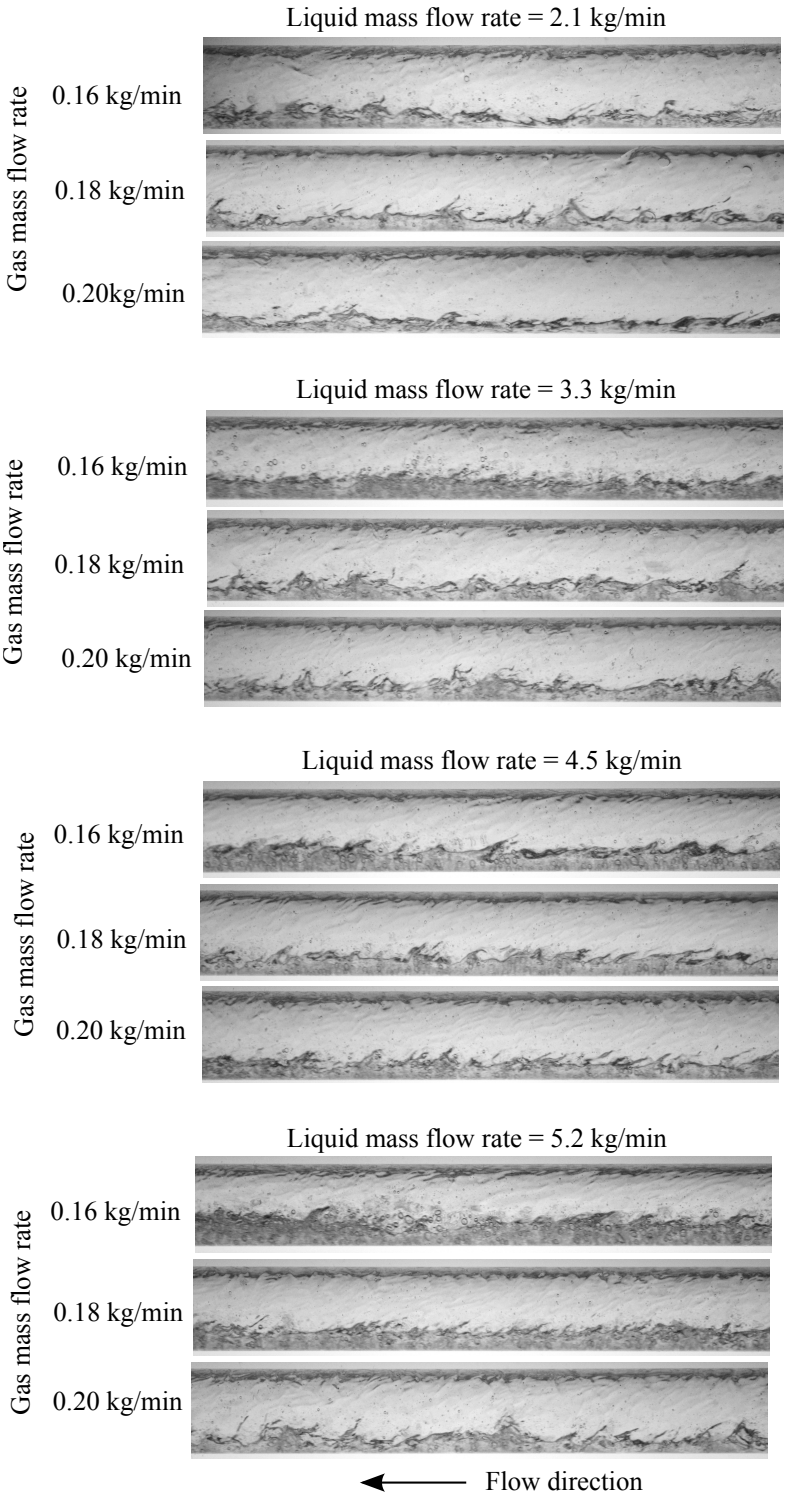

Figure 4.11: Annular flow at varying gas and liquid flow rates in horizontal pipe orientation.

For a fixed liquid and gas flow rate, the effect of increase in the pipe orientation is to make the liquid film distribution more symmetric whereas for a fixed pipe orientation and liquid flow rate, increase in the gas flow rate will reduce the liquid film thickness in contact with the pipe wall. The effect of change in gas and liquid flow rates on the general structure of annular flow in horizontal pipe orientation is depicted in Fig. 4.11. A striking feature observed in annular flow pattern is the entrainment of the tiny liquid droplets into the central fast moving gas core. The liquid entrainment is a consequence of the significant shear at the gas-liquid interface that causes tearing of the liquid waves crests in form of ligaments and may depend on the phase flow rates, pipe diameter and orientation and the surface tension at the interface. The photographic evidences collected in the present study show the entrainment phenomenon to exist for high values of liquid and gas flow rates where a thick liquid film is in contact with the pipe wall. With decreasing liquid flow rates, the entrainment is found to reduce. Two phase flow literature reports different mechanisms such as wave undercutting, rolling wave, wave coalescence and ripple shearing mechanism responsible for the entrainment.

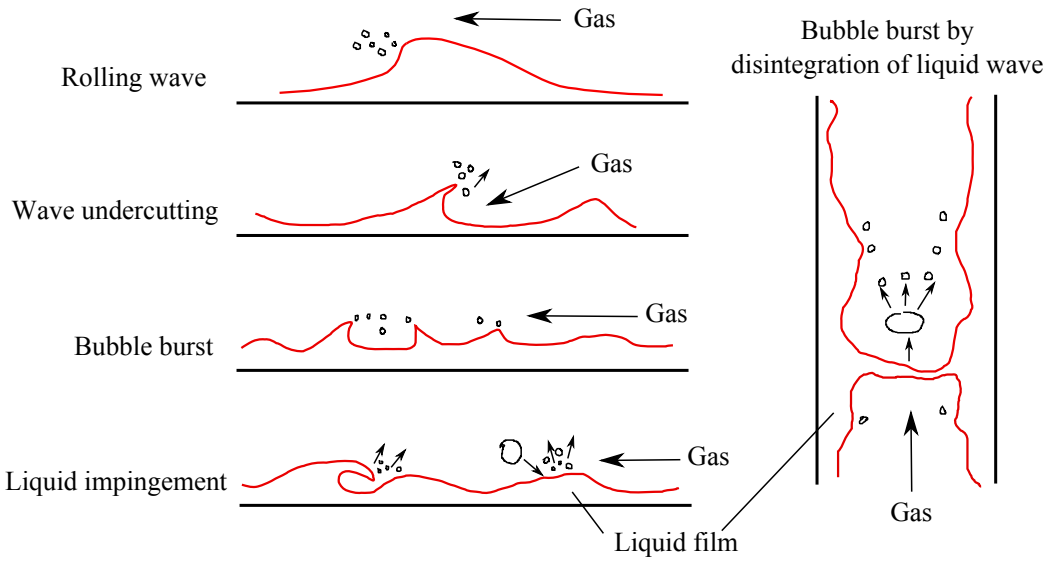

Figure 4.12: Schematics of different entrainment mechanisms.

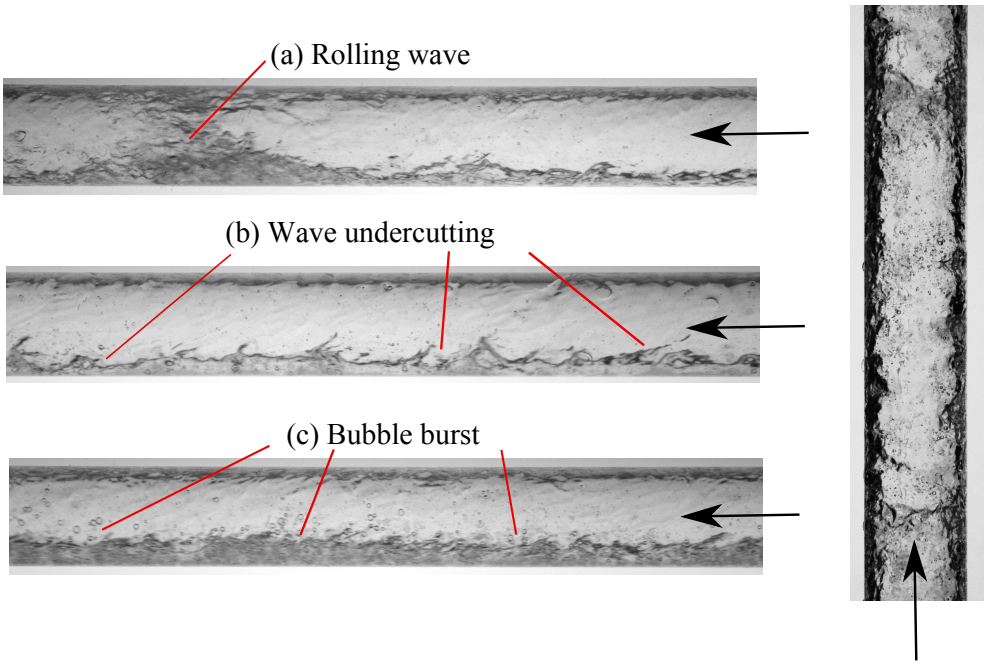

Figure 4.13: Flow visualization of entrainment mechanism in horizontal and vertical upward two phase flow.

Ishii and Grolmes (1975) reported that in addition to wave undercutting and rolling wave mechanisms, 'bubble burst' from the liquid waves crests due to rupture of the liquid film and the 'droplet impingement' mechanism that is essentially an after effect of the rolling wave phenomenon also causes entrainment of the liquid droplets in the gas core. The schematics of these different entrainment mechanisms adopted from work of Ishii and Grolmes (1975) is presented in Fig. 4.12. Out of these different mechanisms, rolling wave, wave undercutting and bubble burst mechanism are clearly observed in the present study as shown in Fig. 4.13. Regardless of the entrainment mechanism, the underlying concept to understand here is that the liquid entrainment phenomenon causes turbulence and instability in two phase flow that definitely contributes towards increased two phase pressure drop. The experimental setup used in this study is not equipped with an entrainment fraction measurement system and hence any quantitative analysis of the entrainment mechanism and entrainment fraction is beyond the scope of this work. So far it is discussed that the structure of two

phase flow patterns is affected by phase flow rates and pipe orientation. However, it is also important to consider the transition between different flow patterns as a function of phase flow rates and the pipe orientation in form of flow pattern maps.

4.1.2 Flow Pattern Maps

As mentioned earlier, the flow pattern map serves as a tool to estimate the sequence of the appearance of different flow patterns with change in the gas and liquid flow rates for a given set of flow conditions. The definitions of flow patterns and their transitions are highly qualitative in nature and are mostly based on the individual's perception. Although some researchers have attempted to develop quantitative methods such as the probabilistic flow regime mapping and power spectral density analysis of the acquired pressure signal to predict the existence of certain flow patterns, these methods are not universal and are mostly limited to certain flow conditions. Moreover, these methods also rely upon prior information of visual inspection of flow patterns. The purpose of this section is to present an overview of the effect of pipe orientation on the transition between different two phase flow patterns. The flow pattern maps for different pipe orientations are presented with reference to the horizontal flow pattern map. It should be mentioned that the flow pattern maps presented in this section are developed for two phase flow of air water through a 12.7 mm I.D. pipe at different orientations and are applicable for similar flow conditions. The flow pattern maps for each orientation in upward and downward inclinations are presented in Figs. 4.14 to 4.17.

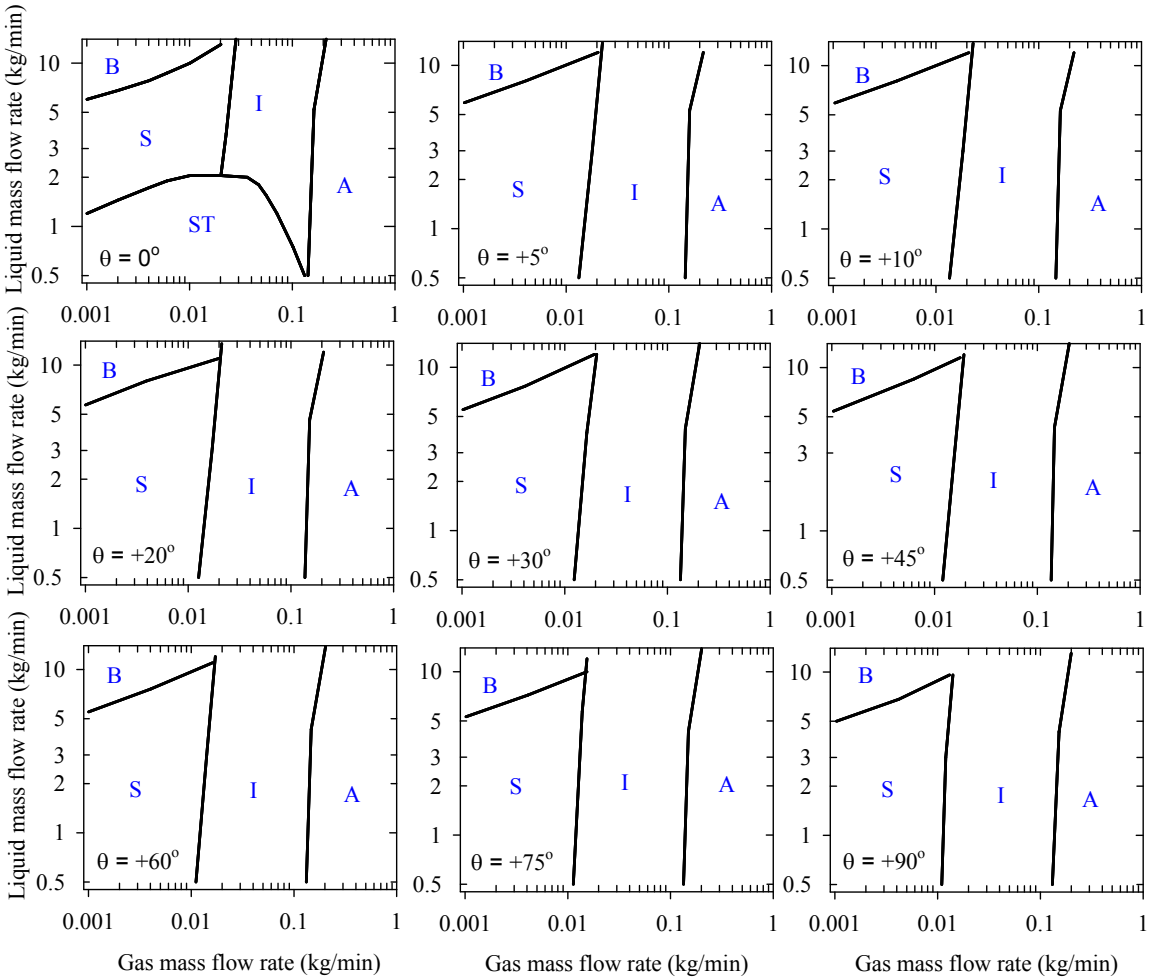

Figure 4.14: Flow pattern map for upward inclined two phase flow (B = Bubbly, S = Slug, I = Intermittent, A = Annular).

In case of both upward (Fig. 4.14) and downward (Fig. 4.16) inclined two phase flow, regardless of the pipe orientation, the bubbly flow occurs for low values of gas and high values of liquid mass flow rates. Whereas, the annular flow exists for low liquid and high values of gas mass flow rates. In the present study for the annular flow regime, due to limitation on the mass flow meters it was possible to visualize annular flow regimes only up to $\dot{m}_L \approx 5.5$ kg/min and $\dot{m}_G \approx 0.2$ kg/min. The separation line between intermittent and annular flow regime is extended further this point for higher liquid mass flow rates based on the trend of the transition line. In case of upward inclined two phase flow, slug flow exists at low to moderate liquid flow rates and low

gas flow rates. The boundary between slug and intermittent flow is influenced by the change in pipe orientation. It is found that the increase in pipe orientation from horizontal causes this transition boundary to shift towards lower gas flow rates. This is possibly because increase in the pipe orientation assists buoyancy and facilitates formation (agglomeration of gas bubbles) and motion of gas slugs.

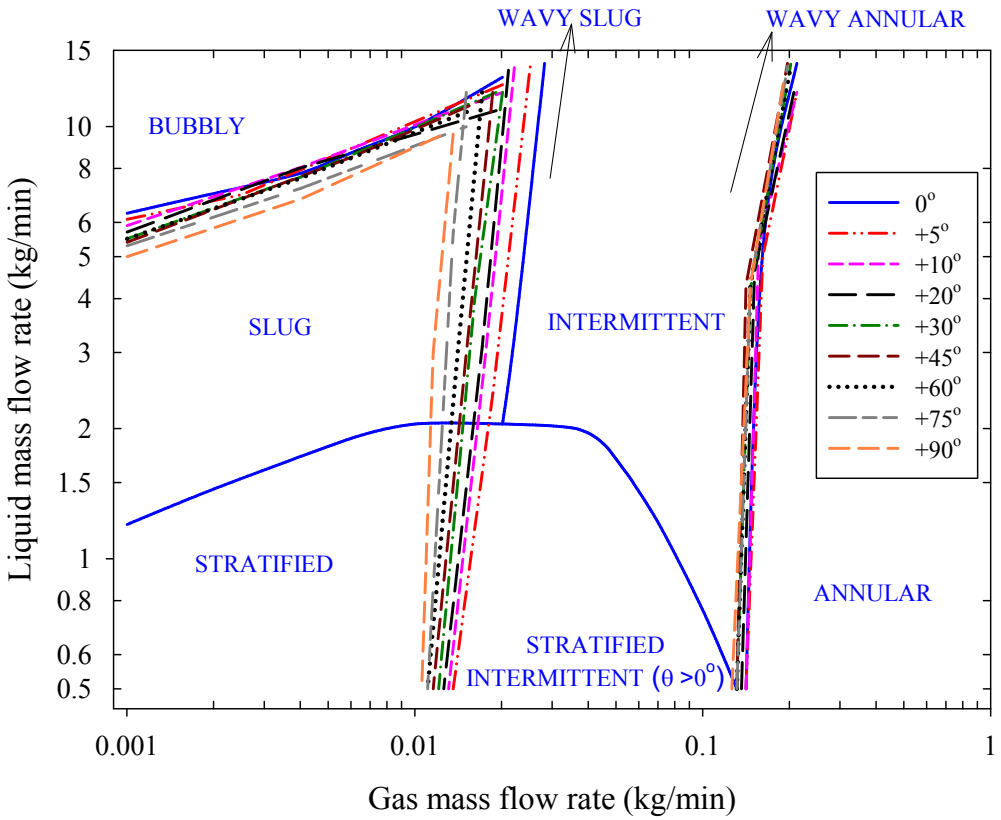

Figure 4.15: Combined flow pattern map for upward inclined pipe orientations.

The transition between intermittent and annular flow regime is virtually unaffected by the pipe orientation due to the fact that this is a shear driven flow regime where the pipe orientation has a little effect on the physical structure of this flow pattern. However, during intermittent flow regime, an early transition from wavy slug to wavy annular flow could be observed with increase in the upward pipe inclination. The transition boundary between bubbly and slug flow is also found to be affected by the change in pipe orientation. The increase in pipe orientation from horizontal

in upward direction causes early transition from slug to bubbly flow. This observation is consistent with the findings of Mukherjee (1979) who experimented with two phase flow of air-kerosene in inclined systems. The transition between bubbly-slug, slug-intermittent and intermittent-annular is evident from Fig. 4.15. In case of horizontal flow at low liquid flow rates, a short region of intermittent flow exists between the transition from stratified to annular. The intermittent flow pattern identified in this narrow range of gas flow rates is mostly wavy-annular in nature. At low liquid flow rates approximately 0.5 kg/min, stratified flow directly transits to annular flow without entering into intermittent flow regime.

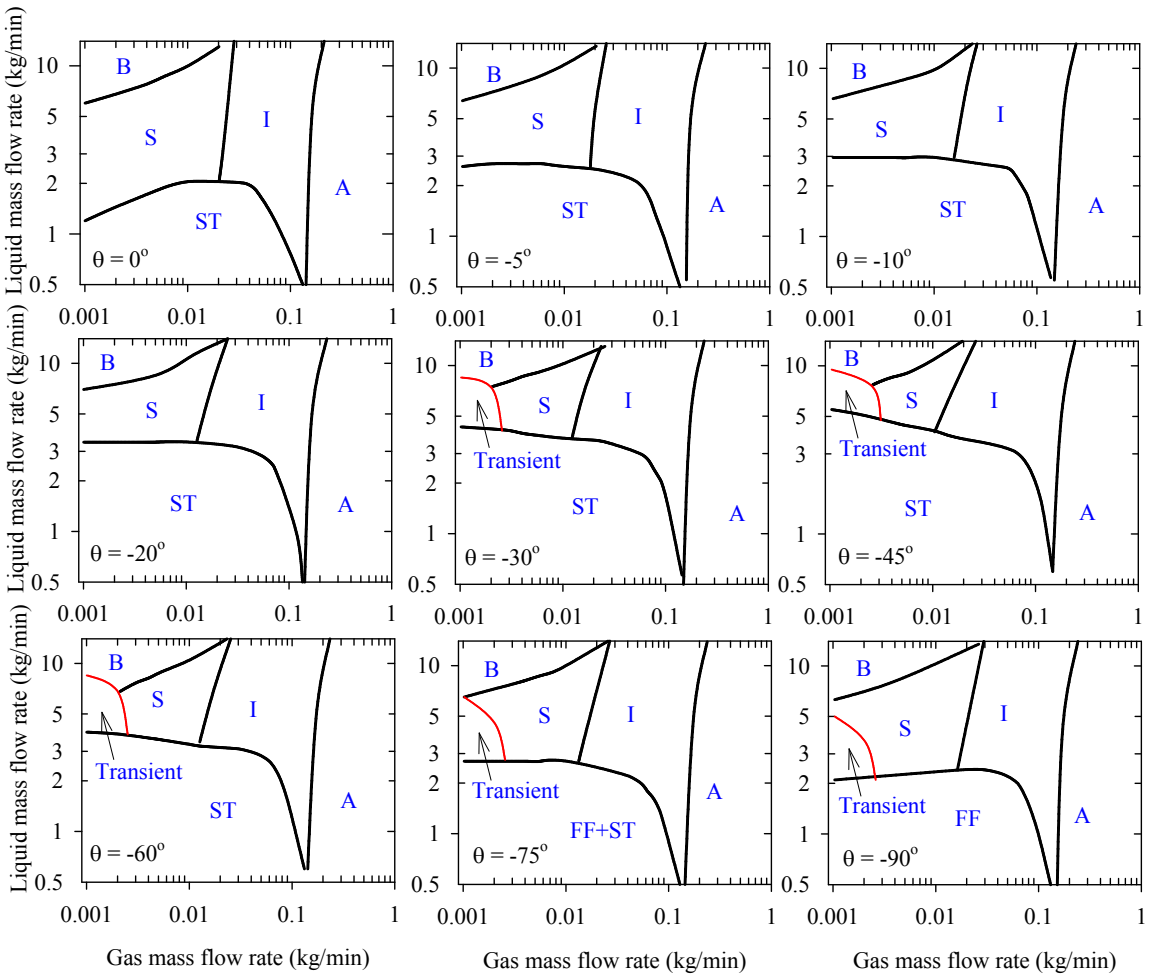

Figure 4.16: Flow pattern map for downward inclined two phase flow (B = Bubbly, S = Slug, I = Intermittent, ST = Stratified, A = Annular, FF = Falling film).

In case of downward inclined two phase flow (Fig. 4.16), the transition between

stratified-slug and slug-intermittent flow regimes is seen to be significantly affected by the change in pipe orientation. As mentioned earlier, the stratified flow appears for low liquid and low to moderate gas flow rates and exist for horizontal and all downward inclinations considered in this study. It is found that the increase in downward pipe inclination expands the region occupied by the stratified flow on the flow pattern map towards higher liquid flow rates and at the expense of slug and intermittent flow regimes.

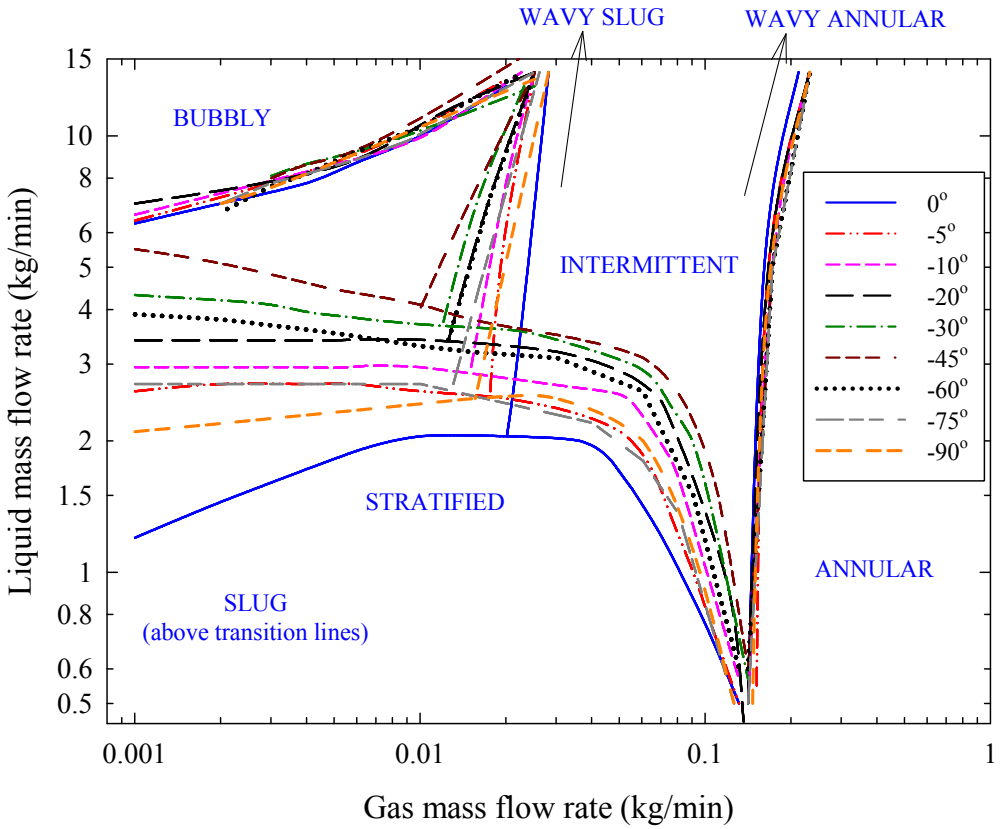

Figure 4.17: Combined flow pattern map for downward inclined pipe orientations.

It is seen from Fig. 4.17 that for low gas flow rates ($\dot{m}_G < 0.01$ kg/min), the transition boundary between stratified and slug flow consistently shifts towards higher liquid flow rates with increase in the gas flow rate up to -45^o from horizontal. With further increase in downward pipe inclination, the transition line between stratified and slug flow shifts back to lower liquid flow rates. For lower gas flow rates, it is found

that the stratified flow exists for liquid flow rates as high as 5.5 kg/min for -45^o pipe orientation. With further increase in pipe orientation at -60^o, the stratified flow cannot sustain beyond liquid flow rate of 4 kg/min. For moderate gas flow rates ($0.01 \leq \dot{m}_G \leq 0.05$ kg/min), the transition between stratified and intermittent flow regime is very gradual (as a function of liquid flow rate and relatively independent of gas flow rate) until a threshold value of the gas flow rate is attained where the gas liquid surface becomes significantly unstable and the liquid phase is splashed frequently on the pipe top wall. This is the point where the flow pattern gradually shifts to intermittent (wavy annular) flow and the transition line between stratified and intermittent flow patterns is steep and very sensitive to the change in gas and liquid flow rates. Fig. 4.17 shows that this threshold value of gas mass flow rate is a function of pipe orientation i.e., it increases until $\theta = -45^o$ and then decreases thereafter. Note that for $\theta = -75^o$, falling film flow coexists with stratified flow at low liquid and low to moderate gas flow rates. At this near vertical pipe orientation, the edges of gas-liquid interface climb up the tube periphery such that it occupies most of the pipe circumference. With increase in liquid flow rate, a thin film of liquid is observed at the pipe upper wall and falling film flow is said to exist. As mentioned earlier, falling film flow is a special case of stratified flow for vertical and near vertical downward pipe orientations and hence no distinction is made between these two phase flow patterns on the flow map in Fig. 4.16. For vertical downward pipe inclination ($\theta = -90^o$), stratified flow is always in form of falling film due to flow symmetry.

Qualitatively, this observation is consistent with the flow visualization experiments of Nguyen (1975) and Crawford et al. (1985). The flow pattern maps in downward pipe inclinations reported by Barnea et al. (1982) show qualitatively similar trends in terms of the increase and decrease in the stratified flow regime at steeper pipe inclinations beyond -45^o from horizontal. However, their flow pat-

tern maps reported in Fig. 4.18 show that for intermediate pipe orientations of $-10^o > \theta > -70^o$, stratified flow directly transits to dispersed bubbly flow without entering the slug/intermittent flow regime. Furthermore, as shown in Fig. 4.18, Barnea et al. (1982) also suggest that at low gas flow rates and steeper downward pipe inclinations ($-70^o > \theta > -89^o$), annular and intermittent flow patterns separate stratified and dispersed bubbly flow.

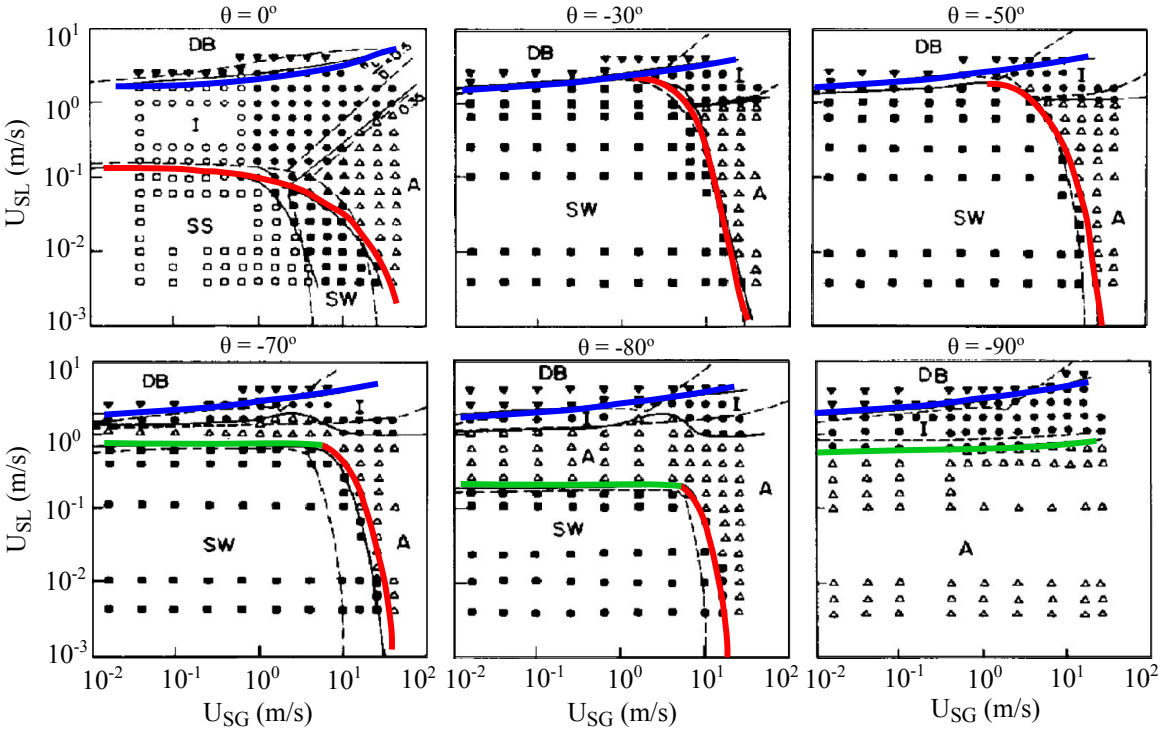

Figure 4.18: Flow pattern maps for downward pipe inclination adapted from Barnea et al. (1982).

Finally, for vertical downward pipe inclination, Barnea et al. (1982) reports existence of annular flow pattern from low to high values of gas flow rates. Considering the flow physics and definition of annular flow pattern (wavy liquid film surrounding fast moving turbulent gas core that results into significant interfacial shear and liquid entrainment), this observation of existence of annular flow pattern at low gas flow rates seems to be unlikely. Moreover, for fixed and low values of gas flow rates, the transition from stratified to annular, then from annular to intermittent and finally from intermittent to dispersed bubbly seems to be improbable. This transition implies

that for fixed gas flow rate and increasing liquid flow rate, void fraction first increases (during stratified-annular flow transition) and then decreases drastically (during annular to dispersed bubbly flow). These observations are inconsistent with the flow visualization experiments carried out in this study as well as those reported in the literature by Crawford et al. (1985) and Nguyen (1975).

In case of transition between slug and intermittent flows, with increase in the downward pipe inclination, the transition boundary is found to shift towards lower gas flow rates up to $\theta = -45^o$ and then slightly moves towards higher gas flow rates thereafter. Similar to upward inclined flows, the transition between intermittent and annular flows is virtually not affected by the change in the pipe orientation. For very low liquid flow rates $\dot{m}_L < 1$ kg/min it is found that the flow pattern shifts directly from stratified to annular without entering the intermittent flow regime. Typically for $\dot{m}_L < 2$ kg/min, the intermittent region is very narrow and is annular wavy in nature.

Another important observation made for downward pipe inclinations is the transient flow behavior at low gas flow rates. Fig. 4.16 show the region of transient two phase flow behavior in the vicinity of stratified-slug-bubbly flow patterns. In addition to the flow visualization, a differential pressure drop signal recorded over a period of time shows significant fluctuations as shown in Fig.4.19. A visual observation of the flow pattern in the transparent test section during the pressure drop data acquisition confirms the transient nature of two phase flow that exhibit combined behavior of stratified/slug/bubbly flow patterns. Visual observations show that these flow patterns repeat one after another continuously over a period of time without establishing one single flow pattern. A plausible explanation for this transient behavior can be given considering the physical structure of flow patterns. For the case of stratified flow with very little gas flow rate, the liquid phase accelerates downstream under the

influence of gravity while the gas phase is believed to either stay virtually stationary or attempt to move upstream under the influence of buoyancy. As the liquid phase

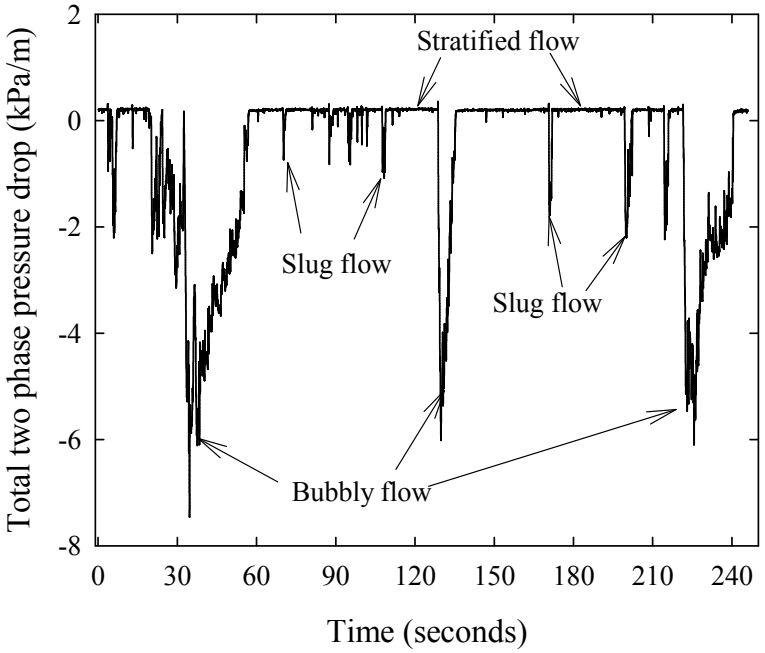

Figure 4.19: Transient nature of two phase flow in downward pipe orientations.

travels downstream it further accelerates and creates unstable gas-liquid interface. These instabilities splash liquid on the pipe upper wall and try to bridge the entire cross section such that it traps a gas pocket in form of slug flow. Slug flow pattern favors dominant buoyancy forces and consequently a pseudo stationary elongated gas pocket (gas slug) is observed in the test section. Meanwhile, the liquid phase coming from downstream direction gets accumulated on the top of pseudo stationary slug which further slips past the elongated gas bubble and eventually forces the gas bubble to move in the downstream direction. During this process, the liquid phase churns the elongated gas bubbles causing it to disintegrate and move further in form of discrete bubbles. After the gas pocket is pushed downstream the incoming two phase flow is in form of stratified flow pattern and this process repeats continuously showing stratified, bubbly and slug flow patterns periodically. A change in flow pattern from one to another (with significantly different flow structure) causes acceleration and

deceleration of the two phase mixture that results into pressure loss and pressure recovery of the system and hence results into an abrupt change in pressure drop signal similar to that shown in Fig. 4.19. It is found that this transient nature of two phase flow aggravates with increase in downward pipe inclination and propagates towards slightly higher gas flow rates.

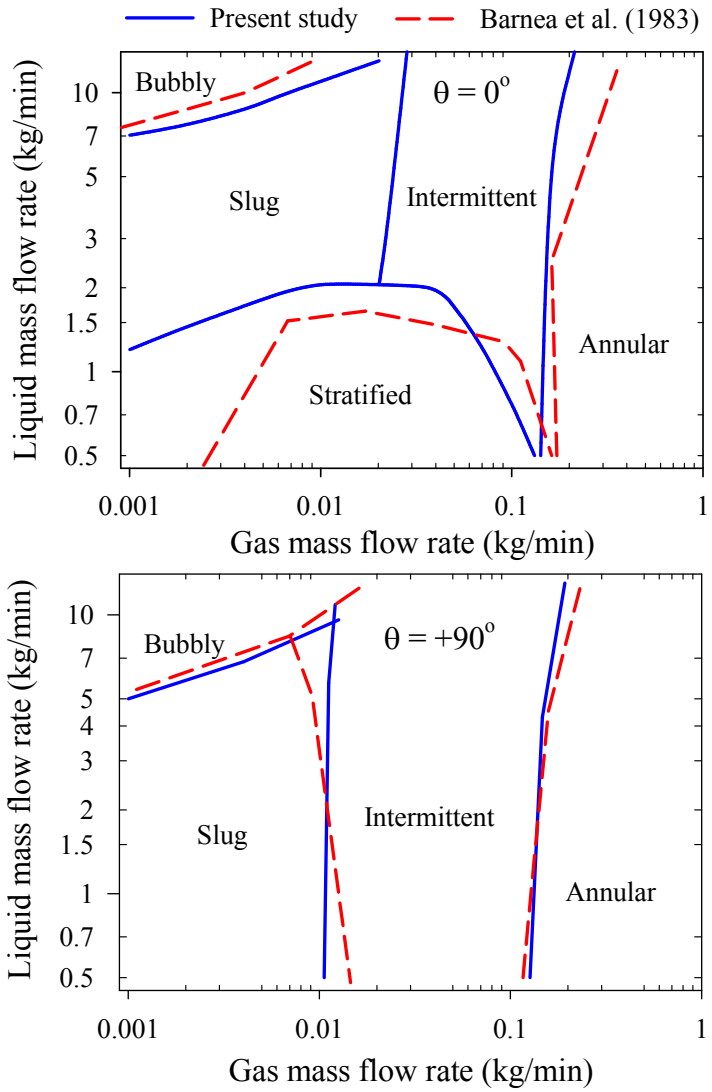

Figure 4.20: Comparison between transition boundaries observed in present study and that of Barnea et al. (1983).

It is also necessary to compare the flow pattern transition boundaries observed in the present study with that available in the literature. However, it should be

understood that any direct comparison between the present work and that available in the literature would be unjust unless the comparison is drawn between experiments having similar pipe diameter, fluid properties and other experimental conditions. Moreover, agreement in the exact appearance of the transition boundaries and hence the flow pattern map totally depends upon individuals understanding and the criteria of defining certain flow patterns. One such flow pattern map for horizontal and vertical upward flow for a 12.3 mm I.D. pipe using air-water fluid combination is presented by Barnea et al. (1983). The comparison between flow pattern maps for horizontal and vertical upward flow observed in present study and by Barnea et al. (1983) is presented in Fig. 4.20. It is seen that for horizontal flow, Barnea et al. (1983) observed late (at higher liquid flow rates) transition from slug to bubbly flow and early (lower liquid and gas flow rates) transition from stratified to slug/intermittent flow regimes. In case of vertical upward flow, a good agreement is observed between the transition lines observed in the present study and that of Barnea et al. (1983). However, Barnea et al. (1983) observed late transition from slug to bubbly flow and slightly early transition between slug and intermittent flow regime for $\dot{m}_L \geq 3$ kg/min. Barnea et al. (1983) also observed the effect of pipe diameter on the transition between different flow patterns for pipe diameters in a range of 4 to 12.3 mm. They concluded that the only transition boundary significantly affected by the change in pipe diameter is the boundary between stratified/slug and stratified/intermittent flows. With a decrease in pipe diameter, the area occupied by stratified flow on a flow pattern map shrinks towards higher gas flow rates and lower liquid flow rates. For small diameter pipes, any disturbance on the gas-liquid interface causes the liquid to touch the pipe wall thereby bridging the entire cross section. This flow situation is very conducive for the formation of slug and intermittent flows and hence for small diameter pipes; slug and intermittent flows occupy a bigger region on a flow pattern map compared to the stratified flow. This also concludes that with increase in the pipe diameter, stratified

flow may become one of the dominant flow patterns occupying a large region on the flow pattern map. Considering the fact that stratified flow exists in all downward inclinations, it can be speculated that the pipe diameter may significantly affect the transition between stratified and slug/intermittent flows in all downward pipe inclinations including the horizontal flow.

4.1.3 Stratified Flow Transition Model

It is presented in the previous section that the transition boundary between stratified-slug and stratified-annular flow is very sensitive to the change in downward pipe inclination. Considering the dependency and practical difficulty in modeling of two phase flow variables such as void fraction, pressure drop and two phase heat transfer in stratified two phase flow, it is desirable to have a stratified flow pattern specific model to predict these parameters. As such, it is first required to be able to correctly predict the existence of stratified flow as a function of phase flow rates, fluid properties and pipe orientation. This section presents a brief review of the mechanistic flow pattern transition model of Taitel and Dukler (1976) and an empirical model of Bhagwat and Ghajar (2015) to predict the transition to stratified flow in horizontal and downward pipe inclinations.

To predict the existence of stratified flow pattern in horizontal and downward inclined pipes, Taitel and Dukler (1976) proposed a mechanistic model based on the momentum balance of gas and liquid phase that requires calculation of several non-dimensional parameters. Additionally, their method also requires use of a graphical method to determine the non-dimensional liquid height in pipe. Using Taitel and Dukler (1976) model, the existence of stratified flow is expressed by Eq. (4.1) in non-dimensional form where F is the Froude number given by Eq. (4.2). The non-dimensional parameters $\tilde{U}_G$ and $\tilde{A}_G$ are function of non-dimensional liquid height

($\tilde{h}_L = h_L/D$). Use of Eq. (4.1) requires a graphical solution for $\tilde{h}_L$ given in Fig. 4.21 where X is the Lockhart and Martinelli (1949) parameter (See Chapter II) and Y is defined by Eq. (4.3), respectively.

$$F^2 \left[\frac{1}{(1-\tilde{h}_L)^2} \frac{\tilde{U}_G \sqrt{1-2(\tilde{h}_L-1)^2}}{\tilde{A}_G} \right] < 1 \tag{4.1}$$

$$F = \frac{U_{SG}}{\sqrt{gD\cos\theta}} \sqrt{\frac{\rho_G}{\rho_L - \rho_G}} \tag{4.2}$$

$$Y = \frac{(\rho_L - \rho_G) g \sin\theta}{|(dP/dL)_G|} \tag{4.3}$$

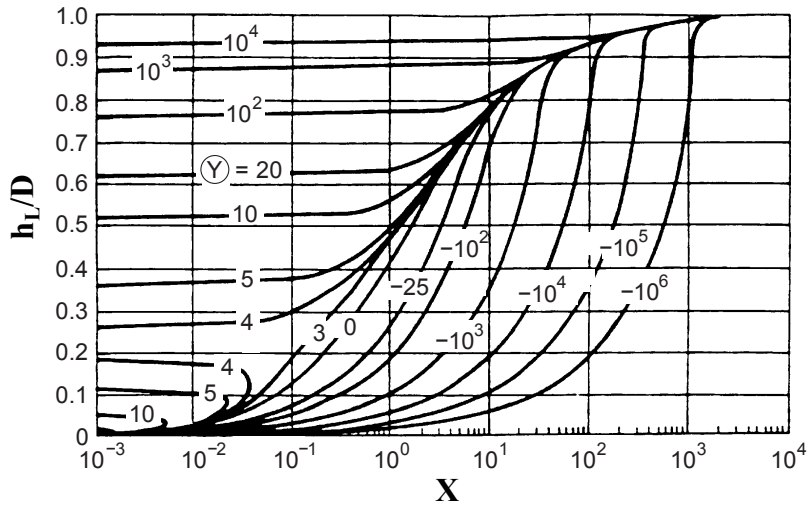

Figure 4.21: Graphical solution for $\tilde{h}_L$ (adapted from Taitel and Dukler (1976)) .

This graphical solution is obtained for equilibrium stratified flow by solving for momentum equation for each phase and is based on the assumption that the pressure drop in gas phase is equal to the pressure drop in liquid phase. Furthermore, it also assumes that the interfacial friction factor is same as that of the gas friction factor i.e., $f_i \approx f_G$ and that during the transition $U_G >> U_i$. Note that the involvement of a graphical solution with log scales for abscissa (X) and Y parameters necessary in determination of $\tilde{h}_L$ and hence calculation of other non-dimensional parameters

makes the use of Taitel and Dukler (1976) model a cumbersome task. Furthermore, it also adds to the uncertainty of the traced values of $\tilde{h}_L$ and hence the solution of Eq. (4.1). An alternate way to circumvent the use of this graphical solution is to solve the momentum balance equation for stratified flow using iterative technique. However, this approach requires several equations to be solved simultaneously to determine the unknown non-dimensional liquid height ($\tilde{h}_L$).

$$\tau_{wG}\frac{p_G}{A_G} - \tau_{wL}\frac{p_L}{A_L} + \tau_i p_i \left(\frac{1}{A_L} + \frac{1}{A_G}\right) - (\rho_L - \rho_G) g \sin\theta = 0 \tag{4.4}$$

$$X^2 \left[(\tilde{U}_L \tilde{D}_L)^{-n} \tilde{U}_L^2 \frac{\tilde{p}_L}{\tilde{A}_L}\right] - \left[(\tilde{U}_G \tilde{D}_G)^{-m} \tilde{U}_G^2 \left(\frac{\tilde{p}_G}{\tilde{A}_G} + \frac{\tilde{p}_i}{\tilde{A}_L} + \frac{\tilde{P}_i}{\tilde{A}_G}\right)\right] + 4Y = 0 \tag{4.5}$$

$$\tilde{A}_L = 0.25\left[\pi - \arccos(2\tilde{h}_L - 1) + (2\tilde{h}_L - 1)\sqrt{1 - (2\tilde{h}_L - 1)^2}\right] \tag{4.6}$$

$$\tilde{A}_G = 0.25\left[\arccos(2\tilde{h}_L - 1) - (2\tilde{h}_L - 1)\sqrt{1 - (2\tilde{h}_L - 1)^2}\right] \tag{4.7}$$

$$\tilde{p}_L = \pi - \arccos(2\tilde{h}_L - 1) \tag{4.8}$$

$$\tilde{p}_G = \arccos(2\tilde{h}_L - 1) \tag{4.9}$$

$$\tilde{p}_i = \sqrt{1 - (2\tilde{h}_L - 1)^2} \tag{4.10}$$

$$\tilde{D}_L = \frac{4\tilde{A}_L}{\tilde{p}_L} \tag{4.11}$$

$$\tilde{D}_G = \frac{4\tilde{A}_G}{\tilde{p}_G + \tilde{p}_i} \tag{4.12}$$

The combined momentum balance equation (for gas and liquid phase) is written in form of Eq. (4.4) and could be expressed in non-dimensional form given by Eq. (4.5). The associated non-dimensional parameters are given by Eqs. (4.6) to (4.12). The exponents m and n are taken to be 1 and 0.2 for laminar and turbulent single phase flows, respectively. The non-dimensional liquid and gas velocity is defined as $\tilde{U}_L = \pi/4\tilde{A}_L$ and $\tilde{U}_G = \pi/4\tilde{A}_G$, respectively. Thus, the use of a graphical solution to

solve for Eq. (4.1) could be avoided only at the expense of solving several equations simultaneously to satisfy Eq. (4.5) and obtain converged values of $\tilde{h}_L$. Note that this method is based on the assumption of $f_i \approx f_G$ (recommended by Taitel and Dukler (1976)) and use of a different closure relationship to model f_i/f_G ratio may yield slightly different values of F and X for which the stratified flow would exist. Although, the Taitel and Dukler (1976) model is a mechanistic model and accounts for the downward pipe inclinations, the goodness of this correlation is found to be restricted to the near horizontal downward pipe inclinations.

Another correlation developed for stratified flow in downward pipe inclinations is that of Crawford et al. (1985). The empirical correlation of Crawford et al. (1985) is in dimensional form and requires solution of two separate equations to determine the existence of the stratified flow. The physical form of the stratified flow criterion of Crawford et al. (1985) is given by Eq. (4.13). This equation if satisfied, separates stratified flow from slug and intermittent two phase flow but does not guarantee distinction between stratified and annular two phase flow. To distinguish between stratified and annular flows, Crawford et al. (1985) have adopted Eq. (4.14) given by Weisman and Kang (1981) for annular flow. Note that Eq. (4.14) is developed to predict existence of annular flow pattern and not the stratified flow. The flow pattern map of Crawford et al. (1985) shows a common boundary between stratified and annular flows and hence if Eq. (4.14) is not satisfied for annular flow, it is intuitive that stratified flow would exist for given two phase flow conditions. In Eq. (4.14), the non-dimensional Kutateladze number is defined as $Ku_{SG} = (U_{SG}\rho_G^2)/(g\Delta\rho\sigma)^{0.25}$. Thus, for stratified flow to exist, Eq. (4.13) must be satisfied as well as the liquid superficial velocity (U_{SL}) must be less than that predicted by Eq. (4.14).

$$U_{SL} < \begin{cases} U_{SG}(4U_{SG}/\sqrt{gD})^{-0.909} & : \theta = 0^o \\ U_{SG}\left[\dfrac{U_{SG}/\sqrt{gD}}{0.32(1+4\times\sin 1.95|\theta|)\exp(12/(3+|\theta|))}\right]^{-0.909} & : -90^o < \theta < 0^o \end{cases} \tag{4.13}$$

$$U_{SL} \geq U_{SG}\left[\frac{1.9}{Ku_{SG}^{0.2}(U_{SG}^2/gD)^{0.18}}\right]^8 \tag{4.14}$$

Above transition model of Crawford et al. (1985) is essentially developed based on the data for downward inclined two phase flow of refrigerant R-113 in 25.4 mm I.D. pipe. Lips and Meyer (2012b) compared correlations of both Crawford et al. (1985) and Taitel and Dukler (1976) against the two phase flow of refrigerant R-134a in downward inclined pipes. They found the correlation of Crawford et al. (1985) to perform better than Taitel and Dukler (1976). They reported Taitel and Dukler (1976) to consistently under predict the two phase mixture mass flux for which stratified flow would exist. Furthermore, they also concluded that since the correlation of Taitel and Dukler (1976) is essentially developed for air-water two phase flow, it cannot handle significantly different physical properties of liquid refrigerant and its vapor and hence needs to be adapted for varying two phase flow conditions.

Thus, considering these complexities in Taitel and Dukler (1976) model and use of different equations for different two phase flow conditions/flow patterns in calculation of stratified flow transition using Crawford et al. (1985) and Weisman and Kang (1981) models, it is desired to have a one single correlation that can predict the transition between stratified and non-stratified flows (slug, intermittent and annular) as one single curve. Bhagwat and Ghajar (2015) presents one such correlation in non-dimensional form using superficial gas Froude number (Fr_{SG}) and Lockhart-Martinelli parameter (X) as coordinates. The parameter X is as defined as $X = \sqrt{(dP/dL)_L/(dP/dL)_G}$ while the gas phase Froude number is the modified form of

Eq. (4.2) presented in Eq. (4.15) such that $Fr_{SG} = F\sqrt{\cos\theta}$. The physical form of the model that separates stratified flow from non-stratified flow patterns is given by Eq. (4.16). Thus, stratified flow will exist for all values of Fr_{SG} that satisfy Eq. (4.16). This equation is developed based on the range of physical parameters shown in Table 4.1.

$$Fr_{SG} = \frac{U_{SG}}{\sqrt{gD}}\sqrt{\frac{\rho_G}{\rho_L - \rho_G}} \tag{4.15}$$

$$Fr_{SG} \leq (0.6 + C_2)\left[\frac{\exp(-Z_1 Z_2 X^{Z_3})}{X^{Z_4}}\right] \tag{4.16}$$

$$Z_1 = 1.3\ln(D/D_{ref}) + 2.5 \tag{4.17}$$

$$Z_2 = \frac{Z_4^{0.65}}{[1 + 2\sin(2|\theta|) \times (1 + 10\tanh(1/|\theta|))]} \tag{4.18}$$

$$Z_3 = \begin{cases} 0.65\left(\Delta\rho/\rho_{ref}\right)\left(D/D_{ref}\right)^{-0.15} & : \rho_L \leq 1000\ \text{kg/m}^3 \\ 0.65\left(D/D_{ref}\right)^{-0.15} & : \rho_L > 1000\ \text{kg/m}^3 \end{cases} \tag{4.19}$$

$$Z_4 = 0.2\sqrt{D_{ref}/D} \tag{4.20}$$

$$G_{max} = (0.6 + C_2)\left[\frac{\exp(-Z_1 Z_2 X^{Z_3})}{X^{Z_4}}\right]\frac{\sqrt{\rho_G(\rho_L - \rho_G)gD}}{x} \tag{4.21}$$

Table 4.1: Summary of the range of experimental data used to develop the proposed model.

Parameter	Range
Pipe diameter (D)	8.9 - 300 mm
Pipe orientation (θ)	$0^o \leq \theta < -90^o$
Liquid density (ρ_L)	780 - 1420 kg/m^3
Gas density (ρ_G)	1.2 - 35 kg/m^3
Liquid viscosity (μ_L)	0.0002 - 0.08 Pa-s

The variables Z_1, Z_2, Z_3 and Z_4 required to solve Eq. (4.16) are expressed by

Eqs. (4.17) to (4.20). Note that the ratio D/D_{ref} is the non-dimensional pipe diameter where D_{ref} = 25.4 mm (1 inch) is the reference pipe diameter used to non-dimensionalize pipe diameter. This particular value of 25.4 mm is chosen as a reference value since the experimental data used for this empirical correlation development exhibited a change in trends of Fr_{SG} vs. X at this threshold value of 25.4 mm I.D. pipe. Similarly, based on the experimental data, liquid density of 1000 kg/m^3 is used as a reference value (ρ_{ref}) to account for the effect of liquid density on the transition to stratified flow. Though the correlation of Bhagwat and Ghajar (2015) is of empirical form, it is explicit in nature, do not require any iterative or graphical solution and very well predicts the transition/separation between stratified and non-stratified (slug, intermittent and annular flow) flow patterns as one single curve. Eq. (4.16) can be also casted in form of two phase mixture mass flux (G) given by Eq. (4.21). The maximum mass flux (G_{max}) calculated using this equation is the limiting value of G below which stratified flow would exist in a given two phase flow system. In Eq. (4.16), variables Z_1 and Z_2 account for the combined effect of pipe diameter and pipe orientation on the shift in transition line. This shift in the transition line obtained by including these variables is in accordance with the observations of Nguyen (1975), Crawford et al. (1985), Ghajar and Bhagwat (2014) and Barnea et al. (1982) that the increase in downward pipe inclination shifts the transition between stratified and non-stratified flow pattern towards higher values of liquid flow rates or alternatively the higher values of X. Note that the hyperbolic tangent term in variable C_2 is to account for the non-linear effect of pipe orientation on the transition line and is adjusted such that it complements the magnitude of sine function only for near horizontal pipe orientations while its contribution to the term Z_2 decreases with increase in the downward pipe inclination. Variable Z_3 ensures that the transition line between stratified and non-stratified flow is shifted towards higher values of X with a decrease in liquid phase density. This trend is consistent with the observation

of Taitel and Dukler (1976) and Barnea et al. (1982) that for the stratified-slug transition, energy of the gas phase must be large enough to lift the liquid phase and splash it on the pipe top wall. As such, the gas phase flow rate required for the inception of interfacial disturbance wave and hence the transition to non-stratified flow is proportional to the liquid phase density. Hence, for a fixed gas flow rate, decrease in liquid density would shift the transition line towards higher values of liquid flow rates or alternatively higher values of X. Based on the experimental data used to develop this model, liquid density of 1000 kg/m^3 is taken as a reference value to account for the effect of phase density on the shift in transition line. The low density liquid data used by Bhagwat and Ghajar (2015) consists of kerosene, light oil and mineral oil while the higher density liquid data consists of glycerol, refrigerants and potassium carbonate (K_2CO_3) solutions. The variables Z_1, Z_2, Z_3 and Z_4 are adjusted such that Z_1, Z_2, Z_3 controls the slope of transition line in the buoyancy driven region (large values of X) while Z_4 controls the slope of transition line in inertia driven region (small values of X). Eq. (4.16) is applicable for a wide range of pipe diameters, liquid phase densities and all downward pipe inclinations including horizontal. Comparison between the performance of Bhagwat and Ghajar (2015) and Taitel and Dukler (1976) model is presented below. Considering the goodness of Crawford et al. (1985) correlation for refrigerant two phase flow, performance of Bhagwat and Ghajar (2015) is also compared against this correlation only for two phase flow of refrigerants in horizontal and downward inclined pipes.

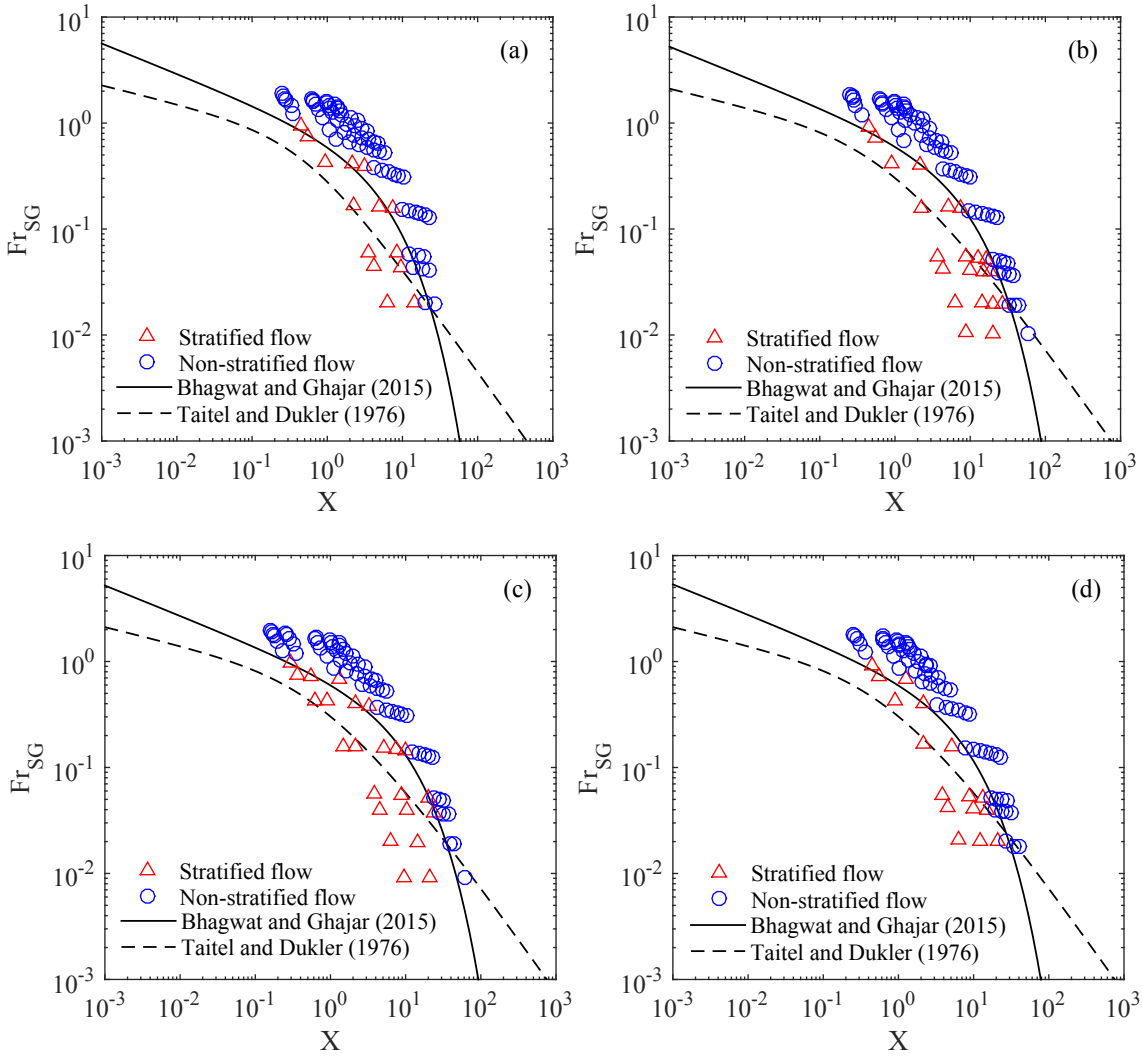

Figure 4.22: Prediction of stratified flow transition for downward inclined two phase flow of air-water in 12.7 mm I.D. pipe (a) -10^o, (b) -30^o, (c) -45^o, (d) -60^o (data measured at Two Phase Flow Lab, OSU).

The comparison between the Bhagwat and Ghajar (2015) and Taitel and Dukler (1976) for downward inclined two phase flow of air-water in 12.7 mm, 25.4 mm and 45.5 mm I.D. pipes is shown in Figs. 4.22, 4.23 and 4.24, respectively. The experimental data for stratified flow indicated by '△' consists of both smooth and wavy stratified flows while the non-stratified flow indicated by '◯' may consist of any or all of the bubbly, slug/intermittent and annular flow patterns. For horizontal two phase flow in both 25.4 mm and 45.5 mm I.D. pipes, Bhagwat and Ghajar (2015) model

gives performance comparable to that of Taitel and Dukler (1976). Overall it appears that the prediction of Taitel and Dukler (1976) improves with increase in the pipe diameter.

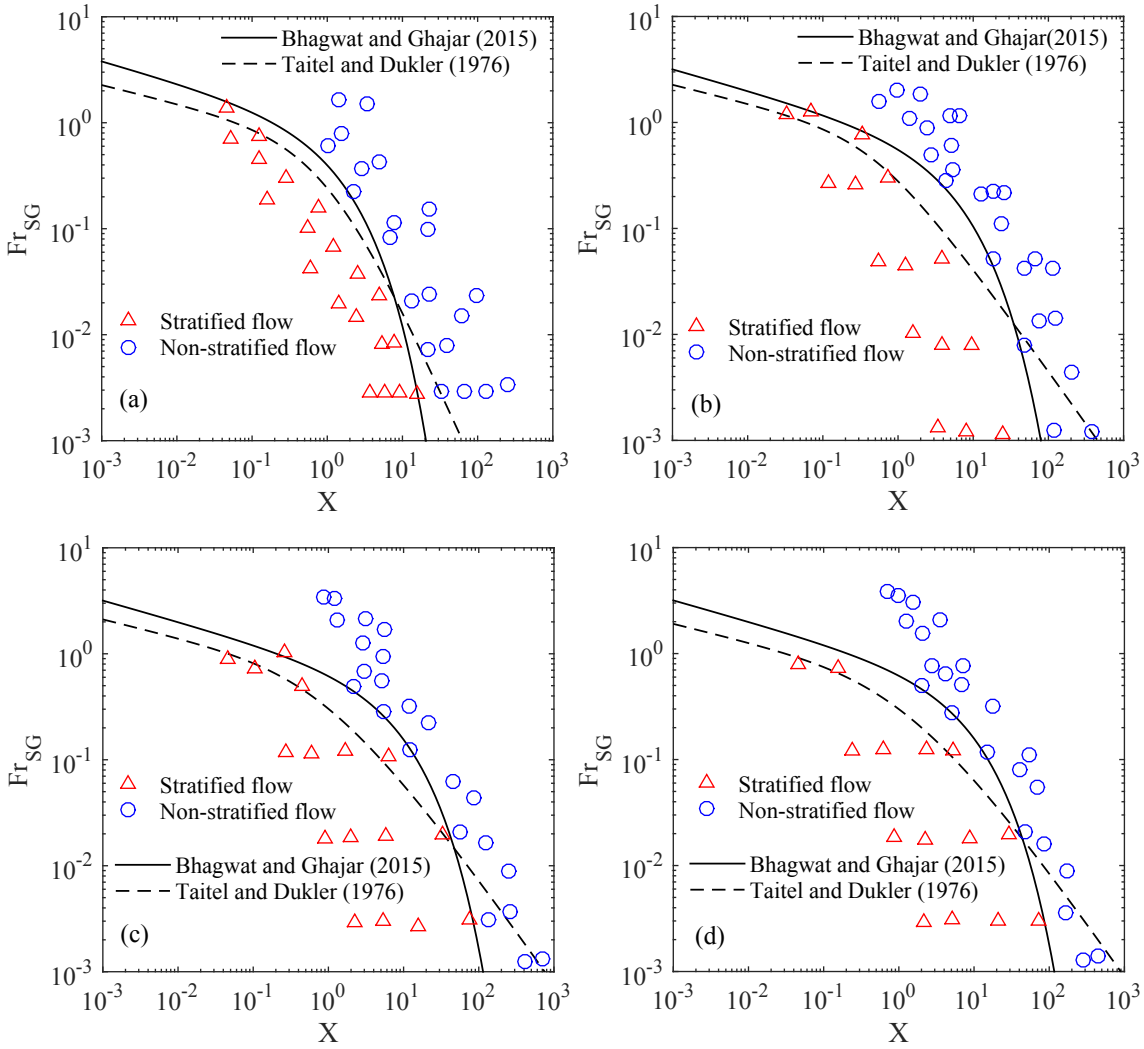

Figure 4.23: Prediction of stratified flow transition for horizontal and downward inclined two phase flow of air-water in 25.4 mm I.D. pipe (a) 0^o, (b) -10^o, (c) -30^o, (d) -50^o (data of Shoham (1982)).

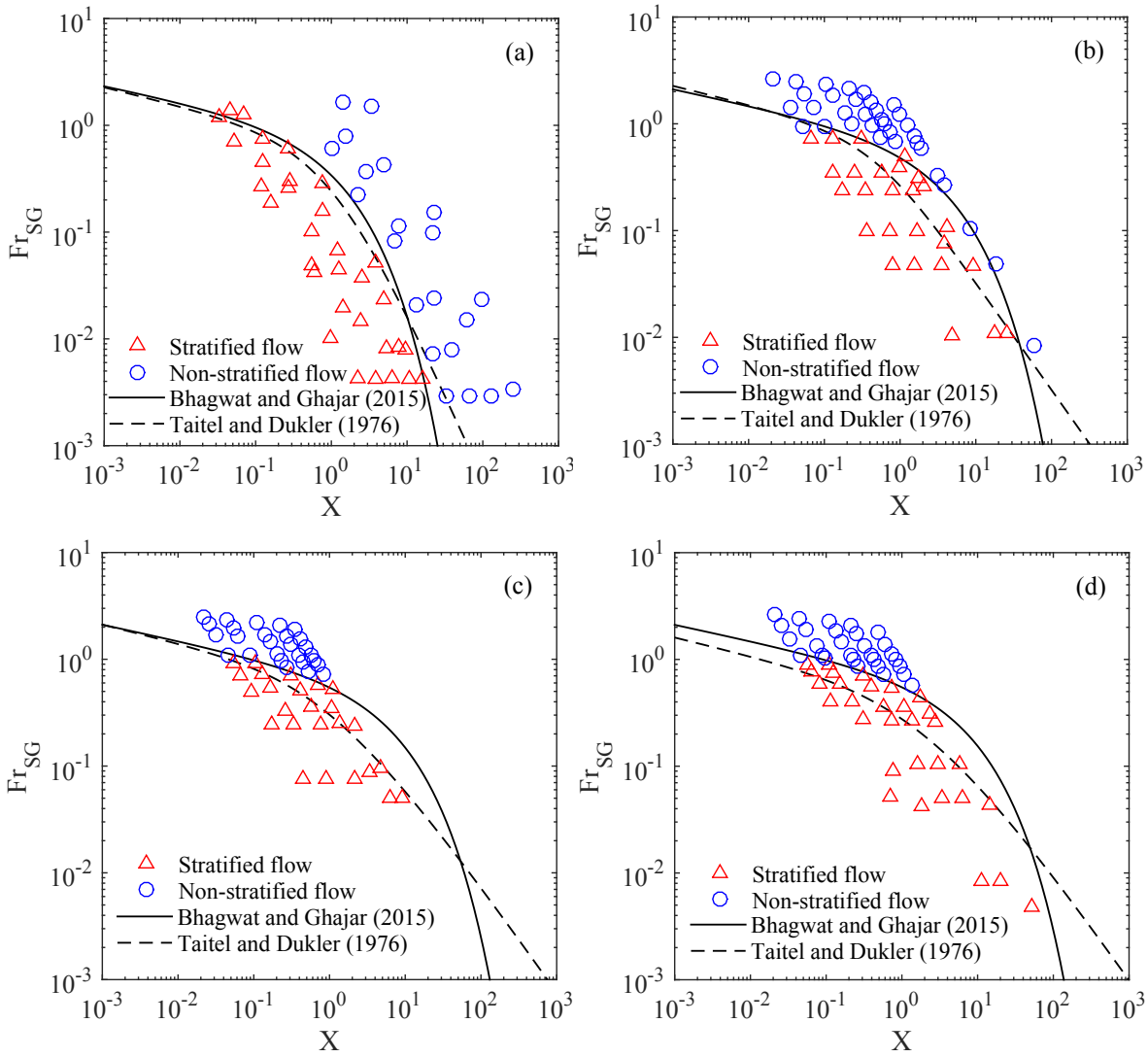

Figure 4.24: Prediction of stratified flow transition for horizontal and downward inclined two phase flow air-water in 45.5 mm I.D. pipe (a) 0^o, (b) -7^o, (c) -20^o, (d) -67^o (data of Nguyen (1975)).

Next, the performance of the Bhagwat and Ghajar (2015) is also compared against that of Taitel and Dukler (1976) for two phase flow of air-oil as shown in Figs. 4.25 and 4.26. It is clear from Fig. 4.25 that Taitel and Dukler (1976) consistently under predict the existence of stratified flow pattern. Comparatively, the Bhagwat and Ghajar (2015) model performs significantly better than Taitel and Dukler (1976) for both pipe orientations. For large pipe diameter of 101 mm (data of Kang

et al. (2002)), there is a rough agreement between the trends of the two models when $X < 0.1$ and $X > 100$. In the intermediate region of X values, the Bhagwat and Ghajar (2015) model performs significantly better than the model of Taitel and Dukler (1976).

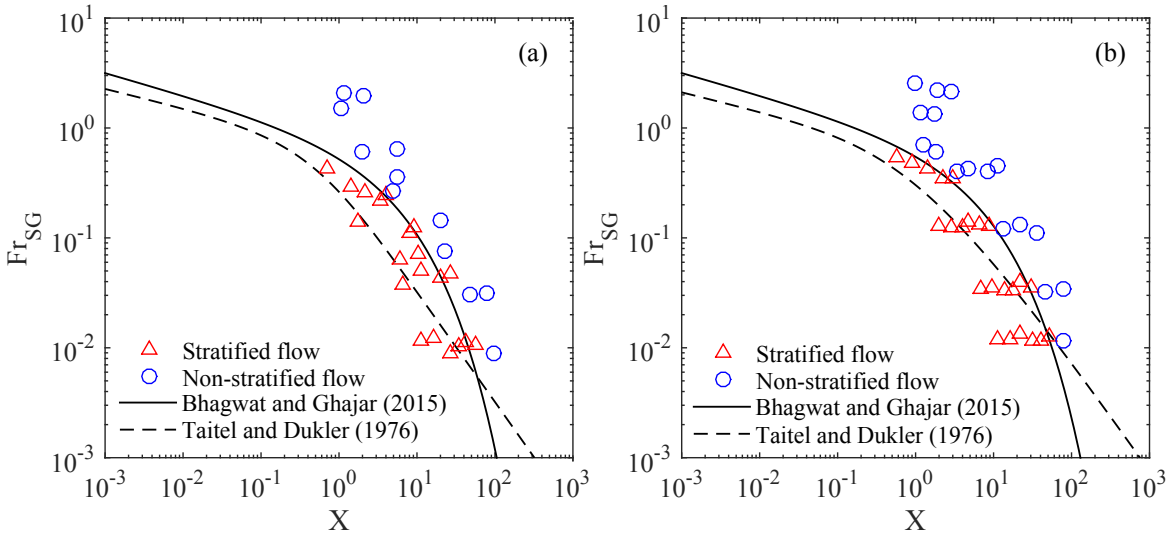

Figure 4.25: Prediction of stratified flow transition for downward inclined two phase flow of air-oil ($\rho_L = 860$ kg/m^3) in 25.4 mm I.D. pipe (a) -5^o and (b) -9^o (data of Kokal and Stanislav (1989a)).

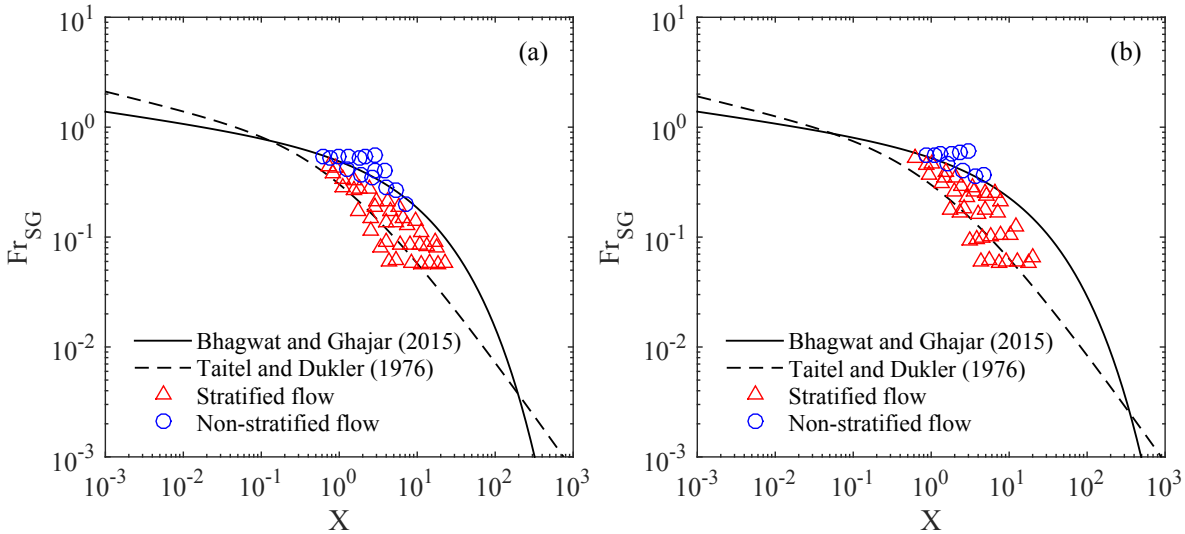

Figure 4.26: Prediction of stratified flow transition for downward inclined two phase flow of air-oil ($\rho_L \approx 910$ kg/m^3) in 101 mm I.D. pipe (a) -15^o and (b) -30^o (data of Kang et al. (2002)).

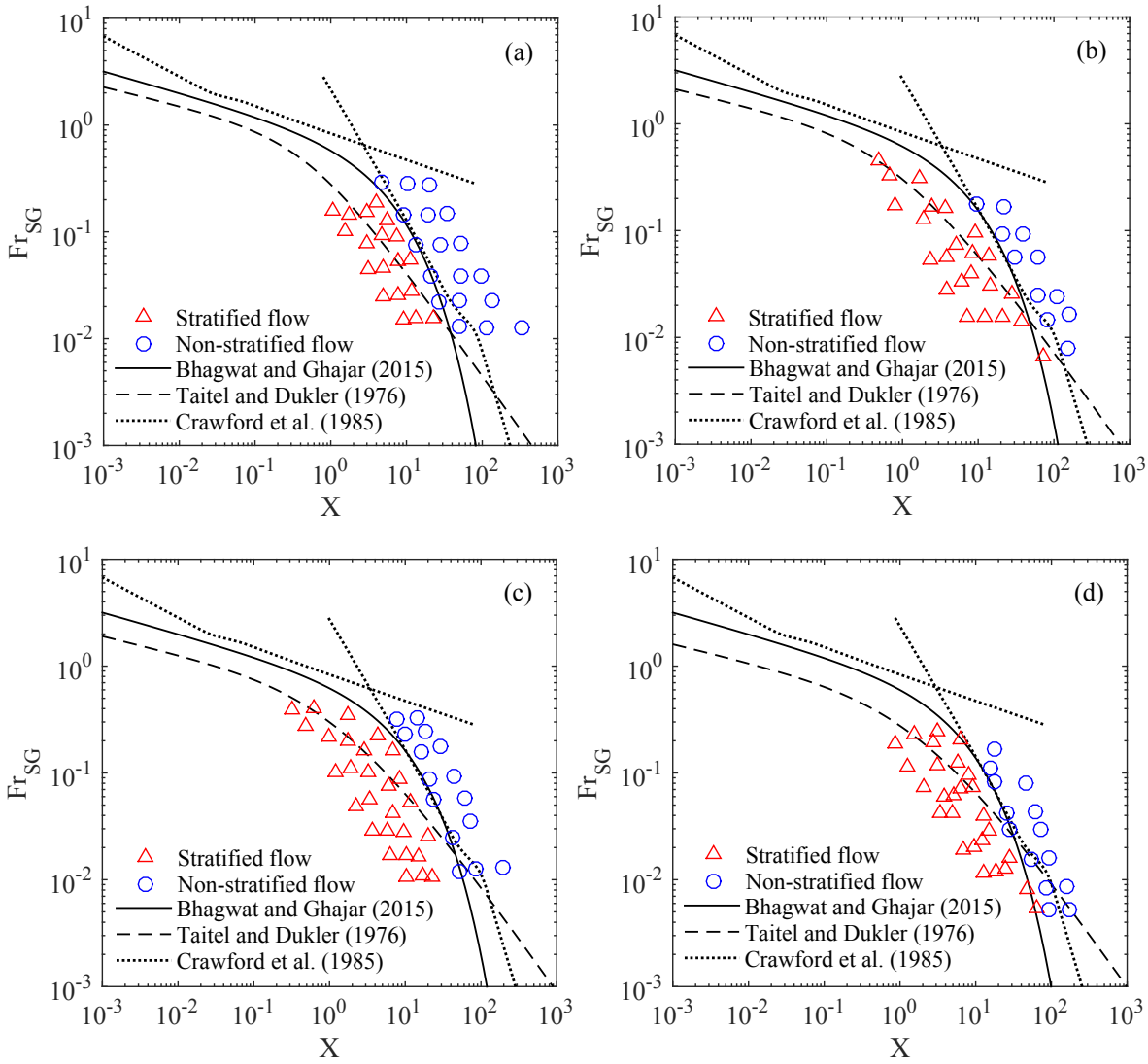

Figure 4.27: Prediction of stratified flow transition for downward inclined two phase flow of R-113 in 25.4 mm I.D. pipe (a) -15^o, (b) -30^o, (c) -45^o, (d) -60^o (data of Crawford et al. (1985)).

The performance assessment of the Bhagwat and Ghajar (2015) correlation for the two phase flow of refrigerants is shown in Figs. 4.27 to 4.29. The experimental data of Crawford et al. (1985) consists of two phase flow of R-113 in downward inclined pipes. As mentioned earlier, the correlation of Crawford et al. (1985) is also used here for comparison purpose. The correlation of Taitel and Dukler (1976) consistently under predicts the existence of stratified flow for all downward pipe inclinations. This

observation is in agreement with the findings of Lips and Meyer (2012b). The Bhagwat and Ghajar (2015) model in general is in good agreement with the predictions of Crawford et al. (1985) model and correctly separates stratified flow pattern from non-stratified flow patterns. Note that the Bhagwat and Ghajar (2015) model gives the transition to stratified flow in form of one single continuous line whereas the model of Crawford et al. (1985) is in form of two straight lines that intersect each other depending upon the two phase flow conditions. The kink observed in these straight lines is due to the shift in friction factor during laminar to turbulent flow transition required to transform the dimensional correlation into a non-dimensional form.

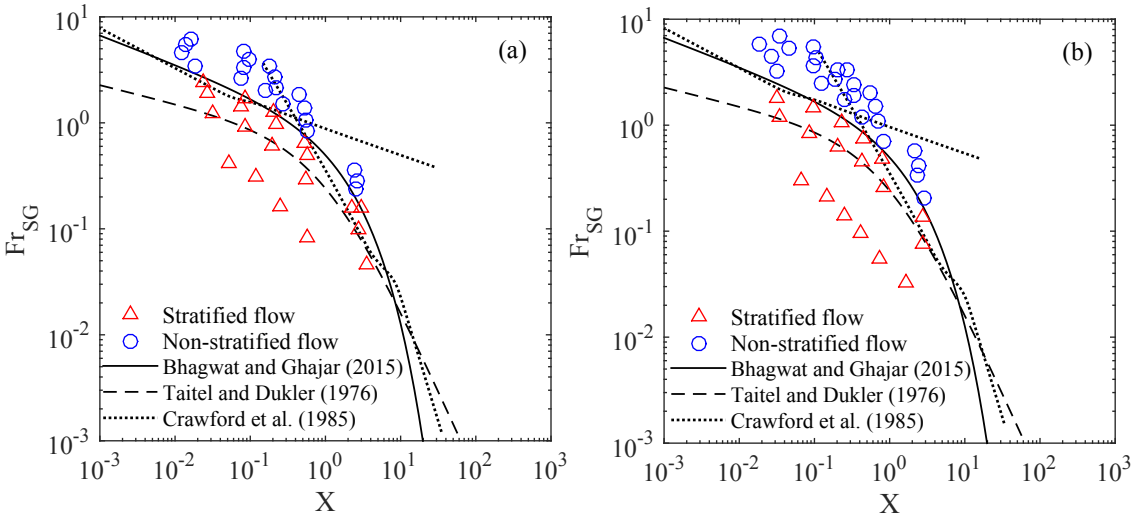

Figure 4.28: Prediction of stratified flow transition for horizontal two phase flow of refrigerants (data of Quiben and Thome (2007)) (a) D = 13.8 mm, ρ_L = 1265 kg/m^3, R-22 and (b) D = 13.8 mm, ρ_L = 1150 kg/m^3, R-410A.

The experimental flow visualization observations reported by Quiben and Thome (2007) in Fig. 4.28 also show a good agreement of the Bhagwat and Ghajar (2015) model with the predictions of Crawford et al. (1985). Similar trends are observed for the evaporating and condensing two phase flow data of Colombo et al. (2012) reported in Fig. 4.29. Based on the overall refrigerant two phase flow data it can be said that Taitel and Dukler (1976) under predicts the existence of stratified flow for

small values of X typically in the region $X < 1$. For the two phase flow of refrigerants, the stratified flow data consists of both stratified and wavy-stratified two phase flow while the non-stratified two phase flow essentially consists of the slug/intermittent, annular and annular-mist flow patterns.

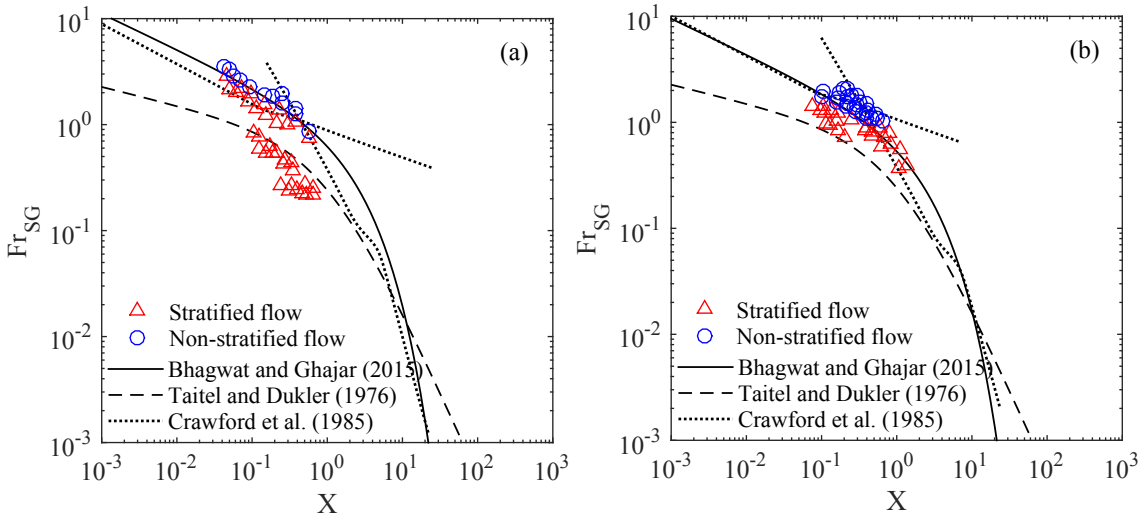

Figure 4.29: Prediction of stratified flow transition for horizontal two phase flow of R-134a in 8.9 mm I.D. pipe (a) evaporating flow and (b) condensing flow (data of Colombo et al. (2012)).

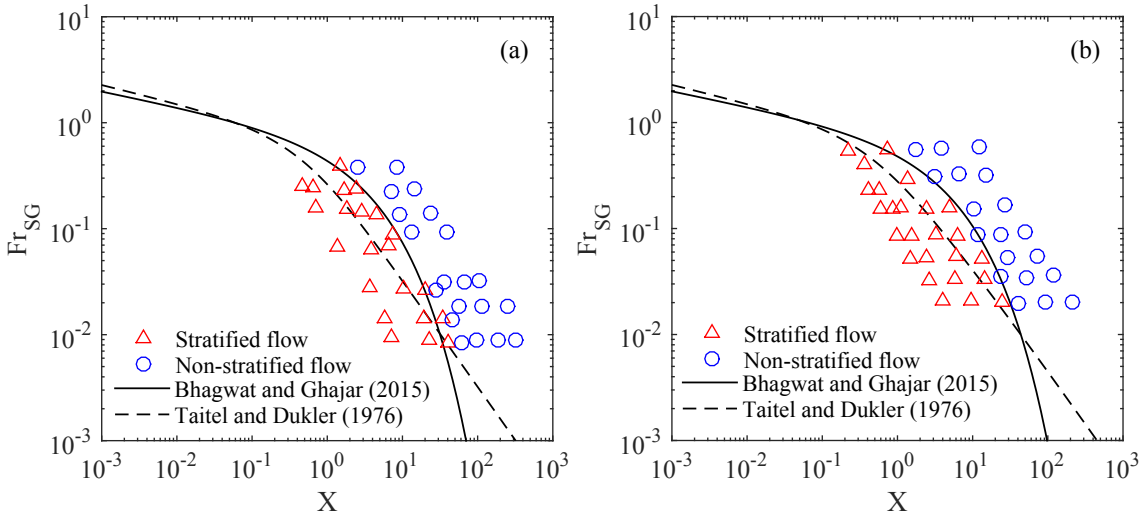

Figure 4.30: Prediction of stratified flow transition for downward inclined two phase flow of air-K_2CO_3 solution ($\rho_L = 1420$ kg/m^3) in 50.1 mm I.D. pipe (a) -2^o and (b) -7^o (data of Gibson (1981)).

Finally, the performance of Bhagwat and Ghajar (2015) and Taitel and Dukler (1976) for some non-conventional two phase flow fluid combinations such as air-potassium carbonate (K_2CO_3) solution is reported in Fig. 4.30. As shown in Fig. 4.30, for the air-potassium carbonate solution, Bhagwat and Ghajar (2015) model slightly under predicts the existence of stratified flow for -2^o of pipe orientation. However, its accuracy is better than that of Taitel and Dukler (1976). For $X < 0.1$, the trend of Bhagwat and Ghajar (2015) model is in good agreement with Taitel and Dukler (1976). From above discussion and comparisons, it is clear that Bhagwat and Ghajar (2015) model performs better than Taitel and Dukler (1976) at steeper downward pipe inclinations. Also, considering the practical difficulty in use of a graphical/iterative solution involved in Taitel and Dukler (1976) method, Bhagwat and Ghajar (2015) may be regarded as a quick explicit method for hand calculations and to get an estimate of the existence of stratified flow in horizontal and downward pipe inclinations. Bhagwat and Ghajar (2015) model is used in subsequent chapters of void fraction and pressure drop modeling to separate stratified flow from non-stratified flow patterns. Remainder of this chapter presents experimental results and a brief discussion on the parametric study of the effect of two phase flow variables on void fraction and two phase pressure drop.

4.2 Void Fraction

The void fraction in gas-liquid two phase flow is found to be influenced by several parameters such as flow rates of individual phases, pipe diameter, pipe orientation and fluid properties. What follows next is a detailed presentation and discussion on the experimental measurements of the void fraction as a function of phase flow rates and pipe orientation. In addition to this, with the aid of data reported in two phase flow literature, the effect of pipe diameter and fluid properties on the void fraction is also explored.

4.2.1 Effect of Phase Flow Rates and Flow Patterns

In the present study, void fraction is measured for flow patterns covering entire range of flow patterns such as bubbly, slug, stratified, intermittent and annular flow regimes. The bubbly flow is associated with the low values of void fraction typically $\alpha < 0.25$, slug, stratified and intermittent flows are found to be associated with the void fraction in a range of $0.25 < \alpha < 0.8$ while the annular flow pattern corresponds to the higher values of void fraction in a range of $0.75 < \alpha < 1$. The void fraction ranges and their association with different flow patterns is an approximation based on the overall data measured in the present study for different pipe orientations. These values are in agreement with the findings of Barnea (1987) and Smith (1969) who suggested a void fraction value of 0.25 and 0.75-0.8 corresponding to the onset of slug (departure from bubbly flow) and annular flows, respectively. The relation between void fraction and different flow patterns as a function of gas and liquid phase flow rates for different upward and downward pipe inclinations is depicted in Figs. 4.31 and 4.32, respectively. Since, the overall effect of phase flow rates on void fraction

is similar for all orientations in upward and downward directions, the experimental data for selected pipe orientations of $\pm 10^o, \pm 30^o, \pm 60^o$ and $\pm 90^o$ is presented.

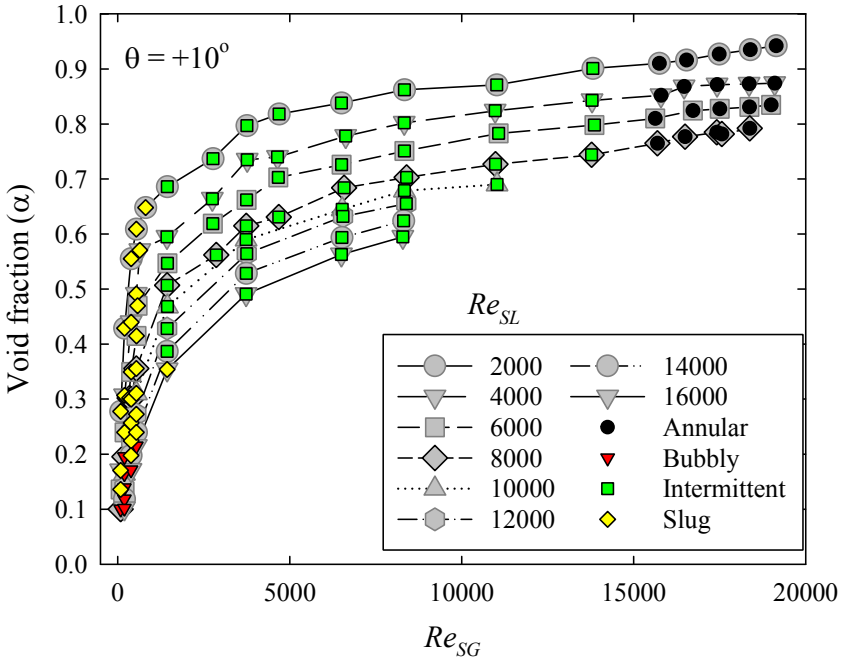

(a) $\theta = +5^o$

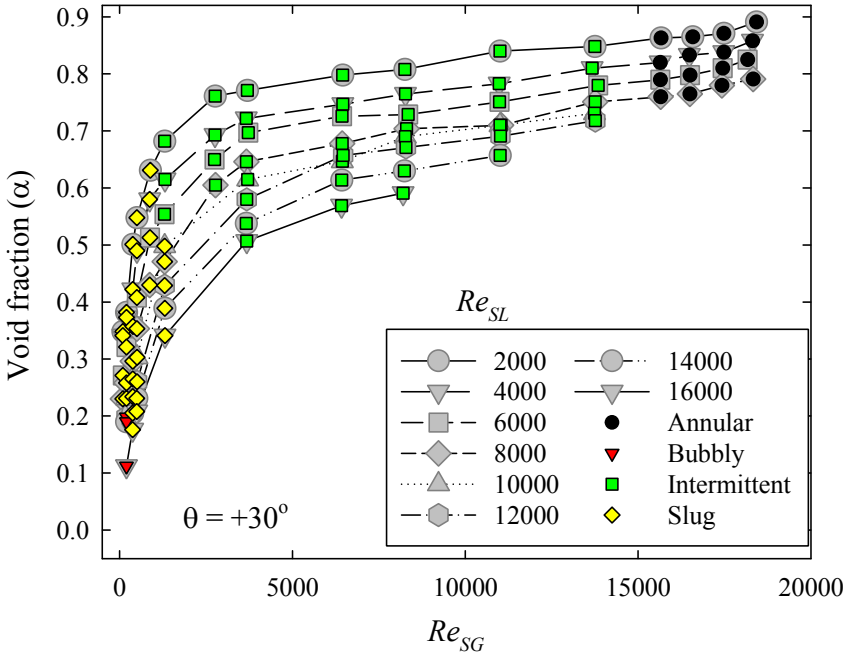

(b) $\theta = +30^o$

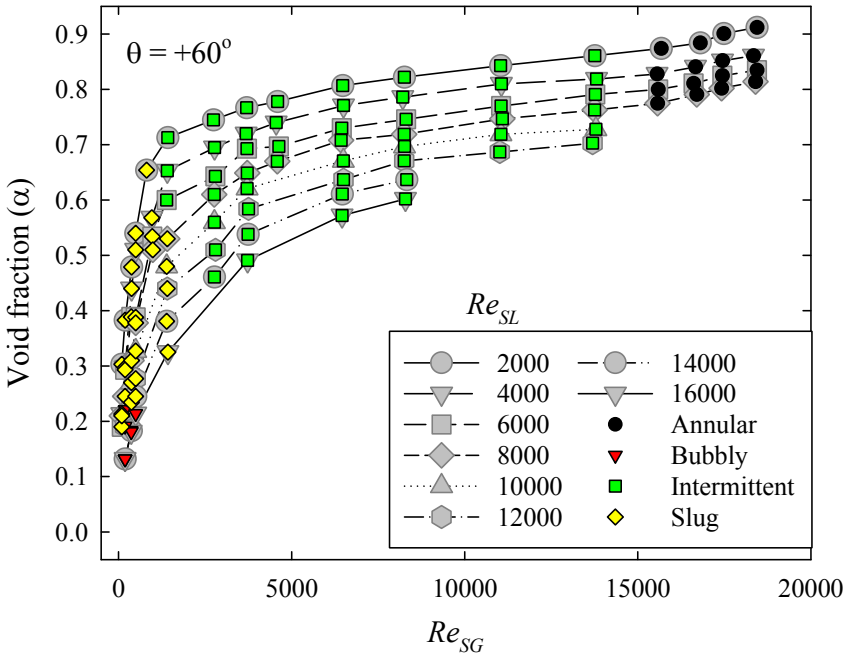

(c) $\theta = +60^o$

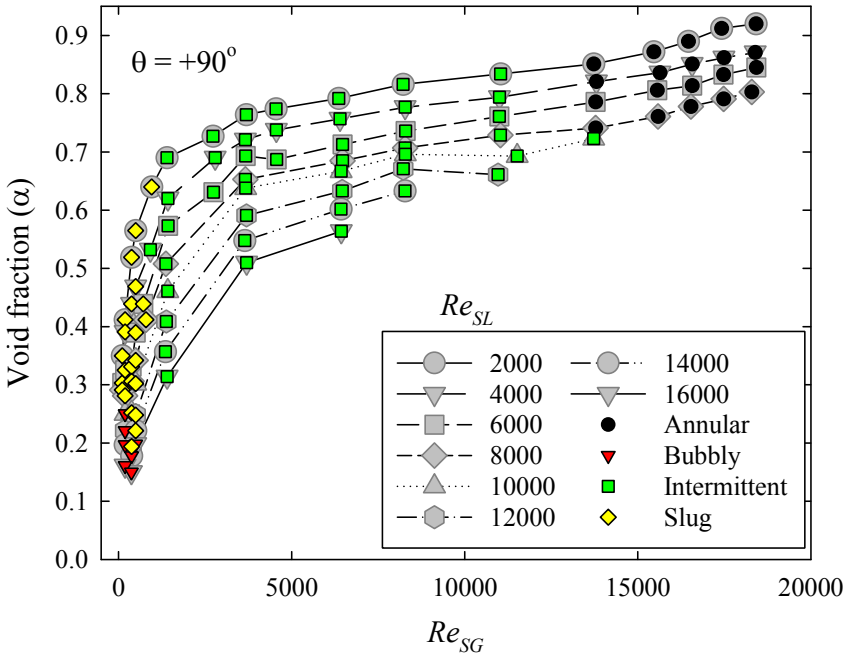

(d) $\theta = +90^o$

Figure 4.31: Effect of phase flow rate on void fraction in upward inclined two phase flow.

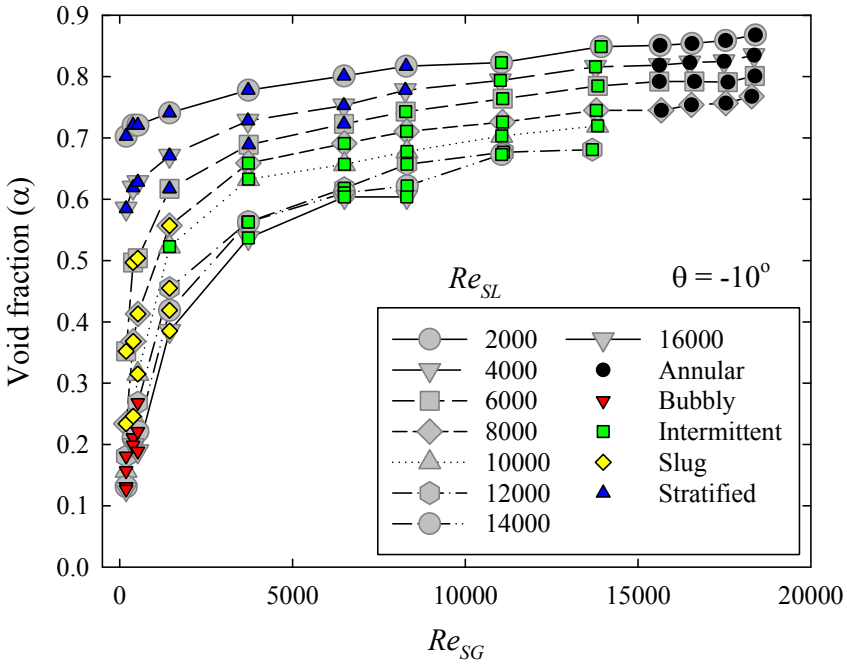

(a) $\theta = -5^o$

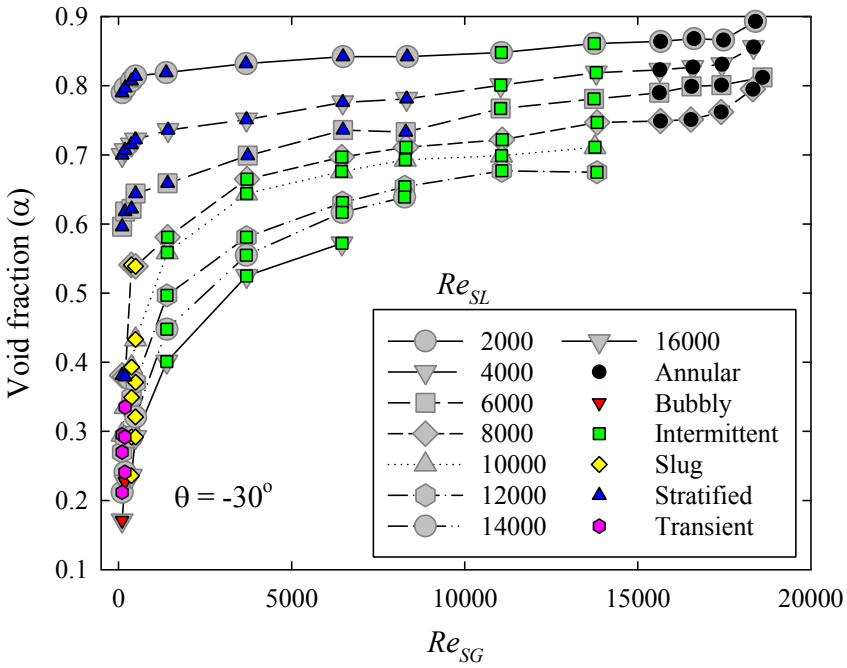

(b) $\theta = -30^o$

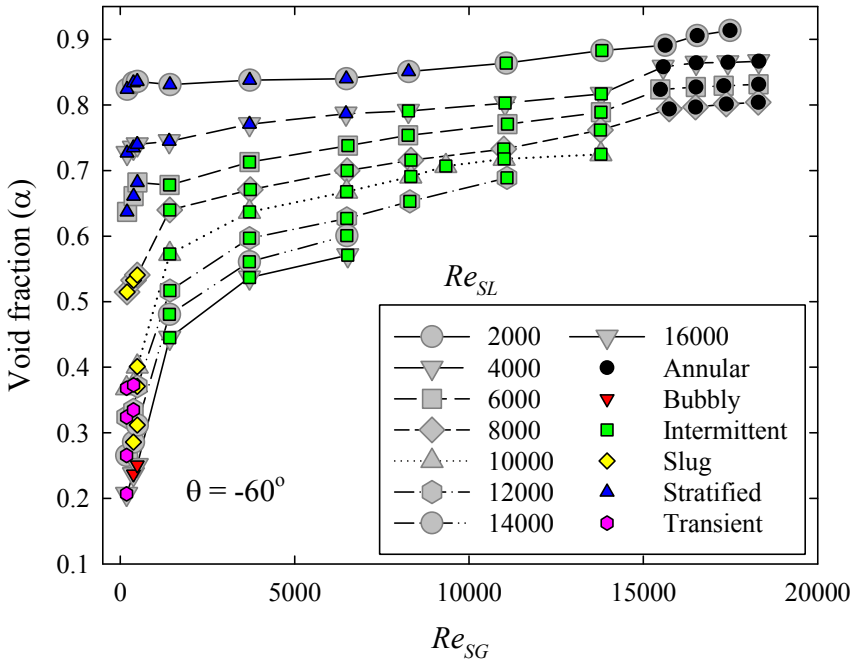

(c) $\theta = -60^o$

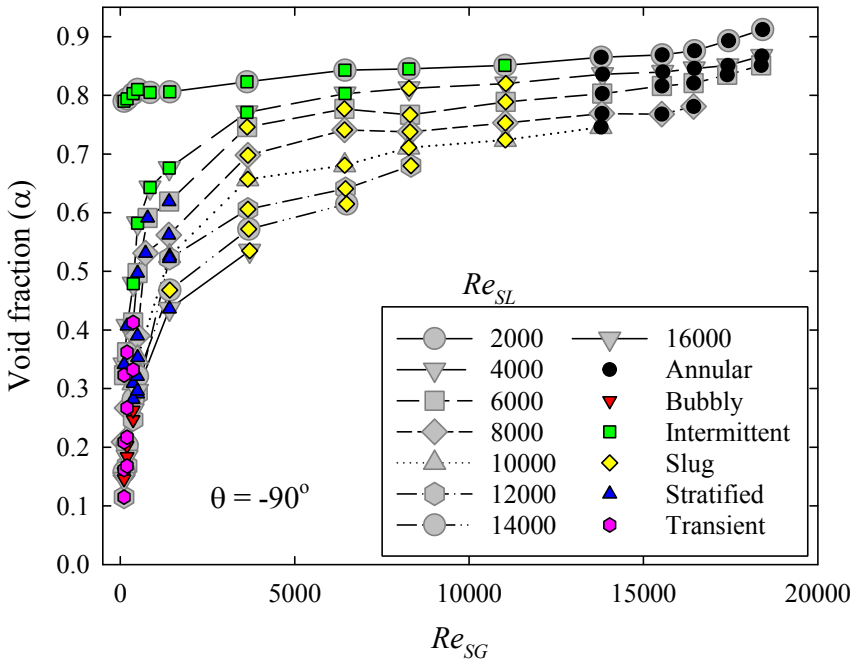

(d) $\theta = -90^o$

Figure 4.32: Effect of phase flow rate on void fraction in downward inclined two phase flow.

Overall it is found that the void fraction is very sensitive to the change in gas flow rates for bubbly and slug flow patterns. In these flow regimes, a small increase in gas flow rate causes the void fraction to increase rapidly. Whereas, in case of intermittent flow, void fraction is found to be sensitive to the gas flow rate during the onset of intermittent (slug wavy) flow. For higher gas flow rates, void fraction becomes relatively insensitive to the increase in gas flow rates corresponding to wavy and annular-wavy flow regimes. Finally for the annular flow regime, the void fraction is found to be virtually independent of the increase in gas flow rates. Similar relationship between flow patterns (phase flow rates) and void fraction is found to exist for all pipe orientations. In Figs. 4.31 and 4.32, void fraction data for selected liquid flow rates (Re_{SL}) is presented such that these flow rates cover all flow patterns and the entire range of void fraction. A comparison between void fraction data for upward and downward pipe inclinations at low liquid flow rates ($Re_{SL} \leq 4000$) and $Re_{SG} < 1400$ show that the void fraction in downward pipe inclinations is considerably higher than the upward inclinations. This is because the existence of stratified flow regime at these low liquid flow rates in downward inclinations promotes higher void fraction compared to slug flow in upward pipe orientations. More discussion on the effect of pipe orientation on void fraction is presented in next section.

In addition to phase flow rates, the measured void fraction is also plotted against the gas volumetric flow fraction (β) and is compared against the case of homogeneous void fraction assuming no slip condition ($\alpha = \beta$). The condition of $\alpha < \beta$ implies that the buoyancy acting on the gas phase is in the direction of flow and that there is a significant slippage ($S > 1$) between gas and liquid phase. As against this, the condition of $\alpha > \beta$ implies that the buoyancy force acting on the gas phase is in direction opposite to that of the two phase flow which retards the motion of gas phase (increases the residence time of the gas phase in test section) and would result in $S < 1$. As shown in Fig. 4.33 for all upward inclined pipe orientations

void fraction is always less than the gas volumetric flow fraction ($\alpha < \beta$) indicating that the buoyancy always acts on the gas phase in the direction of flow and slip ratio between the two phases is always greater than unity. In case of downward pipe inclinations it is seen from Fig. 4.34 that increase in the downward pipe inclination favors the effect of buoyancy force acting on the gas phase in direction opposite to that of the mean flow.

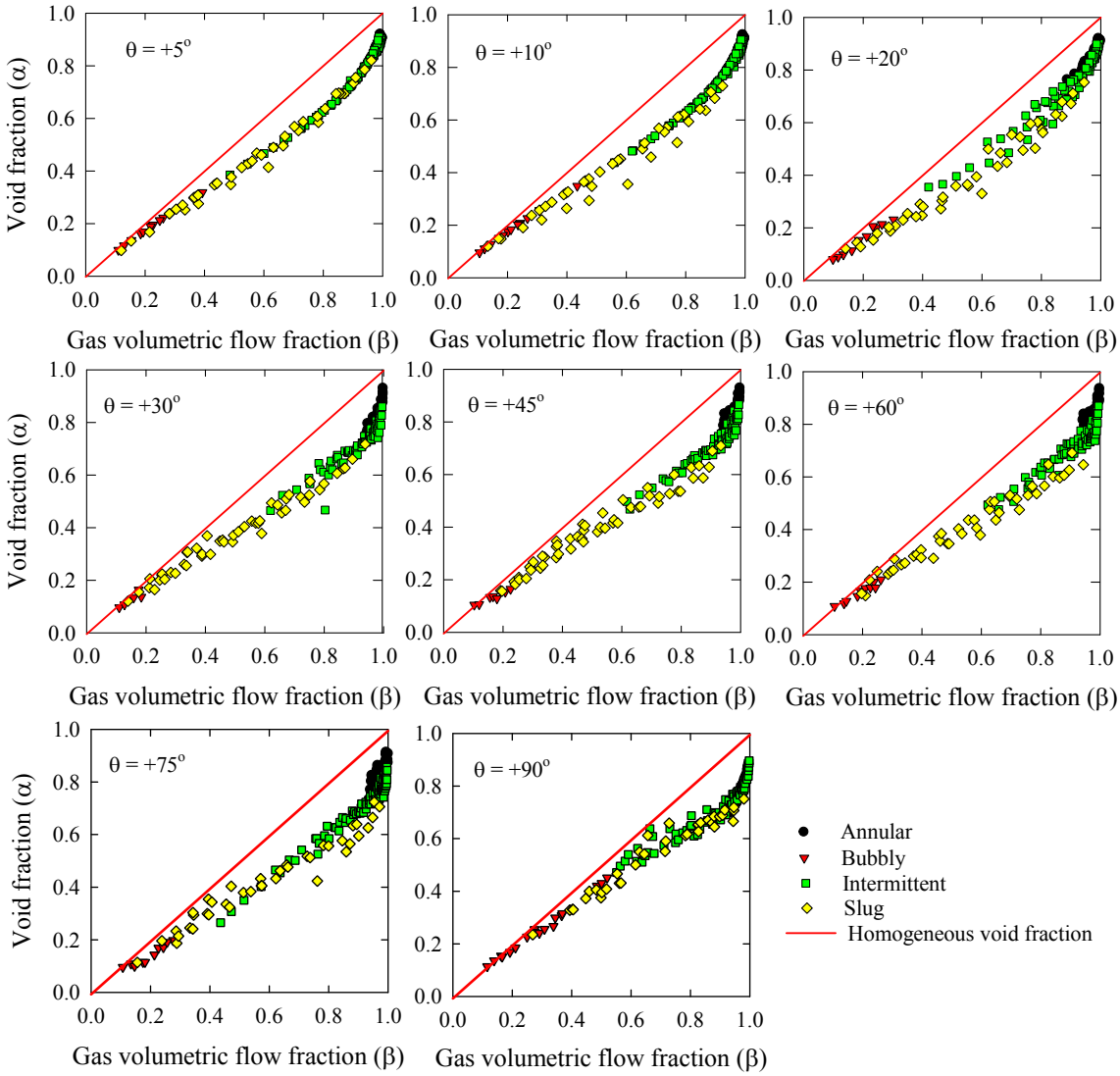

Figure 4.33: Void fraction vs. gas volumetric flow fraction for different upward inclined pipe orientations.

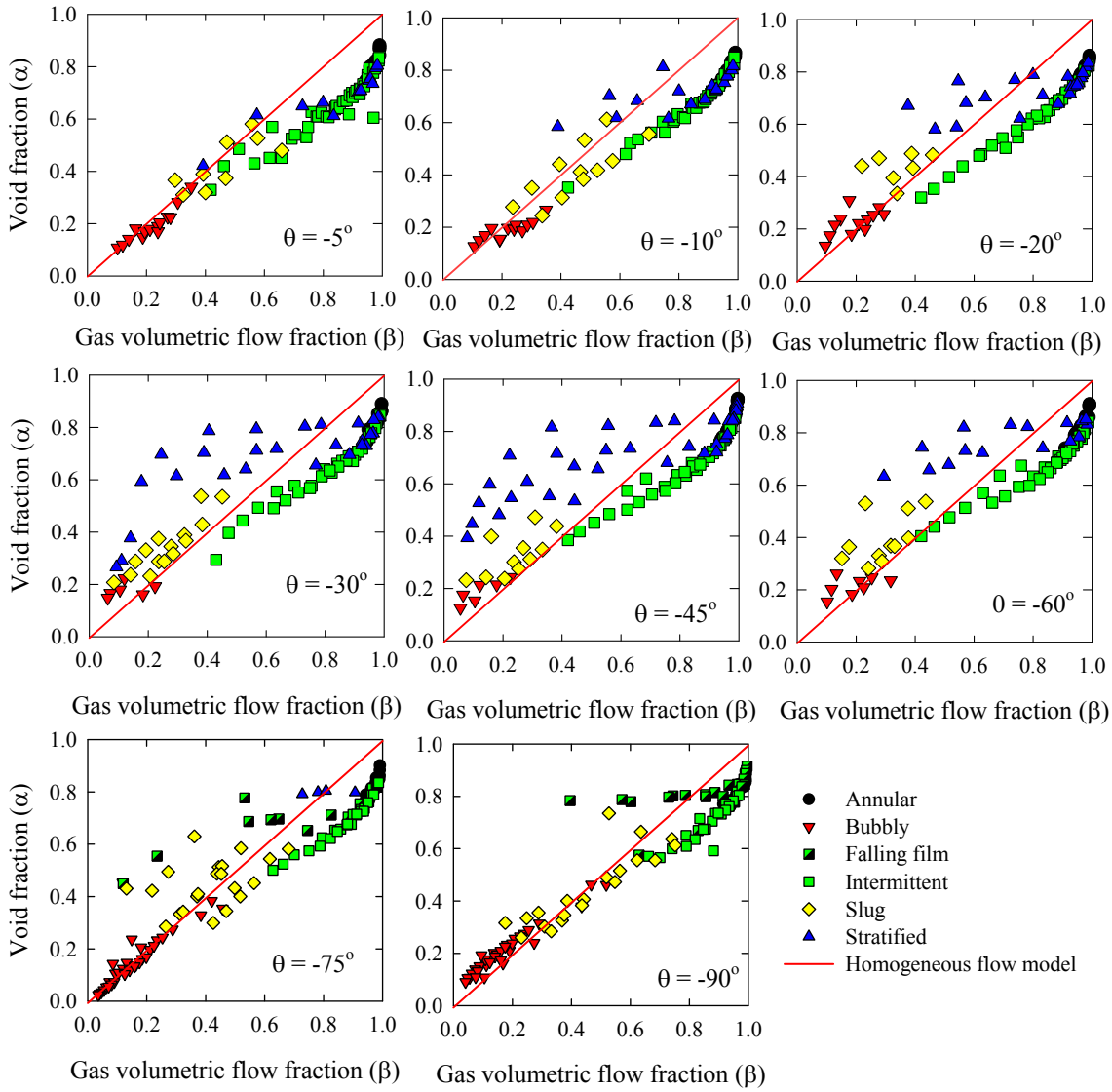

Figure 4.34: Void fraction vs. gas volumetric flow fraction for different downward inclined pipe orientations.

Thus, for steeper downward inclinations, more number of data points exhibit $\alpha > \beta$ behavior indicating higher residence time of the gas phase in the test section. It should be noted that the behavior following relationship $\alpha > \beta$ is only for bubbly, slug and stratified flow (flow patterns with low to moderate gas flow rates) where the buoyancy forces are dominant than the inertia forces. In case of intermittent and annular flow patterns, the relationship $\alpha < \beta$ is valid indicating that buoyancy forces

are weaker in comparison to the inertia forces and do not resist the motion of the gas phase. All data points that lie on the line of $\alpha = \beta$ imply that there is negligible slippage between the two phases and the two phase flow may be regarded as quasi homogeneous flow.

4.2.2 Effect of Pipe Orientation

In addition to the phase flow rates, the pipe orientation also has a remarkable effect on the void fraction. Most of the experimental void fraction data available in the literature is concentrated over a narrow range of pipe orientations and phase flow rates (or alternatively the flow patterns). In this study, the void fraction measured at 17 different pipe orientations ($0^o, \pm 5^o, \pm 10^o, \pm 20^o, \pm 30^o, \pm 45^o$, $\pm 60^o$, $\pm 75^o$ and $\pm 90^o$) consists of a wide range of void fraction ($0.09 \leq \alpha \leq 0.94$) and cover all important flow patterns observed in gas-liquid two phase flow. The variation of void fraction with respect to change in pipe orientation is illustrated for different phase flow rates in Fig. 4.35 (a)-(d). The four liquid flow rates are selected such that the representative data occupies entire range of the void fraction and all flow patterns observed in this study. The effect of pipe orientation on the void fraction is essentially due to the change in flow pattern or the structure of the flow pattern due to change in pipe orientation measured at fixed gas and liquid flow rate. As shown in Fig. 4.35 (a), the effect of pipe orientation on the void fraction is significant at low values of liquid flow rates. For low Re_{SL} and Re_{SG}, the flow pattern in downward inclinations is falling film and stratified whereas for upward orientations the flow pattern is in form of slug flow characterized by elongated gas slugs moving through liquid medium. In case of falling film (special form of stratified flow in vertical downward orientation) and stratified flows in downward inclinations, the liquid phase (water) flows downstream under the influence of gravity however, the flow of gas phase in downstream direction

is opposed by the buoyancy forces acting on it in the upstream direction which further increases the residence time of the gas phase in the test section.

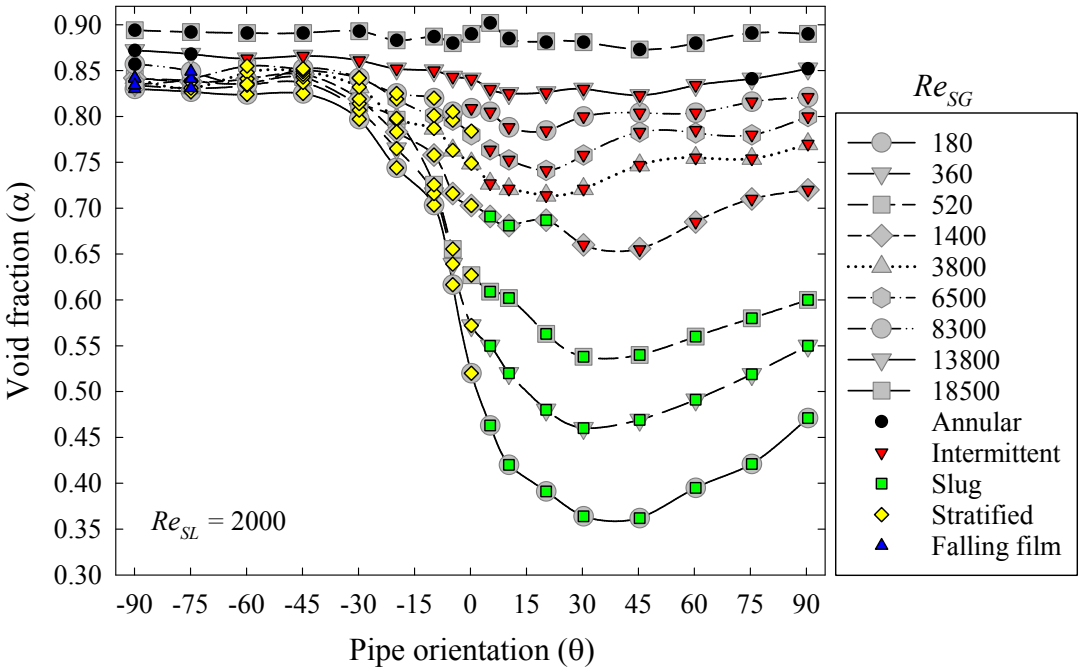

(a) $Re_{SL} = 2000$

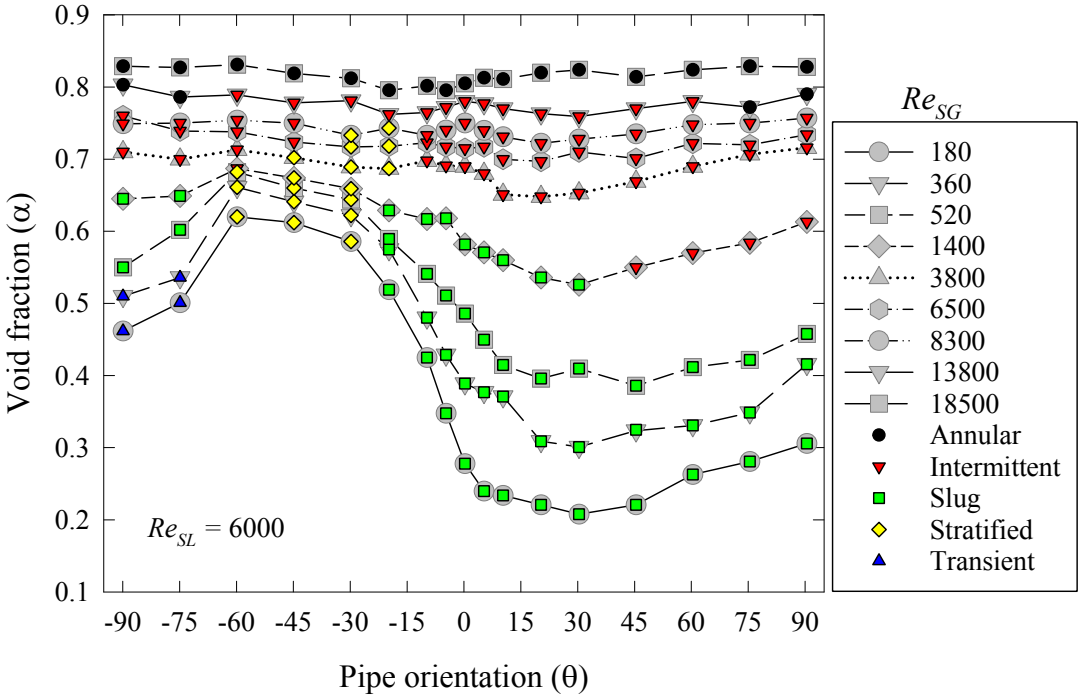

(b) $Re_{SL} = 6000$

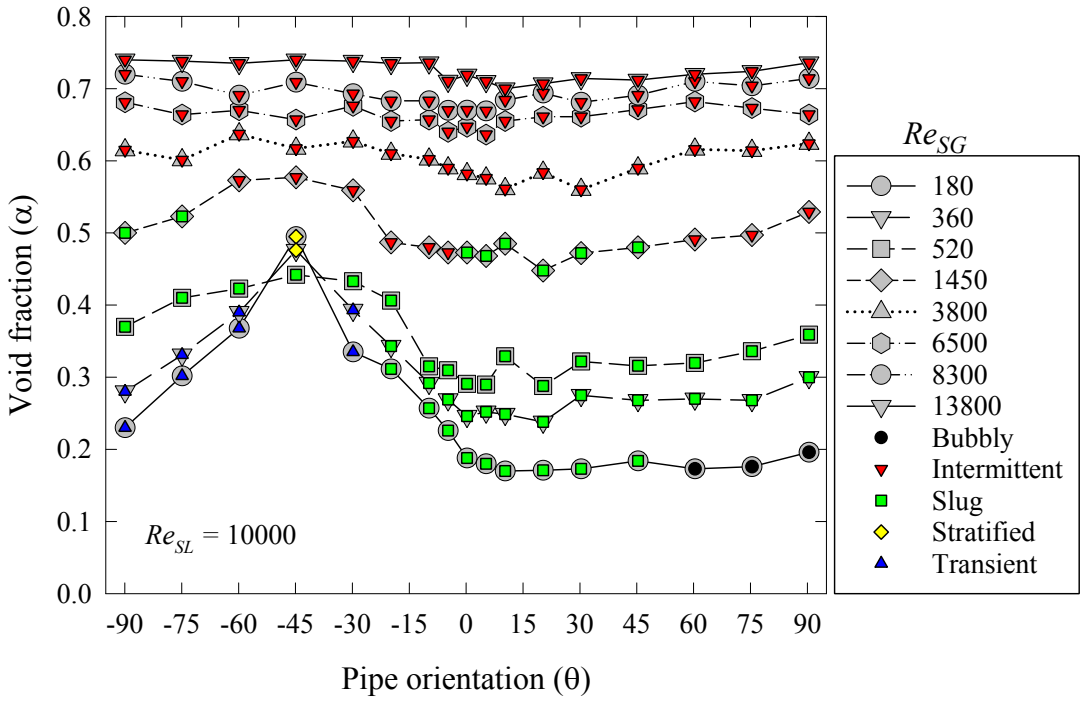

(c) $Re_{SL} = 10000$

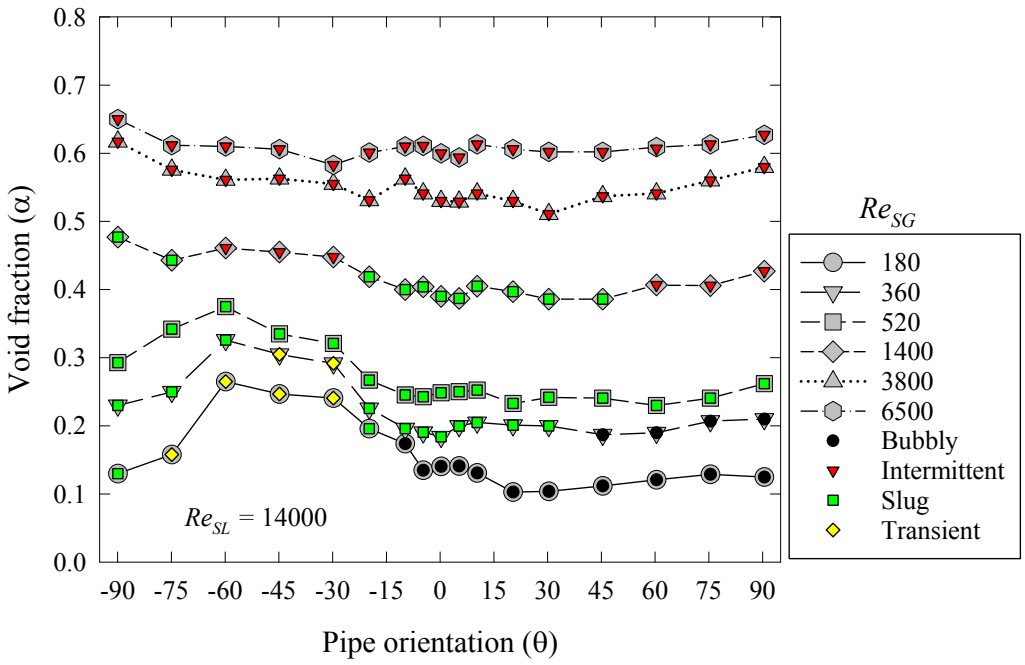

(d) $Re_{SL} = 14000$

Figure 4.35: Effect of the change in pipe orientation on void fraction.

In case of upward inclined two phase flow at low Re_{SL} and Re_{SG}, the buoyancy acts on the gas phase in the direction of flow and hence reduces the residence time of the gas phase in the test section. Thus, the higher residence time of the gas phase in downward inclined stratified flow and smaller residence time of the gas phase in slug flow results in high and low values of the void fraction, respectively. With increase in gas flow rates, typically in annular flow regime, the void fraction is found to be virtually independent of the pipe orientation. This trend is expected since for shear driven flow structures, the inertia forces are significant compared to the buoyancy forces and hence the effect of pipe orientation on the void fraction is negligible. For $Re_{SL} = 2000$ and $Re_{SG} = 180$, a change in pipe orientation from $+90^o$ to -90^o causes the void fraction to increase from 0.46 to 0.83 ($\approx$80% increase). The void fraction minimum as a function of pipe orientation is observed between $+30^o$ and $+45^o$ pipe orientation for low Re_{SG}. With increase in the gas flow rate, the void fraction minimum is found to gradually shift towards lower pipe inclinations. It appears that for upward pipe inclinations the lowest value of void fraction at certain pipe orientation is associated with the translational or propagation velocity ($U_T = C_o U_M + U_{GM}$) of the gas phase. Experimental measurements of the translational velocity at different pipe inclinations reported in the literature by Bendiksen (1984) and Gokcal et al. (2009) show that, U_T is maximum somewhere in between 30^o and 40^o i.e., the U_T increases from horizontal up to the pipe orientation in this range and then decreases with increase in the pipe orientation. The translational velocity of the gas phase is also the measure of the residence time of the gas phase in the test section which in turn is directly proportional to the void fraction. Thus, higher translational velocity results into lower void fraction values. Opposite holds true for lower translational velocities observed at $\theta < +30^o$ and $\theta > +45^o$. It is also observed that for $Re_{SL} = 2000$ for steeper downward inclinations, void fraction is insensitive to the increase in gas flow rate. Even if the gas flow rate is increased from 0.002 kg/min to 0.2 kg/min

($180 \leq Re_{SG} \leq 18500$), the void fraction is merely increased by 8%. However, in case of upward inclined orientations a maximum of about 93% increase in the void fraction is observed for the smallest and largest values of the gas flow rates. This implies that for stratified flow observed in downward pipe inclinations, the increase in gas flow rate doesn't contribute significantly to the increase in the void fraction. However, with increase in liquid flow rate ($Re_{SL} = 6000$), it is observed that the gas flow rate affect the magnitude of void fraction in stratified flow in steep downward inclinations. Even at $Re_{SL} = 6000$, the void fraction in downward inclinations is significantly higher than that in the upward inclination up to $Re_{SG} \leq 3800$. Any further increase in the gas flow rate makes void fraction relatively independent of the pipe orientation. For higher values of liquid flow rates, the stratified flow does not exist however a noticeable effect of pipe orientation on the void fraction is observed. It is also seen that for $Re_{SL} \geq 6000$, the void fraction is maximum between $-45^o \geq \theta \geq -60^o$ while for further steeper orientations, void fraction decreases consistently. This is due to the fact that at $Re_{SL} = 6000$, flow pattern up to $\theta = -60^o$ is stratified while that in $\theta < -60^o$ is slug flow. For $Re_{SL} = 10000$, stratified flow exists at $\theta = -45^o$ while slug flow exists for further steeper orientations. Finally for highest liquid flow rate at $Re_{SL} = 14000$, flow pattern at low gas flow rates in $\theta = -60^o$ is slug while that in $\theta = -75^o$ and $\theta = -90^o$ is bubbly in nature.

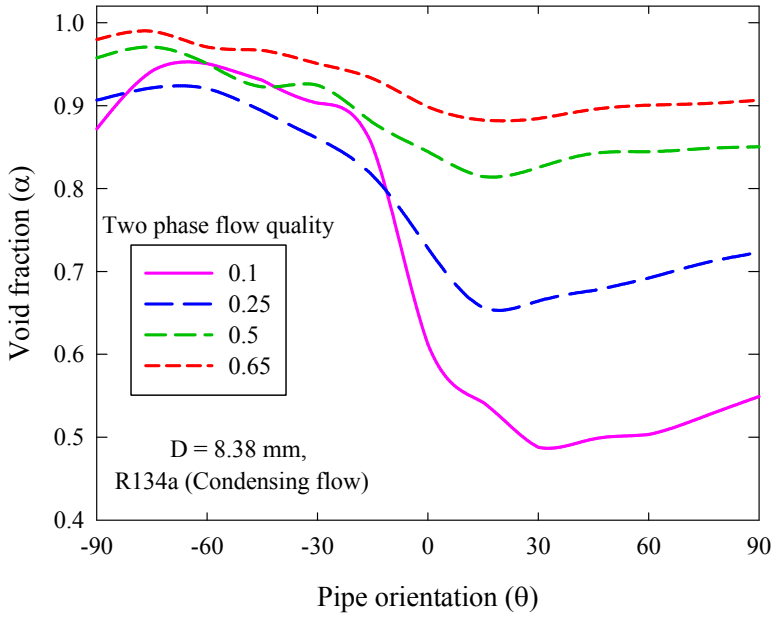

Figure 4.36: Variation of void fraction as a function of pipe orientation for condensing flow of R134a.

Overall it is concluded that the effect of pipe orientation on the void fraction is essentially due to the effect of pipe orientation on the physical structure of the flow patterns. Similar type of the void fraction dependency on the pipe orientation is reported by Lips and Meyer (2012c) for condensing flow of R134a refrigerant in 8.38 mm I.D. pipe. The variation of void fraction as a function of pipe orientation measured by Lips and Meyer (2012c) is illustrated in Fig. 4.36. It is evident that for condensing flow of R134a, void fraction is sensitive to pipe orientation at low qualities (bubbly/slug flow) and with increase in two phase flow quality, void fraction gradually becomes insensitive to void fraction. This resemblance in void fraction trends as a function of pipe orientation infers that independent of the nature of two phase flow i.e., with or without phase change, the void fraction significantly depends on the pipe orientation.

4.2.3 Effect of Pipe Diameter

The effect of pipe diameter on gas-liquid void fraction is not as significant as the flow patterns and the pipe orientation. However, the void fraction is found to be inversely proportional to the pipe diameter. The increase in void fraction with decrease in pipe diameter for certain flow patterns may be significant and hence cannot be neglected. Based on the two phase flow literature, the pipe diameter is found to affect the void fraction in conjunction with the flow patterns, i.e., the effect of pipe diameter on void fraction is different for different flow patterns or alternatively the range of void fraction. As shown in Fig. 4.37, the effect of pipe diameter on the measured values of void fraction is found to be prominent for low values of void fraction (typically bubbly and slug flow regime). Whereas, for the high values of void fraction corresponding to that in annular flow regime (shear driven flow) typically $\alpha > 0.8$, the void fraction is relatively insensitive to the pipe diameter. This observation is in agreement with the work of Kaji and Azzopardi (2010) who investigated the effect of pipe diameter in a range of 5 mm to 70 mm on void fraction in vertical upward annular flow regime for non-boiling two phase flow. They found that the effect of pipe diameter on void fraction in the annular flow regime is negligible. The higher values of void fraction in small diameter pipes can be justified considering the flow structure and wall effects on the gas phase. In case of two phase flow through small diameter pipes, typically at low gas flow rates, the two phase flow is in form of bubble train (quasi spherical or equal length elongated bubbles that occupy entire pipe cross section) whereas the flow structure in large diameter pipes may be in form of dispersed bubbles.

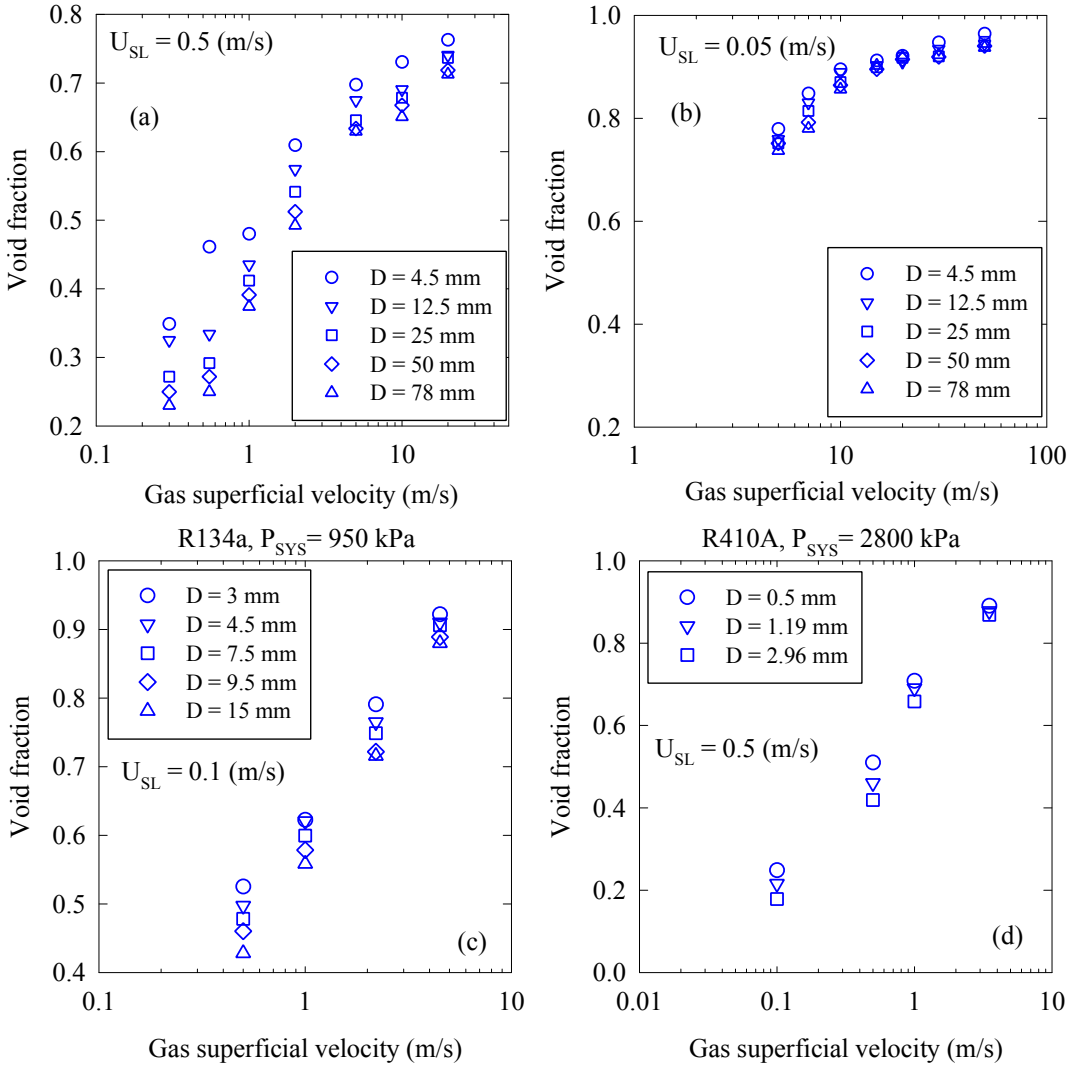

Figure 4.37: Effect of pipe diameter on void fraction.

The small pipe dimensions confine the motion of gas bubbles/slug due to wall induced drag and increases its residence time in the test section which ultimately results in increased void fraction. Thus, for correct prediction of void fraction over a range of pipe diameters, a robust void fraction correlation must account for the effect of pipe diameter on the change in flow structure and hence the void fraction. The consideration of the effect of pipe diameter on the void fraction modeling parameters such as the distribution parameter and drift velocity is discussed in next chapter.

4.2.4 Effect of Fluid Properties

The two important fluid properties that are known to affect the void fraction are the gas phase density and the liquid phase dynamic viscosity. The effect of gas phase density on the void fraction is essentially in a case of high system pressure flow such as that observed in nuclear cooling applications and the refrigeration industry whereas, the effect of liquid phase dynamic viscosity on the void fraction is of significant interest in chemical engineering processes and the oil and gas industry applications that involve viscous oils having dynamic viscosity up to an order of 500 compared to that of liquid water at room temperature and pressure. The increase in system pressure or alternatively increase in the gas phase density reduces the slippage between the two phases and also reduces the void fraction measured at similar mass flow rate. A denser gas phase (lower specific volume) will occupy less volume in the test section and hence would result in reduced void fraction. As shown in Fig. 4.38, the slope of void fraction vs. quality is a function of the phase density ratio and in the limiting case of $\rho_G = \rho_L$, there is a negligible slippage between the two phases and there exists a linear relationship between void fraction and two phase flow quality i.e., the two phase flow void fraction becomes equal to the homogeneous flow void fraction. Shedd (2010) and Keinath (2012) reported a similar trend of void fraction as a function of gas phase density for two phase flow of refrigerants. They found the void fraction to decrease with increase in refrigerant saturation temperature (increase in saturation or system pressure).

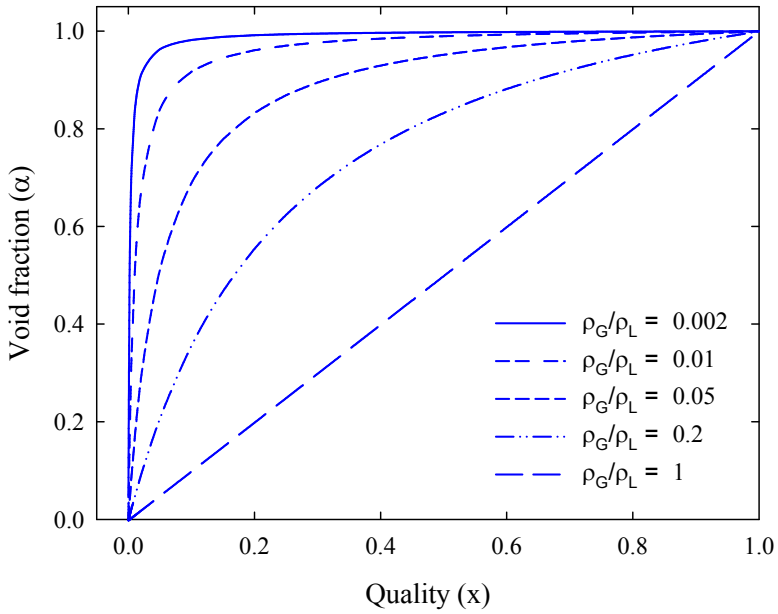

Figure 4.38: Variation of void fraction with respect to change in quality as a function of phase density ratio.

Two phase flow literature also reports the experimental results of the effect of liquid phase dynamic viscosity on the void fraction. Gokcal (2008) and Jeyachandra (2011) measured the void fraction in a 50.2 mm I.D. pipe using air and oil of dynamic viscosity in a range of 0.18 Pa-s to 0.58 Pa-s. Overall they found the void fraction to slightly decrease with increase in the liquid dynamic viscosity. Similar results are reported by Oshinowo (1971) who measured void fraction in vertical upward and downward pipes using air-water and air and four different concentrations of ethylene glycol. Mukherjee (1979) measured void fraction using air-kerosene and air-oil fluid combinations in upward and downward pipe inclinations. He observed that the viscous drag on liquid phase reduces its velocity and tends to accumulate in the test section and hence decreases in-situ void fraction. Effect of liquid dynamic viscosity on void fraction reported by Gokcal (2008) is shown in Fig. 4.39.

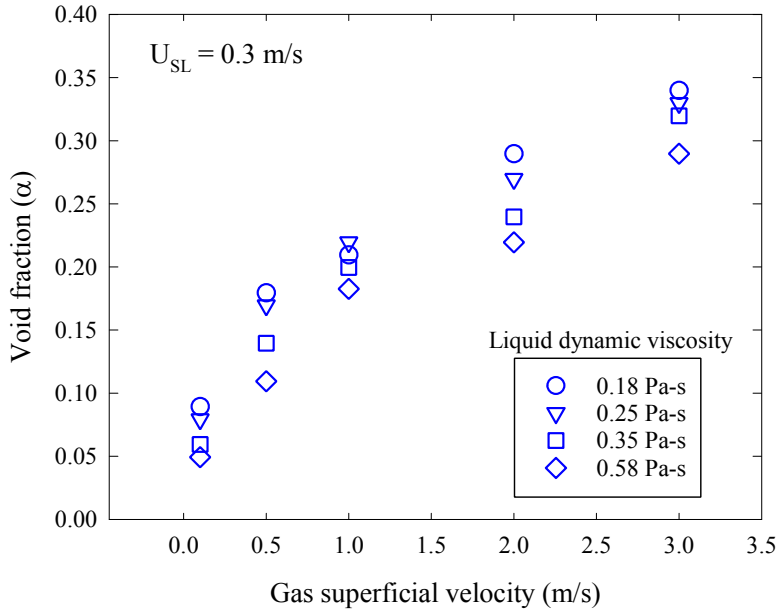

Figure 4.39: Effect of liquid dynamic viscosity on void fraction (adapted from Gokcal (2008)).

4.3 Two Phase Pressure Drop

As mentioned earlier in Chapter II, the total pressure drop in gas-liquid two phase flow consists of the hydrostatic, acceleration and frictional components. In case of non-boiling two phase flow applications, the contribution of accelerational component of the total two phase pressure drop is negligible and hence can be ignored. The contribution of the hydrostatic and the frictional components to the total pressure drop depends upon the flow patterns (phase flow rates), pipe diameter and the pipe orientation. Before proceeding further on the discussion of the parametric study of the two phase pressure drop it is worthwhile to get a glimpse of the contribution of each of the two phase pressure drop components to the total two phase pressure drop.

4.3.1 Contribution of Different Components to the Total Two Phase Pressure Drop

The contribution of hydrostatic pressure drop to the total two phase pressure drop component is significant in cases of bubbly flows (small range of void fraction), large diameter pipes and those oriented in vertical direction. Whereas, the contribution of frictional component to the total two phase pressure drop is noticeable for annular flow regime (large values of void fraction) and small diameter pipes. As shown in Fig. 4.40, the hydrostatic pressure drop is maximum for small values of void fraction and vertical two phase flow. The hydrostatic pressure drop is calculated using the separated flow model definition of two phase mixture density. As the pipe orientation decreases, the impact of void fraction values on the two phase hydrostatic pressure drop decreases and it is finally zero at $\theta = 0^o$ indicating absence of hydrostatic pressure drop component in horizontal two phase flow.

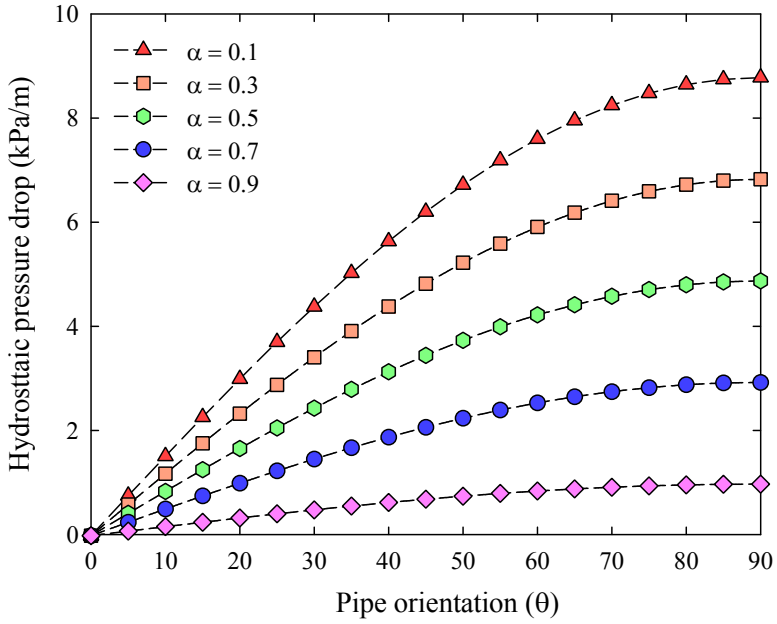

Figure 4.40: Interrelationship between void fraction, pipe orientation and hydrostatic pressure drop.

It is also necessary to highlight the sensitivity of the hydrostatic pressure drop to

the void fraction. In fact the sensitivity of hydrostatic component to the void fraction is related to the void fraction weighted form of the two phase mixture density. The error incurred in the prediction of the void fraction is observed to have significant impact on the correct estimation of the hydrostatic component. Most of the correlations available in the two phase flow literature claim to predict the void fraction within ±20% error bands. From a pragmatic point of view, in case of the estimation of hydrostatic pressure drop where the void fraction is required as an input; the percentage error in prediction of void fraction can be a misleading term since; a ±10% to ±30% error in its prediction can have different magnitudes of impact on the two phase mixture density and hence the hydrostatic pressure drop.

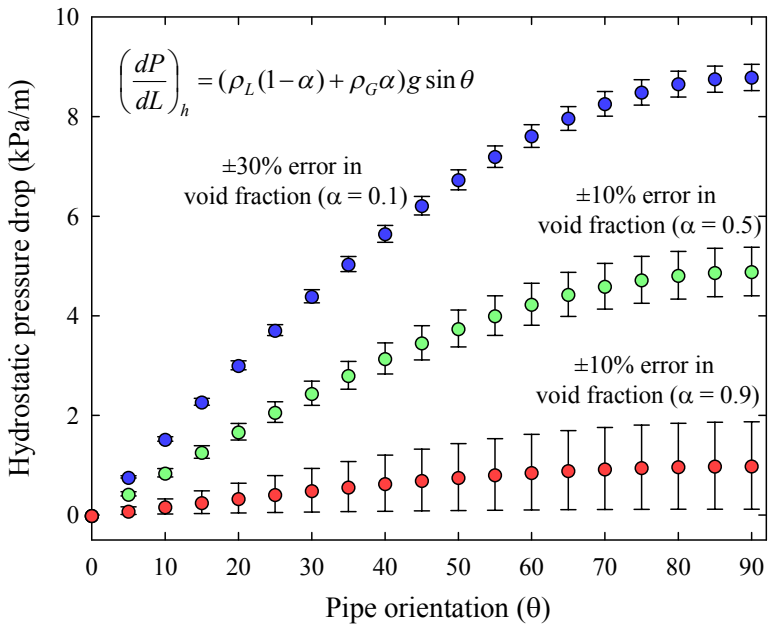

Figure 4.41: Effect of error in void fraction on prediction of two phase hydrostatic pressure drop.

This issue of sensitivity of hydrostatic pressure drop to the void fraction is exemplified through Fig. 4.41. For small values of void fraction i.e., $\alpha = 0.1$ corresponding to that of bubbly flow, a ±10% error in prediction of void fraction can cause an error of up to ±1.2% in estimation of the hydrostatic component. Whereas, for large values

of void fraction i.e., $\alpha = 0.9$ corresponding to annular flow, a $\pm 10\%$ error in prediction of void fraction can cause an error of up to $\pm 35\%$ in estimation of the hydrostatic component. For the case of $\alpha = 0.1$, error bands of $\pm 30\%$ is used in Fig. 4.41 since the error induced in hydrostatic pressure drop due to $\pm 30\%$ error in void fraction is insignificant and cannot be noticed in the graph. It is also seen that impact of error in void fraction on hydrostatic component decreases with decrease in pipe orientation toward horizontal. Thus, it can be inferred that, highest accuracy in prediction of void fraction is required in vertical and near vertical pipe orientations for correct estimation of hydrostatic pressure drop. Based on this argument the acceptable error criteria in the estimation of void fraction is discussed later in next chapter.

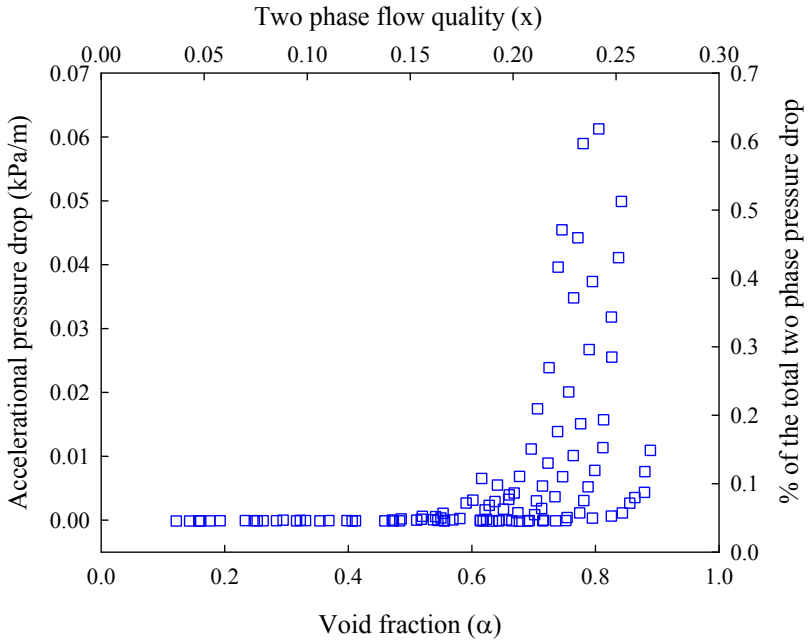

Figure 4.42: Contribution of accelerational component to the total two phase pressure drop in vertical upward flow.

It was mentioned in Chapter 2 that the contribution of accelerational component of the pressure drop to the total two phase pressure drop depends upon the diabatic or adiabatic flow conditions. For adiabatic flow condition, the accelerational component is usually very small since there is no expansion of the two phase mixture due to phase change process. In the present study, the accelerational component of the two

phase pressure drop is calculated for vertical upward flow accounting for the change in gas and liquid phase density corresponding to the drop in absolute pressure at a downstream location. As shown in Fig. 4.42, the maximum percentage contribution of the accelerational component to the total two phase pressure drop is even less than 1%. For low values of void fraction corresponding to bubbly flow, accelerational component is negligible but increases with increase in the void fraction or alternatively as the flow pattern shifts to intermittent or annular flow. In case of one component two phase flow i.e., boiling or condensing flow, the two phase mixture continuously undergoes further phase change process in the test section and hence accelerational component of two phase pressure drop exists due to change in specific volume of two phase mixture. The experimental results of Tran (1998), Lim (2005) and Lips and Meyer (2012a) show that for boiling two phase flow as is the case with flow of refrigerants, the accelerational component of two phase pressure drop can be up to 10 to 20% of total two phase pressure drop.

A consolidated view of the contribution of hydrostatic and frictional components to the total pressure drop is presented in Fig. 4.43. It is clearly seen that the contribution of hydrostatic component to the total pressure drop is significant for the low values of void fraction (bubbly flow) which further decreases with increase in the void fraction. The frictional pressure drop for small values of void fraction (bubbly flow) is small and goes on increasing with increase in void fraction. It is also observed that the two components of pressure drop become equal at a certain void fraction that is inversely proportional to liquid mass flux. For high liquid velocity of 1.16 m/s or liquid mass flux of 1100 kg/m^{2}s, the flow pattern is typically bubbly and the void fraction increases linearly with increase in the gas flow rate and hence the hydrostatic component also reduces gradually. It should also be noted that trends presented in Fig. 4.43 is for vertical upward flow. With decrease in the pipe orientation towards horizontal, the contribution of hydrostatic component to the total two phase pressure

drop will decrease and will be zero at horizontal pipe orientation. In addition to the phase flow rates, the role of pipe diameter in contribution of hydrostatic and frictional components to the total two phase pressure drop cannot be overlooked.

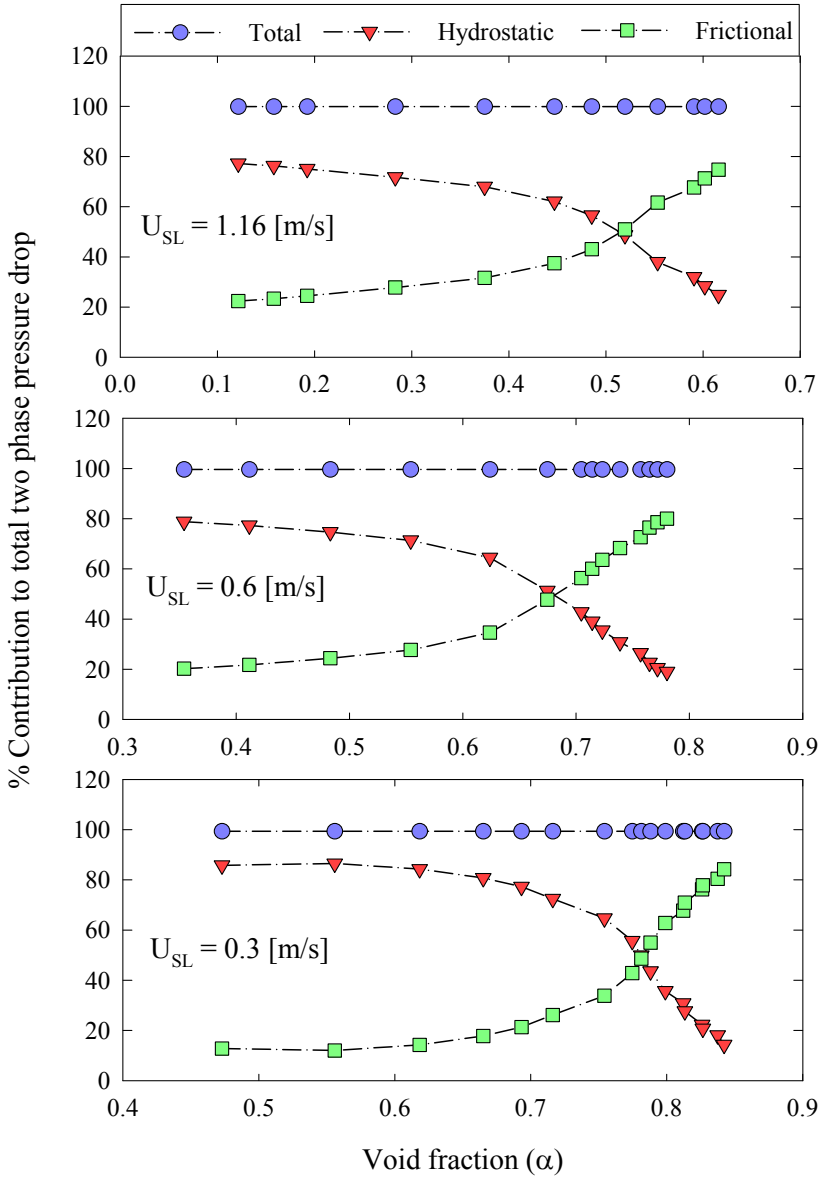

Figure 4.43: Contribution of hydrostatic and frictional components to the total pressure drop in vertical upward two phase flow.

As illustrated in Fig. 4.44 the hydrostatic component of a large diameter pipe offers more contribution to the total two phase pressure drop than the comparatively small diameter pipes. However, the frictional component of smaller diameter pipe

offers more contribution to total two phase pressure drop compared to larger diameter pipes. It should also be noted that the relative magnitude of each of these components also strongly depend upon the void fraction or alternatively the flow pattern. Thus it can be concluded that depending upon the range of void fraction (or flow pattern), for large diameter pipes, correct determination of hydrostatic pressure drop is equally or even of greater importance compared to frictional component whereas for smaller diameter pipes, correct estimation of frictional component is crucial.

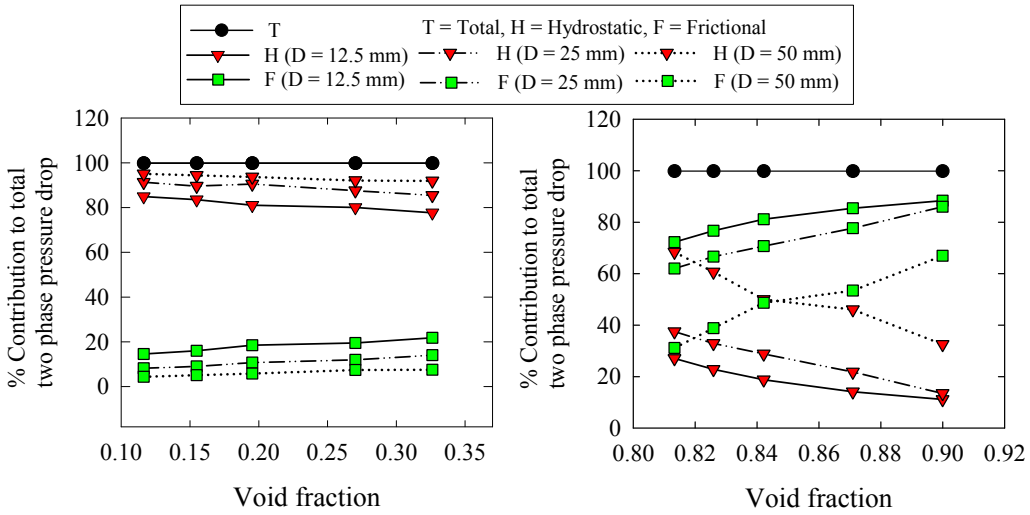

Figure 4.44: Contribution of hydrostatic and frictional components of two phase pressure drop to the total two phase pressure drop.

4.3.2 Effect of Phase Flow Rates and Flow Patterns

The effect of phase flow rates (or alternatively the flow patterns) on two phase pressure drop is essentially due to change in void fraction and the physical structure of the flow patterns. For a fixed liquid flow rate and increasing gas flow rates, the contribution of the hydrostatic two phase pressure drop to the total two phase pressure drop decreases while that of frictional component increases. In such a case the flow pattern may transit from bubbly to annular flow regimes during which both void fraction and the physical structure of flow pattern changes drastically. In this section,

the effect of change in phase flow rates (or alternatively the physical structure of flow patterns) on the frictional component of two phase pressure drop is presented in Figs. 4.45 to 4.47. The gas and liquid flow rates are varied such that the experimental conditions include all flow patterns typically observed in two phase flow. In case of horizontal flow as illustrated in Fig. 4.45, it is seen that at low liquid and gas flow rates, two phase frictional pressure drop is insensitive to increase in gas flow rates, the region corresponding to slug and stratified flow patterns. At these low flow rates of $Re_{SL} < 4000$ a sharp increase in $(dP/dL)_f$ is observed for $Re_{SG} > 8000$. Further this gas flow rate, the flow pattern is intermittent (wavy and wavy annular) and annular that causes rapid increase in pressure drop. In comparison to all other flow patterns, annular flow has large interfacial area which contributes to the frictional losses in addition to the friction of single phase liquid at the pipe wall. At higher liquid flow rates ($Re_{SL} > 8000$), $(dP/dL)_f$ is found to increase consistently with increase in the gas flow rates.

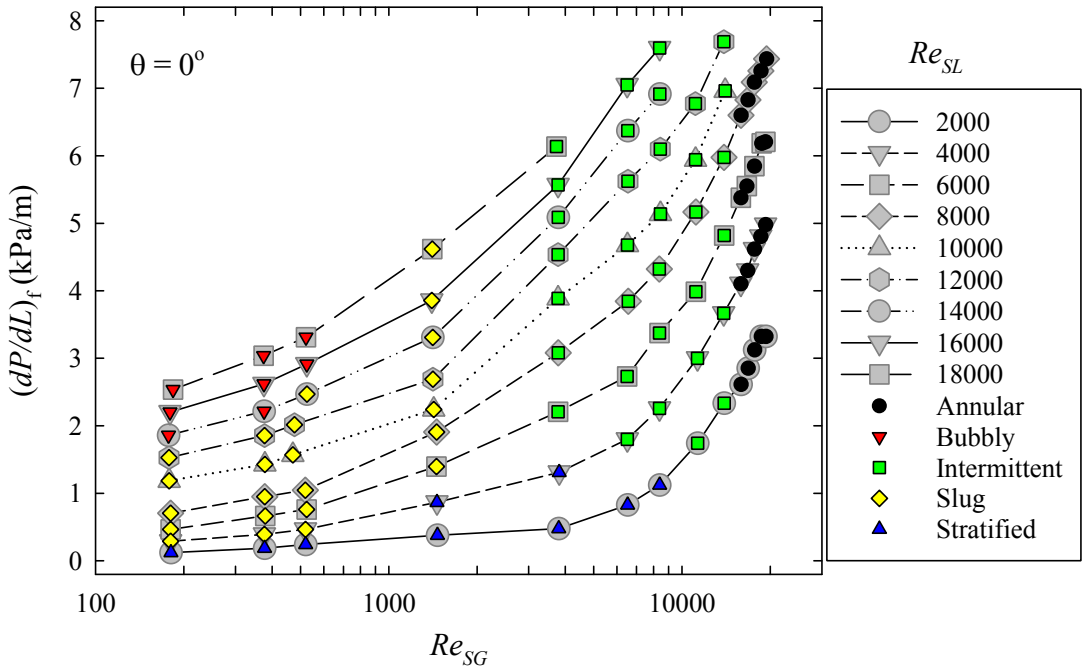

Figure 4.45: Effect of phase flow rates (flow patterns) on two phase frictional pressure drop in horizontal flow.

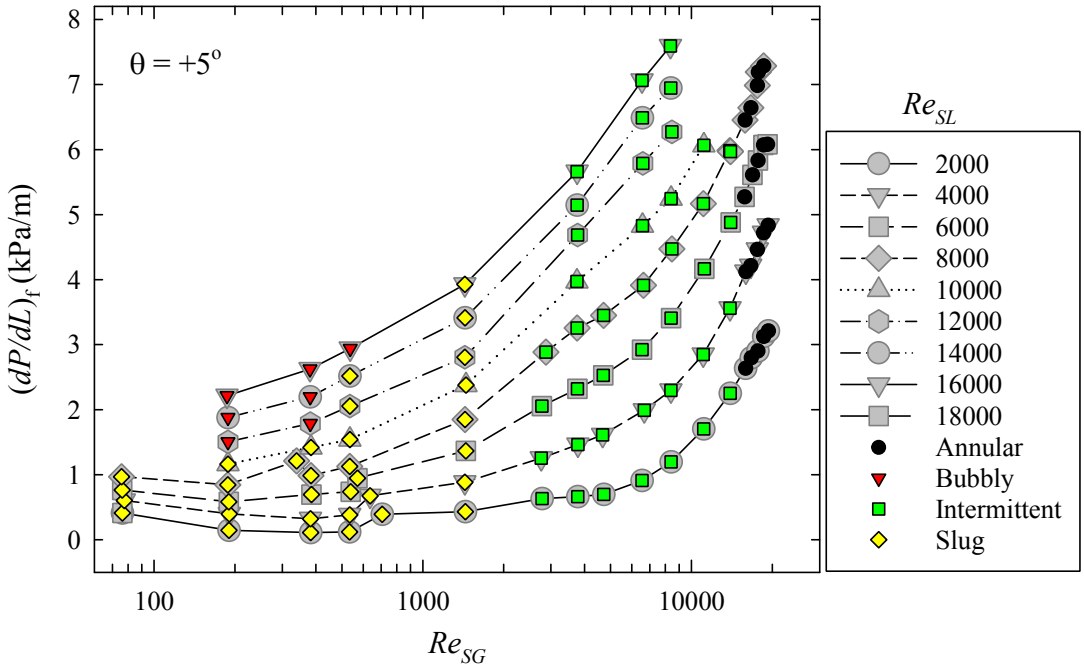

(a) $\theta = +5^o$

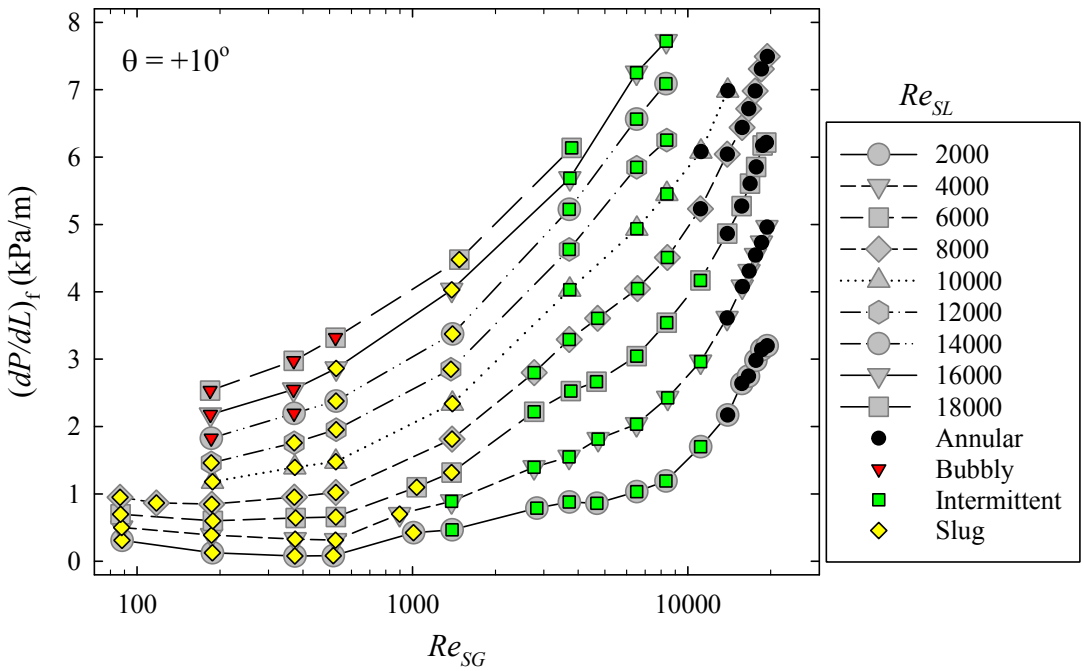

(b) $\theta = +10^o$

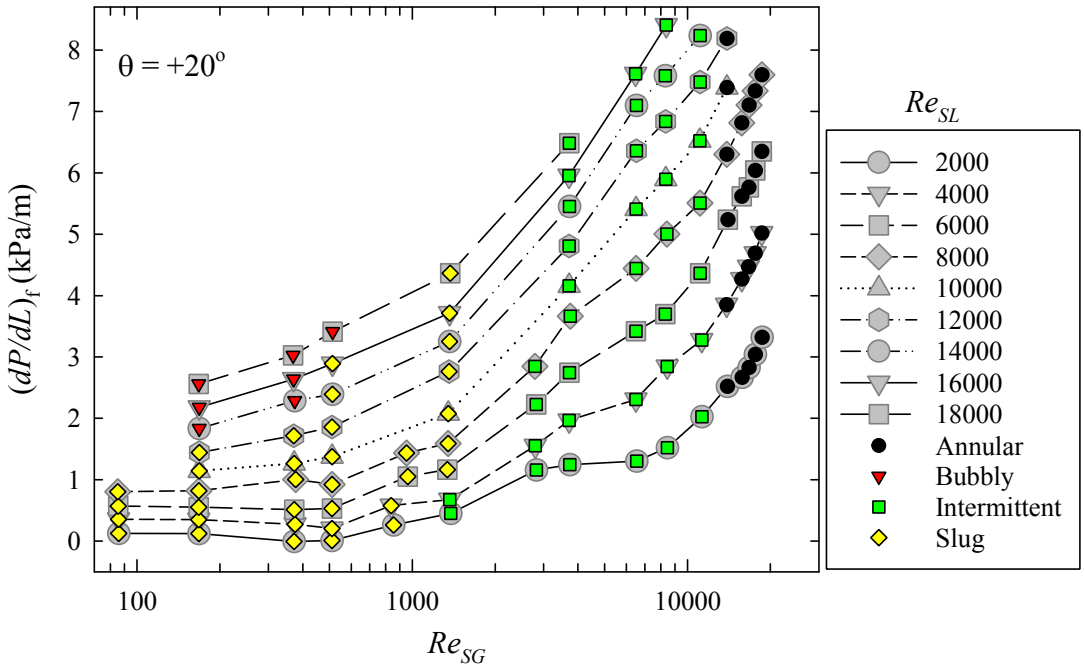

(c) $\theta = +20^o$

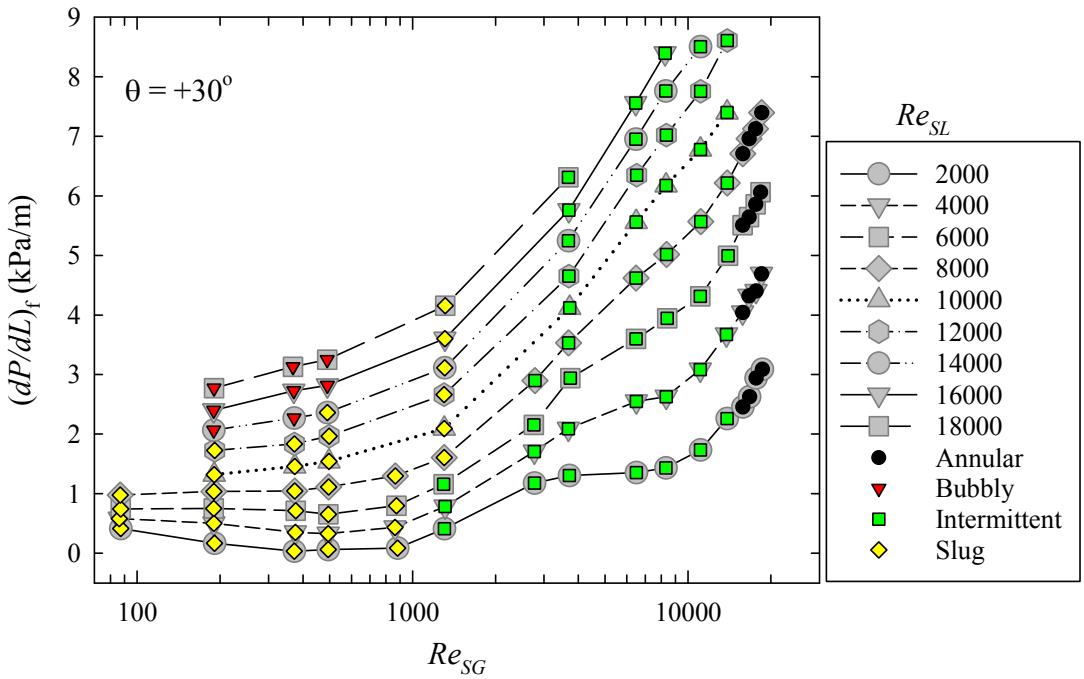

(d) $\theta = +30^o$

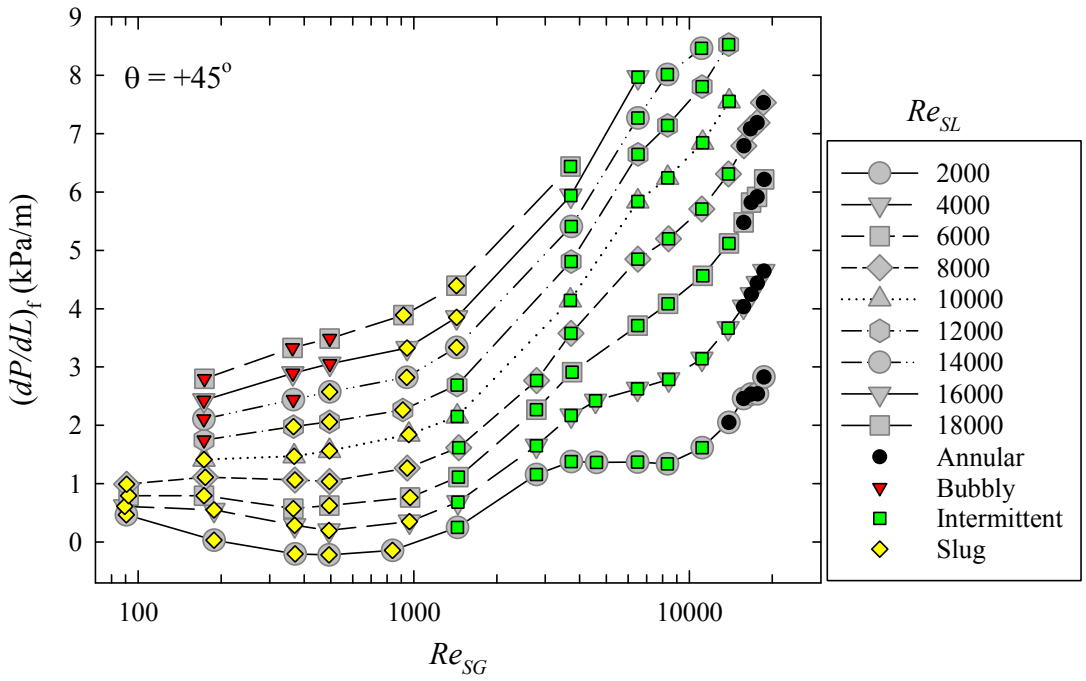

(e) $\theta = +45^o$

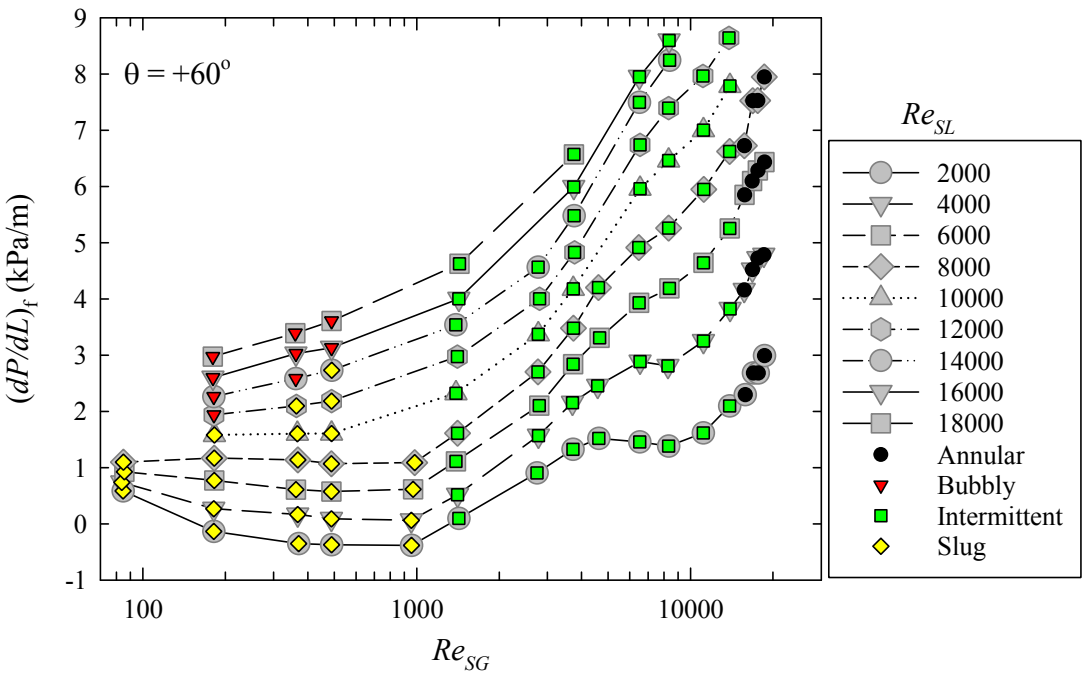

(f) $\theta = +60^o$

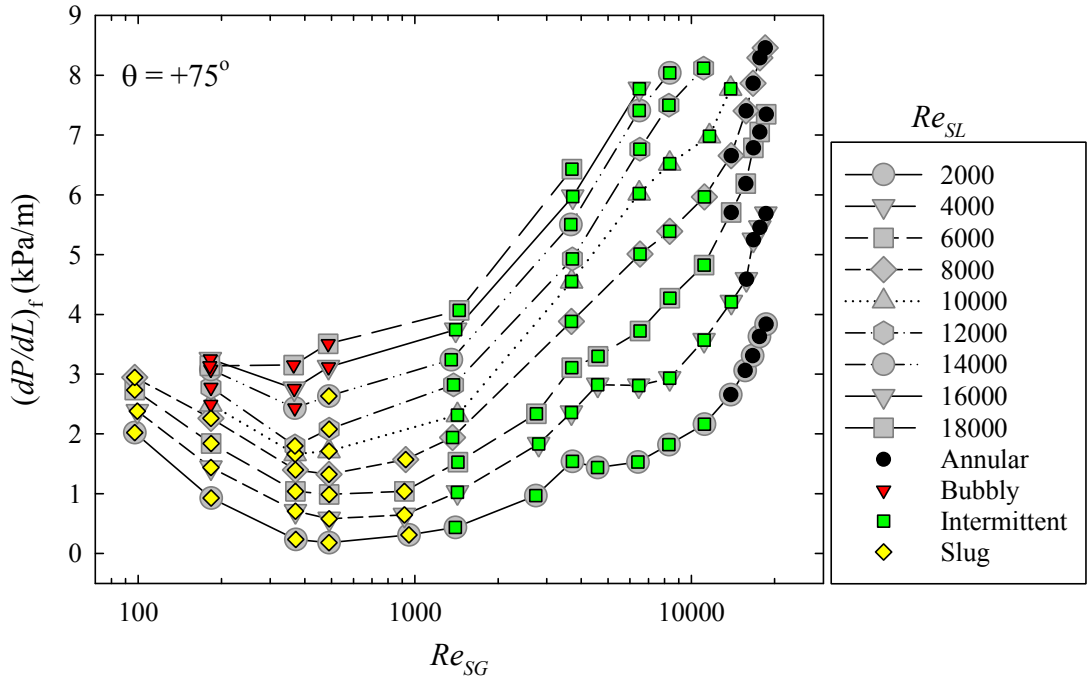

(g) $\theta = +75^o$

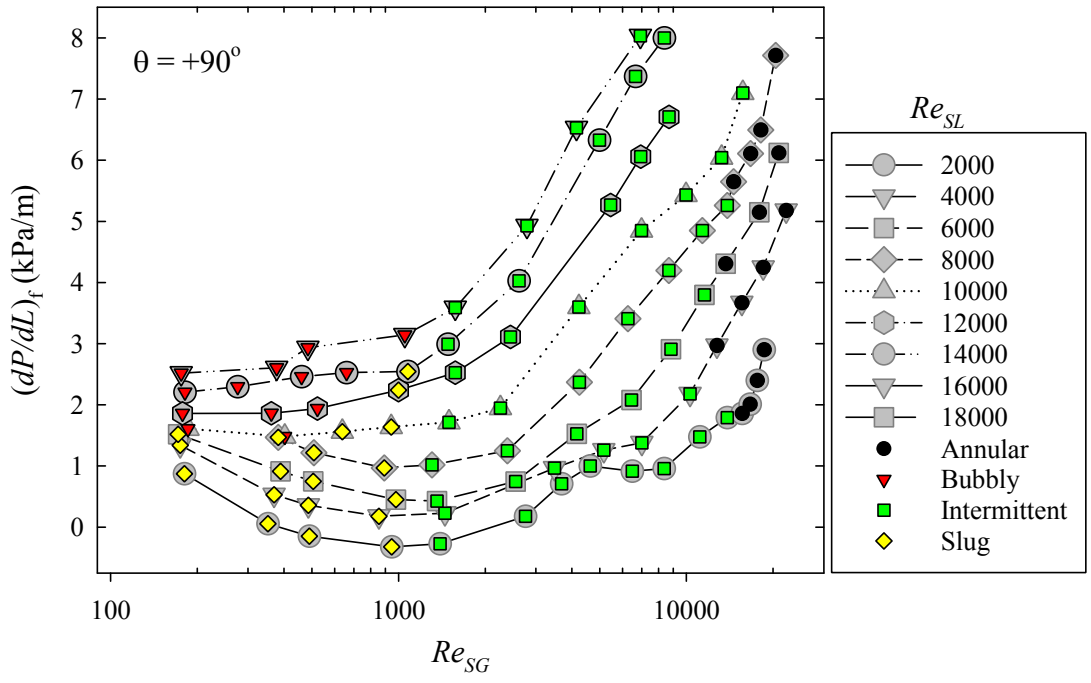

(h) $\theta = +90^o$

Figure 4.46: Effect of phase flow rates (flow patterns) on two phase frictional pressure drop in upward pipe inclinations.

The effect of phase flow rates (flow patterns) on frictional pressure drop in upward inclined flow is presented in Fig. 4.46 (a)-(h). In comparison to horizontal flow at low liquid and gas flow rates, a decreasing tendency of $(dP/dL)_f$ is observed with increase in the gas flow rates. This decreasing tendency of $(dP/dL)_f$ is found to exist for slug flow regime and aggravates with increase in pipe orientation towards vertical upward flow. For near horizontal upward inclinations, decreasing frictional pressure drop tendency prevails mainly for $Re_{SL} < 4000$ and $Re_{SG} \lessapprox 500$ whereas, for vertical and near vertical pipe orientations, decreasing trend of $(dP/dL)_f$ exists up to $Re_{SL} \approx 8000$ and $Re_{SG} \lessapprox 1000$. It is also seen that at low liquid flow rate ($Re_{SL} = 2000$) increasing trend of frictional pressure drop beyond $Re_{SG} > 500$ and $Re_{SG} > 1000$ for near horizontal and near vertical pipe orientations, respectively; tends to plateau at $Re_{SG} \approx 3000$. In fact for very small liquid flow rates ($400 < Re_{SL} < 2000$), yet another decreasing trend of $(dP/dL)_f$ is observed with further increase in gas flow rates. These two decreasing trends of frictional pressure drop, one at low gas flow rates and another at moderate to high gas flow rates are discussed in detail later in this chapter. In case of bubbly flow it is found that increase in upward pipe orientation from horizontal retards the increasing tendency of $(dP/dL)_f$ with increase in the gas flow rate. However, for intermittent (at high gas flow rates) and annular flow regimes, no significant effect of pipe orientation on the overall trends of $(dP/dL)_f$ is observed. The frictional pressure drop trends of intermittent flow at the beginning and end of the flow pattern (as a function of gas flow rates) is similar to that of slug and annular flow, respectively. This is in accordance with the definition of intermittent flow pattern that at beginning of intermittent flow, the flow structure is slug wavy while at the end of intermittent flow regime, flow pattern is annular wavy. Overall it is concluded that similar to void fraction trends, effect of pipe orientation on two phase frictional pressure drop is appreciable for buoyancy dominated flows while the shear driven flow patterns such as intermittent and annular flow remain

virtually unaffected by the change in pipe orientation.

The variation of $(dP/dL)_f$ with increase in gas superficial Reynolds number (Re_{SG}) for different downward pipe inclinations is presented in Fig. 4.47 (a)-(h). In comparison to near horizontal upward inclinations (Fig. 4.46), two phase frictional pressure drop trends with respect to increase in gas flow rates for near horizontal downward inclinations (Fig. 4.47) resembles the trends observed in horizontal flow (Fig. 4.45). Unlike upward pipe inclinations no decreasing tendency of $(dP/dL)_f$ is observed in downward pipe inclinations. For all downward pipe inclinations, at low liquid flow rates, the frictional pressure drop is found to be insensitive to the increase in gas flow rates. This flow region attributing to low liquid and low to moderate gas flow rate corresponds to stratified flow. It can be inferred that in stratified flow regime, increase in liquid flow rate has first order effect on the two phase frictional pressure drop while that of the gas flow rate is of secondary. The flat trend of $(dP/dL)_f$ extends to higher gas flow rates with increase in downward pipe inclination up to -45^o. This tendency is in agreement with the observation that beyond -45^o, the tendency of flow stratification gradually decreases with increase in the downward pipe inclination. In vertical downward falling film flow, the trend of $(dP/dL)_f$ with change in gas flow rate is similar to that of stratified flow in downward pipe inclinations. This supports the fact that falling film flow is indeed a special case of uniformly distributed symmetric stratified flow. As described earlier in flow pattern maps, transient (unsteady) two phase flow behavior exists at steeper pipe inclinations ($-30^o \geq \theta \geq -90^o$). This transient flow regime that exists at moderate liquid flow rates and low gas flow rates is characterized by the existence of more than one flow pattern in the test section. Plots in Fig. 4.47 (d)-(h) distinctly shows the data points affected by the transient behavior of two phase flow. For these pipe orientations, no distinct trend of two phase frictional pressure drop vs. Re_{SG} are observed because since the flow behavior is transient, the measured values of pressure drop are sensitive

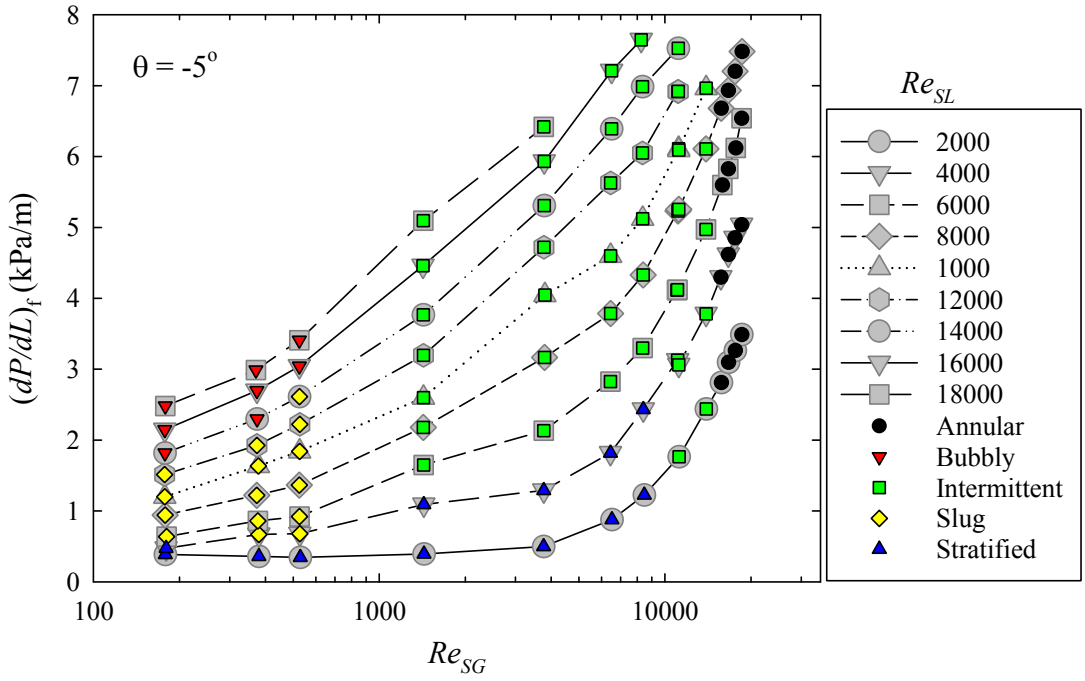

(a) $\theta = -5^o$

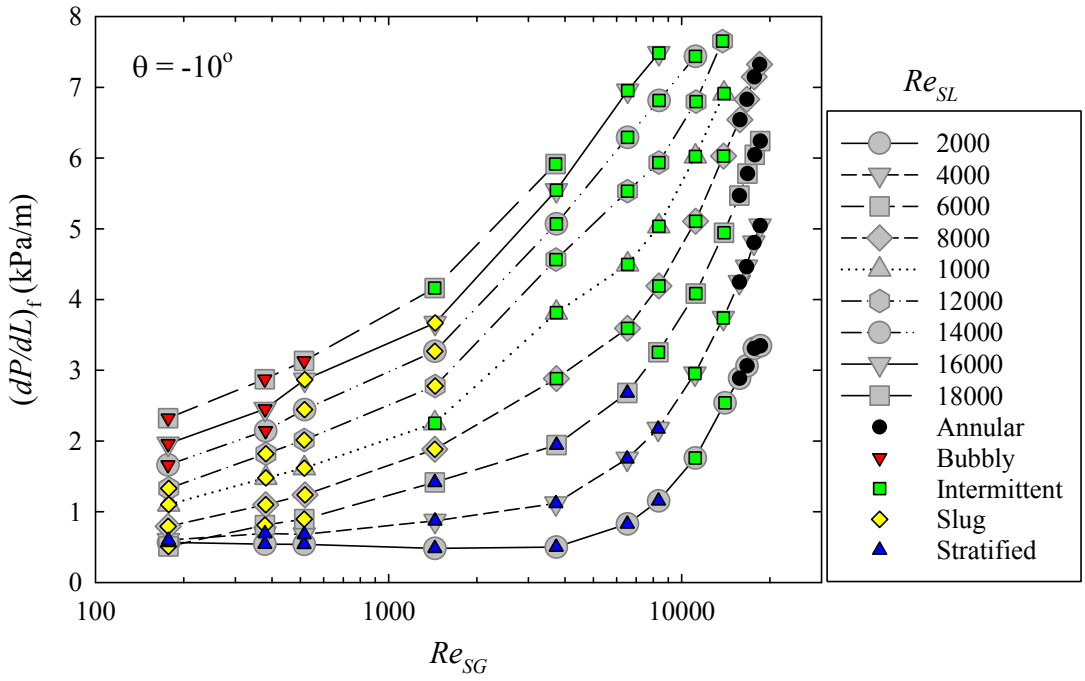

(b) $\theta = -10^o$

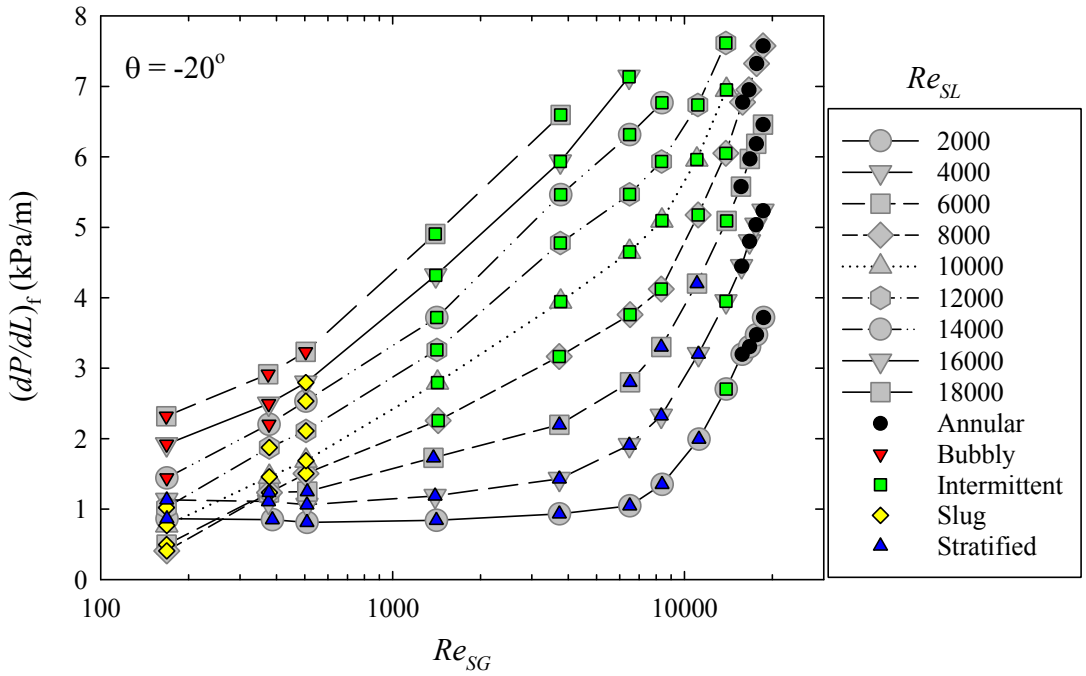

(c) $\theta = -20^o$

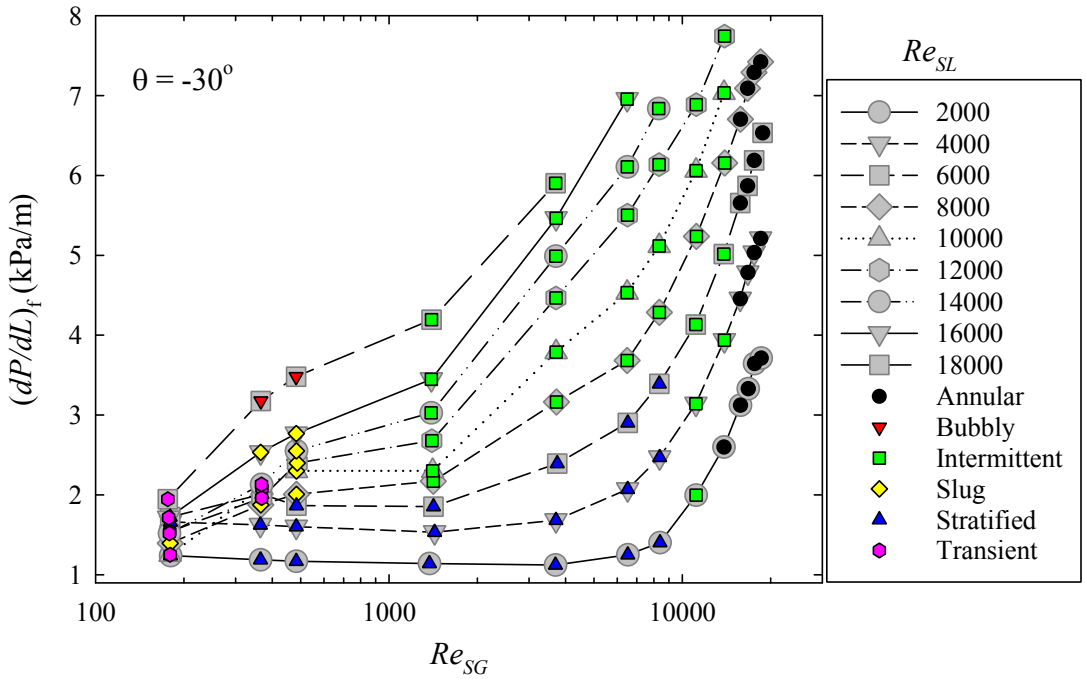

(d) $\theta = -30^o$

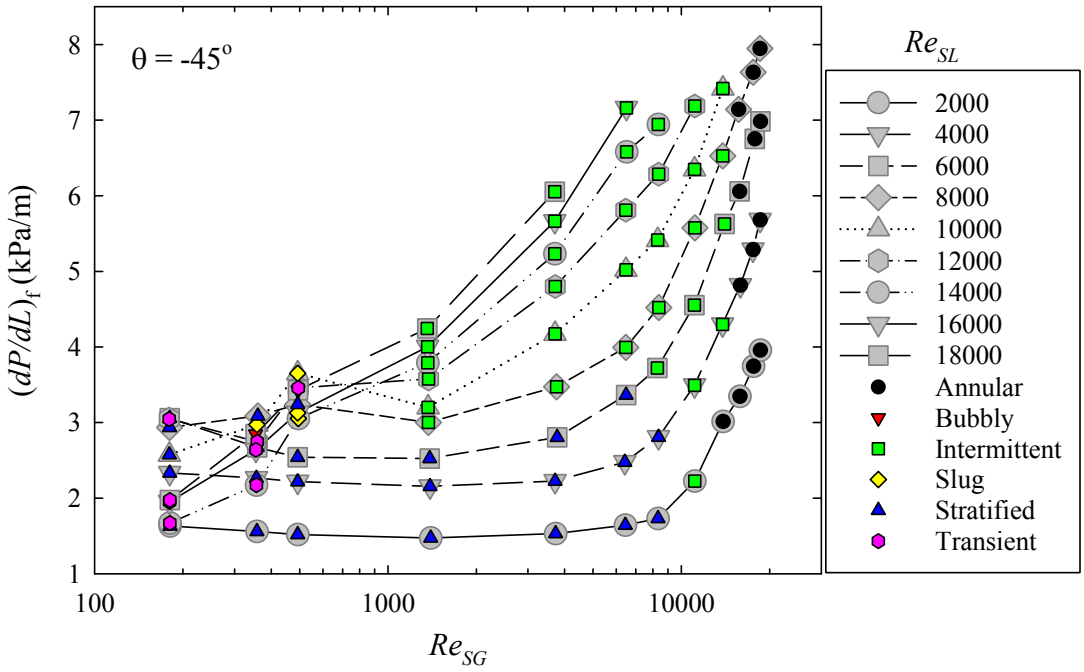

(e) $\theta = -45^o$

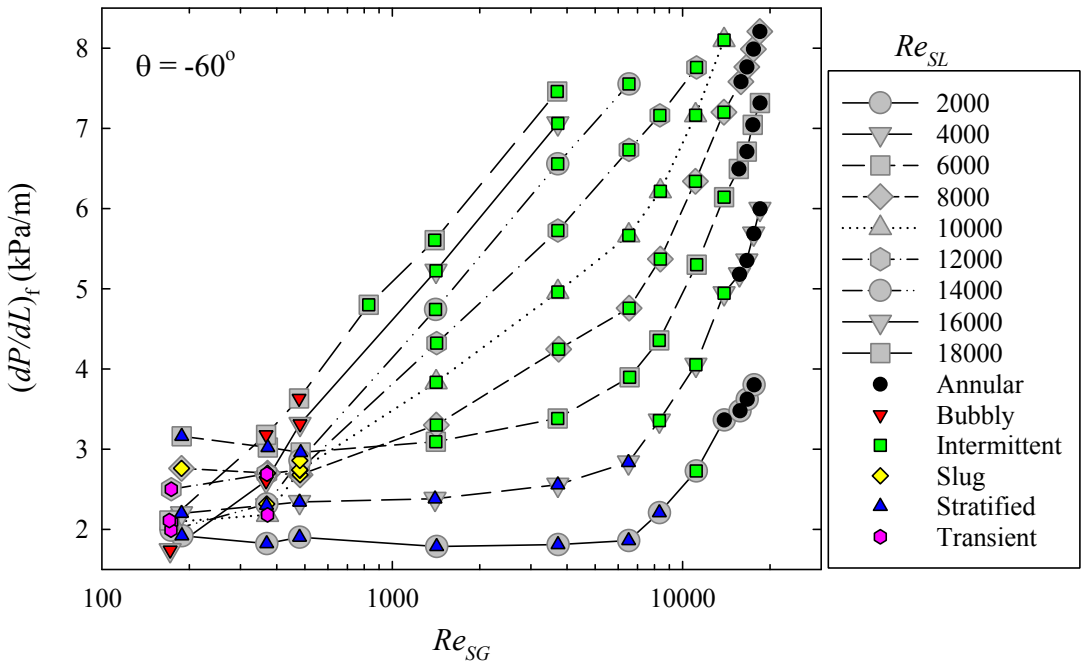

(f) $\theta = -60^o$

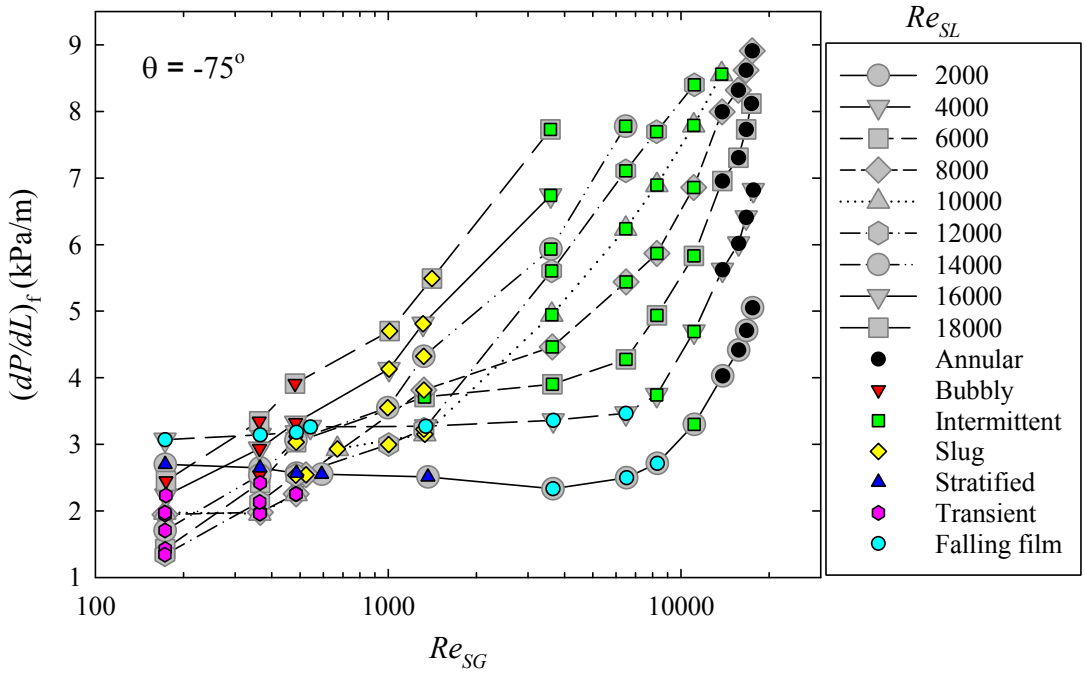

(g) $\theta = -75^o$

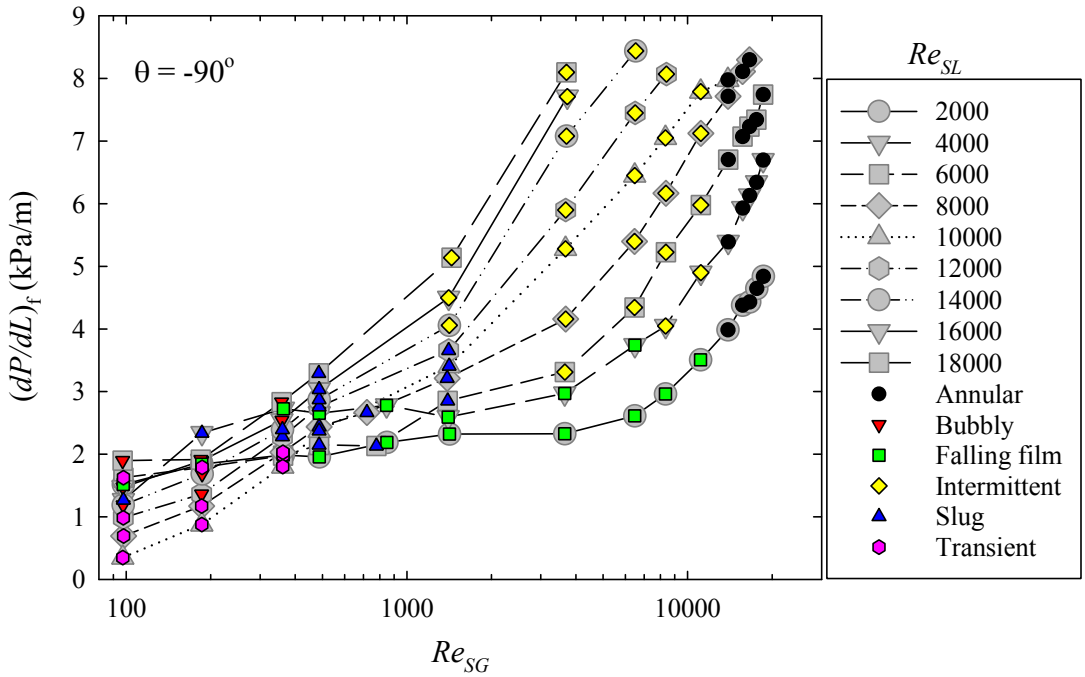

(h) $\theta = -90^o$

Figure 4.47: Effect of phase flow rates (flow patterns) on two phase frictional pressure drop in downward pipe inclinations.

to the sampling process (total number of measurements as a function of time). For this flow regime, steady state conditions are hardly attained and a different sampling time would yield a different magnitude of two phase pressure drop. As such, the transient region in downward inclined two phase flow has little significance with no definite flow structure and hence this region must be avoided for all practical purpose. For all downward pipe inclinations, the qualitative trends of frictional pressure drop for intermittent (annular wavy) and annular flow patterns are found similar to those in horizontal and upward inclined two phase flow. This again concludes that intermittent (annular wavy) and annular flow patterns are fairly insensitive to the change in pipe orientation. It is also of interest to check the effect of coring phenomenon in bubbly flow (discussed in Section 4.1.1) on the two phase frictional pressure drop. The non-dimensional form of two phase frictional pressure drop (Φ_L^2) is presented as a function of gas flow rate in Fig. 4.48. The ratio of $\Phi_L^2 = 1$ indicates that two phase pressure drop is equal to single phase pressure drop measured/calculated at equivalent mass flow rate. Thus, $\Phi_L^2 < 1$ would mean that two phase frictional pressure drop is less than its single phase counterpart. It is seen from Fig. 4.48 that for high liquid flow rates (Re_{SL}), two phase frictional multiplier is less than unity. With increase in Re_{SG}, Φ_L^2 gradually increases and eventually becomes greater than unity.

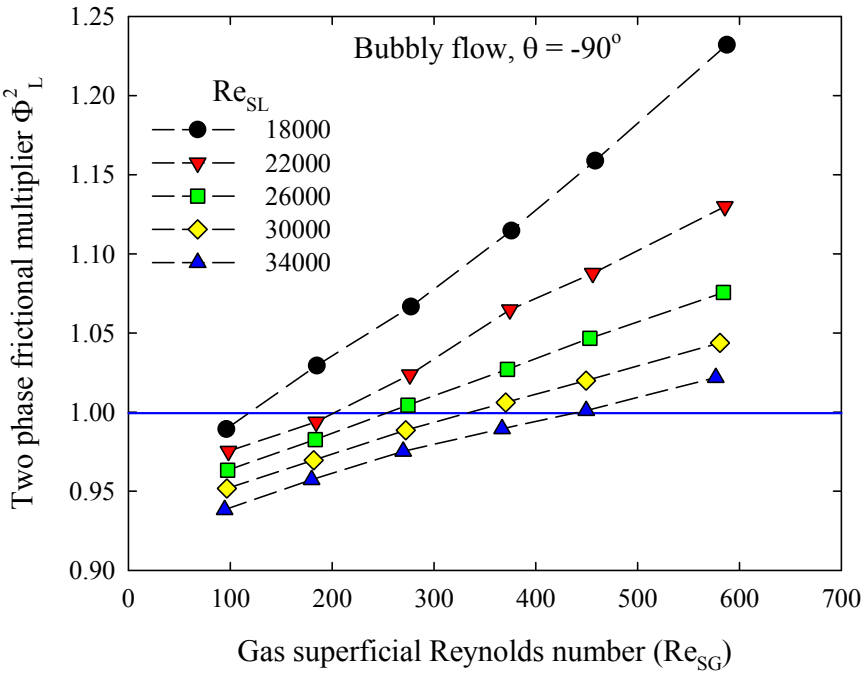

Figure 4.48: Effect of coring phenomenon on two phase frictional pressure drop in vertical downward bubbly flow.

A probable explanation for $\Phi_L^2 < 1$ can be given considering the flow physics of coring bubbly flow. It was discussed in section 4.1.1 that the coring phenomenon is a consequence of wall repulsion forces acting in a direction towards centerline. It is speculated that these repulsive forces tend to increase the viscous sublayer thickness that alters the wall shear stress and velocity profile becomes less steeper within the boundary layer. This change in velocity profile reduces the two phase frictional pressure drop. It was seen in Fig. 4.2 that the coring phenomenon reduces with decrease in liquid flow rate and/or increase in gas flow rates. This conclusion obtained from flow visualization is very well in agreement with the results in Fig. 4.48 i.e., with increasing liquid flow rates, higher gas flow rates are required to overcome the coring effect such that the two phase pressure drop exceeds single phase pressure drop.

4.3.3 Effect of Pipe Orientation

In addition to the effect of phase flow rates (flow patterns) it is also vital to analyze the effect of pipe orientation on total two phase pressure drop. A preliminary analysis of measured two phase pressure drop data showed that the effect of pipe orientation on total component of two phase pressure drop is very significant compared to its effect on frictional component. This means that the effect of pipe orientation on total two phase pressure drop is essentially through the effect of pipe orientation on the hydrostatic component as a function of void fraction. The effect of pipe orientation on $(dP/dL)_t$ as a function of Re_{SG} is presented for different liquid superficial Reynolds numbers in Fig. 4.49 (a)-(d). At low liquid flow rates ($Re_{SL} = 2000$) and low gas flow rates, total two phase pressure drop is relatively insensitive to decrease in downward pipe inclination from $\theta = -90^o$ till the pipe is in horizontal orientation. For upward pipe inclinations, total two phase pressure drop increases rapidly with increase in pipe orientation. At higher gas flow rates, $(dP/dL)_t$ is found to be insensitive to the change in pipe orientation. It is interesting to note that for vertical and near vertical upward pipe orientations, highest total two phase pressure drop occurs at lower gas flow rates with a maximum $(dP/dL)_t$ occurring at $\theta = +75^o$. The high values of $(dP/dL)_t$ at low gas flow rates compared to that at high gas flow rates appear to be due to relative magnitudes of hydrostatic and frictional components of pressure drop. At low liquid and low gas flow rates, void fraction in upward inclinations is low and hence causes significantly higher hydrostatic pressure drop such that it is greater than the frictional pressure drop in annular flow regime at high gas flow rates. Similar observations are reported by Spedding et al. (1982) for two phase flow of air-water in a 45 mm I.D. pipe. They found the maximum total two phase pressure drop to occur at $\theta = +70^o$ and concluded that the maximum two phase pressure drop at $\theta = +70^o$ is essentially due to the minimum void fraction and hence maximum

contribution of hydrostatic component at this pipe orientation. Later Spedding et al. (2000) further investigated two phase pressure drop in 26 mm I.D. vertical and near vertically upward oriented pipe using air-water fluid combination. They reported that the total two phase pressure drop in near vertical pipe orientations was equal (at high gas flow rates) or higher (at low gas and liquid flow rates) than that in vertical upward pipe orientation. Spedding et al. (2000) suggested that in comparison to vertical upward flow, the flow structure (liquid and gas phase distribution) across the pipe cross section in near vertical inclined pipes exhibits anisotropy which favors additional liquid holdup. This anisotropy reduces the uplift action of liquid slug rising in the wake region of the Taylor bubble (elongated slug) and hence results in further pressure loss in the downstream direction. In the present study as well as that of Spedding et al. (1982), total two phase pressure drop was observed to decrease with decrease in pipe diameter for $\theta \lessapprox 75^o$. This observation infers that the threshold pipe orientation at which the anisotropy of two phase flow structure increases two phase pressure drop is in the range of $70^o < \theta < 75^o$. From the experimental data of Spedding et al. (1982) it is found that the liquid and gas flow rates at which the total two phase pressure drop at $\theta = +75^o$ is greater than that in vertical upward pipe orientation are in the range of $0.01 \leq U_{SL} \leq 0.51$ m/s and $0.09 \leq U_{SG} \leq 10$ m/s, respectively. In comparison to this, the present study finds the tendency of $(dP/dL)_t$ to maximize at $\theta = +75^o$ when the liquid and gas flow rates are in the range of $0.03 \leq U_{SL} \leq 0.45$ m/s and $0.09 \leq U_{SG} \leq 13$ m/s, respectively.

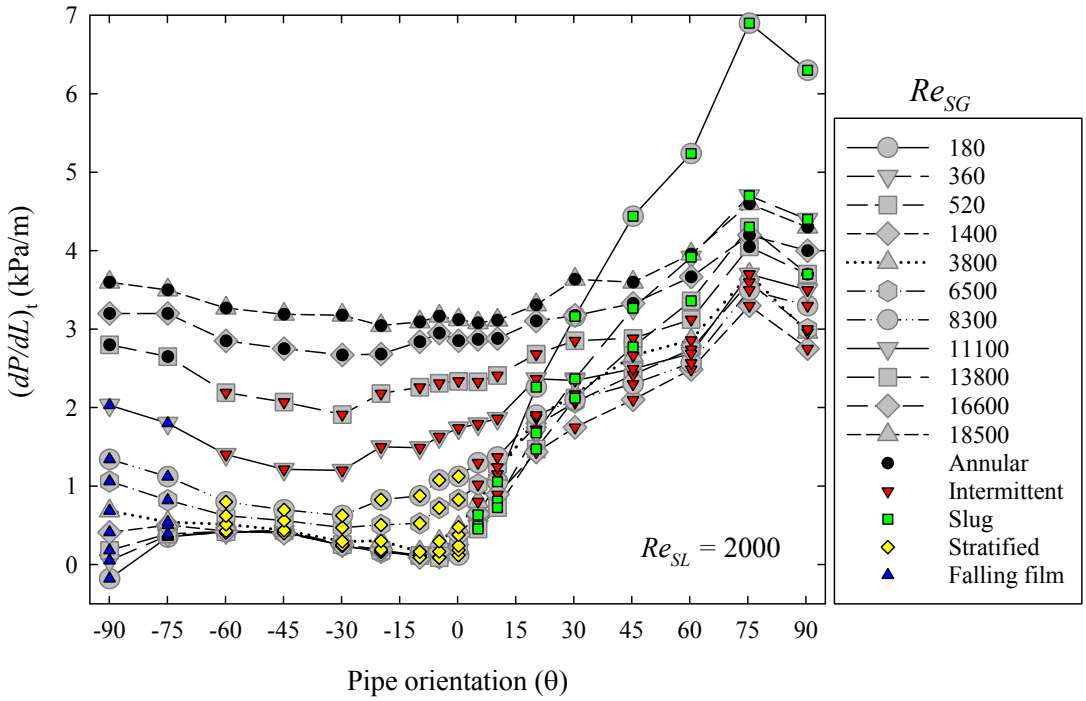

(a) $Re_{SL} = 2000$

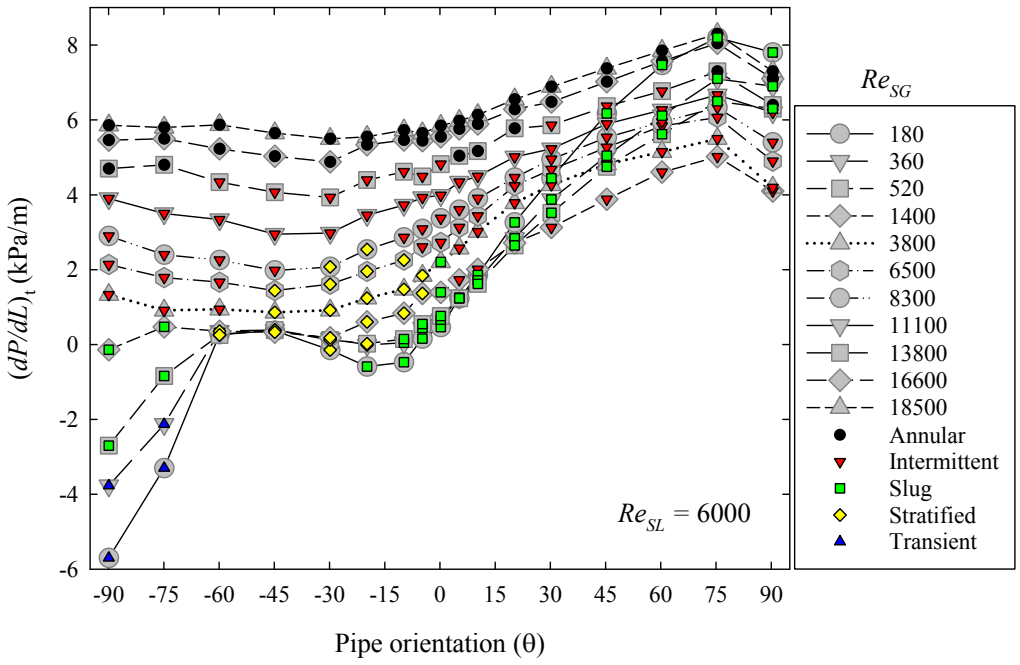

(b) $Re_{SL} = 6000$

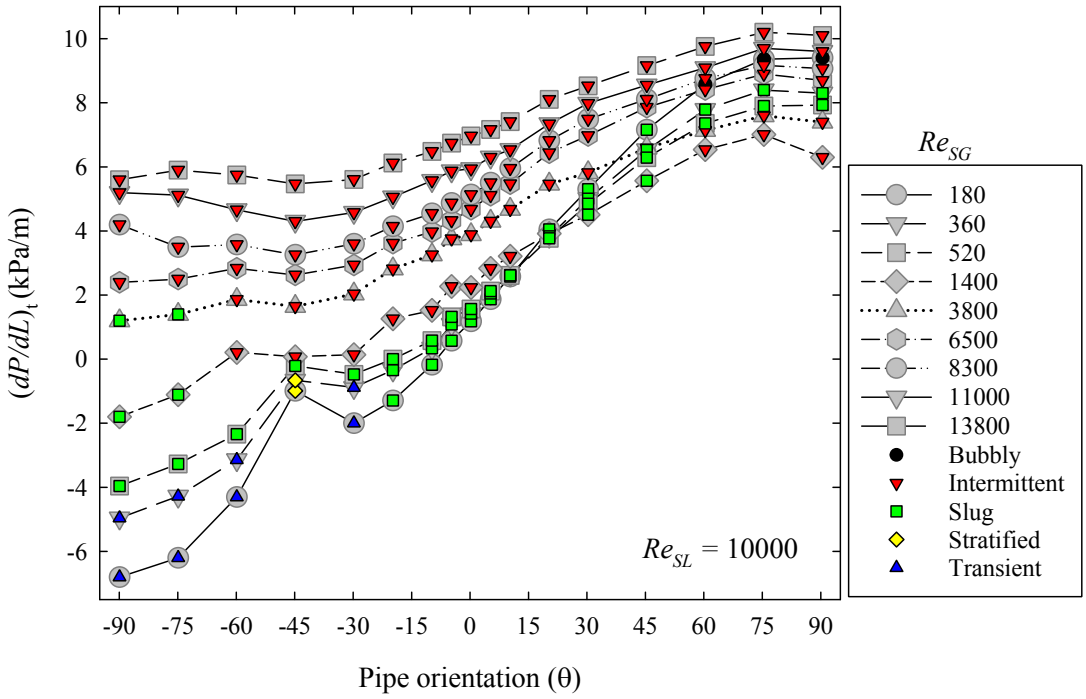

(c) $Re_{SL} = 10000$

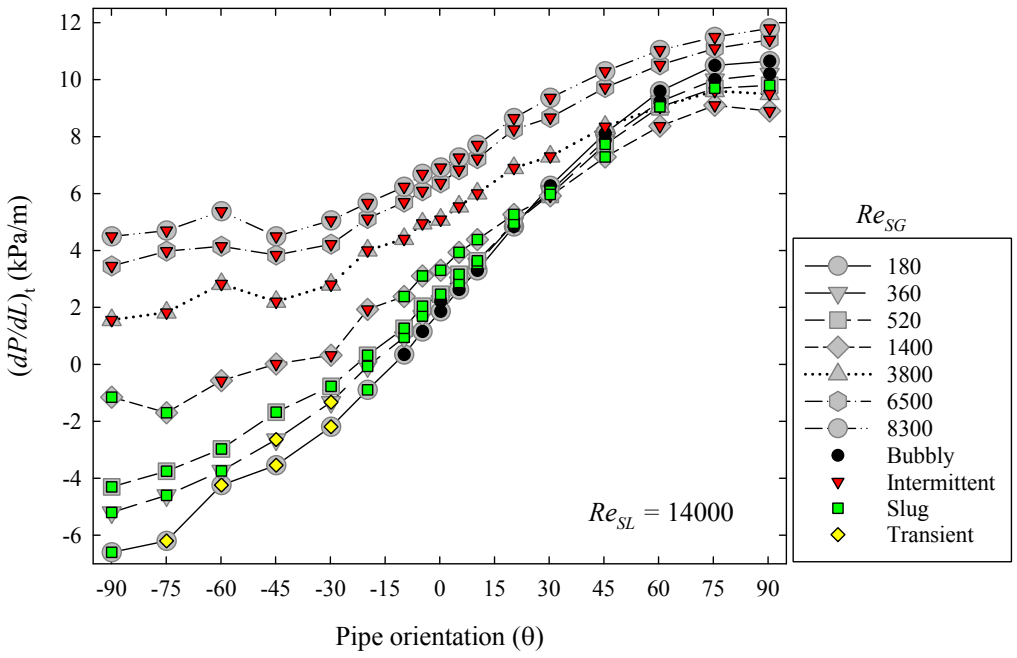

(d) $Re_{SL} = 14000$

Figure 4.49: Effect of pipe orientation on total two phase pressure drop.

It is seen that for stratified flow in downward pipe inclinations, total two phase

pressure drop is insensitive to the change in pipe orientation. This is because both hydrostatic pressure drop (as a function of void fraction) and frictional pressure drop for stratified flow remains insensitive to pipe orientation. Slightly higher values of $(dP/dL)_t$ in falling film flow at -75^o and -90^o compared to stratified flow can also be attributed to the flow structure. In stratified flow, partial pipe circumference is in contact with liquid phase while the remaining portion is in contact with gas phase. Comparatively in falling film flow, entire pipe circumference is in contact with liquid phase that increases the total two phase pressure drop. For increased liquid flow rates, trends of total two phase pressure drop similar to that at $Re_{SL} = 2000$ are observed at low and high gas flow rates. However, for $-90^o \leq \theta \leq -60^o$, a sharp decrease in total two phase pressure drop is observed. This is due to the fact that for $\theta \geq -60^o$, stratified flow exists while for further increase in downward pipe orientation two phase flow is in form of slug or transient flow. The negative values of total two phase pressure drop in downward inclined slug flow are essentially due to the pressure recovery i.e., pressure gain due to hydrostatic two phase pressure drop being greater than irreversible pressure loss due to friction.

For further increase in liquid flow rates at $Re_{SL} = 10000$ and $Re_{SL} = 14000$, a continuously increasing trend of total two phase pressure drop as a function of pipe orientation is observed. It needs to be mentioned that at these high liquid flow rates, the tendency of maximum total two phase pressure drop at near vertical upward pipe inclinations gradually goes away. With increase in liquid flow rates, the magnitude of pressure recovery in near vertical downward pipe inclinations is observed to increase. A comparison between total two phase pressure drop measured at vertical upward and downward orientation for $Re_{SL} = 14000$ and $Re_{SG} = 180$ show that about 60% of total two phase pressure drop incurred in vertical upward flow is recovered in vertical downward flow at identical phase flow rates. Thus, a consecutive upward and downward inclined piping system arrangement in industrial applications may

help to reduce overall total two phase pressure drop by having partial pressure drop recovery during two phase flow in downward inclinations. The qualitative resemblance between the trends of total two phase pressure drop as function of pipe orientation for different combinations of gas and liquid flow rate is observed for the experimental data of Spedding et al. (1982) and Lips and Meyer (2012c) shown in Figure 4.50. In comparison to present study and Spedding et al. (1982), data of Lips and Meyer (2012c) do not show a tendency of $(dP/dL)_t$ to maximize at $\theta = +75^o$. However, a saturating trend of $(dP/dL)_t$ is observed at near vertical pipe orientations.

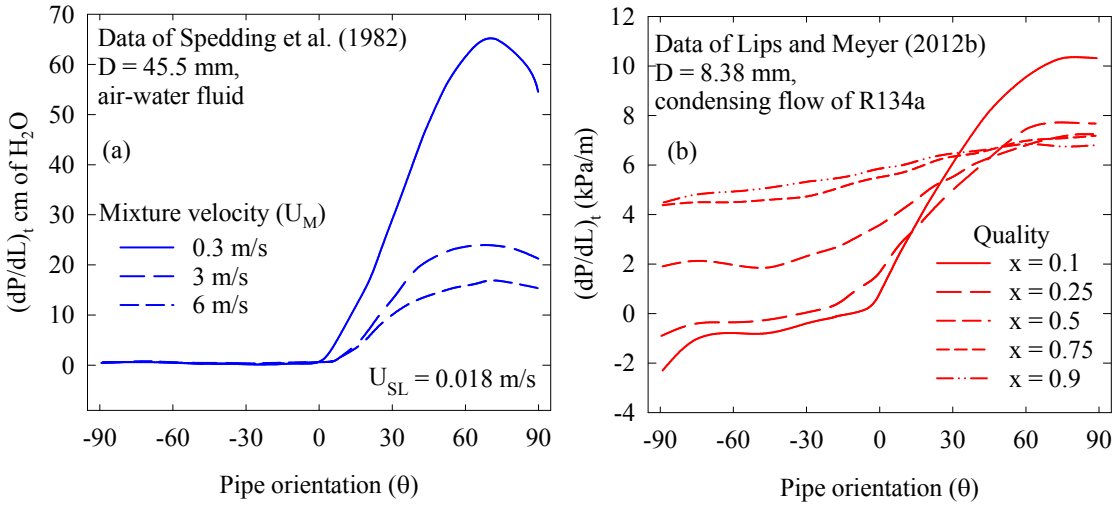

Figure 4.50: Effect of pipe orientation on total two phase pressure drop for (a) air-water data (b) R134a data.

4.3.4 Effect of Surface Roughness

One of the objectives of this work is to investigate the effect of pipe wall surface roughness on frictional component of two phase pressure drop. The effect of pipe surface roughness on two phase pressure drop is crucial in applications involving two phase flow through steel or micro-finned tubes. The internally ribbed or micro-finned tubes are used in air-conditioning and refrigeration applications to improve the tube side heat transfer however at the expense of enhanced pressure drop. Most of the two phase flow research reported in the literature is carried out in a transparent (smooth pipe) while the effect of pipe surface roughness on the frictional two phase pressure drop is so far the least investigated issue in the two phase literature. Some of the known studies available in the literature that investigate the effect of surface roughness on two phase pressure drop are that of Wongs-ngam et al. (2004) and Shannak (2008). Wongs-ngam et al. (2004) experimentally measured pressure drop of R134a refrigerants in a 8.9 mm I.D. micro-finned tube with a fin height of 0.2 mm. They found that compared to smooth tube, the pressure drop in micro-fined tube increased by about 60% for a combination of high mass flux and high two phase flow quality. Even at low qualities, the two phase pressure drop in micro-finned tube measured 10% higher than that in smooth tube. Shannak (2008) experimentally measured frictional two phase pressure drop in a 52.5 mm I.D. pipe (horizontal and vertical) with two different surface roughness using air-water fluid combination. He found that the pipe surface roughness enhanced the frictional component of two phase pressure drop by up to 20% especially at high mass fluxes and high two phase flow quality. However, he did not report the combined effect of individual flow patterns and the pipe orientation on the frictional two phase pressure drop for two different

relative surface roughness.

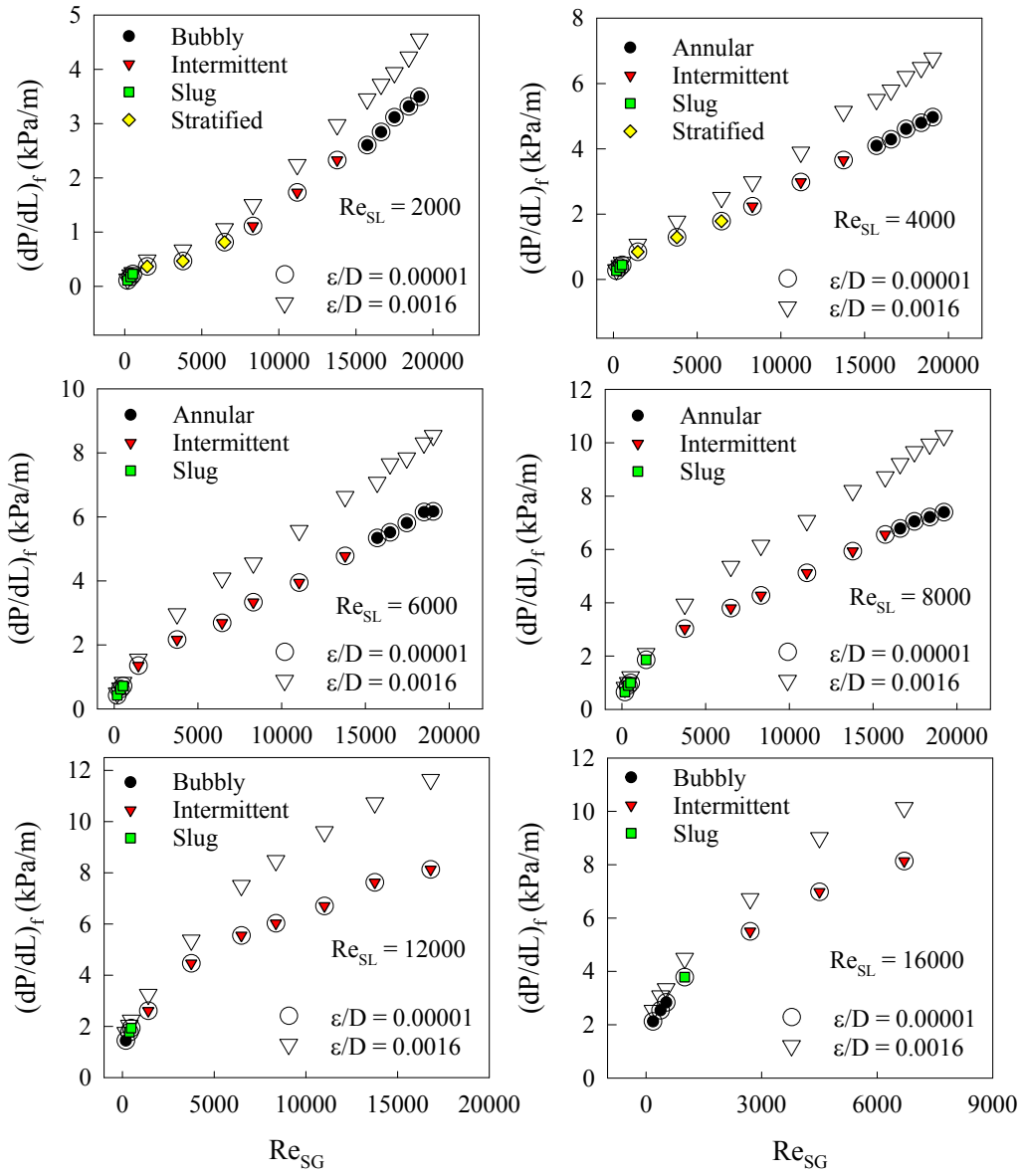

Figure 4.51: Effect of pipe surface roughness on frictional pressure drop for horizontal flow (present study).

In the present study, two phase frictional pressure drop is measured in a smooth (polycarbonate material) and rough (stainless steel) pipe. The surface roughness of the polycarbonate and stainless steel pipe is taken to be 0.00015 mm and 0.02 mm thus giving ϵ/D ratio of 0.00001 and 0.0016, respectively. The pressure drop measurements

are carried out in both polycarbonate and stainless steel pipes at seven different pipe orientations covering all flow patterns and the entire range of void fraction. Assuming void fraction to be independent of the pipe surface roughness, the void fraction values measured in polycarbonate pipe is used to extract frictional pressure drop from total two phase pressure drop. The effect of pipe surface roughness on two phase frictional pressure drop for horizontal pipe orientation is evident from Fig. 4.51. It is seen that for a fixed liquid flow rate or Re_{SL}, the effect of pipe surface roughness on two phase frictional pressure drop is noticeable for high values of gas flow rates or Re_{SG}. The difference between frictional pressure drop in smooth and rough pipe increases with increase in liquid flow rates. At $Re_{SL} = 2000$ and $Re_{SG} = 16500$, the two phase frictional pressure drop in rough pipe is about 26% higher than that in smooth pipe whereas for similar Re_{SG} but at higher Re_{SL} of 12000, the frictional pressure drop in rough pipe is about 44% higher than that in smooth pipe. This result is in agreement with the observations of Shannak (2008) and Wongs-ngam et al. (2004) that the effect of pipe surface roughness on two phase pressure drop is significant for high mass fluxes and high two phase flow quality i.e., high gas and liquid mass flow rates. The experimental measurements of Shannak (2008) are presented in Figure 4.52.

In addition to the combined effect of Re_{SL} and Re_{SG}, it is also of interest to check the combined effect of pipe orientation (θ), Re_{SL} and Re_{SG} on the two phase frictional pressure drop for smooth and rough pipes. Fig. 4.53 shows the percentage increase in the frictional pressure drop due to the two phase flow in rough pipe compared to a smooth pipe for six different pipe orientations measured at similar gas and liquid flow rates. It is evident that there is no combined effect of pipe orientation and the phase flow rates i.e., for a fixed pipe diameter and fluid properties, the increase in frictional pressure drop due to pipe surface roughness depends only on the relative roughness (ϵ/D) and gas and liquid phase flow rates.

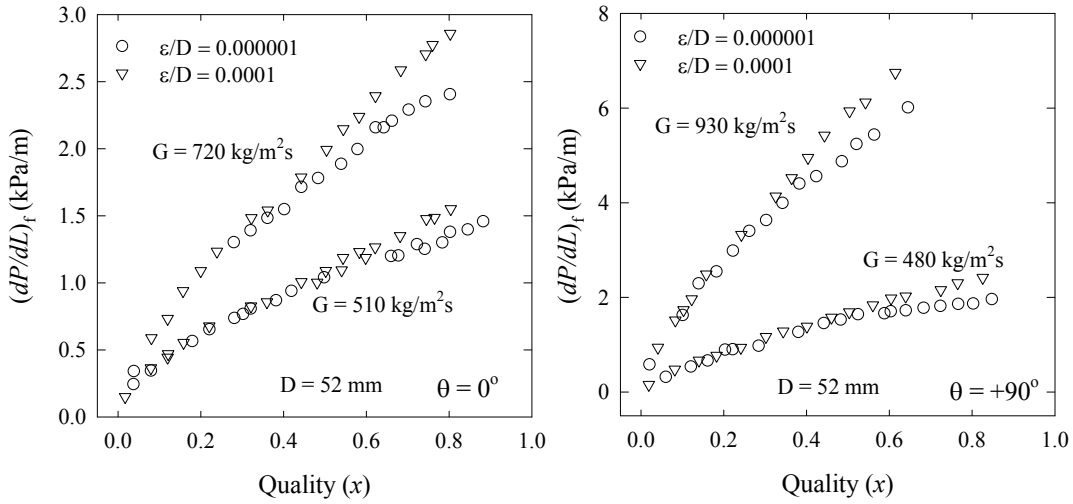

Figure 4.52: Effect of pipe surface roughness on frictional two phase pressure drop (Air-water data of Shannak (2008), $D = 52$ mm).

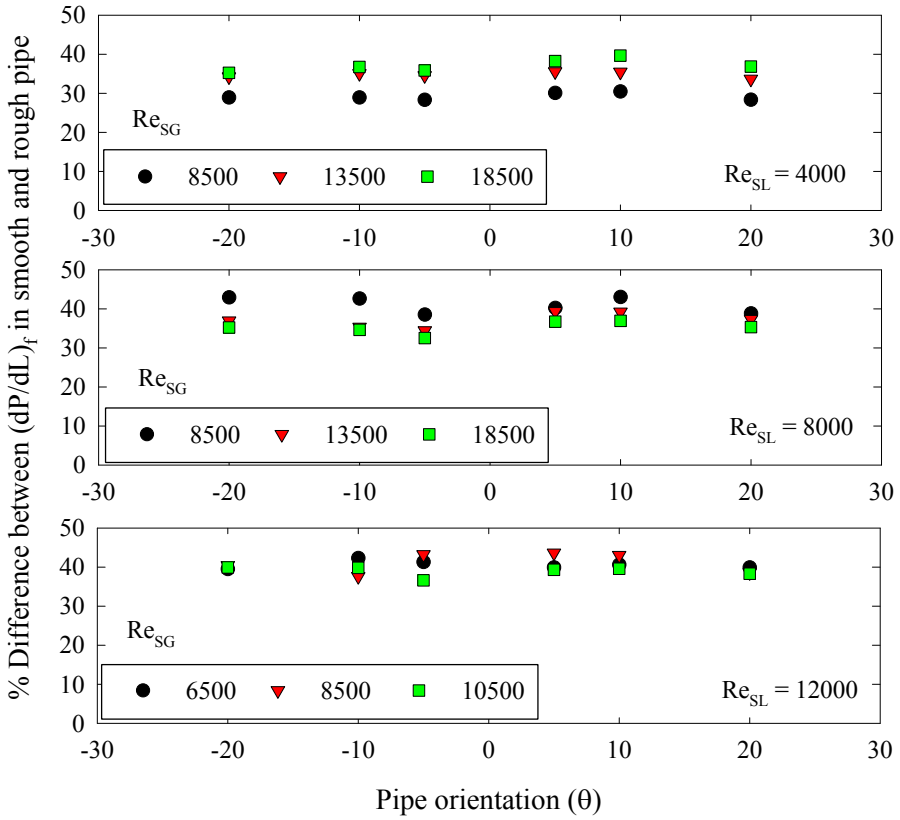

Figure 4.53: Combined effect of pipe orientation and phase flow rates on percentage increase in frictional pressure drop due to pipe wall surface roughness.

4.3.5 Effect of Pipe Diameter

Similar to the single phase flow, two phase flow pressure drop is also inversely proportional to the pipe diameter. Moreover, based on the data available in the literature it is found that the effect of pipe diameter on two phase frictional pressure drop depends on the flow pattern structure to a great extent and is expected to be independent of the fluid combination. As shown in Fig. 4.54, the two phase frictional pressure drop is plotted against the two phase flow quality covering the entire range of void fraction and flow patterns. The effect of pipe diameter on two phase frictional pressure drop is significant for higher values of quality representing the wavy annular and annular flow regimes. For lower two phase flow qualities, the effect of pipe diameter on $(dP/dL)_f$ gradually reduces.

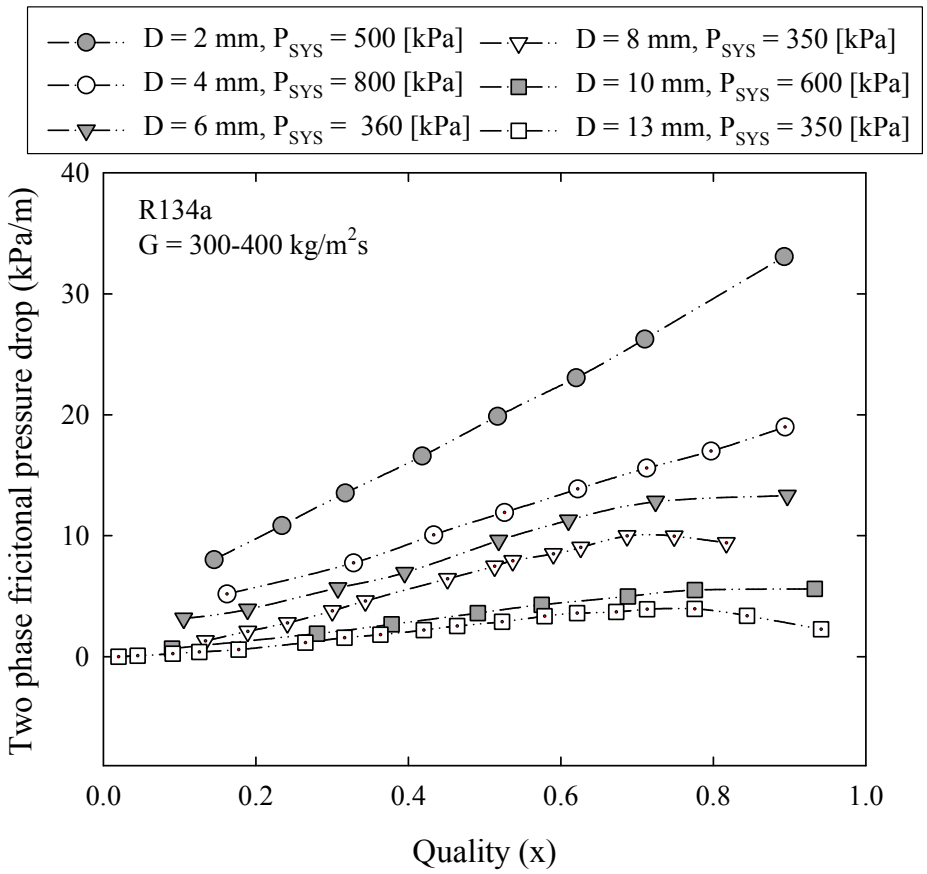

Figure 4.54: Effect of pipe diameter on two phase frictional pressure drop.

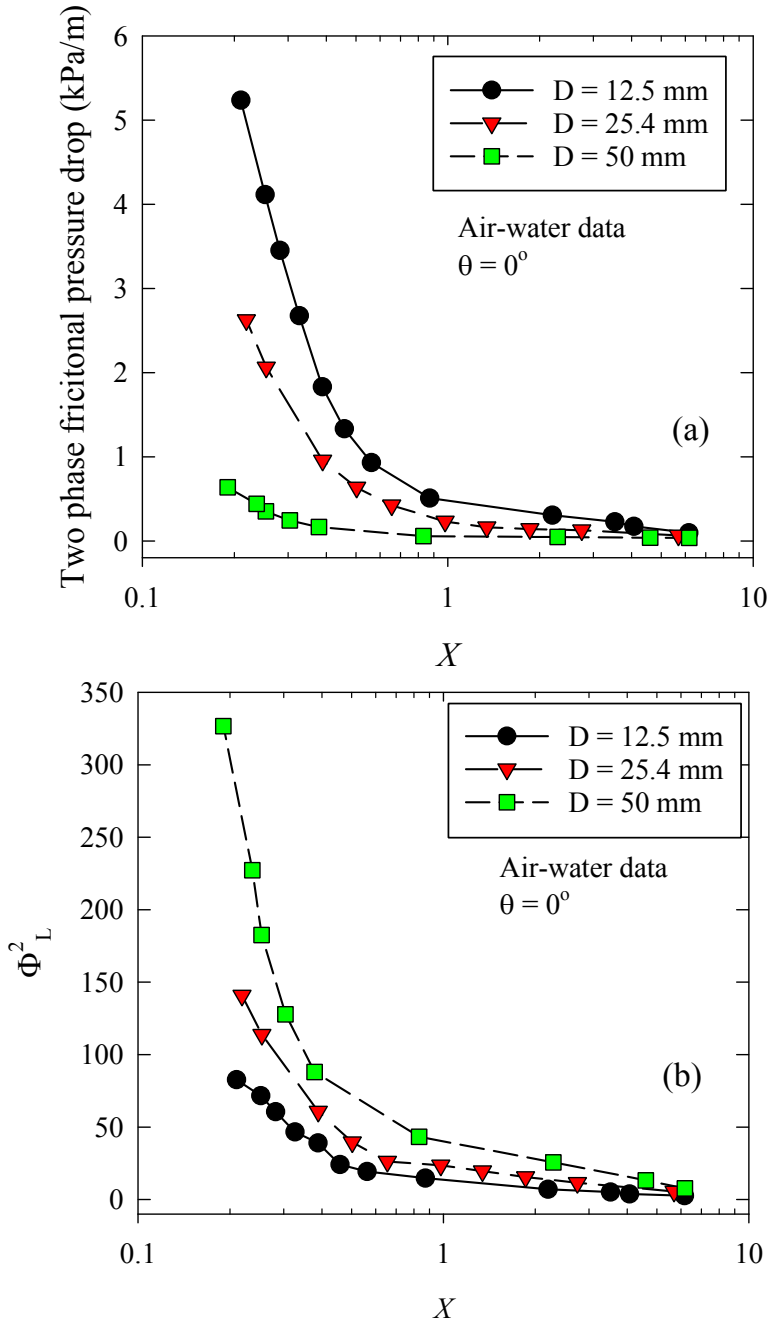

Figure 4.55: Effect of pipe diameter on frictional pressure drop and two phase frictional multiplier.

Similar relation between pipe diameter and frictional pressure drop is observed for the air-water data as shown in Fig. 4.55. The Lockhart and Martinelli (1949) parameter X is used to compare the frictional pressure drop and two phase frictional

multiplier (Φ_L^2) for three different pipe diameters. The small values of X correspond to the annular (shear driven flow region) where the effect of pipe diameter on frictional pressure drop is significant. Whereas, the large values of X belong to buoyancy driven flows such as slug flow and only a marginal effect of change in pipe diameter is observed on the two phase frictional pressure drop. It is also interesting to check the effect of pipe diameter on non-dimensional frictional pressure drop represented in terms of two phase frictional multiplier (Φ_L^2) proposed by Lockhart and Martinelli (1949). It is seen from Fig. 4.55(b), the two phase frictional multiplier increases with increase in gas flow rate (decrease in 'X') and decrease in the pipe diameter. As against this, the two phase frictional pressure drop increases with decrease in pipe diameter. The increasing trend of Φ_L^2 with increase in pipe diameter is essentially due to increase in gas-liquid interfacial area. Thus for any correlation to account for the effect of pipe diameter on two phase frictional pressure drop, it is necessary that the correlation considers combined effect of the pipe diameter and flow pattern structure.

4.3.6 Effect of Fluid Properties

It was seen earlier that the gas density and liquid phase dynamic viscosity are the two parameters that can significantly influence the two phase flow parameters. To investigate this issue further, effect of gas phase density (system pressure) and the liquid phase dynamic viscosity on the two phase frictional pressure drop is analyzed in this section. The increase in system pressure increases the gas phase density and hence reduces the specific volume occupied by the gas phase. This results into decrease in void fraction and hence reduces slippage between the two phases. Reduction in gas liquid slippage reduces the interfacial velocity or the shear at gas liquid interface and hence reduces the overall two phase frictional pressure drop. The decreasing trend of two phase frictional pressure drop with increase in the gas (vapor) phase density is illustrated in Fig. 4.56 for two phase flow of refrigerants in two different pipe diameters. It is clearly seen that for $D = 6$ mm, the $(dP/dL)_f$ for CO_2 having a vapor density of 61 kg/m^3 is lowest compared to other refrigerants with smaller gas density. Similar conclusion can be drawn for the two phase flow of refrigerants in 10 mm I.D. pipe shown in Fig. 4.56. Based on the trends of $(dP/dL)_f$ with change in two phase flow quality it is anticipated that the effect of gas phase density on two phase frictional pressure drop is significant for higher flow qualities (typically that in annular flow) and will reduce with decrease in flow quality. A close observation reveals that approximately for $x > 0.9$, the two phase pressure drop tends to decrease with further increase in flow quality. Similar trend was also observed for $D \geq 8$ mm presented in Fig. 4.54. This inflection point at which the decreasing trend of $(dP/dL)_f$ is observed represents onset of mist flow. In the mist flow, gas (vapor) phase flows in contact with the pipe wall and liquid phase in form of small droplets moves through the pipe core region. This situation when the liquid phase in contact with the pipe wall is replaced by the gas (vapor) phase, a decreasing tendency of

$(dP/dL)_f$ with increase in two phase flow quality is observed.

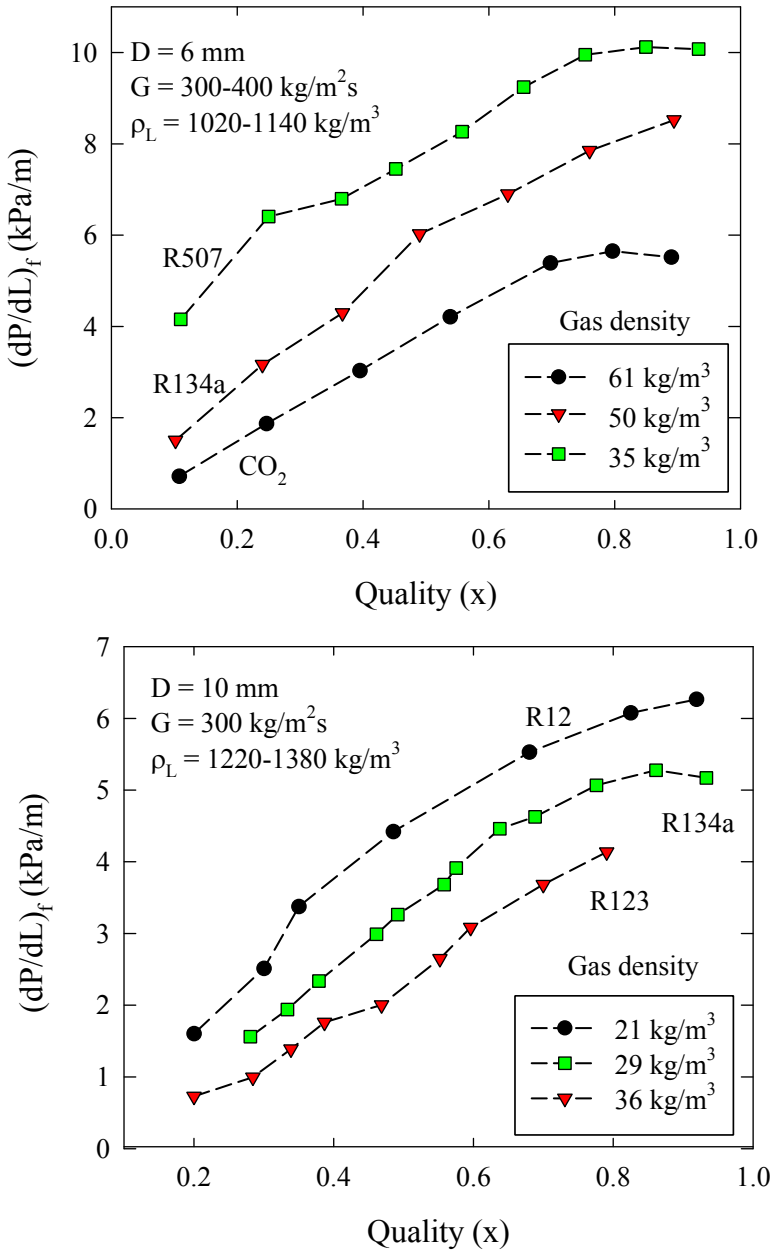

Figure 4.56: Effect of gas (vapor) phase density on two phase frictional pressure drop.

This type of a flow situation is of more relevance in boiling two phase flow where the flow pattern transits from annular to mist flow before reaching the complete dry out condition. In the present study, this type of decreasing frictional pressure

drop trend with increase in gas flow rate i.e., the mist flow was not observed due to limitations in the mass flow meters. Moreover, the occurrence of mist flow is also accompanied by the practical difficulty in measurements of void fraction and entrainment of gas phase in pressure transducer connecting lines that is considered to affect two phase pressure drop.

Another fluid property that affects the two phase pressure drop is liquid phase dynamic viscosity. Two phase flow literature of Oshinowo (1971), Mukherjee (1979), Fukano and Furukawa (1998), Hlaing et al. (2007), Abduvayat et al. (2003),Gokcal (2008) and Kajero et al. (2012) shows that the effect of increase in liquid phase dynamic viscosity is to increase the two phase frictional pressure drop. Oshinowo (1971), Fukano and Furukawa (1998) and Hlaing et al. (2007) experimented with air-water and air-water-glycerol fluid combinations while Abduvayat et al. (2003), Gokcal (2008) and Kajero et al. (2012) carried out pressure drop measurements for oil with significantly higher dynamic viscosities. The experimental data measured by Gokcal (2008) is presented in Fig. 4.57 for two different liquid superficial velocities. It is seen that the effect of increase in liquid dynamic viscosity is small at low gas and liquid flow rates and increases with increase in gas flow rate for a fixed liquid flow rate. The region of high gas flow rate is typically the annular flow which is shear driven in nature. Liquids with higher viscosity exert higher wall and interfacial shear resulting in increased two phase pressure drop. Kajero et al. (2012) also found that the increase in liquid viscosity increases the liquid film thickness which also contributes to increase in the two phase pressure drop.

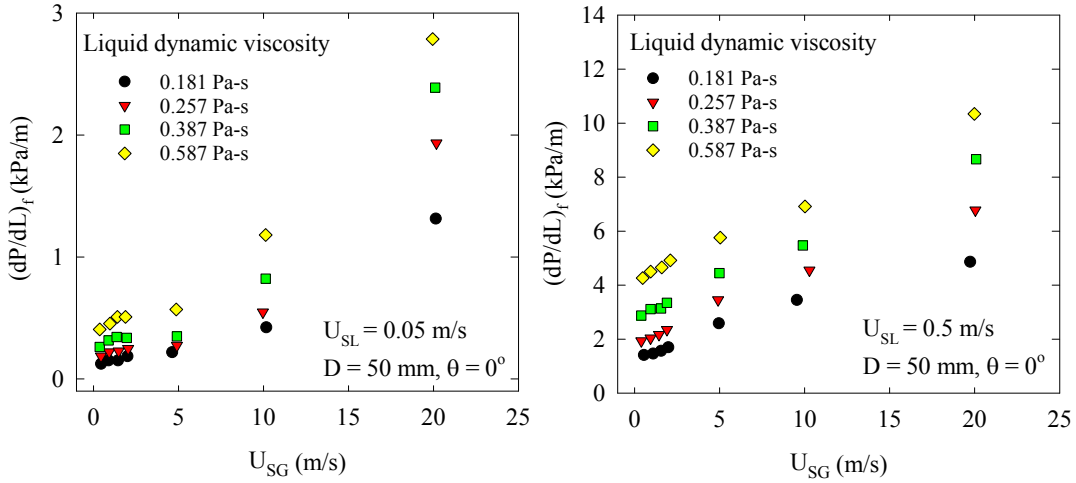

Figure 4.57: Effect of liquid dynamic viscosity on two phase frictional pressure drop.

4.4 Pressure Drop Minimum and Flow Reversal in Upward Inclined Flow

In co-current gas-liquid two phase flow, at low liquid flow rates, although the net two phase flow is observed in the upward direction, reversal of liquid film in contact with the pipe wall is observed under the influence of gravity forces. This reversal of liquid film may be partial reversal or complete reversal depending upon the gas and liquid flow rates. At fixed liquid flow rate, with increase in gas flow rate a point is reached where the gas phase does not have enough potential to carry liquid phase along with it in the downstream direction. At this point, the liquid phase in contact with the pipe wall appears to oscillate or move in the downward direction. Thus, this flow situation in co-current upward inclined flow at certain gas and liquid flow rates where a partial or complete downward flow of liquid phase exists and that gives rise to a momentary counter-current flow is recognized as flow reversal.

Two phase flow literature of Hewitt et al. (1985) and Mao and Dukler (1993), reports the technique of analyzing pipe wall shear stress to determine the onset and departure of the flow reversal. They proposed that the partial downward flow of liquid

phase would result in the decreasing wall shear stress or the frictional pressure drop and a point is reached where the wall shear stress is zero ($\tau_w = 0$). This condition could be described assuming constant phase density and uniform circumferential film thickness in upward inclined flow can be given by Eq. (4.22) where d is any location along the pipe diameter (see Hewitt and Hall-Taylor (1970) and Collier and Thome (1996) for more details).

$$\tau = \tau_i \left(\frac{D - 2\delta}{d} \right) + \frac{1}{4} \left(\rho_L g \sin\theta + \frac{dP}{dL} \right) \left(\frac{(D - 2\delta)^2 - d^2}{d} \right) \tag{4.22}$$

Using the boundary condition of zero wall shear stress ($\tau_w = 0$) at $d = D$ for the case of stationary liquid film in contact with the pipe wall, Eq. (4.22) can be expressed as Eq. (4.23).

$$\tau_w = \tau_i \left(\frac{D - 2\delta}{d} \right) + \frac{1}{4} \left(\rho_L g \sin\theta + \frac{dP}{dL} \right) \left(\frac{(D - 2\delta)^2 - d^2}{d} \right) = 0 \tag{4.23}$$

Assuming negligible acceleration in the gas core and negligible entrainment of liquid drops in the gas core, the interfacial shear stress exerted by the gas phase on the liquid film can be expressed as,

$$\tau_i = \frac{D - 2\delta}{4} \left(\frac{dP}{dL} + \rho_G g \sin\theta \right) \tag{4.24}$$

After combining Eqs. (4.23) and (4.24) and considering that $\delta << D$, following relationship given by Eq. (4.25) is obtained. Following the assumption of negligible liquid entrainment and uniform film thickness distribution, the void fraction can simply be expressed as that by Eq. (4.26). Using this definition of void fraction, it is evident that right hand side of Eq. (4.25) is indeed the hydrostatic component of

two phase pressure drop.

$$\left(\frac{dP}{dL}\right)_{\tau_w=0} = \left[\rho_G\left(\frac{(D-2\delta)^2}{D^2}\right) + \rho_L\left(1 - \frac{(D-2\delta)^2}{D^2}\right)\right] g\sin\theta \tag{4.25}$$

$$\alpha = \frac{A_G}{A} = \frac{(D-2\delta)^2}{D^2} = 1 - \frac{4\delta}{D} \tag{4.26}$$

The physical implication of Eq. (4.25) is that as long as there is a balance between interfacial shear stress and hydrostatic pressure drop, liquid film in contact with the pipe wall with either remain stationary or oscillate giving a zero wall shear stress. Thus, when the interfacial shear stress is large enough to supersede the gravity forces, the net flow of two phase mixture will be in upward direction without any reversal of liquid film. Practically, it is not possible to have a stagnant liquid film in contact with the pipe wall. The zero values of wall shear stress result from the averaged values of positive and negative all shear stress incurred due to oscillating nature of two phase flow. Negative values of wall shear stress would correspond to the complete flow reversal of the liquid film while a decreasing trend would indicate partial reversal of the liquid phase. Two phase flow literature reports that in churn flow regime even if the gas flow rate is increased, a decreasing trend of two phase pressure drop is observed until a pressure drop minimum point is reached. Beyond this point, the two phase flow pattern is annular and two phase pressure drop increases consistently with increase in gas flow rate. What follows is a brief discussion on the partial flow reversal based on the trends between non-dimensional two phase pressure drop and non-dimensional gas and liquid phase velocities.

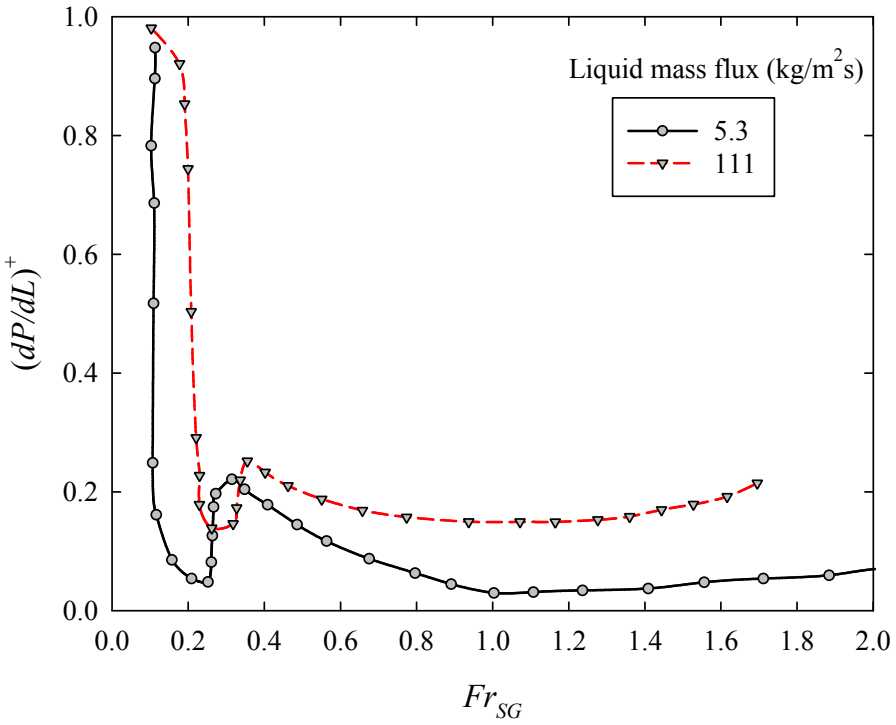

Figure 4.58: Measured non-dimensional pressure drop as a function of non-dimensional gas velocity in air-water vertical upward two phase flow (experimental data of Owen (1986)).

Owen (1986) experimented with air-water two phase flow in a 38 mm I.D. vertical pipe. The gas and liquid flow rates were varied over a wide range and system pressure was maintained approximately at 2.4 bar. He presented the experimental data in form of non-dimensional total two phase pressure drop (Eq. 4.27) and non-dimensional gas velocity (Eq. 4.28) as shown in Fig. 4.58. It is seen that starting with single phase liquid flow, after the gas phase is introduced, the pressure drop or the wall shear stress would decrease until the pressure minimum point is reached. This region of first pressure drop minimum is approximately in the range of $0.2 < Fr_{SG} < 0.3$. After this pressure drop minimum point, further increase in the gas flow rate would cause the two phase pressure drop to increase approximately in the range of $0.3 < Fr_{SG} < 0.4$. Now, any increase in gas flow rate further $Fr_{SG} > 0.4$ would again cause the to phase pressure drop to decrease until $Fr_{SG} \approx 1$. This is the region of second pressure drop

minimum which indicates the end of churn-annular transition region. Further this point of second pressure drop minimum, two phase flow is in form of annular flow pattern and two phase pressure drop increases with increase in gas flow rate.

A thorough two phase flow literature review reveals that almost all of the experimental work related to the flow reversal is carried out in vertical upward pipe orientation with hardly any investigation done for the qualitative and quantitative existence of this phenomenon in inclined systems. Based on the two phase flow mechanism it can be anticipated that the flow reversal exists at all steeper pipe orientations in the upward direction and hence to address this issue, in the present study, the onset and departure of the partial or complete reversal of liquid film is identified by analyzing the trends of the non-dimensional two phase pressure drop $(dP/dL)^+$ plotted against the non-dimensional gas flow rate (Fr_{SG}). The two phase pressure drop and phase superficial velocity are non-dimensionalized similar to that done by Owen (1986) and are shown in Eqs. (4.27) to (4.29).

$$\left(\frac{dP}{dL}\right)^+ = \frac{(dP/dL)_t}{(\rho_L - \rho_G)g} \tag{4.27}$$

$$Fr_{SG} = U_{SG}\sqrt{\frac{\rho_G}{gD(\rho_L - \rho_G)}} \tag{4.28}$$

$$Fr_{SL} = U_{SL}\sqrt{\frac{\rho_L}{gD(\rho_L - \rho_G)}} \tag{4.29}$$

As seen from Fig. 4.59 (a)-(h), the plots of $(dP/dL)^+$ vs. Fr_{SG} for different upward inclined pipe orientations clearly show two distinct regions of pressure drop minimum. Due to limitations of the mass flow meters used in this study, it was not possible to measure any data between $0.2 < Fr_{SG} < 0.35$. Although it appears that the first pressure drop minimum for vertical upward flow is in the vicinity of $Fr_{SG} \approx 0.2$, considering the slope of pressure drop trends in a range of $0.2 < Fr_{SG} < 0.35$,

it is anticipated that the actual minimum point of $(dP/dL)^+$ is approximately at $Fr_{SG} = 0.3$. Following this consideration, the region of first pressure drop minimum is in agreement with the findings of Owen (1986). The flow pattern corresponding to the first trend of decreasing pressure drop is the slug and slug wavy flow. It is also seen that the Fr_{SG} corresponding to first pressure drop minimum decreases with decrease in pipe orientation. For $\theta < +45^o$ it is clearly seen that the first pressure drop minimum occurs at $Fr_{SG} < 0.2$. For all pipe orientations, any increase in Fr_{SG} beyond the first pressure minimum point increases $(dP/dL)^+$ until $Fr_{SG} \approx 0.4$. A close observation shows that for $\theta < +45^o$, the pressure drop maximum (after first pressure drop minimum) is at $Fr_{SG} < 0.4$. After the maximum of $(dP/dL)^+$ is reached (at $Fr_{SG} \approx 0.4$), increase in gas flow rate results into decrease in non-dimensional pressure drop until $Fr_{SG} \approx 1$. This region between $0.4 < Fr_{SG} < 1$ is typically the churn-annular transition region. The region of second pressure drop minimum is $Fr_{SG} \approx 1$ independent of pipe orientation with the exception of $\theta < +20^o$. For near horizontal pipe orientations, the slope of decreasing pressure drop is very small and hence can be ignored. It is also seen that for a fixed pipe orientation, the value of Fr_{SG} corresponding to second pressure drop minimum remains independent of the liquid flow rate. The region of second pressure drop minimum identified in this study for vertical upward flow is in agreement with the work of Wallis (1969) who found that the pressure drop minimum in vertical upward air-water two phase flow occurs at Fr_{SG} between 0.8 and 1. Furthermore, he also suggested that this location of the pressure drop minimum is not appreciably affected by the liquid flow rate. The region of Fr_{SG} at which second pressure minimum is observed in this study is also compared with some of the investigations available in the literature for flow reversal in vertical upward co-current flow. The details of pipe diameter, fluid combinations and the range of Fr_{SG} and Fr_{SL} over which the experiments were carried out are reported in Table 4.2.

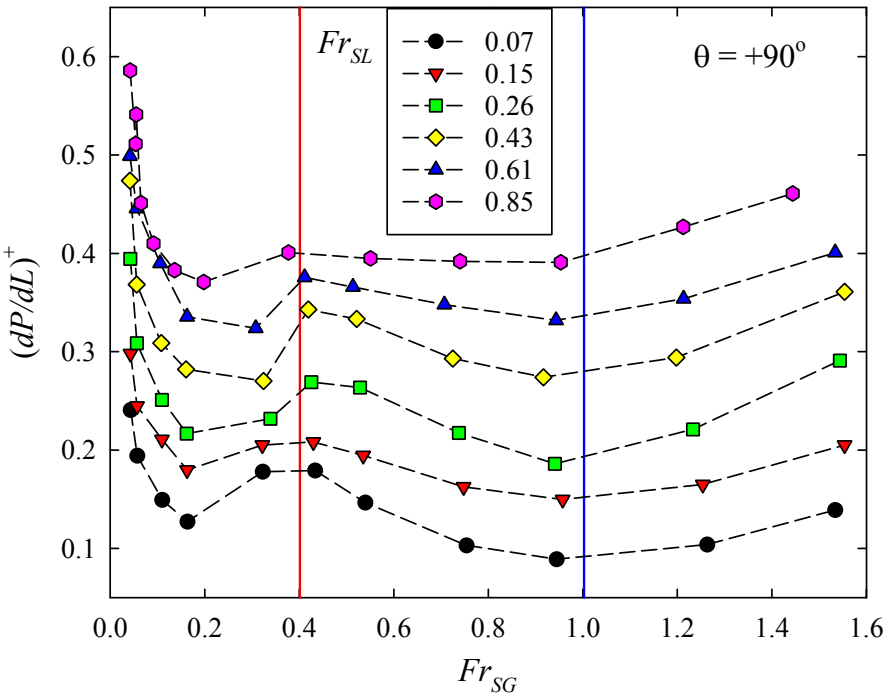

(a) $\theta = +90^o$

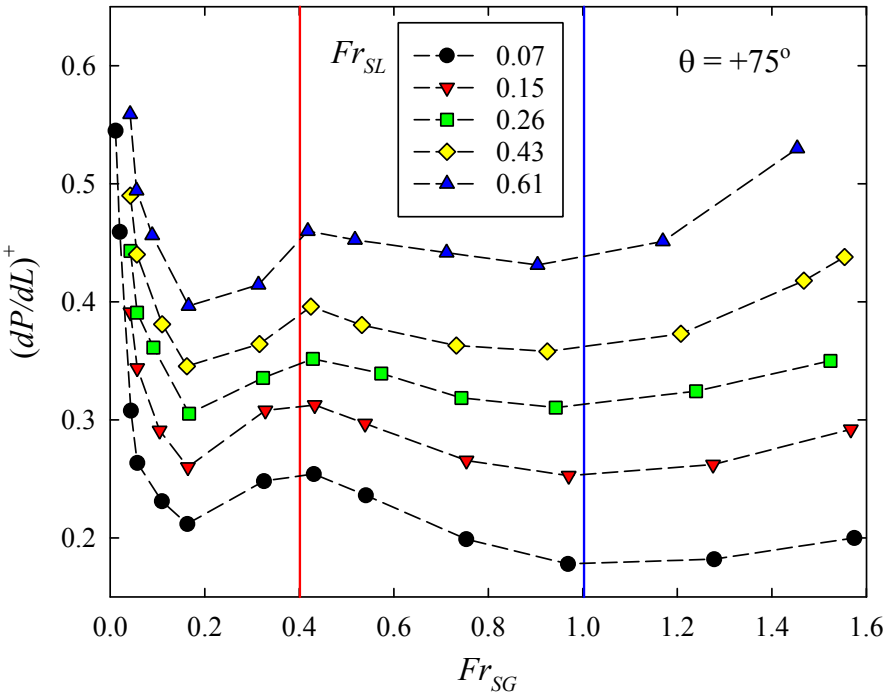

(b) $\theta = +75^o$

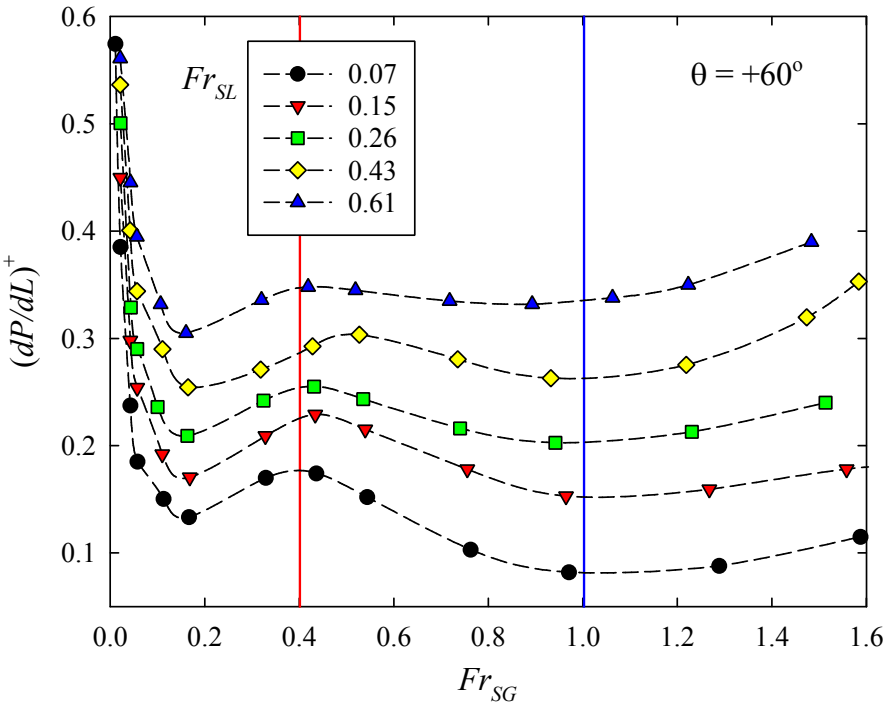

(c) $\theta = +60^o$

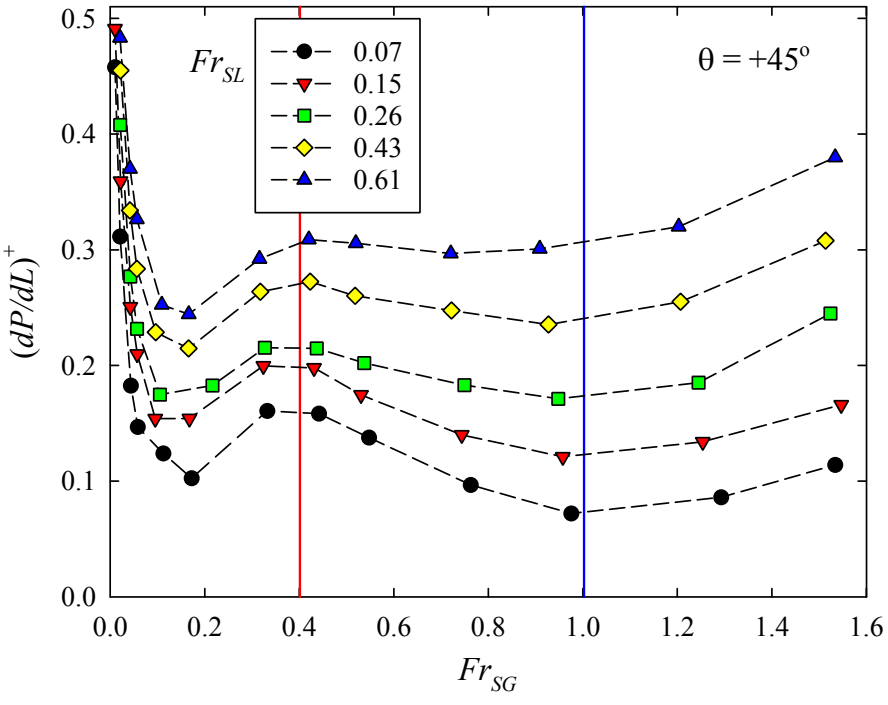

(d) $\theta = +45^o$

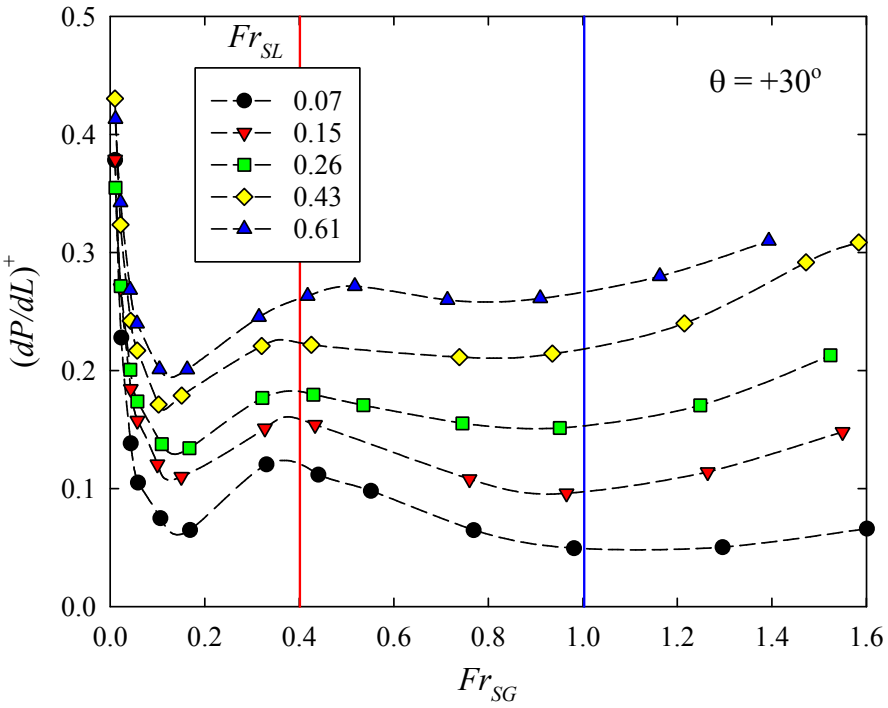

(e) $\theta = +30^o$

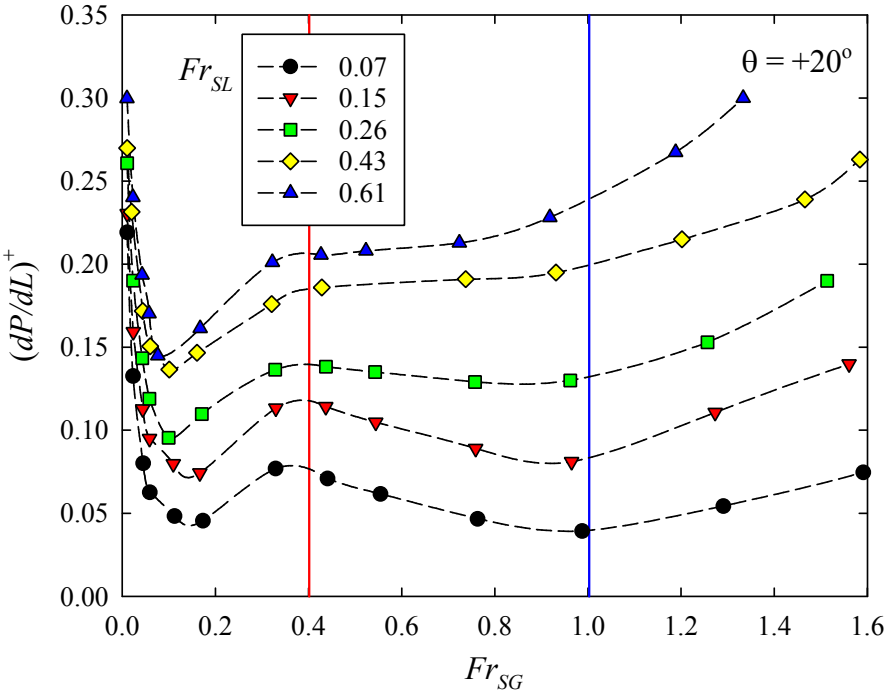

(f) $\theta = +20^o$

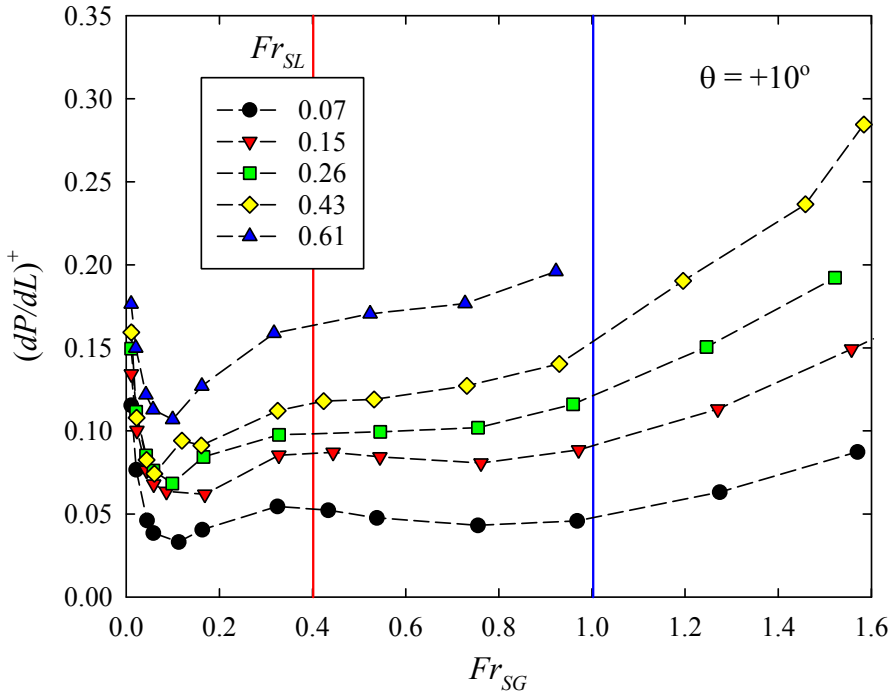

(g) $\theta = +10^o$

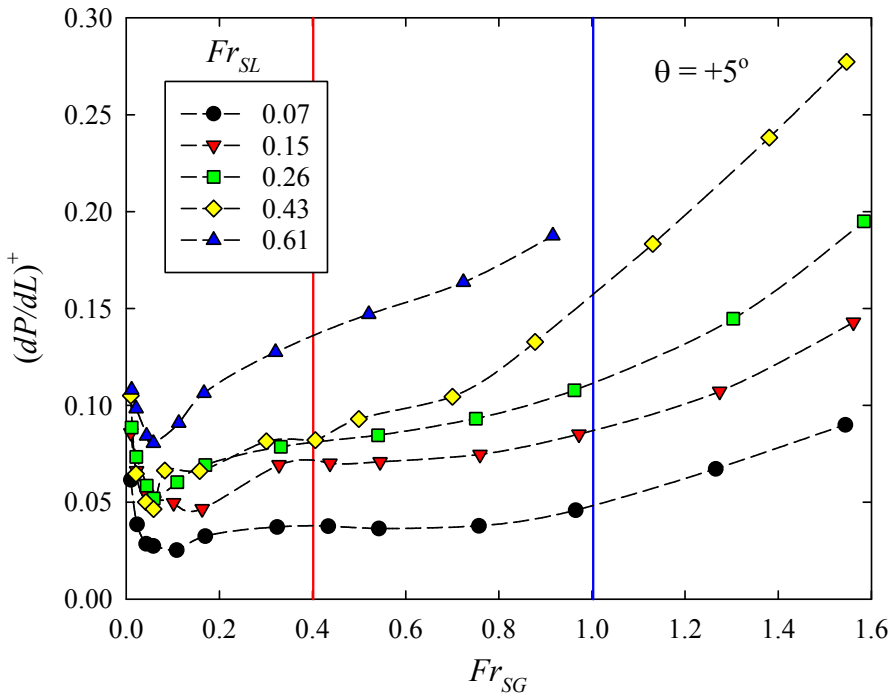

(h) $\theta = +5^o$

Figure 4.59: Distribution of non-dimensional pressure gradient against non-dimensional gas velocity for different pipe orientations.

Table 4.2: Fr_{SL} and Fr_{SG} corresponding to the second pressure drop minimum in vertical upward two phase flow for different pipe diameters.

Source	D (mm)	Fluid	Fr_{SL}	Fr_{SG}
Present study	12.7	air-water	0.07-0.7	0.95 - 1
Guo and Jeong (2014)	7	air-water	0.06-0.58	0.86
Guo and Jeong (2014)	7	air-oil	0.06-0.58	1.11
Kaji and Azzopardi (2010)	19	air-water	0.07-0.58	0.97
Oshinowo (1971)	25.4	air-water	0.1-0.65	0.98
Oshinowo (1971)	25.4	air-glycerin	0.1-0.25	1
Barbosa et al. (2002)	31	air-water	0.09-0.55	≈ 1
Owen (1986)	31.8	air-water	0.009-0.36	≈ 1
Hewitt et al. (1965)	38	air-water	0.004-0.07	0.9-1.1
Nguyen (1975)	45.5	air-water	0.01-0.66	0.98
Belt et al. (2009)	50.5	air-water	0.015 - 0.15	0.95

It is evident from Table 4.2 that for the pipe diameters in a range of $7 \leq D \leq 50$ mm, the second pressure minimum always occur in the vicinity of Fr_{SG} and is independent of liquid flow rates. For the case of air-oil data of Guo and Jeong (2014), the second pressure drop minimum is delayed up to $Fr_{SG} = 1.1$. It is intuitive that viscous liquid phase would require higher gas flow rates to increase the disturbance wave frequency so as to avoid the reversal of liquid film. It can be inferred that the non-dimensional gas velocity defined by Eq. (4.28) can be regarded as a universal criteria to estimate the region of second pressure drop minimum. Beyond this point, the two phase pressure drop always increases with increase in gas flow rate as long as the flow pattern is annular in nature. In case of very low liquid and very high gas flow rates such that the mist flow exists after the annular flow, a third decreasing trend of two phase pressure drop can be anticipated.

A careful look at the decreasing pressure drop trends at different pipe orientations show that the liquid flow rate below which decreasing trend of $(dP/dL)^+$ is always present depends considerably on upward pipe inclination from horizontal. For vertical

upward flow, the decreasing trend of $(dP/dL)^+$ is present for all liquid flow rates shown in Fig. 4.59 (a) and tend to seize only for $0.61 < Fr_{SG} < 0.76$. With decrease in pipe orientation from vertical, Fr_{SL} corresponding to end of decreasing trend of $(dP/dL)^+$ decreases. For the case of near horizontal pipe orientation ($\theta = +20^o$), the decreasing trend of two phase pressure drop is not observed beyond $Fr_{SL} \approx 0.21$. The non-dimensional gas and liquid velocity corresponding to the region of second pressure minimum observed in this study are presented graphically in Fig. 4.60. Considering

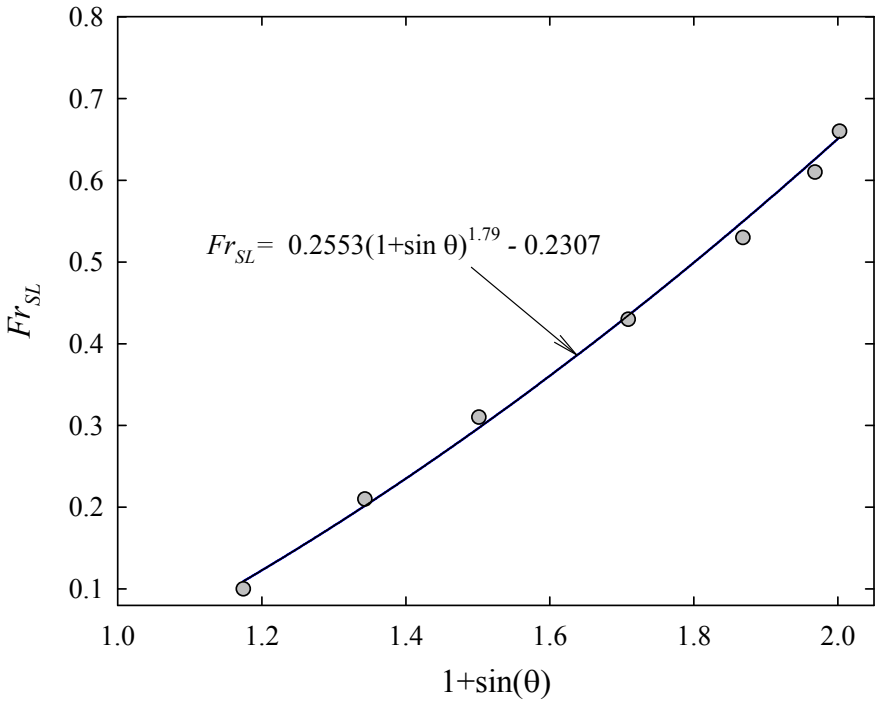

Figure 4.60: Threshold liquid superficial velocity for decreasing pressure drop trend at different pipe orientations.

the combined effect of liquid flow rate and the pipe orientation on the second pressure drop minimum, a relationship between Fr_{SL} and pipe orientation can be expressed as shown by Eq. (4.30). The value of Fr_{SL} represents the threshold value of liquid flow rate below reversal of liquid film always exist.

$$Fr_{SL} = 0.2553 \times (1 + \sin\theta)^{1.79} - 0.2307 \tag{4.30}$$

Due to lack of experimental data in two phase flow literature, it is difficult at this moment to verify the universality of this equation for a range of two phase flow conditions. However, considering the fact that liquid superficial velocity is non-dimensionalized using similar parameters used for Fr_{SG} and that the Fr_{SL} listed in Table 4.2 for different pipe diameters are all within the prediction of Eq. (4.30); it can be assumed that the criteria defined by Eq. (4.30) to predict the upper limit of Fr_{SL} can be applied for air-water two phase flow and pipe diameters in a range of 7 to 50 mm. Any liquid flow rate below this predicted value of Fr_{SL} will experience a decreasing pressure drop trend up to $Fr_{SG} \approx 1$.

The two decreasing trends of pressure drop and two regions of pressure drop minimum shown in Fig. 4.59 are consequence of two different two phase flow mechanisms. The initial decreasing trend of $(dP/dL)^+$ and hence the first pressure drop minimum occurring at low gas flow rates is essentially due to the downward flow of liquid film surrounding the gas slug where as the second trend of decreasing pressure drop and hence the pressure drop minimum occurring at moderate to high gas flow rate attributes to the phenomenon of partial or complete reversal of the liquid film under the influence of gravity. As shown in Fig. 4.4, the liquid phase in contact with the pipe wall will travel in downward direction to maintain the continuity of flow. The downward motion of liquid phase results into decreasing trend of pressure drop and may even yield negative values of frictional pressure drop for steeper pipe inclinations as observed in Fig. 4.46. Based on the flow visualization and investigations reported in two phase flow literature, second pressure drop minimum typically occurs during the transition from churn to annular two phase flow. The pressure drop minimum point represents end of churn (oscillating and intermittent) flow and onset of annular two phase flow. Beyond this point, annular flow always exist and the two phase pressure drop increases with increase in the gas flow rate. As shown in Fig. 4.61, during the transition between churn (intermittent) to annular, large disturbance waves (b)

travel in the downstream direction. Hewitt et al. (1985) reported that these disturbance waves are prime mechanism of liquid phase transport. Once the disturbance wave crosses certain pipe cross section, a liquid film close to the pipe wall begins to move downward under the influence of gravity. As shown in Fig. 4.61, the liquid phase in the crest region (c) of wavy film moves upward due to fast moving gas core whereas, the liquid phase in the trough region of wavy liquid film travel downward under the influence of gravity. This falling liquid film merges with the upstream liquid (d) to accumulate and again form a wavy liquid film. Further, a disturbance wave coming from upstream direction carries the wavy liquid film downstream followed by a trailing liquid film (a) in contact with the pipe wall and the process is repeated continuously.

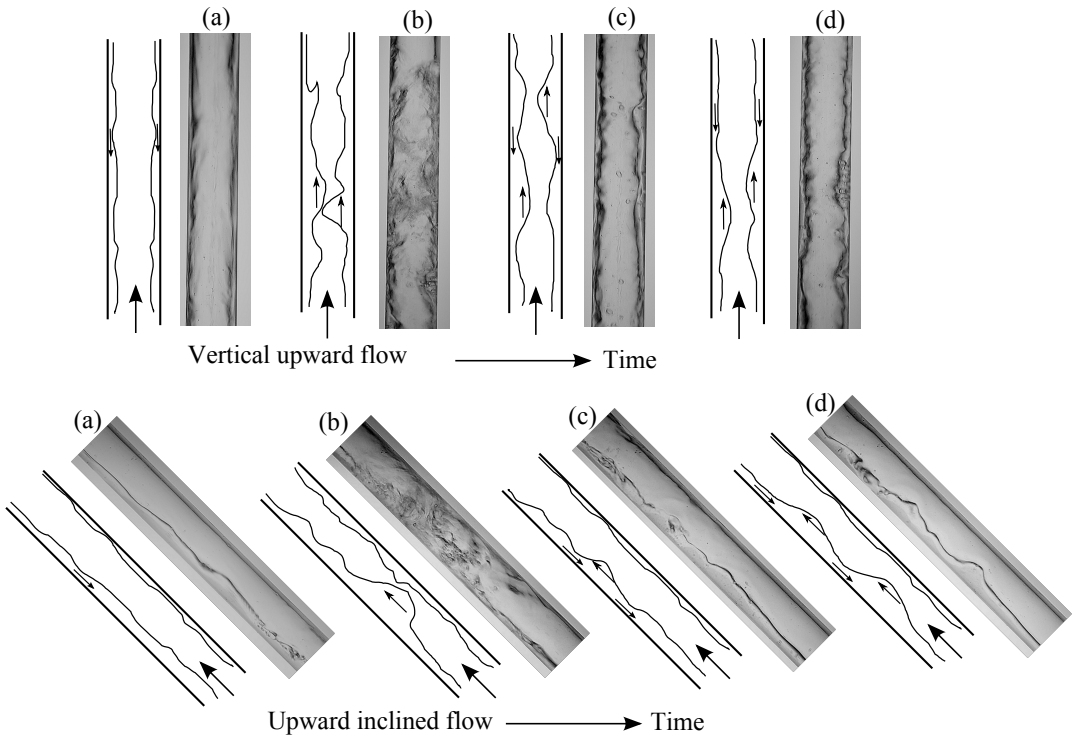

Figure 4.61: Flow reversal mechanism responsible for second pressure drop minimum.

The disturbance wave frequency that serves as a prime mechanism of liquid transport governs the extent of the decreasing trend of the pressure drop. With increase in the disturbance wave frequency, the falling liquid film will be more often

carried in the upward direction and eventually at the sufficient high wave frequency the liquid no more moves downward and the decreasing trend of two phase pressure drop is seized. Nedderman and Shearer (1963), Taylor Hall et al. (1963) and Azzopardi (1986) have experimentally confirmed that the disturbance wave frequency increases with increasing liquid and gas flow rates. Thus the gradual elimination of decreasing pressure drop trend with increase in the gas and liquid flow rates observed in Fig. 4.59 is essentially due to increase in the disturbance wave frequency. Based on the flow physics responsible for decreasing pressure drop trend it can be anticipated that the flow reversal phenomenon (reversal of liquid film) will continue to aggravate for large diameter pipes while it may not exist for small pipe diameters.

4.5 Chapter Summary

This chapter presents the experimental observations of the physical structure of the flow patterns and their transition boundaries as a function of pipe orientation. Additionally, experimental results of the void fraction and two phase pressure drop as a function of several parameters such as gas and liquid flow rates, flow patterns, pipe orientation and surface roughness are presented. Furthermore, based on experimental data available in two phase flow literature, the dependency of these measured two phase flow variables on pipe diameter and fluid properties is also briefly discussed. It is found that the both the phase flow rates (or alternatively the flow patterns) and the pipe orientation significantly affects the void fraction and two phase pressure drop. This effect of pipe orientation is noticeable for low values and liquid and gas flow rates and is little for inertia driven flow regime observed at high liquid and gas flow rates. Finally, the phenomenon of decreasing trend of pressure drop and pressure drop minimum due to partial flow reversal in upward inclined two phase flow is presented and the flow mechanism governing these trends are discussed.

CHAPTER V

MODELING OF VOID FRACTION

Realizing the practical significance of void fraction in several calculations related to two phase flow, the main objective of this chapter is to develop a flow pattern independent void fraction model applicable for a wide range of two phase flow conditions. Based on some of the top performing correlations presented in Chapter II, the key parameters that influence the void fraction are identified. The correlation presented in this chapter is based on the general concept of drift flux model (DFM) and provides expressions for distribution parameter (C_o) and drift velocity (U_{GM}) as a function of several two phase flow variables. What follows next is a brief background of the importance of void fraction and shortcomings of the current state of knowledge, a concise theory of the drift flux model and the proposal of equations to calculate distribution parameter and drift velocity required in drift flux model. Finally, the performance of developed void fraction model is verified against a comprehensive data bank and other top performing correlations available in the literature. The void fraction model presented in this chapter is published in Bhagwat and Ghajar (2014) and henceforth the proposed void fraction correlation will be alternatively referred to as Bhagwat and Ghajar (2014) correlation.

5.1 Background

As discussed in the preceding chapters, the knowledge of two phase flow parameters such as flow patterns, void fraction, pressure drop and heat transfer is crucial in design and optimization of all these industrial processes and equipment. Out of all these two phase flow parameters, void fraction is the most fundamental and crucial parameter as it is required as an input in almost every two phase flow calculation such as two phase mixture density, two phase mixture viscosity and actual velocities of each phase. In addition to this, the correct knowledge of void fraction is also decisive in determination of two phase pressure drop (hydrostatic and accelerational components), refrigerant charge inventory in evaporators and condensers, two phase heat transfer coefficient and the liquid film thickness in annular flow under the assumption of negligible liquid entrainment. Due to its significance, the concept of void fraction has received significant attention by several investigators resulting into numerous void fraction measurement experiments and development of different models for its prediction. However, these experiments and modeling work has been confined mostly to the horizontal and vertical pipe orientations with very little attention paid to the two phase flow in inclined systems and with various fluid combinations. It was seen in literature review (Chapter II) that one of the major short comings of some of these models is that they are developed for a specific flow pattern or need additional information related to the flow pattern to be fed into the model beforehand which is in most of the cases is not known to the user. Although, there are few mathematical and graphical tools available in the literature for estimation of the flow pattern in a two phase flow system; these tools are developed based on limited experimental data and flow conditions with flow patterns often identified qualitatively merely by visual observations and hence cannot guarantee correct estimation of a certain flow pattern over a wide range of operating conditions. Moreover, in case if the flow con-

ditions are in the vicinity of the transition of one flow pattern to another, then the correct estimation of the flow pattern and hence the selection of corresponding void fraction correlation depends on sheer subjective judgment of an individual. Thus, it is very much desired to have a correlation that can predict the void fraction and other two phase flow variables accurately without making any reference to the flow patterns. Another pitfall related to the failure of void fraction correlations is that a good number of these correlations are limited to certain pipe orientations and can work accurately only for a short range of pipe diameters and fluid combinations. The comprehensive study of Woldesemayat and Ghajar (2007) identified over 68 void fraction correlations available in the literature based on seperated flow model (SFM) model, $k - \alpha$ model and drift flux model (DFM). They found the drift flux model based void fraction correlations to be more flexible and fairly accurate as compared to other types of correlations for void fraction data in horizontal, upward inclined and vertical upward pipe orientations. Other recent studies of Godbole et al. (2011) and Bhagwat and Ghajar (2012) have also recommended the use of drift flux model based correlations for vertical upward and downward pipe orientations. It is observed from these studies that although the top performing correlations predict the void fraction with desired accuracy, their performance is not consistent over a broad range of operating conditions. For example, certain correlations which perform outstandingly for higher values of void fraction are found to fail for small values of void fraction or those correlations which predict void fraction data accurately for vertical pipe orientation fail in case of inclined pipe orientations. Moreover, these studies analyzed the correlations and made recommendations based on majority of the data for air-water two phase flow with no verification done against the data for refrigerants, steam-water and high viscosity oils. Our preliminary results showed that, the recommended correlations by the above mentioned studies tend to lose their accuracy in case of high pressure steam-water data, very small and large diameter pipes and

fluids with dynamic viscosity considerably higher than that of the water. In short, the two phase flow literature lacks a closure relationship to predict the void fraction independent of the flow patterns, void fraction range, pipe diameter, pipe orientation and most importantly the fluid properties. To overcome these problems and use one single correlation instead of multiple correlations based on specific flow conditions, it is attempted in this study to develop a drift flux model based flow pattern independent correlation that can predict the void fraction over a wide range of system pressures, pipe diameters, and fluid properties. The developed void fraction correlation represents the two parameters in the drift flux model namely, the distribution parameter and the drift velocity as a function of two phase flow variables such as pipe diameter, pipe orientation, fluid properties and the void fraction. It is shown that the new equations developed for distribution parameter and drift velocity adhere to the two phase flow physics and account for almost all two phase flow variables that influence the void fraction in gas-liquid two phase flow. Certain correction factors are introduced in the general structure of the proposed correlation to extend its application to non-circular pipes (rectangular and annular geometry), large diameter pipes and very high dynamic viscosity liquids.

5.2 Theory of Drift Flux Model

Since the proposed correlation is based on the concept of one dimensional drift flux model that represents the distribution parameter and drift velocity as a function of several two phase flow variables, it is first necessary to take a brief review of the drift flux model and the relevant literature. The general concept of drift flux model was first envisaged by Zuber and Findlay (1965) and later developed and contributed by Wallis (1969) and Ishii (1977). The one dimensional drift flux model is essentially an approximate formulation compared to more detailed two fluid (separated) flow

model. However, it is preferred due to its simplicity and flexibility over the two fluid flow model. The main assumptions involved with the formulation of one dimensional drift flux model are:

1. All two phase flow parameters are time averaged.

2. All two phase flow parameters are averaged across the pipe cross section as shown in Eq. (5.1) where F is any two phase flow parameter under consideration.

$$\langle F \rangle = \frac{1}{A} \int_A F dA \tag{5.1}$$

The cross sectional and void fraction weighted actual gas velocity can be written as given in Eq. (5.2) where $\langle U_M \rangle = \langle U_{SL} \rangle + \langle U_{SG} \rangle$ is the two phase mixture velocity. Multiplying each term in Eq. (5.2) by the cross sectional averaged void fraction yields Eq. (5.3).

$$\langle \langle U_G \rangle \rangle = \langle U_M \rangle + (\langle \langle U_G \rangle \rangle - \langle U_M \rangle) \tag{5.2}$$

$$\langle U_{SG} \rangle = \langle \alpha U_M \rangle + (\langle \alpha (U_G - U_M) \rangle) \tag{5.3}$$

The second term of Eq. (5.3) is the gas drift flux and both terms involving void fraction are the averages of the product of two quantities and are difficult to calculate analytically and hence drift flux model require definition of two empirical parameters namely, distribution parameter (C_o) and drift velocity (U_{GM}) as defined by Eqs. (5.4) and (5.5), respectively.

$$C_o = \frac{\langle \alpha U_M \rangle}{\langle \alpha \rangle \langle U_M \rangle} \tag{5.4}$$

$$\langle \langle U_{GM} \rangle \rangle = \frac{\langle \alpha U_{GM} \rangle}{\langle \alpha \rangle} = \frac{\langle \alpha (U_G - U_M) \rangle}{\langle \alpha \rangle} \tag{5.5}$$

Now using the definitions of C_o and U_{GM}, Eq. (5.3) can be recast as Eq. (5.6) and hence the void fraction can be expressed as Eq. (5.7).

$$\langle U_{SG} \rangle = C_o \langle \alpha \rangle \langle U_M \rangle + \langle \alpha \rangle \langle \langle U_{GM} \rangle \rangle \tag{5.6}$$

$$\langle \alpha \rangle = \frac{\langle U_{SG} \rangle}{C_o \langle U_M \rangle + \langle \langle U_{GM} \rangle \rangle} \tag{5.7}$$

Based on the general structure of drift flux model it is clear that Eq. (5.7) resembles the equation for a straight line. Thus one of the simplest ways to determine these drift flux variables is to curve fit the plot of (U_{SG}/α) vs. $(U_{SL} + U_{SG})$ such that slope of the graph gives the distribution parameter (C_o) and the y intercept gives drift velocity (U_{GM}) as shown in Fig. 5.1 . Although, this is the simplest of all methods, it is approximate, depends on the scatter of experimental data and is highly impractical in remote and real time applications since void fraction information is required in advance to plot the data.

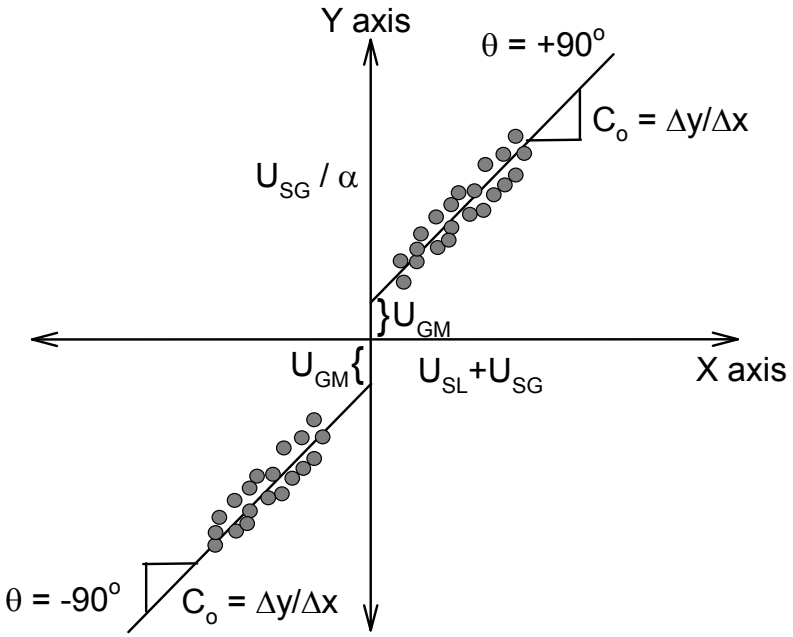

Figure 5.1: Estimation of C_o and U_{GM} using experimental data.

The distribution parameter is a representation to account for the distribution of the gas phase across the pipe cross section (concentration profile) and also serves as a correction factor to the homogeneous flow theory (that assumes no local slip between the two phases) to acknowledge the fact that the concentration profile and the two phase flow velocity profile can vary independently of each other across the pipe cross section. Whereas, the physical interpretation of drift velocity is the cross sectional void fraction weighted average of the local relative velocity of the gas phase with respect to the two phase mixture velocity at the pipe volume center. The local relative motion between the gas and the two phase mixture is considerable and uniform across the pipe cross section when there is a strong coupling between the two phases as in case of the flow of dispersed bubbles in continuous liquid medium, i.e., dispersed bubbly flow. As the two phase flow transits to annular flow regime, the local relative velocity of the gas phase with respect to the two phase mixture at the pipe volume center becomes negligible and so does the drift velocity. Analogous to the drift velocity, we can also define the slip velocity or relative velocity that represents the difference between the cross sectional averaged actual velocity of the gas and liquid phase. The slip velocity of the relative velocity is defined by Eq. (5.8). Ishii (1977) showed that with some manipulation and combining Eqs. (5.4), (5.5) and (5.8) following relation expressed in Eq. (5.9) can be obtained.

$$U_S = \langle\langle U_G \rangle\rangle - \langle\langle U_L \rangle\rangle = \frac{\langle U_{SG} \rangle}{\langle \alpha \rangle} - \frac{\langle U_{SL} \rangle}{1 - \langle \alpha \rangle} \tag{5.8}$$

$$U_S = \frac{\langle\langle U_{GM} \rangle\rangle + (C_o - 1)\langle U_M \rangle}{1 + \langle \alpha \rangle} \tag{5.9}$$

Although the one dimensional drift flux model is used in context of cross sectional averaged void fraction, there are several drift flux model based correlations available in the literature that can be practically implemented for void fraction calculations

based on volumetric void fraction experimental data instead of the cross sectional void fraction. The parity between the cross sectional and volumetric void fraction holds true in case of non-boiling two phase flow (two component two phase flow) where the cross sectional distribution of the gas phase with respect to the liquid phase remains virtually unaltered over a short length of pipe. Henceforth, without making any distinction between the cross sectional and volumetric void fraction, the void fraction is simply expressed as $\langle\alpha\rangle = \alpha$. Similar justification is applicable for all the cross sectional averaged quantities involved in Eqs. (5.1) to (5.9). Ishii (1977) reported that the use of drift flux model is more appropriate when there is strong coupling and local relative motion between the two phases. Two phase flow literature review shows that the application of drift flux model is justified when the drift velocity is significant approximately $U_{GM} > 0.05U_M$. Thus, theoretically the use of drift flux model is more apt for dispersed bubbly, bubbly and slug flow patterns and unsuitable for separated or shear driven flow patterns like stratified and annular flow. However, the performance of some recent correlations such as Hibiki and Ishii (2003) and Woldesemayat and Ghajar (2007) show that the drift flux model based correlations can successfully predict the void fraction in separated or shear driven two phase flow regimes such as annular flow with an acceptable accuracy by empirically accounting for the effect of change in flow patterns on the distribution parameter and the drift velocity. It is shown later in this chapter that only those drift flux model based correlations which consider the flow physics of annular flow regime are the top performing correlations and their accuracy is comparable to the correlations exclusively developed for annular flow regime.

5.3 Distribution Parameter

Prior to deciding upon the physical form of the distribution parameter it is first necessary to explore and understand both the qualitative and quantitative forms of the distribution parameter associated with the change in two phase flow variables. Let us first consider the effect of change in physical structure of flow patterns on the distribution parameter. As seen from Eq. (5.4), the mathematical form of distribution parameter as a function of void fraction implies that, the distribution parameter must change with change in the void fraction or alternatively the flow patterns. Thome (2006) discussed the relationship between the distribution parameter and the flow patterns (as a function of cross sectional void fraction distribution) as shown in Fig. 5.2 (a)-(c). It is seen that in case of subcooled boiling, i.e., initiation of bubbly flow regime in boiling two phase flow, the void fraction profile peaks at the pipe wall (pipe wall at both sides of centerline) and for such a condition the recommended value of distribution parameter is less than unity ($C_o < 1$). For a case of bubbly and slug flow in vertical pipes, the void fraction profile peaks at the pipe center that corresponds to the distribution parameter in the vicinity of 1.2. In the event of annular flow regime, the void fraction profile is almost flat except at the near wall region and as the void fraction reaches unity, distribution parameter must approach unity indicating the absence of liquid phase. In case of non-boiling two phase flow shown in Fig. 5.3, except for the case (a) in Fig. 5.2, other two cases of the void fraction distribution (alignment of gas phase with liquid phase) (b) and (c) for bubbly, slug and annular flow, respectively are analogous to the void fraction distribution in boiling two phase flow. Hence, the distribution parameter must be modeled in such a way that independent of the boiling or non-boiling nature of the two phase flow it should take a value close to 1.2 for vertical bubbly and slug flow while approach unity as the flow pattern shifts to annular flow regime. Unlike the void fraction peak

at both pipe walls in subcooled boiling Fig. 5.2 (a), the bubbly and slug flow in horizontal and upward inclined pipes show the concentration of the gas phase (void profile peak) only at the upper pipe wall.

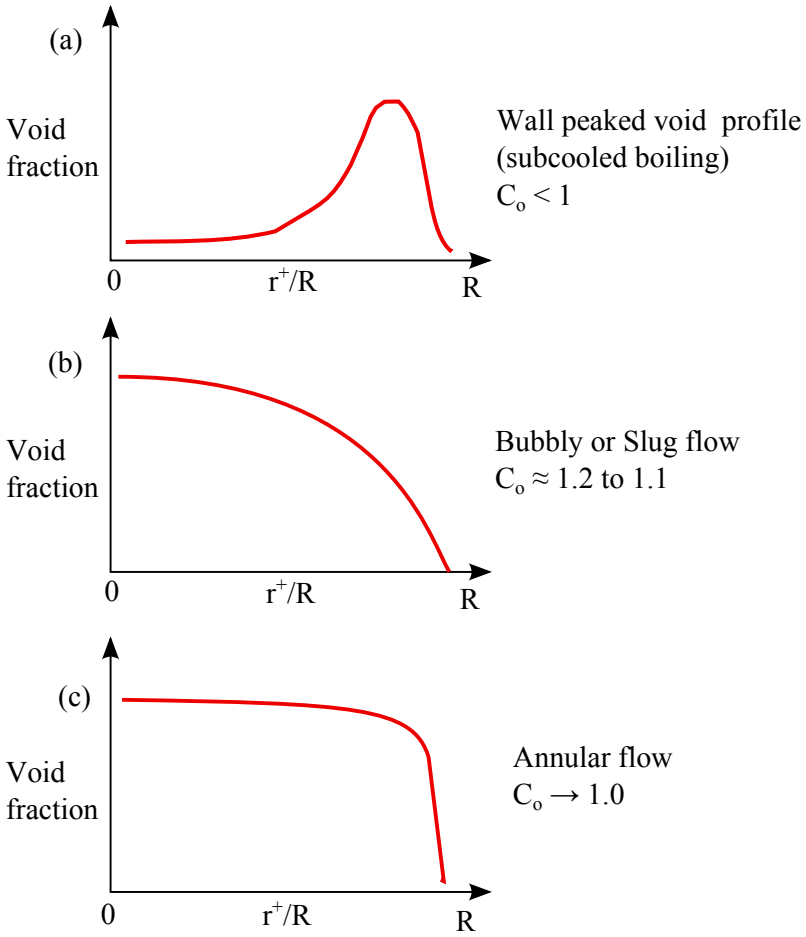

Figure 5.2: Distribution parameter as a function of cross sectional distribution of void fraction in vertical pipe (adapted from Thome (2006)).

In addition to the work of Thome (2006), the approximate values of distribution parameter for different two phase flow structures can be calculated based on the resemblance of the velocity and void profiles for different flow patterns. In case of dispersed bubble flow, tiny bubbles can be assumed to travel downstream at local two phase mixture velocity. Ishii (1977) and Nassos and Bankoff (1967) considered the similarity of the void fraction distribution profile with the velocity profile in fully developed single phase turbulent flow and assuming symmetric flow and radial profile

approximated by the power law, the two distributions can be expressed by Eqs. (5.10) and (5.11), respectively.

$$\frac{\langle U_M \rangle}{U_c} = 1 - \left(\frac{r^+}{R}\right)^m \tag{5.10}$$

$$\frac{\langle \alpha \rangle - \alpha_w}{\alpha_c - \alpha_w} = 1 - \left(\frac{r^+}{R}\right)^n \tag{5.11}$$

By substituting Eqs. (5.10) and (5.11) in Eq. (5.4), distribution parameter as shown in Eq. (5.12) can be obtained.

$$C_o = 1 + \frac{2}{m+n+2}\left(1 - \frac{\alpha_w}{\langle \alpha \rangle}\right) \tag{5.12}$$

Assuming a power law velocity profile in fully developed turbulent flow, the value of exponent 'm' used in velocity distribution may be taken as m $\approx$ 6 to 7. The local velocity and concentration profile measurements by Zuber and Findlay (1965) and Nassos and Bankoff (1967) show that the exponent 'n' for void fraction profile is $n \approx 2$ for bubbly flow and $n \approx 4$ for slug flow. Thus for bubbly flow with $n \approx 2$, the distribution parameter would be $C_o \approx 1.18 - 1.2$ and for slug flow with $n \approx 4$ and hence $C_o \approx 1.15 - 1.16$. In case of annular flow where the void fraction distribution can be approximated to be uniform throughout the pipe cross section, the relationship $\langle \alpha \rangle \approx \alpha_w \approx \alpha_c$ is valid and hence the distribution parameter approaches unity. On the other hand, for case of wall peaked void profile as in case of sub-cooled boiling, $\alpha_w > \alpha_c$ and hence $C_o < 1$.

As shown in Fig. 5.3 for air-water two phase flow in horizontal pipe, the gas phase is concentrated only at one side of the pipe wall, i.e., at the pipe upper wall for bubbly and slug flows. Similar type of flow structure is observed for these flow

patterns in inclined pipes. Franca and Lahey (1992) found that for the low values of gas flow rates in horizontal flow, the distribution parameter is close to unity which is less than that found in vertical and upward inclined pipe orientations. Their value of distribution parameter was obtained by curve fitting the experimental data with equation of straight line.

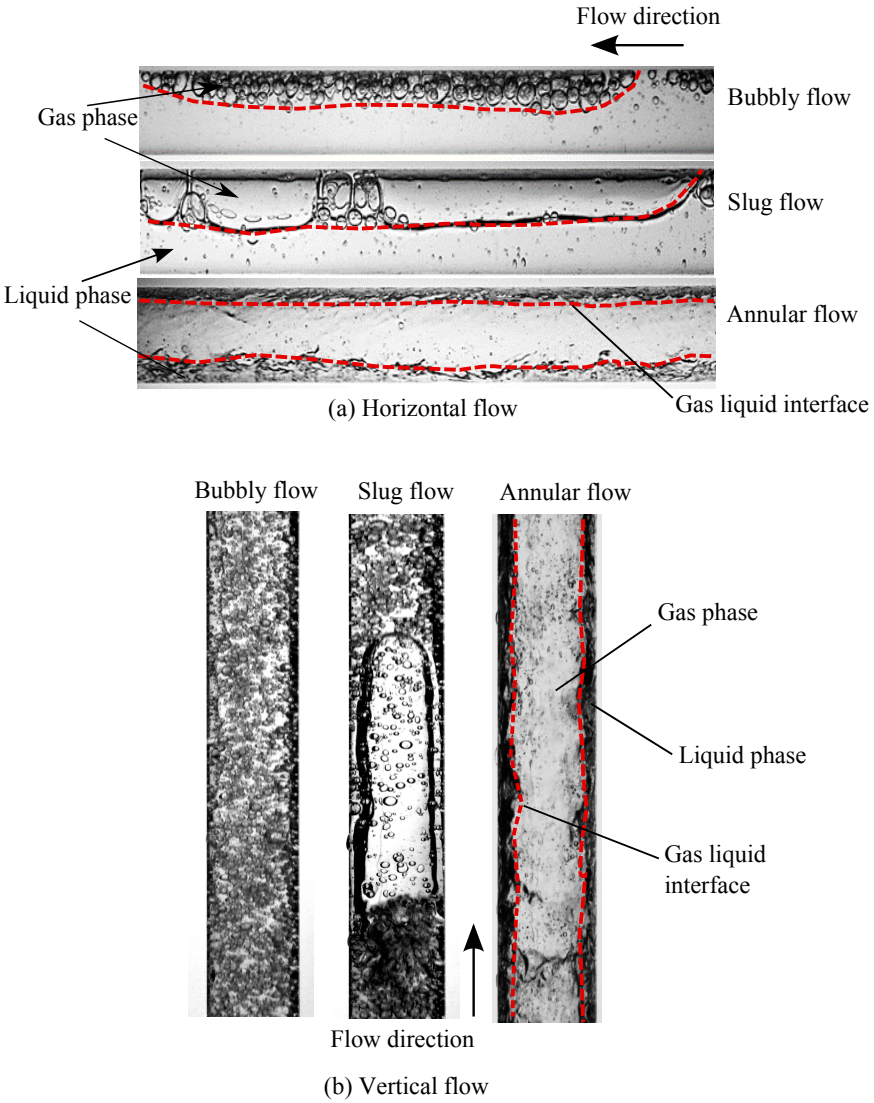

Figure 5.3: Two phase flow structure in horizontal and vertical upward non-boiling two phase flow.

Thus, for the modeling purpose, in the present study it is assumed that in case of bubbly and slug flow in horizontal and inclined pipes, the distribution parameter

is greater than unity but less than 1.2 such that it varies between 1 and 1.1. This assumption is based on interpolated value of C_o for a case of wall peaked void profile ($C_o < 1$) at both pipe walls and center peaked void profile ($C_o = 1.2$). In case of near horizontal downward inclined pipe orientations ($0^o > \theta \geq -30^o$), Bendiksen (1984) found that when the average velocity of the liquid phase is less than the critical liquid velocity, the distribution parameter is less than unity. This type of a flow situation is potentially encountered in plug, slug and stratified flow regimes in near horizontal downward inclined flows and is characterized by the dominant buoyancy forces that increases the residence time of the gas phase in the test section. This type of a flow situation for example in downward inclined slug flow would cause a pointed slug tail and a relatively flat nose as shown in flow visualization section of Chapter IV. Bendiksen (1984) reported that quantitative approach to identify such a flow situation in terms of critical liquid velocity would require additional information of liquid film thickness and the liquid film velocity. This additional information is very specific to the flow conditions and is not readily available in practical applications. He also concluded that for such a flow situation distribution parameter should be less than unity.

In case of horizontal and near horizontal downward inclined two phase flow, our preliminary data analysis showed that almost all drift flux model based correlations tend to under predict the void fraction data meaning that the measured void fraction in these orientations is higher compared to other pipe orientations measured at similar flow rates. From the drift flux model it is seen that the distribution parameter is inversely proportional to the void fraction, and hence for such a case the experimentally measured higher values of void fraction would correspond to $C_o < 1$ for correct estimation of the void fraction. Based on the available experimental data it is found that for $0^o > \theta \geq -50^o$ when $Fr_{SG} \leq 0.1$, then the distribution parameter less than unity predicts the measured void fraction data better than other drift flux

models available in the literature. Fr_{SG} is the Froude number based on gas superficial velocity and the phase densities defined by Eq. (5.13).

$$Fr_{SG} = \sqrt{\frac{\rho_G}{\rho_L - \rho_G}} \frac{U_{SG}}{\sqrt{gD_h \cos\theta}} \tag{5.13}$$

For high values of void fraction, i.e., annular flow regime, the flow structure is found to be unaffected by the pipe orientation. In case of annular flow regime in horizontal flow, the gas phase is concentrated in the center near pipe axis region while liquid phase occupies the near wall region. This distribution of the gas and liquid phase in horizontal annular flow regime is very similar to that observed in vertical upward annular flow as shown in Fig. 5.3. However, in case of horizontal and inclined flows, the liquid film thickness at the pipe bottom wall is more than that at the pipe top wall. Whereas, the liquid film in vertical pipe orientation is symmetrical about the pipe axis. In the present study, this effect of asymmetric distribution of the liquid phase on distribution parameter is assumed to be negligible. Kaji and Azzopardi (2010) compared the void fraction data in annular flow regimes for pipe diameters in a range of 5 to 50 mm. They concluded that the void fraction in annular flow regime remains virtually unaffected by the pipe diameter. Additionally, in Chapter IV it was concluded that for a fixed pipe diameter, void fraction in annular flow regime remains virtually independent of the pipe orientation. It was found that void fraction is sensitive to the pipe orientation only for small values of void fraction corresponding to bubbly and slug flows. Thus, considering the similarity between visual observations for annular flow regime in horizontal and vertical pipe orientations and conclusions of Chapter IV and that of Kaji and Azzopardi (2010), the distribution parameter is to be modeled independent of the pipe orientation and pipe diameter (for annular flow) such that the distribution parameter must approach a value close to unity for high values of void fraction. In addition to the pipe orientation, pipe diameter

and the flow patterns, another two phase flow variable that significantly affects the distribution parameter is the liquid phase viscosity. Gokcal (2008) experimentally determined the distribution parameter in slug flow by measuring the void fraction and drift velocity at different phase flow rates and liquid dynamic viscosities. He found that unlike the distribution parameter in a range of 1.1-1.2 in air-water two phase slug flow, the high viscosity liquid can cause the distribution parameter to go as high as 2.0. This large value of distribution parameter is probably due to the laminarization (due to high viscosity oil) of the two phase flow and hence results into centrally peaked void profile that is steeper than that compared to relatively flat void profile in turbulent two phase flow of air-water. The quantitative criteria used to differentiate between laminar and turbulent two phase flow in this work is similar to that of the single phase flow but is based on two phase Reynolds number Re_{TP}. Thus, it is evident that in order to account for the effect of liquid viscosity on the slope of cross sectional void fraction profile, the distribution parameter must be modeled as a function of liquid phase viscosity. Other two phase flow parameters that influence the distribution parameter are system pressure and the phase flow rates. It is seen from the correlations of Hibiki and Ishii (2003) and Woldesemayat and Ghajar (2007) that the effect of system pressure on the distribution parameter is considered by including the ratio of gas and liquid phase density. Since, the gas phase is compressible in nature, the distribution parameter will vary with variation in the system pressure. The effect of phase flow rates on the distribution parameter is captured by the Woldesemayat and Ghajar (2007) and Rouhani and Axelsson (1970) correlations through inclusion of phase superficial velocities and the two phase quality, respectively.

5.3.1 Proposed Model for Distribution Parameter

Following the above discussion, the proposed correlation for the distribution parameter is modeled such that it accounts for the effect of phase density ratio (also accounts for the effect of system pressure on gas phase), two phase mixture Reynolds number (includes effect of two phase mixture velocity, liquid phase density and dynamic viscosity and hydraulic pipe diameter), gas volumetric flow fraction (defined as a function of phase superficial velocities), two phase flow quality (defined in terms of mass flow rate of gas and liquid phase), pipe orientation and void fraction (considers the effect of flow patterns on the distribution parameter). In addition to these parameters, the proposed distribution parameter is also modeled as the function of two phase friction factor based on two phase Reynolds number.

$$C_o = C_o\left(\frac{\rho_G}{\rho_L}, \frac{U_M \rho_L D_h}{\mu_L}, \frac{U_{SG}}{U_{SG}+U_{SL}}, \frac{\dot{m}_G}{\dot{m}_G+\dot{m}_L}, f_{TP}, \theta, \alpha\right) \tag{5.14}$$

Following the functional form of Eq. (5.14), the proposed correlation for distribution parameter is expressed by Eq. (5.15).

$$C_o = \frac{2-(\rho_G/\rho_L)^2}{1+(Re_{TP}/1000)^2} + \frac{\left[\sqrt{(1+(\rho_G/\rho_L)^2\cos\theta)/(1+\cos\theta)}^{1-\alpha}\right]^{2/5} + C_{o,1}}{1+(1000/Re_{TP})^2} \tag{5.15}$$

Where $C_{o,1}$ is defined by Eq. (5.16) in terms of gas to liquid phase density ratio (ρ_G/ρ_L), gas volumetric flow fraction (β), two phase friction factor (f_{TP}) and two phase flow quality (x). The pipe orientation term used in distribution parameter equation is to be measured from horizontal.

$$C_{o,1} = \left(C_1 - C_1\sqrt{\rho_G/\rho_L}\right)\left[(2.6-\beta)^{0.15} - \sqrt{f_{TP}}\right](1-x)^{1.5} \tag{5.16}$$

The constant C_1 is 0.2 for circular and annular channels and 0.4 for rectangular channels. With reference to the previous discussion on the flow pattern physical structure in horizontal and downward pipe inclinations, use of Eq. (5.17) to calculate $C_{o,1}$ is recommended for a specific flow condition determined in terms of Fr_{SG} as a function of gas phase superficial velocity, pipe diameter, phase densities and the pipe orientation. This equation is based on the recommendations of Bendiksen (1984) and Franca and Lahey (1992) in order to make distribution parameter less than unity.

$$C_{o,1} = 0 \ \ (0^o \geq \theta \geq -50^o \text{ and } Fr_{SG} \leq 0.1) \tag{5.17}$$

Based on the experimental data bank used in this work, this specific flow condition is found to prevail only for a very narrow range of two phase flow. It should also be noted that if both conditions of Eq. (5.17) are not satisfied then Eq. (5.16) must be used to determine $C_{o,1}$. The two phase friction factor required in Eq. (5.16) is determined using Colebrook (1939) equation for single phase flow based on two phase mixture Reynolds number. The two phase friction factor and two phase Reynolds number can be calculated from Eqs. (5.18) and (5.19), respectively.

$$\frac{1}{\sqrt{f_{TP}}} = -4.0 \log_{10} \left(\frac{\epsilon/D_h}{3.7} + \frac{1.256}{Re_{TP}\sqrt{f_{TP}}} \right) \tag{5.18}$$

$$Re_{TP} = \frac{U_M \rho_L D_h}{\mu_L} \tag{5.19}$$

So far, all the discussion was based on the distribution parameter in circular pipes. In case of rectangular pipes, owing to the flow geometry, the cross sectional distribution of void fraction and hence the distribution parameter is expected to be different than that in circular pipes. Based on the data for turbulent bubbly flows, Ishii (1977) has proposed that the distribution parameter in rectangular channels is

greater than that in circular pipes. He suggested that depending upon the system pressure the distribution parameter can be up to 1.35 compared to the value of 1.2 in circular pipes. Based on the experimental data available in literature use of $C_1 = 0.4$ is recommended such that in case of turbulent bubbly flows, the maximum value of C_o is 1.4 for high values of Re_{TP}.

The pipe orientation term used in Eq. (5.15) causes the distribution parameter to vary as a function of pipe orientation and the void fraction or alternatively the flow patterns such that the effect of pipe orientation on distribution parameter is made considerable only for the small values of void fractions typically corresponding to the bubbly and slug flows. For large values of void fraction corresponding to those observed in annular flow, this term approaches unity. For example, the pipe orientation term in Eq. (5.15) will cause C_o to vary by about 15 to 20% in case of small void fraction values (bubbly flow regime) as the pipe orientation changes from horizontal to vertical. Whereas, for high void fraction values (annular flow regime), as the pipe orientation changes from horizontal to vertical, this term will change C_o only by 0.1 to 0.2%. Thus, this trend is in agreement with our previous assumptions and conclusions that the distribution parameter is a strong function of pipe orientation only for the small values of void fraction and its dependency on the pipe orientation is trivial for high values of void fraction. The ratio of gas to liquid phase density used in Eq. (5.15) is to account for the effect of system pressure or the gas phase density on the distribution parameter. The physical significance of these terms and their role in determining the distribution parameter in a limiting case is justified in the next section. The use of two phase flow quality term $(1 - x)^{1.5}$ and gas volumetric flow fraction and two phase friction factor term $[(2.6 - \beta)^{0.15} - \sqrt{f_{TP}}]$ is to ensure that the distribution parameter is a decreasing function of the void fraction. In particular, the use of the later term involving β and f_{TP} ensures that the distribution parameter is sensitive to the low values of void fraction and follows a saturated trend as the void

fraction approaches unity for any given pipe orientation.

For low values of two phase Reynolds number ($Re_{TP} < 1000$), the first term on the left hand side is dominant while the second term is nominal. Opposite is true for the case of high values of Reynolds number ($Re_{TP} > 10000$). The variation of the proposed form of distribution parameter against the two phase Reynolds number is illustrated in Fig. 5.4 (a)-(b). In Fig. 5.4 (a), the trends of C_o are plotted for a case of vertical two phase flow and low system pressure such that $\rho_G << \rho_L$. It is seen that, for low values of Reynolds number typically $Re_{TP} < 1000$, the distribution parameter follows a continuous and smooth trend whereas for higher values of Re_{TP}, the distribution parameter is found to vary between 1.2 and 1.0 based on the two phase flow conditions. As shown in Fig. 5.4 (a), the different values of parameter $C_{o,1}$ varying between 0.2 and 0.0 correspond to different two phase flow conditions such that for small values of density ratio ($\rho_G << \rho_L$), $C_{o,1} = 0.2$ represents the region of small values of void fraction and make the distribution parameter 1.2. Whereas, $C_{o,1} = 0.04$ corresponds to large values of void fraction as that in annular flow and makes the distribution parameter approach unity. It is also seen that for $Re_{TP} < 1000$, distribution parameter is independent of $C_{o,1}$ and for $Re_{TP} > 10000$, the distribution parameter is a function of $C_{o,1}$ and stays unaffected by any variation in the two phase Reynolds number.

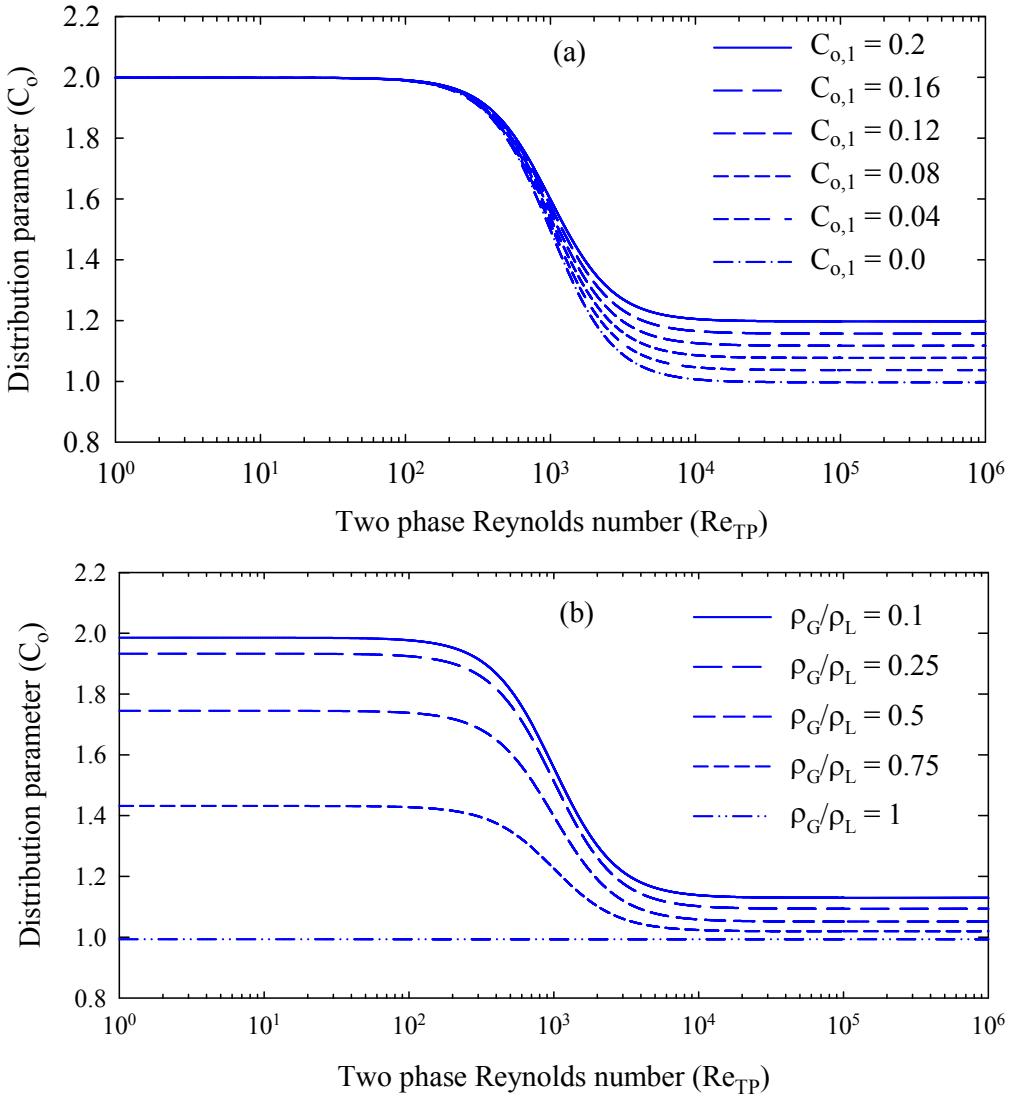

Figure 5.4: Variation of C_o with change in Re_{TP} for vertical upward pipe orientation (a) Effect of $C_{o,1}$ when $\rho_G << \rho_L$ (b) Effect of phase density ratio.

Considering another situation of varying ratios of (ρ_G/ρ_L) for small values of void fraction, the distribution parameter as a function of two phase Reynolds number is illustrated Fig. 5.4 (b). It is seen that in contrast to the trend of C_o shown in Fig. 5.4 (a), C_o can have significantly different values even for $Re_{TP} < 1000$. In the limiting case when $\rho_G/\rho_L = 1$, the distribution parameter becomes unity and is independent of two phase mixture Reynolds number. The justification of $C_o = 1$ for

the case of $\rho_G = \rho_L$ is explained later in this chapter. For a case when $Re_{TP} < 1000$ and $\rho_G << \rho_L$, Eq. (5.15) can be simplified to $C_o \approx 2/(1 + (Re_{TP}/1000)^2$ and its graphical illustration is seen from Fig. 5.4. In the limit of large values of the two phase Reynolds number ($Re_{TP} > 10000$) typically those encountered in case of air-water, refrigerants and steam-water two phase flow, the first term on the right hand side will approach zero and the denominator of the second term will approach unity. In case of vertical two phase flow when $Re_{TP} > 10000$, then to be in agreement with the trends shown Fig. 5.4 (a), Eq. (5.15) reduces to $C_o = 1 + C_{o,1}$. In case of non-vertical pipe orientations, the trends of C_o with respect to the change in $Re_{TP}, C_{o,1}$ and (ρ_G/ρ_L) will be qualitatively similar to that shown in Figure 5.4 except that their slopes will be offset by a proportionate magnitude of the pipe orientation term used in Eq. (5.15).

5.4 Drift Velocity

As seen in the literature review, most of the available DFM void fraction correlations model the drift velocity as a function of pipe diameter, pipe orientation, fluid properties and the void fraction or alternatively the flow patterns. Before deciding upon the physical form of the drift velocity equation, it is first necessary to understand both qualitative and quantitative effects of different two phase flow variables on the drift velocity. Let's first consider the effect of pipe orientation on the drift velocity. Two phase literature reports that an experimental method to determine the drift velocity is to measure the rise or propagation velocity of the gas bubbles in continuous liquid phase. The rise velocity of the gas phase results from the interaction between the gravity, buoyancy, surface tension and inertia forces. In vertical upward flows, the drift velocity is due to the interaction between buoyancy and interfacial drag and depends upon the pipe diameter. Dumitrescu (1943) analyzed inviscid flow

theory for vertical upward two phase flow and found the drift or rise velocity of the gas phase to be proportional to $\sqrt{gD}$ with the proportionality constant being 0.35. Nicklin et al. (1962) experimentally measured drift (rise) velocity of two phase slug flow in vertical pipes and also found the proportionality constant to be 0.351 which in agreement with the findings of Dumitrescu (1943). Some of the previous studies related to drift flux modeling in two phase flow such as those of Wallis (1969) and Dukler and Hubbard (1975) assumed drift velocity in the horizontal pipe orientations to be zero since there is no effect of buoyancy on the gas phase. In contrary to this assumption, Benjamin (1968), Nicholson et al. (1978) and Weber (1981) found that the drift velocity exists in horizontal flows as a consequence of the balance between lateral and axial pressure gradients and may exceed the drift velocity in case of vertical two phase flow. Benjamin (1968) found that similar to vertical upward flow, the drift velocity in horizontal pipe orientation is also proportional to $\sqrt{gD}$ with proportionality constant of 0.54. However, Gokcal et al. (2009) found that the drift velocity in horizontal flow is less than the theoretical value and hence based on their experimental measurements of drift velocity, in the present study, the proportionality constant for horizontal flows is taken to be 0.45.

Another two phase flow variable that affects the drift velocity is the liquid phase dynamic viscosity. Gokcal et al. (2009) experimentally measured the combined effect of pipe orientation and the liquid phase dynamic viscosity on the drift velocity. They found the liquid phase dynamic viscosity to have considerable effect on the drift velocity at different pipe orientations measured from horizontal to vertical upward direction. Fig. 5.5 shows the combined effect of pipe orientation and the liquid phase dynamic viscosity on the drift velocity. It is seen that for a fixed pipe orientation, the drift velocity decreases with increase in the liquid dynamic viscosity. For a 0.645 Pa-s viscosity fluid, the drift velocity is found to reduce by 35% compared to water having a dynamic viscosity of 0.001 Pa-s. Thus, it is necessary to express the drift

velocity as a function inversely proportional to the liquid phase dynamic viscosity.

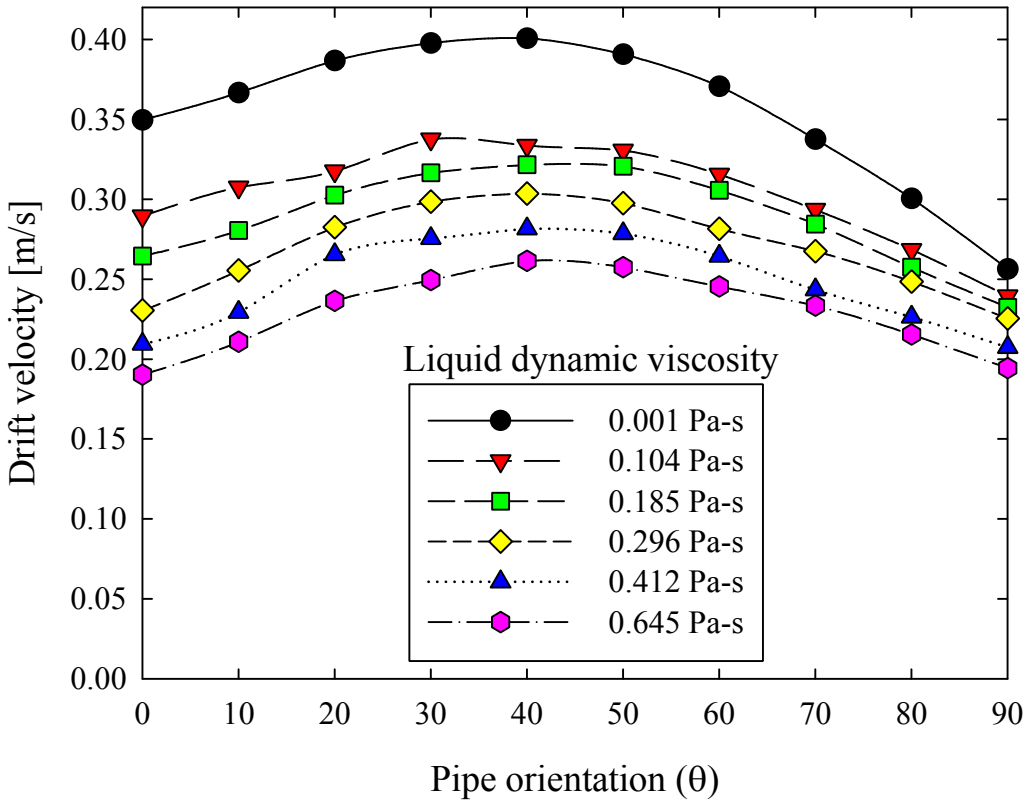

Figure 5.5: Effect of liquid dynamic viscosity on drift velocity (adapted from Gokcal et al. (2009)).

In addition to pipe orientation and liquid viscosity, it is also crucial to understand the relation between pipe diameter and drift velocity. The drift flux model based void fraction correlations listed in Chapter II such as Hibiki and Ishii (2003), Shipley (1982) and Woldesemayat and Ghajar (2007) will result into unreasonably high drift velocity for very large pipe diameters. In case of small diameter pipes ($D \leq 6$ mm), Mishima and Hibiki (1996) found that due to narrow flow passage, the pipe wall induced drag on the gas phase is significant causing the drift velocity to be negligible and hence it can be assumed to be zero. Whereas, in case of large diameter pipes, Kataoka and Ishii (1987) argued that when the pipe diameter is too large there is negligible effect

of pipe wall induced drag on the motion of the gas phase (bubbles) and hence the drift velocity. Furthermore, they also experimentally verified that for the motion of gas bubbles through non-dimensional pipe diameter (D_h^*) larger than 40, a typical gas slug cannot exist since for such a large pipe diameter, the gas bubbles tend to grow in a lateral direction (normal to flow direction) as compared to their growth in longitudinal direction for relatively small diameter pipes. This lateral expansion of the gas phase retards the rate of increase of the drift velocity with increase in the pipe diameter. Consequently, the drift velocity remains virtually independent of the pipe diameter when $D_h^* \geq 40$. From this discussion, it is evident that the drift velocity must be corrected for the reduced wall drag effects in large diameter pipes (based on the threshold value of La).

5.4.1 Proposed Model for Drift Velocity

Considering the parametric effects of different two phase flow parameters on the drift velocity, the proposed correlation for the drift velocity is represented by Eq. (5.20) where the pipe orientation term θ is measured from horizontal and the variables C_2, C_3 and C_4 are defined by Eqs. (5.21), (5.22) and (5.23), respectively. The term $(0.35 \sin\theta + 0.45 \cos\theta)$ is used to account for the effect of pipe orientation on the drift velocity. Thus, for vertical and horizontal flows, use of Eq. (5.20) will give a proportionality constant of 0.35 and 0.45, respectively. This pipe orientation terms gives maximum drift velocity at around $\theta = +40^o$ which is in agreement with the void fraction trends reported in Chapter 4.‘ The variable C_2 defined in Eq. (5.21) accounts for the effect of liquid phase dynamic viscosity on the drift velocity. In case of $(\mu_L/0.001) > 10$, the variable C_2 is defined in terms of the logarithm of the non-dimensional liquid dynamic viscosity. The dynamic viscosity of the given liquid is made non-dimensional by dividing it with the dynamic viscosity of water measured

at standard pressure and temperature conditions to be taken as 0.001 Pa-s.

$$U_{GM} = (0.35 \sin\theta + 0.45 \cos\theta)\sqrt{\frac{gD_h(\rho_L - \rho_G)}{\rho_L}}(1-\alpha)^{0.5} C_2 C_3 C_4 \tag{5.20}$$

$$C_2 = \begin{cases} \left(\dfrac{0.434}{\log_{10}(\mu_L/0.001)}\right)^{0.15} & : (\mu_L/0.001) > 10 \\ 1 & : (\mu_L/0.001) \leq 10) \end{cases} \tag{5.21}$$

$$C_3 = \begin{cases} (La/0.025)^{0.9} & : La < 0.025 \\ 1 & : La \geq 0.025 \end{cases} \tag{5.22}$$

$$C_4 = \begin{cases} 1 & \\ -1 & : (0^o > \theta \geq -50^o \text{ and } Fr_{SG} \leq 0.1) \end{cases} \tag{5.23}$$

Preliminary results based one the experimental data available in the literature show that, the effect of liquid phase dynamic viscosity on the drift velocity approximately up to $(\mu_L/0.001) \leq 10$ is very little and hence can be ignored. With reference to the previous discussion on the drift velocity in large diameter pipes corresponding to $D_h^* > 40$, or alternatively the Laplace number (inverse of D_h^*) $La < 0.025$, a correction factor is incorporated in the drift velocity expression through variable C_3 defined by Eq. (5.22). The Laplace number is defined in terms of phase density difference, surface tension and pipe hydraulic diameter as $La = \sqrt{\sigma/(g\Delta\rho)}/D_h$ Further, it can also be seen that for very small diameter pipes typically those corresponding to mini and micro dimensions, the drift velocity will be negligibly small due to small pipe diameter and is in agreement with the conclusions of Mishima and Hibiki (1996).

The void fraction term $\sqrt{1-\alpha}$ used in Eq. (5.20) ensures that the drift velocity is a function of flow pattern such that for low values of void fraction (bubbly flow) the drift velocity is maximum as $\sqrt{1-\alpha} \approx 1$ and as void fraction approaches unity (annular flow regime), the drift velocity becomes negligibly small.

Finally, the use of C_4 is required when both conditions in Eq. (5.23) are satisfied. The limitations imposed on the variable C_4 are on similar grounds as discussed in the preceding section for distribution parameter. It should also be noted that pipe orientation criteria in Eq. (5.23) excludes the case of $\theta = 0^o$ since the drift velocity cannot be negative in horizontal two phase flow. The switching of C_4 values between 1 and -1 ensures that the drift velocity is a positive and negative quantity based on the Fr_{SG} values. In principle, the positive and negative values of drift velocity for near horizontal downward inclined pipe orientations are to be used to take into consideration the dominant buoyancy force acting on the gas phase compared to the inertia force of the liquid phase. This condition is imposed only on $(0^o > \theta \geq -50^o)$ since for $\theta < -50^o$, the physical from of Eq.(5.20) will render the drift velocity as a negative quantity. The impact of using positive and negative values of drift velocity on the prediction of the void fraction is documented by Bhagwat and Ghajar (2012).

5.5 Boundedness of the Proposed Correlation

Since, the proposed correlation for the void fraction is expressed in terms of distribution parameter and the drift velocity as a function of void fraction, the solution of the proposed drift flux model based correlation is to be obtained using iterative technique. It is necessary to verify the correctness of the trends of these drift flux variables so that the value of void fraction always stays within the lower and upper limits of 0 and 1, respectively. In case, if the continuity of C_o and U_{GM} with respect to void fraction is not followed, it might result into multiple values of C_o and U_{GM} and hence multiple values of void fraction resulting into numerical oscillations and divergence of the solution for the void fraction. In the preceding sections we discussed that in order to make the drift flux model based correlations independent of the flow patterns, it is necessary to model the drift flux parameters, i.e., distribution parameter and the drift velocity as variables that account for the change in two phase flow behavior. For any two phase flow physical system under consideration, the void fraction must be a continuous function of the phase flow rates except when the general trends of the two phase flow phenomenon change abruptly. Accordingly, the distribution parameter and the drift velocity must be modeled such that the void fraction values are constrained between lower and upper limits of 0 and 1. Based on the relation between void fraction profile and the distribution parameter, it is that the upper limit of C_o should be 2 for laminar two phase flow and 1.2 for turbulent two phase flow. Further, as the flow pattern transits to annular flow regime, C_o should approach unity. This concludes that the functional form of the distribution parameter must be such that $(\partial C_o/\partial\alpha) < 0$. Furthermore, as void fraction approaches unity, distribution parameter tends to follow a saturated trend and hence in the limit as $\alpha \rightarrow 1$, $(\partial C_o/\partial\alpha) = 0$. Similarly, from the definition of the drift velocity, it is seen that U_{GM} must be a decreasing function of the void fraction and the condition of $(\partial U_{GM}/\partial\alpha) < 0$

must be satisfied. The proposed correlations for distribution parameter are designed such that for a smooth variation of the two phase flow conditions they satisfy this mathematical requirement and are a decreasing function of the void fraction.

It is also necessary to check the upper and lower limits of both distribution parameter and the drift velocity for different two phase flow conditions including the limiting cases. One of the most important limiting case considered in non-boiling two phase flow literature is when the gas phase density is equal to that of the liquid phase density i.e., $\rho_G/\rho_L = 1$. Ishii (1977) reported that for a fully developed turbulent bubbly flow, the distribution parameter is a function of phase density ratio (ρ_G/ρ_L) and when $\rho_G = \rho_L$ then $C_o = 1$. From the theory of drift flux model and the mathematical definition of drift velocity, it is evident that when both phases have the same density, they will move with the same velocity and no slip condition will exist at the gas liquid interface resulting into a zero drift velocity. Moreover, from Eq. (5.9), it can be seen that for such a case, slip velocity (U_S) approaches zero. Thus from Eq. (5.9) we get, $(C_o - 1)U_M = 0$ and hence $C_o = 1$. It can be easily shown that the proposed correlations for C_o and U_{GM} adhere to this limiting case. From the physical structure of the proposed correlation for the distribution parameter Eq. (5.15), it is evident that, for $\rho_G/\rho_L = 1$, $C_o = 1$. The decreasing trend of distribution parameter with increase in the system pressure or alternatively the gas to liquid density ratio is illustrated in Figure 5.4. The drift velocity correlated by Eq. (5.20) will become zero since $\rho_L - \rho_G = 0$. These limiting values of distribution parameter and drift velocity are valid regardless of whether it is a laminar or turbulent two phase flow. Cioncolini and Thome (2012a) reported that depending on the system pressure, the void fraction changes with change in the two phase flow quality such that for low values of system pressure, the rate of increase of void fraction is rapid and gradual for low and high values of two phase quality, respectively. With increase in the system pressure, the rate of increase of the void fraction with respect to the change in flow quality becomes

more uniform and in the limiting case when $\rho_G/\rho_L = 1$, then void fraction is equal to the two phase flow quality ($\alpha = x$). This limiting case is also found to be valid for the proposed correlation by rearranging Eq. (5.7) in terms of gas volumetric flow fraction such that, $\alpha = \beta/(C_o + U_{GM}/U_M)$. In the event of $\rho_G = \rho_L$, it is shown that $C_o = 1$ and $U_{GM} = 0$. Thus the void fraction becomes equal to the gas volumetric flow fraction, i.e., $\alpha = \beta$. The gas volumetric flow fraction defined in terms of the phase superficial velocities can be rearranged as, $\beta = \dot{m}_G\rho_G^{-1}/(\dot{m}_G\rho_G^{-1} + \dot{m}_L\rho_L^{-1})$. Thus, for the case of $\rho_G/\rho_L = 1$, $\beta = x$. Hence, from the principle of transitivity, the void fraction is equal to the two phase flow quality ($\alpha = x$). This result is in agreement with that of Cioncolini and Thome (2012a) and thus it can be concluded that with proper formulations of distribution parameter and drift velocity, the application of drift flux model can be extended to the limiting cases. In case of boiling two phase flow, this limiting case can be expressed in terms of the system pressure such that, when $P_{SYS} \geq P_{CRIT}$, vapor and liquid phases cannot be distinguished from one another and for such a case we have $\rho_G = \rho_L$. Following the above discussion it can be concluded that when $P_{SYS} \geq P_{CRIT}$, $C_o = 1$ and $U_{GM} = 0$ and hence the two phase flow can be considered as homogeneous flow such that $\alpha = \beta$. Another limiting case arises for very high values of void fraction such that the void fraction approaches unity. In event of $\alpha \to 1$, due to relatively high mass flow rate of gas and considerably low mass flow rate of liquid, we have $x \to 1$. For all the experimental void fraction data considered in this work, it is observed that the void fraction approaches unity for high values of two phase mixture Reynolds number typically $Re_{TP} > 20000$. For these high Reynolds numbers and the fact that $x \to 1$ when $\alpha \to 1$, the distribution parameter defined by Eq. (5.15) will approach unity. Whereas, from the definition of drift velocity it is clear that for void fraction approaching unity, $(1 - \alpha) \to 0$ and hence $U_{GM} \to 0$. These limiting values of distribution parameter and drift velocity resembles those for the case of very high system pressure or when $\rho_G = \rho_L$ and hence

we conclude that, as void fraction approaches unity, the two phase flow will behave more like a homogeneous flow and the relation $\alpha = \beta$ will be valid. The limiting case when void fraction becomes zero is of no practical importance since for $\alpha = 0$, the two phase flow becomes single phase liquid flow and thus eliminates need of void fraction correlation. However, regardless of the bounds on the proposed distribution parameter and drift velocity, the drift flux model will predict zero void fraction for single phase liquid flow since the numerator of Eq. (5.7) will be zero due to absence of gas or vapor phase.

5.6 Validation of the Proposed Void Fraction Correlation

The drift flux model based void fraction correlation developed in this chapter is now onwards referred to as Bhagwat and Ghajar (2014) correlation in the remaining text and is validated against a comprehensive data base consisting of 10225 data points with 5294 data points for air-water, natural gas-water and argon-water fluid combinations, 1404 data points for liquid refrigerants and their vapors (R11, R12, R22, R134a, R114, R410A, R290, R1234yf, Ammonia and Carbon Dioxide), 892 data points for steam-water with system pressure in a range of 1 to 18.1 MPa, 733 data points for air-oil with liquid phase dynamic viscosity ranging from 0.005 to 0.6 Pa-s and 1902 data points for other fluid combinations such as air-kerosene, air-glycerin, argon-ethanol, argon-acetone and argon-alcohol. This experimental data bank is collected from more than 70 sources in the two phase flow literature and consists of pipe orientations in a range of $-90^o \leq \theta \leq +90^o$ and hydraulic pipe diameters ranging from 0.5 mm to 305 mm covering the micro to macroscale two phase flow phenomenon. Table 5.1 summarizes the diverse experimental data bank used to validate the performance of different void fraction correlations. Some of the data sources that represent majority of this data are listed in Appendix.

Table 5.1: Experimental data for the assessment of void fraction correlations.

Air-water data (5294)	
Pipe diameter (D_h) [mm]	4.5 - 305
Pipe orientation (θ)	$-90^o \leq \theta \leq +90^o$
Density ratio (ρ_L/ρ_G)	20 - 875
Mass flux (G) [kg/m^{2}s]	10 - 8450
Two phase flow quality (x)	0.000085 - 0.96
Void fraction (α)	0.003 - 0.995
Mixture Reynolds number (Re_{TP})	500 - 2×10^6
Refrigerants (1404 data) (R11, R12, R22, R114, R134a, R410A, R290, CO_2, NH_3 and R1234yf)	
Pipe diameter (D_h) [mm]	0.5 - 50.8
Pipe orientation (θ)	$-90^o \leq \theta \leq +90^o$
Density ratio (ρ_L/ρ_G)	6 - 250
Mass flux (G) [kg/m^{2}s]	60 - 1050
Two phase flow quality (x)	0.002 - 0.98
Void fraction (α)	0.05 - 0.99
Mixture Reynolds number (Re_{TP})	2000 - 3×10^6
Air-oil (733 data points)	
Pipe diameter (D_h) [mm]	25 - 189
Pipe orientation (θ)	0^o, $\pm5^o$, $\pm10^o$ and $\pm90^o$
Density ratio (ρ_L/ρ_G)	30 - 775
Liquid dynamic viscosity (μ_L) [Pa-s]	0.005 - 0.6
Mass flux (G) [kg/m^{2}s]	50 - 2450
Two phase flow quality (x)	0.0001 - 0.97
Void fraction (α)	0.01 - 0.99
Mixture Reynolds number (Re_{TP})	10 - 7×10^5
Air-Kerosene, Air-Glycerin, Air-Acetone, Argon-Alcohol, Argon-Ethanol (1902 data)	
Pipe diameter (D_h) [mm]	2 - 80
Pipe orientation (θ)	$-90^o \leq \theta \leq +90^o$
Density ratio (ρ_L/ρ_G)	20 - 290
Liquid dynamic viscosity (μ_L) [Pa-s]	0.0003 - 0.015
Mass flux (G) [kg/m^{2}s]	10 - 7000
Two phase flow quality (x)	0.00008 - 0.92
Void fraction (α)	0.01 - 0.99
Mixture Reynolds number (Re_{TP})	200 - 3×10^6
Steam-water data (892 data), $\theta = +90^o$	
Pipe diameter (D_h) [mm]	6 - 25
Density ratio (ρ_L/ρ_G)	6 - 375
Mass flux (G) [kg/m^{2}s]	100 - 5000
Two phase flow quality (x)	0.0001 - 0.45
Void fraction (α)	0.005 - 0.97
Mixture Reynolds number (Re_{TP})	15000 - 4.5×10^6

The experimental void fraction data for refrigerants and steam-water consists of both adiabatic and diabatic (boiling and condensing) flow conditions. In fact, about 36% of the refrigerant data and 62% of the steam-water data is for diabatic conditions. The diabatic two phase flow data for steam-water consists of non-circular (rectangular) pipes with dimensions 11.1 mm x 93.6 mm, 6.35 mm x 50.8 mm and 12.7 mm x 50.8 mm obtained from Marchaterre (1956) and Marchaterre et al. (1960). The performance of the proposed correlation is verified against this comprehensive data bank and is also compared with the performance of other drift flux model and separated flow model based correlations available in the literature. The experimental void fraction data is divided into three different ranges of void fraction based on the two phase flow physics and associated flow patterns. The first range of void fraction of $0 < \alpha \leq 0.25$ is based on the bubbly flow pattern where the gas phase is dispersed into the continuous liquid phase and there is a strong coupling between the two phases. The next range of the void fraction is selected for the slug and intermittent type of flow patterns that approximately occupies a void fraction range of $0.25 < \alpha \leq 0.75$. Finally, the third range of the void fraction is considered based on shear driven flows such as annular flow that approximately occupies a void fraction range of $0.75 < \alpha < 1$. It must be emphasized that the two phase flow literature reports appropriateness of the drift flux model for the bubbly flow pattern or alternatively the first range of void fraction ($0 < \alpha \leq 0.25$) under consideration while recommends the use of separated flow models for shear driven flows such as annular flow, i.e., the last range of void fraction of $0.75 < \alpha < 1$. In order to check the ability of proposed correlation and other drift flux model based correlations to predict the void fraction in annular flow regime their performance is also compared against some of the frequently referenced correlations in the two phase flow literature developed for annular flow such as Lockhart and Martinelli (1949), Yashar et al. (2001), Smith (1969), Permoli et al. (1971) and Cioncolini and Thome (2012a). With

the exception of Cioncolini and Thome (2012a), all other correlations mentioned above are based on the concept of separated flow model while the correlation of Cioncolini and Thome (2012a) is based on a mathematical function used in biochemical kinetics.

A preliminary comparison of the different void fraction correlations against the experimental data base show that for the first range of void fraction, a small absolute difference between the measured and predicted values of void fraction corresponds to a relatively high percentage error essentially due to the small value of void fraction. For example, an absolute difference of 0.05 between measured and predicted values of void fraction for a measured void fraction of 0.1 translates to an error of 50%. Whereas, a similar magnitude of absolute difference for a measured void fraction of 0.9 gives an error of 5.5%. Thus it is clear that a similar assessment criteria based on percentage error cannot be used for different ranges of the void fraction. Based on the performance of different void fraction correlations and considering the fact that the percentage error between measured and predicted values of the void fraction is biased by the actual magnitude of the void fraction, an error of up to $\pm 30\%$ is considered acceptable for the first range of void fraction i.e., $0 < \alpha \leq 0.25$. On similar grounds, for the next range of void fraction ($0.25 < \alpha \leq 0.75$), a percentage error of $\pm 20\%$ is considered acceptable. Finally, for the last range of void fraction, the most stringent performance criteria is applied and the performance of the void fraction correlations is assessed based on the percentage of data points predicted within $\pm 7.5\%$ error bands. Ghajar and Bhagwat (2013) reported that the choice of any particular void fraction correlation must be according to its impact on the calculated variables such as the two phase mixture density. They concluded that the two phase mixture density defined as $\rho_{TP} = \rho_G \alpha + (1 - \alpha)\rho_L$ is biased due to its void fraction weighted physical form such that a considerable error in small values of void fraction would give a small error in calculation of ρ_{TP} while a small error for large values of void fraction would

render a considerable error in prediction of two phase mixture density. Thus, the use of three different acceptable error criteria to predict void fraction mentioned above also considers its effect on calculated variables such as two phase mixture density which is further required in calculation of hydrostatic pressure drop. The accuracy of the proposed correlation is also gauged based on the statistical parameters such as mean relative deviation (MRD) and mean absolute relative deviation (MARD) of the percentage error between experimentally measured and predicted values of the void fraction. The mean relative deviation (MRD) and the mean absolute relative deviation (MARD) of the percentage error are determined using Eqs. (5.24) and (5.25).

$$\text{MRD} = \frac{1}{N}\sum_{1}^{N}\frac{\alpha_{\text{exp}} - \alpha_{\text{pred}}}{\alpha_{\text{exp}}} \times 100 \tag{5.24}$$

$$\text{MARD} = \frac{1}{N}\sum_{1}^{N}\frac{|\alpha_{\text{exp}} - \alpha_{\text{pred}}|}{\alpha_{\text{exp}}} \times 100 \tag{5.25}$$

The performance of different void fraction correlations against the experimental data listed in Table 5.1 is presented for different fluid combinations in Tables 5.2 to 5.7. In case of air-water data, for the lowest range of void fraction ($0 < \alpha \leq 0.25$), Bhagwat and Ghajar (2014) gives comparable performance as that of Gomez et al. (2000) and predicts 73% and 85% of data points within ±10% and ±20% error bands, respectively. It is evident that the drift flux model based void fraction correlations perform better than the separated flow models for the low range of void fraction. For the second range of void fraction i.e., $0.25 < \alpha \leq 0.75$, Bhagwat and Ghajar (2014) and Choi et al. (2012) give the highest and comparable performance. Among the separated flow models, Smith (1969) gives best accuracy by predicting 76% and 84% of data points within ±15% and ±20% error bands, respectively.

Table 5.2: Performance comparison of different void fraction correlations for the air-water data ($-90^o \leq \theta \leq +90^o$).

Void fraction range	$(0 < \alpha \leq 0.25)$				$(0.25 < \alpha \leq 0.75)$				$(0.75 < \alpha < 1)$			
No. of data points	(738 data points)				(2530 data points)				(2026 data points)			
			% of data in				% of data in				% of data in	
Correlation	MRD	MARD	±20%	±30%	MRD	MARD	±15%	±20%	MRD	MARD	±5%	±7.5%
Bhagwat and Ghajar (2014)	-6.8	23.3	73	85	2.4	14.9	83	89	-1.4	6.0	74	87
Bonnecaze et al. (1971)	-24	20	63	62	-6	16	78	84	-10	8.1	32	41
Choi et al. (2012)	-10.1	24.9	69	83	2.4	14.9	83	89	-6.6	7.8	39	54
Gomez et al. (2000)	-6	26	73	85	4	17	77	86	-3	7	38	59
Rouhani and Axelsson (1970)	-17.2	28.4	53	69	-4.3	17.6	74	82	-10.4	12.3	49	56
Woldesemayat and Ghajar (2007)	72.6	102.5	16	29	0.5	16.5	74	83	-1.4	8.2	56	78
Cioncolini and Thome (2012a)	242	391	0	0	17.5	21.4	57	66	1.1	6.5	67	83
Homogeneous	33.2	120.6	50	62	23.8	22.6	21	33	11.7	8.6	25	34
Chen (1986)	86.4	154	28	62	8.7	20.2	70	78	2.8	7.3	56	75
Lockhart and Martinelli (1949)	15.7	92.4	49	71	-12.2	19.8	48	62	-1.9	8.8	68	81
Permoli et al. (1971)	33.1	120	50	62	23.6	22.5	31	66	11.6	8.7	35	61
Smith (1969)	17.6	100	55	68	-0.2	18	76	84	1.3	8	58	75
Yashar et al. (2001)	38.1	80.3	42	68	-16.3	15.7	56	62	-4.2	10.7	62	74
Xu and Fang (2014)	26.3	99.5	51	63	10	16.5	68	79	4.9	9.1	50	64
Zivi (1964)	111	182	11	20	18.6	18.8	38	61	5.9	7.8	43	56

For the last range of void fraction ($0.75 < \alpha < 1$), the best performance is given by Bhagwat and Ghajar (2014) followed by Cioncolini and Thome (2012a) and Lockhart and Martinelli (1949) correlations. Correlations of Cioncolini and Thome (2012a) and Lockhart and Martinelli (1949) are expected to give good accuracy for this range of void fraction since they are derived based on the data for annular flow regime and are applicable for separated type of two phase flow. Graphical performance of Bhagwat and Ghajar (2014) for air-water data in horizontal, vertical upward and vertical downward pipe orientation is shown in Figs. 5.6 and 5.7. As shown in Fig. 5.6, for horizontal flow, Bhagwat and Ghajar (2014) predicts more than 90% of data points within ±20% error bands while for vertical upward and downward flow, Bhagwat and Ghajar (2014) correlation predicts 88.3% and 94.6% of data within ±20% error bands.

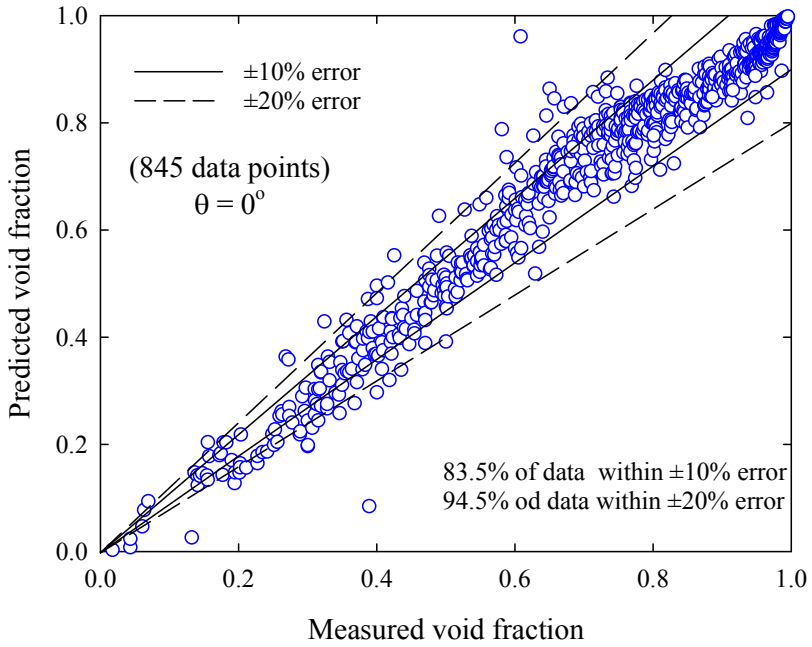

Figure 5.6: Performance of the Bhagwat and Ghajar (2014) against data in air-water horizontal two phase flow.

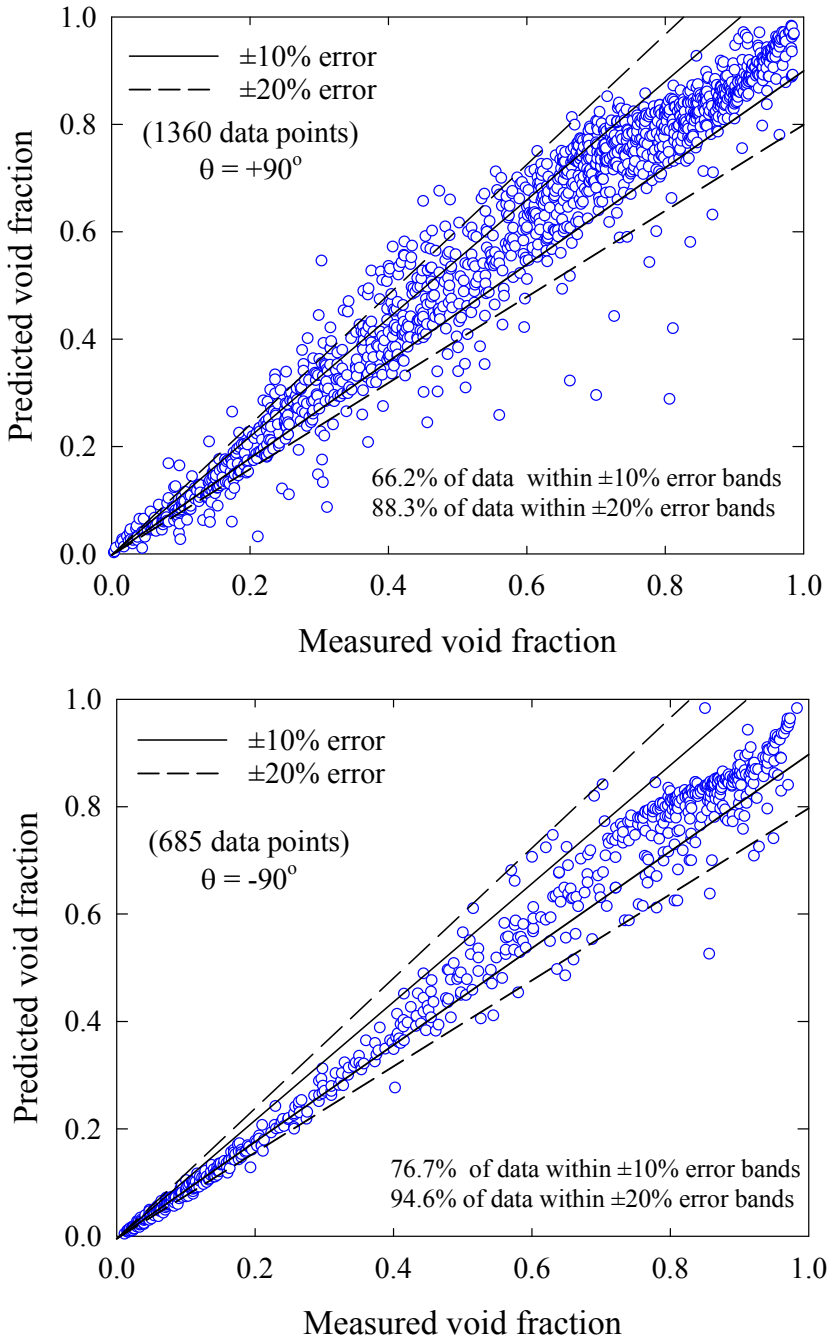

Figure 5.7: Performance of the Bhagwat and Ghajar (2014) correlation against data in air-water vertical upward and downward two phase flow.

It is seen from Fig. 5.7 that in comparison to vertical upward flow, Bhagwat and Ghajar (2014) gives better accuracy for vertical downward flow. For the vertical downward flow with void fraction in a range of $0 < \alpha \leq 0.5$, Bhagwat and Ghajar

(2014) predicts 92% of data points within ±20% error bands whereas comparatively, Woldesemayat and Ghajar (2007) predicts only 17% of data points within ±20% error bands. This enhanced accuracy of Bhagwat and Ghajar (2014) correlation is due to correct modeling of distribution parameter and drift velocity. The lower accuracy of Woldesemayat and Ghajar (2007) is due to the low values of distribution parameter ($C_o < 1$) exhibited by their correlation in addition to zero drift velocity at vertical downward pipe orientation. The graphical performance of Bhagwat and Ghajar (2014) correlation for air-water void fraction data in upward and downward inclined flow is depicted in Figs. 5.8 and 5.9. It is seen that the performance of Bhagwat and Ghajar (2014) correlation deteriorates for downward pipe inclinations.

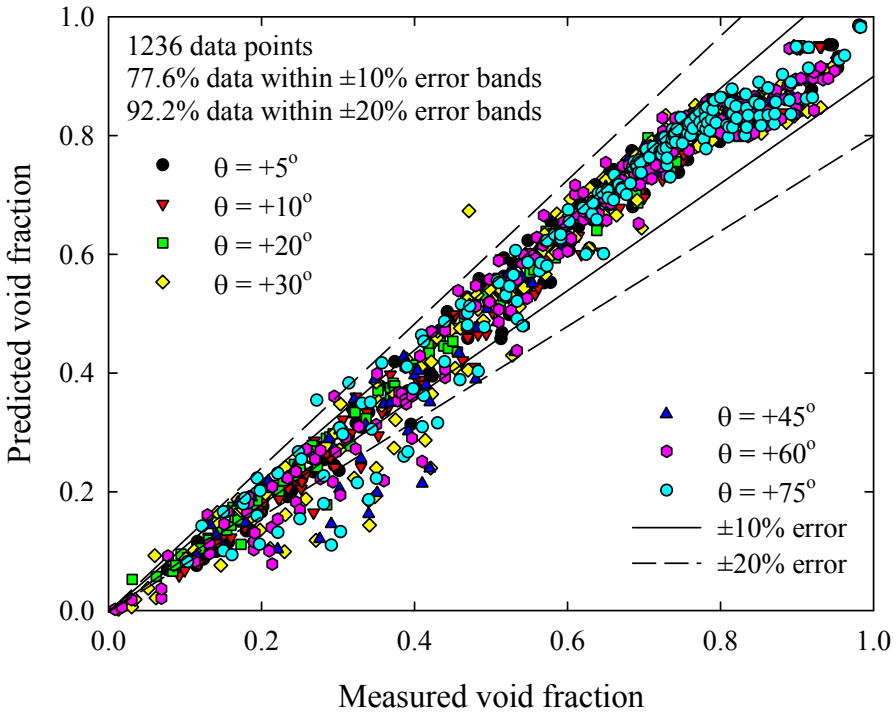

Figure 5.8: Performance of Bhagwat and Ghajar (2014) correlation in air-water upward inclined flow.

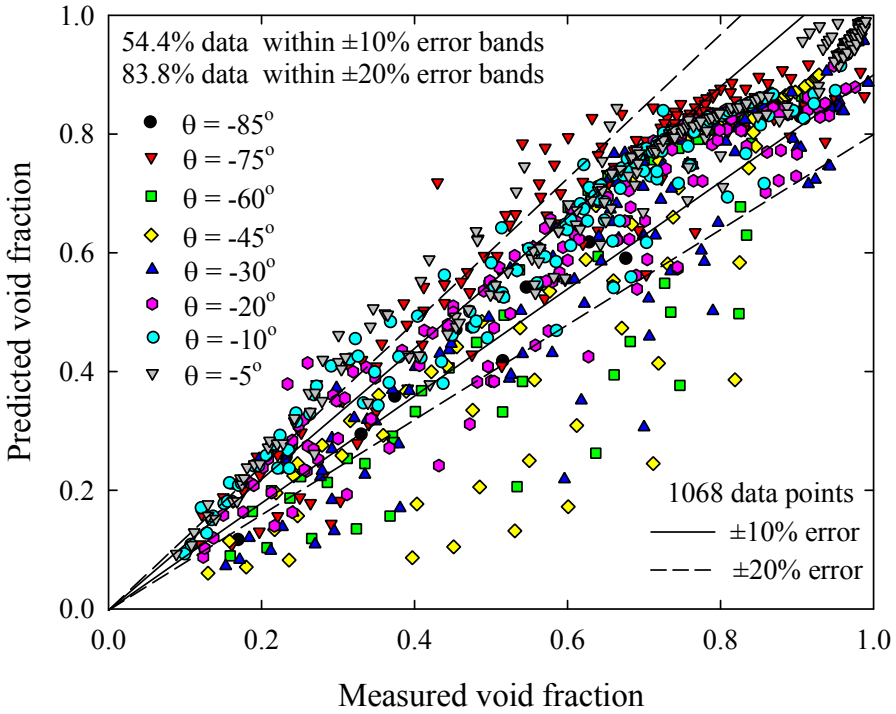

Figure 5.9: Performance of Bhagwat and Ghajar (2014) correlation in air-water downward inclined flow.

The inaccuracies involved in prediction of void fraction in downward inclinations is essentially due to the flow stratification that causes the slip ratio to decrease and follow the relationship $\alpha > \beta$. It was seen in Chapter IV that for all downward pipe inclinations, for slug and stratified flow, the relation $\alpha \geq \beta$ holds true. The performance of different void fraction correlations tested here would be undermined if their accuracy is not checked separately against the two different flow situations of $\alpha \geq \beta$ and $\alpha < \beta$, respectively. Since, the data presented in Fig. 5.9 contains data measured in this work as well data from literature without information of associated flow pattern, the flow condition of $\alpha \geq \beta$ is used to separate out the data for stratified and slug flow affected by the dominant buoyancy force in a direction opposite to mean flow. Using this criteria, 244 out of 1068 data points satisfy the condition of $\alpha \geq \beta$. It is found that all drift flux and separated flow model based correlations considered

in this study exhibit an under prediction tendency for all downward pipe inclinations when $\alpha \geq \beta$. A comparison of the performance of different void fraction correlations for downward pipe inclinations for two different flow situations i.e., $\alpha \geq \beta$ and $\alpha < \beta$ is reported in Table 5.3. For the flow condition of $\alpha \geq \beta$, the accuracy of void fraction correlations is assessed based on the percentage of data points predicted within $\pm 20\%$ and $\pm 30\%$ error bands. Whereas, for the case $\alpha < \beta$, a stricter error criteria of $\pm 10\%$ and $\pm 20\%$ is used to gauge the accuracy of void fraction correlations. For the first case of $\alpha \geq \beta$, Bhagwat and Ghajar (2014) predicts highest number of data points within $\pm 30\%$ error bands. Interestingly, the homogeneous flow model which assumes no slippage between the gas and liquid phase i.e., $\alpha = \beta$, predicts highest number of data points within $\pm 20\%$ error bands. It is found that for the case of $\alpha \geq \beta$ most of the data points are in the vicinity of gas volumetric flow fraction (β) values. Among separated flow models, comparable performance is given by Permoli et al. (1971), Xu and Fang (2014) and Zivi (1964). For the second flow condition of $\alpha < \beta$, most of the correlations predict more than 85% of data points within $\pm 20\%$ error bands. The best performance is given by seperated flow model based correlations of Smith (1969) and Yashar et al. (2001) by predicting 85.1% and 94.6% of data points within $\pm 10\%$ and $\pm 20\%$ error bands, respectively. In comparison to this, among all DFM based correlations, Bhagwat and Ghajar (2014) gives overall best accuracy by predicting 84.1% and 91.4% of data points within $\pm 10\%$ and $\pm 20\%$ error bands, respectively. Based on the accuracies in Table 5.3, it appears that Bhagwat and Ghajar (2014) correlation works fine for $\alpha < \beta$ however, for $\alpha \geq \beta$, it needs to be modified for better accuracy.

The performance of different void fraction correlations against the data for liquid refrigerants and their vapors is tabulated in Table 5.4. Due to lack of data in low range of void fraction, the first range of void fraction is taken as $0 < \alpha \leq 0.5$ while the second and third range of void fraction is taken as $0.5 < \alpha \leq 0.75$ and $0.75 < \alpha < 1$,

Table 5.3: Performance of void fraction correlations against data in downward inclined two phase flow.

Flow condition	$\alpha \geq \beta$ (244 data)		$\alpha < \beta$ (824 data)	
Correlation	% of data within		% of data within	
	±20%	±30%	±10%	±20%
Bhagwat and Ghajar (2014)	56.1	77.1	84.1	91.4
Bonnecaze et al. (1971)	10.2	32.4	61.1	95.3
Choi et al. (2012)	41.8	61.7	66.1	92.3
Gomez et al. (2000)	44.6	63.5	58.3	92.7
Rouhani and Axelsson (1970)	12.3	31.9	57.7	85.7
Woldesemayat and Ghajar (2007)	31.1	53.3	75.8	91.3
Cioncolini and Thome (2012a)	33.6	50.4	76.3	88.4
Homogeneous	61.1	73.4	25.4	51.1
Chen (1986)	37.7	54.1	78.8	95.2
Lockhart and Martinelli (1949)	22.6	38.5	65.1	87.4
Smith (1969)	20.1	53.2	85.1	94.6
Permoli et al. (1971)	49.5	66.4	25.7	52.1
Yashar et al. (2001)	25.4	46.3	85.1	94.6
Xu and Fang (2014)	43.4	65.2	59.1	85.7
Zivi (1964)	45.5	61.1	43.5	92.7

respectively. It is seen that for the first range of void fraction, correlation of Bhagwat and Ghajar (2014) predicts highest number of data points i.e., 61% and 80% of data points within ±20% and ±30% error bands, respectively. The second and third best performance is given by Smith (1969) and Choi et al. (2012) correlations, respectively. For the second range of void fraction, performance of Bhagwat and Ghajar (2014) is comparable to that of Smith (1969) however with slightly larger mean relative deviation (MRD) and mean absolute relative deviation (MARD). For the last range of void fraction, Bhagwat and Ghajar (2014) correlation gives highest accuracy and is also comparable to the performance of separated flow models. The accuracy of Bhagwat and Ghajar (2014) is comparable to that of Cioncolini and Thome (2012a) correlation exclusively developed for annular flow ($0.75 < \alpha < 1$). It is worthwhile

to mention that the Bhagwat and Ghajar (2014) correlation performs slightly better than the Xu and Fang (2014) correlation developed exclusively for predicting void fraction in two phase flow of refrigerants. It should be noted that the drift flux model based correlations such as Bonnecaze et al. (1971), Choi et al. (2012) and Gomez et al. (2000) that perform relatively well for low values of void fraction fail to predict the data accurately for higher values of void fraction typically in annular flow regime. These inaccuracies are attributed to the fact that these correlations do not model distribution parameter and drift velocity as a function of flow patterns. The graphical performance of Bhagwat and Ghajar (2014) correlation for different refrigerants is given in Fig. 5.10 (a)-(b). In Fig. 5.10 (a), Bhagwat and Ghajar (2014) under predicts the void fraction data for CO_2. The under prediction tendency for this data is justified later in this section. In Fig. 5.10 (b), Bhagwat and Ghajar (2014) over predicts the void fraction for R22 and R134a in the range of $0.5 \leq \alpha \leq 0.7$. The experimental data for R22 is measured by Sacks (1975) whose uncertainty is not reported. In case of R134a, the over predicted data belong to the experimental work of Bowers and Hrnjak (2010) who measured the void fraction in pipe diameters in a range of 7 mm to 15 mm through the pixel analysis of the images obtained by high speed visualization. The reliability of these measurements needs further examination since they did not report uncertainty of the measured void fraction data and did not make any comparison regarding its agreement with other measurement techniques or with the predictions of available void fraction correlations. As reported in Table 5.5, for steam-water two phase flow, Bhagwat and Ghajar (2014) predicts highest percentage of data points within $\pm 20\%$ and $\pm 30\%$ error bands with minimum MRD and MARD for the first range of void fraction ($0 < \alpha \leq 0.25$). For $0.25 < \alpha \leq 0.75$, Bhagwat and Ghajar (2014) and Choi et al. (2012) give comparable performance by predicting more than 70% and 80% of data points within $\pm 15\%$ and $\pm 20\%$ error bands, respectively.

Table 5.4: Performance comparison of different void fraction correlations for the refrigerant data ($-90^o \leq \theta \leq +90^o$).

Void fraction range	$(0 < \alpha \leq 0.5)$				$(0.5 < \alpha \leq 0.75)$				$(0.75 < \alpha < 1)$			
No. of data points	(97 data points)				(363 data points)				(944 data points)			
			% of data in				% of data in				% of data in	
Correlation	MRD	MARD	±20%	±30%	MRD	MARD	±15%	±20%	MRD	MARD	±5%	±7.5%
Bhagwat and Ghajar (2014)	6.4	53.6	61	80	3.1	13.2	79	82	1	4	82	91
Bonnecaze et al. (1971)	-5.8	48.4	52	70	-9.1	11.1	44	84	-14	4.1	12	37
Choi et al. (2012)	5.3	52.2	55	73	-1.8	12.6	59	81	-9.4	4.1	18	34
Gomez et al. (2000)	11.5	53.3	52	66	1.1	12.3	59	83	-7	5.1	24	42
Rouhani and Axelsson (1970)	-2.5	50.9	52	73	-3.1	13.9	49	78	-4.1	5.3	61	76
Woldesemayat and Ghajar (2007)	14.6	57.5	54	71	1.5	11.9	65	84	-2.4	4.1	79	94
Cioncolini and Thome (2012a)	49.4	70.6	18	34	8.5	11.4	66	76	2.2	4.1	79	89
Homogeneous	28.6	61.1	35	46	16.4	13.9	49	77	6.7	5.2	46	66
Chen (1986)	109.1	102.3	14	25	19.8	13.2	23	61	4.1	5.3	65	79
Lockhart and Martinelli (1949)	71.3	80.3	15	23	11.1	11.5	52	66	1.9	3.9	79	88
Permoli et al. (1971)	-17.5	37.8	45	68	-24.5	13.4	32	61	-3.3	9.1	33	65
Smith (1969)	7.6	50.3	58	76	0.2	12.6	77	81	-1.1	4.8	72	88
Yashar et al. (2001)	50.5	78.8	35	57	5.1	11.9	72	80	1.2	5.1	77	87
Xu and Fang (2014)	19.5	57.1	53	69	1.9	11.6	83	86	0.1	5.1	73	89
Zivi (1964)	39.1	62.6	39	46	6.1	11.9	76	81	0.1	3.8	80	92

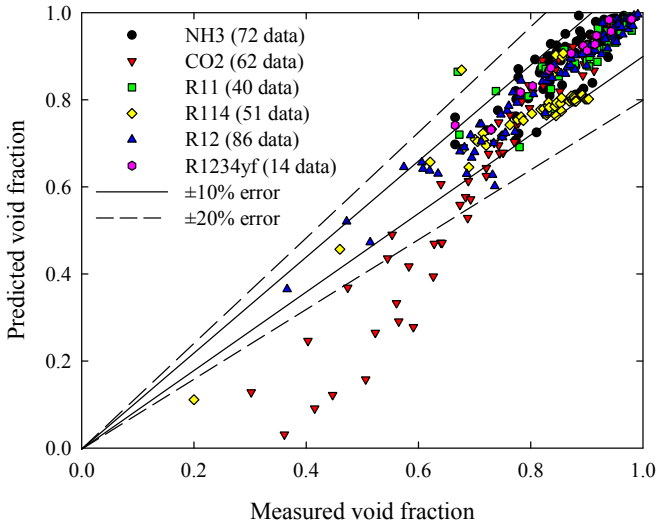

(a) $\theta = 0^o$ and $+90^o$ (R114)

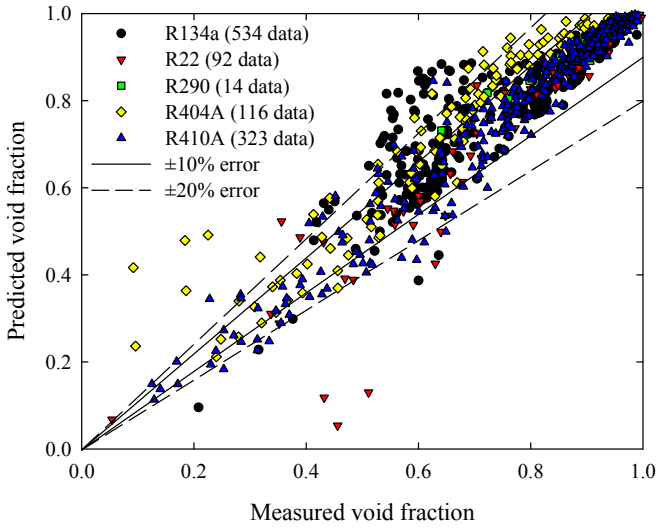

(b) $\theta = 0^o$ and $-90^o \leq \theta \leq +90^o$ (R134a)

Figure 5.10: Performance of Bhagwat and Ghajar (2014) correlation for refrigerant data.

For the highest range of void fraction, Bhagwat and Ghajar (2014) is undoubtedly the best performer that predicts more than 80% of data points within ±5% error bands. In comparison to first two ranges of void fraction ($0.75 < \alpha < 1$), the accuracy of separated flow model based correlations increase for higher values of void fraction.

Table 5.5: Performance comparison of different void fraction correlations for the steam-water data ($\theta = +90^o$).

Void fraction range	$(0 < \alpha \leq 0.25)$				$(0.25 < \alpha \leq 0.75)$				$(0.75 < \alpha < 1)$			
No. of data points	(97 data points)				(527 data points)				(268 data points)			
			% of data within				% of data within				% of data within	
Correlation	MRD	MARD	±20%	±30%	MRD	MARD	±15%	±20%	MRD	MARD	±5%	±7.5%
Bhagwat and Ghajar (2014)	2.8	20.8	69	87	4.7	14.4	75	84	-2.5	3.4	81	94
Bonnecaze et al. (1971)	10.2	24.3	55	78	8.2	16.6	65	82	-13.9	16.4	12	25
Choi et al. (2012)	4.6	25.5	62	78	7.1	16.5	71	84	-11.7	6.1	16	23
Gomez et al. (2000)	9.1	26.3	49	75	12.3	17.5	53	71	-10.1	6.7	21	31
Rouhani and Axelsson (1970)	11.6	27.7	48	72	13.6	19.3	60	79	-1.9	7.1	63	75
Woldesemayat and Ghajar (2007)	57.1	61.1	21	38	16.3	26.8	49	62	-2.7	6.6	62	75
Cioncolini and Thome (2012a)	119.9	178.8	0	4	30.8	24.6	40	57	-1.9	6.5	65	78
Homogeneous	56.9	33.1	11	13	37.1	22.7	24	36	3.9	7.7	57	70
Chen (1986)	170.4	158.3	1	5	47.4	30.8	17	33	0.5	6.2	65	81
Lockhart and Martinelli (1949)	151.6	141.3	0	3	26.2	23.4	33	46	-2.7	6.1	62	76
Permoli et al. (1971)	21.1	57.9	23	39	-12.3	47.9	47	57	-19.3	9.6	23	45
Smith (1969)	37.1	29.6	21	39	10.3	17.6	59	71	-4.5	7.8	51	78
Yashar et al. (2001)	101.2	121.1	5	18	19.3	19.4	45	67	-1.2	6.2	70	82
Xu and Fang (2014)	13.3	36.7	59	76	11.5	18.3	49	68	-3.6	5.7	71	86
Zivi (1964)	93.7	102.1	0	4	28.8	21.9	35	56	-2.6	7.5	54	68

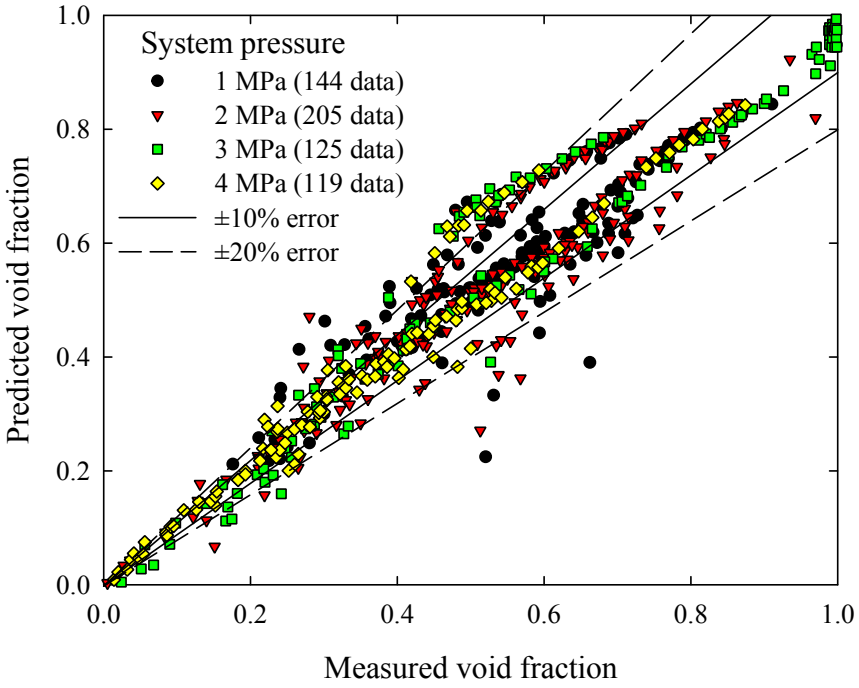

(a)

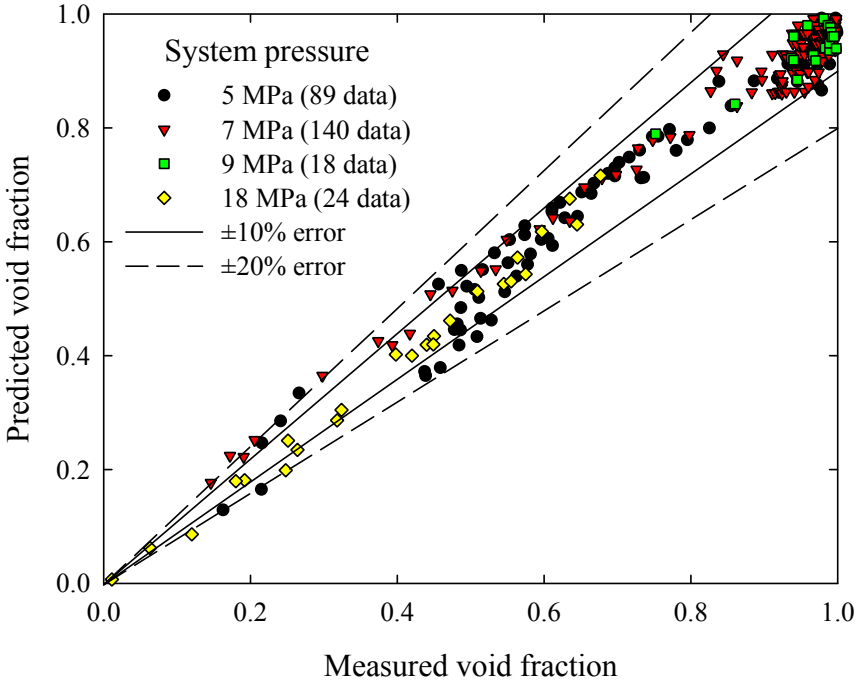

(b)

Figure 5.11: Performance of Bhagwat and Ghajar (2014) for high system pressure steam-water data ($\theta = +90^o$).

Among SFM based correlations, Yashar et al. (2001) and Xu and Fang (2014) give better performance than other correlations. It is important to mention that the void fraction data for steam-water flows consists of the data measured in rectangular and annular pipe geometries and hence the correlations not developed for these pipe geometries obviously fail to predict void fraction correctly. The steam-water flow data is typically measured at high system pressures and since the correlation of Bhagwat and Ghajar (2014) accounts for the effect of system pressure (through the phase density ratio) on void fraction, its relevant here to illustrate its performance against the data consisting of different system pressures. In Fig. 5.11 (a)-(b), the performance of Bhagwat and Ghajar (2014) is presented for a wide range of system pressures. Since the objective of the void fraction modeling undertaken in this work was to make the void fraction correlation independent of the fluid properties, it is imperative to check the performance of Bhagwat and Ghajar (2014) against the experimental data measured for fluids with high viscosity. The accuracy of Bhagwat and Ghajar (2014) and other correlations against the data of air-oil fluid combination is tabulated in Table 5.6. For the low and intermediate range of void fraction it is evident that Bhagwat and Ghajar (2014) and Choi et al. (2012) correlations perform reasonably well whereas other correlations based on both DFM and SFM fail to predict the void fraction data correctly. For first two ranges of void fraction, Choi et al. (2012) perform slightly better than Bhagwat and Ghajar (2014) correlation. However, for the last range of void fraction, accuracy of the later correlation is significantly higher than the former. Among all DFM correlations listed in Table 5.6, only Bhagwat and Ghajar (2014) and Choi et al. (2012) account for the effect of liquid dynamic viscosity on the void fraction and hence perform well for the air-viscous oil void fraction data. It is also observed that compared to all other fluid combinations, the accuracy of Cioncolini and Thome (2012a) for the high values of void fraction in air-oil fluid combination is relatively low. This is probably because their correlation

only considers the effect of phase densities and the two phase flow quality on the void fraction and do not account for the effect of liquid viscosity on the void fraction. The performance of Bhagwat and Ghajar (2014) correlations against void fraction data with different liquid dynamic viscosities in a range of 0.005 Pa-s to 0.59 Pa-s is presented in Fig. 5.12. Better performance of Bhagwat and Ghajar (2014) over Choi et al. (2012) correlation for the large values of void fraction can be attributed to the correct modeling of distribution parameter as a function of flow patterns in terms of void fraction. Finally for the miscellaneous fluid combinations, the performance of different void fraction correlations is documented in Table 5.7. It is seen that for the low values of void fraction ($0 < \alpha \leq 0.25$), both Bhagwat and Ghajar (2014) and Choi et al. (2012) predict more than 90% of data points within ±30% error bands.

For the last range of void fraction, Bhagwat and Ghajar (2014), Woldesemayat and Ghajar (2007), Cioncolini and Thome (2012a) and Chen (1986) are among the top performers. So far based on the performance of different void fraction correlations it is quite evident that with the exception of Bhagwat and Ghajar (2014) correlation, all other drift flux model based correlations perform well for the low to intermediate range of void fraction while separated flow model based correlations perform well for large values of void fraction. Since the drift flux model expression of Bhagwat and Ghajar (2014) correlations introduces a correction factor to account for the effect of pipe diameter on drift velocity, it is also of interest to check the accuracy of Bhagwat and Ghajar (2014) correlation for pipe diameters of mini and macro scale. Following the thumb-rule given by Kandlikar (2002), $0.5 \leq D \leq 3 \sim 4$ mm are considered as mini channels while pipe diameter greater than this threshold value are recognized as conventional or macro channels.

Table 5.6: Performance comparison of different void fraction correlations for the air-oil data ($(\theta = 0^o, \pm 5^o, \pm 10^o$ and $\pm 90^o)$.

Void fraction range	$(0 < \alpha \leq 0.25)$				$(0.25 < \alpha \leq 0.75)$				$(0.75 < \alpha < 1)$			
No. of data points	(154 data points)				(404 data points)				(175 data points)			
			% of data in				% of data in				% of data in	
Correlation	MRD	MARD	±20%	±30%	MRD	MARD	±15%	±20%	MRD	MARD	±5%	±7.5%
Bhagwat and Ghajar (2014)	12.5	66.2	61	77	2.9	20.8	73	85	-0.3	6.5	69	75
Bonnecaze et al. (1971)	20.8	47.8	53	59	14.2	31.4	49	53	-11.3	9.9	17	37
Choi et al. (2012)	12.4	34.3	64	77	2.9	17.2	74	88	-8.3	8.2	37	50
Gomez et al. (2000)	60.2	70.6	23	36	37.1	39.3	24	36	-2.6	6.5	51	65
Rouhani and Axelsson (1970)	28.1	53.7	51	60	20.7	36.9	43	50	-9.6	15.3	31	40
Woldesemayat and Ghajar (2007)	93.6	139.7	14	27	22.9	32.1	43	54	0.1	11.7	43	66
Cioncolini and Thome (2012a)	279.3	315.6	0	0	47.6	36.8	21	37	3.8	8.1	36	61
Homogeneous	95.1	88.2	11	25	61.1	46.9	7	21	11.9	7.7	29	38
Chen (1986)	141.9	123.4	13	19	35.7	33.4	35	48	3.8	7.6	42	62
Lockhart and Martinelli (1949)	59.1	74.2	34	45	14.1	33.4	46	58	-0.4	10.1	38	59
Permoli et al. (1971)	7.2	83.9	18	30	-6.2	61.6	29	43	-16.6	14.5	37	46
Smith (1969)	68.1	74.5	17	30	33.2	40.1	31	38	3.1	9.5	30	54
Yashar et al. (2001)	82.1	129.8	29	37	2.1	26.5	56	74	-4.1	14.9	27	50
Xu and Fang (2014)	19.5	57.1	53	69	1.9	11.6	83	86	0.1	5.1	73	89
Zivi (1964)	169	154.7	3	9	51.3	40.8	22	36	6.8	8.1	27	45

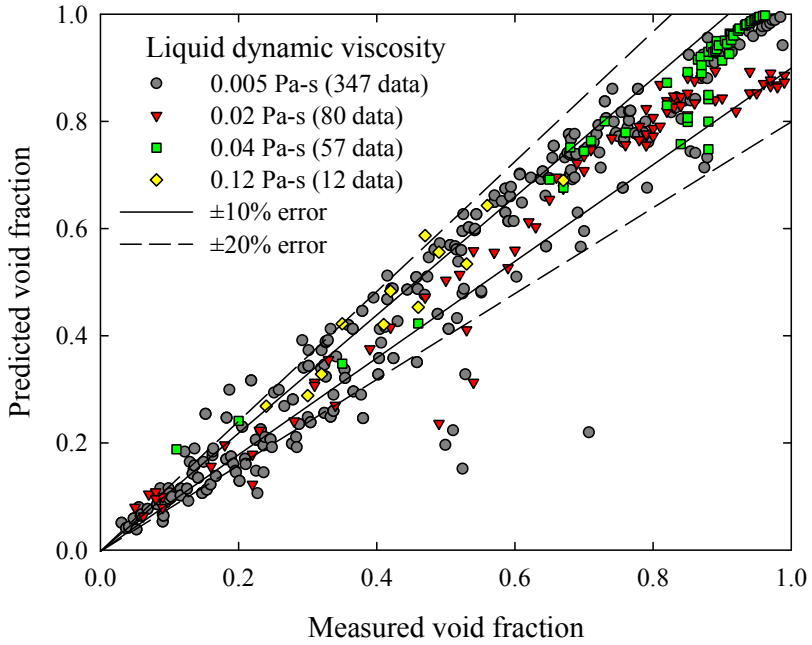

(a) $\theta = 0^o, \pm 5^o, \pm 10^o$ and $\pm 90^o$

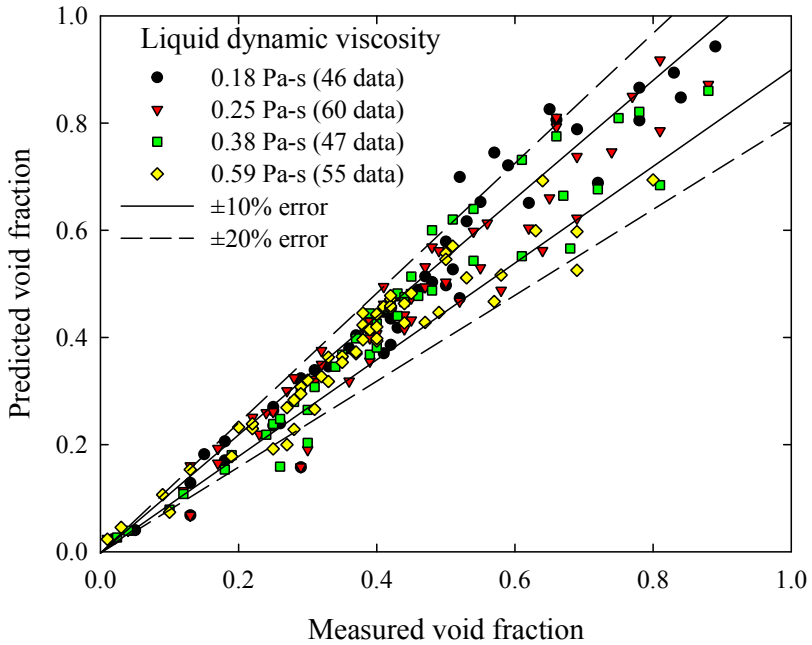

(b) $\theta = 0^o$

Figure 5.12: Performance of Bhagwat and Ghajar (2014) correlation for viscous oil data.

Table 5.7: Performance comparison of different void fraction correlations for the air-miscellaneous fluid data ($-90^o \leq \theta \leq +90^o$).

Void fraction range	$(0 < \alpha \leq 0.25)$				$(0.25 < \alpha \leq 0.75)$				$(0.75 < \alpha < 1)$			
No. of data points	(271 data points)				(612 data points)				(1019 data points)			
			% of data in				% of data in				% of data in	
Correlation	MRD	MARD	±20%	±30%	MRD	MARD	±15%	±20%	MRD	MARD	±5%	±7.5%
Bhagwat and Ghajar (2014)	-7.1	20.1	66	90	-4.7	15.2	79	86	-2.6	5.1	67	85
Bonnecaze et al. (1971)	1.3	23.1	62	84	-7.5	18.3	63	76	-12.2	5.9	9	17
Choi et al. (2012)	-5.8	18.2	74	92	-5.1	15.6	76	86	-8.9	5.8	21	36
Gomez et al. (2000)	18.8	33.7	50	64	3.7	21.8	71	81	-5.9	5.7	34	52
Rouhani and Axelsson (1970)	-0.7	21.4	72	87	-5.1	18.3	66	78	-11.2	9.5	30	42
Woldesemayat and Ghajar (2007)	103.3	97.5	13	20	2.3	16.4	73	81	-1.7	6.3	66	80
Cioncolini and Thome (2012a)	303.5	299.5	0	0	20.5	24.7	50	66	0.1	6.6	67	80
Homogeneous	28.6	61.1	35	46	16.4	13.9	35	49	7.8	5.1	46	65
Chen (1986)	116.2	89.2	3	6	19.3	23.1	49	61	1.9	6.1	72	83
Lockhart and Martinelli (1949)	34.3	52.7	44	56	-2.6	20.9	57	73	-1.8	7.6	61	77
Permoli et al. (1971)	29.6	49.7	45	61	-17.9	21.2	23	41	-9.3	10.8	33	55
Smith (1969)	29.1	41.7	45	58	0.1	22.4	57	73	-0.5	7.6	58	75
Yashar et al. (2001)	92.8	94.6	26	37	-10.3	16.1	54	70	-3.5	9.2	59	71
Xu and Fang (2014)	40.4	41.5	40	51	9.8	18.6	76	88	2.5	7.3	62	75
Zivi (1964)	141.2	97.4	10	24	19.2	23.7	50	61	3.1	6.7	64	78

In the present study, pipe diameters less than 5 mm are recognized as small diameter pipes while pipe diameters greater than $La < 0.025$ are recognized as large (macroscale) diameter pipes. All pipe diameters between this upper and lower limit are classified as conventional pipe diameters. Out of the 10225 data points, 515 data points are for $D \leq 4.5$ mm while 291 data points are for $La < 0.025$. The graphical performance of Bhagwat and Ghajar (2014) correlation for $D \leq 4.5$ mm is shown in Fig. 5.13 (a). Bhagwat and Ghajar (2014) predicts 77% of data points within $\pm 10\%$ and 92% of data points within $\pm 20\%$ error bands. It is of interest to compare the performance of Bhagwat and Ghajar (2014) with the prediction of Cioncolini and Thome (2012a), Choi et al. (2012) and homogeneous flow model. Cioncolini and Thome (2012a) is based on the experimental data of Shedd (2010) for $0.5 < D < 3$ mm while Choi et al. (2012) correlation includes two phase mixture Reynolds number (as a function of pipe diameter) in its physical structure to account for the decrease of pipe diameter on void fraction. Performance of homogeneous flow model ($\alpha = \beta$) also needs to be tested since a decrease in pipe diameter is known to offer resistance to the flow and hence reduce slippage between the two phases. Cioncolini and Thome (2012a), Choi et al. (2012) and homogeneous flow model predicts 74.5%, 60.7% and 56.5% of data points, respectively within $\pm 10\%$ error bands. The under predicted data for D = 1 mm is for CO_2 measured in 14 port parallel channels using quick closing valve by Adams et al. (2006). They found that different flow patterns may exist in different parallel channels leading to uneven distribution of void fraction in each channel. The reason for under prediction of Bhagwat and Ghajar (2014) is probably the uneven distribution of the void fraction in parallel channels. The performance of Bhagwat and Ghajar (2014) correlation for macro size pipes ($La < 0.025$) is shown in Fig. 5.13 (b). Out of 291 data points, 181 data points (62.2%) and 236 data points (81%) are predicted within $\pm 10\%$ and $\pm 20\%$ error bands, respectively.

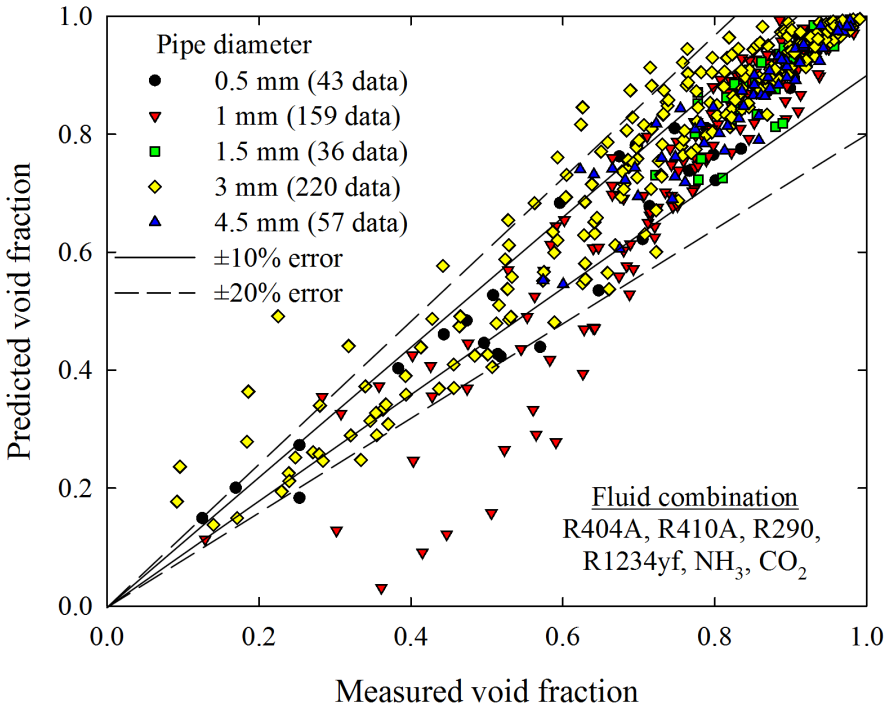

(a) Small diameter data $D < 4.5$ mm, $\theta = 0^o$

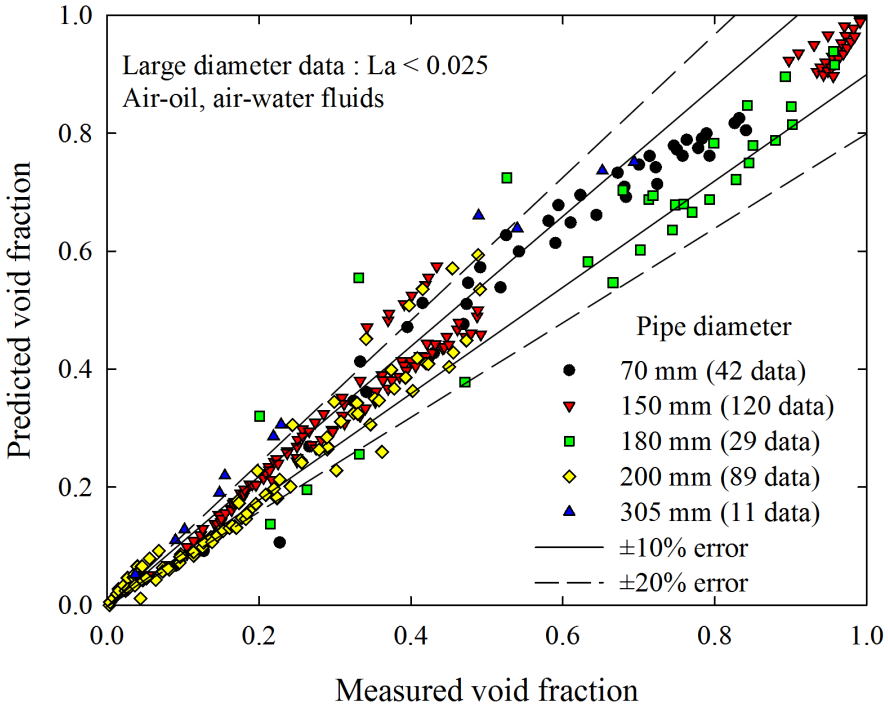

(b) Large diameter data $La < 0.025$, $\theta = +90^o$

Figure 5.13: Performance of Bhagwat and Ghajar (2014) correlation for mini and macro scale diameter pipes.

In addition to the range of pipe diameters, validity of Bhagwat and Ghajar (2014) correlation is also extended to rectangular and annular pipe geometries as depicted in Fig. 5.14 (a)-(b). For rectangular pipe geometries, it is recommended to use a value of 0.4 for C_1. The void fraction data for annular pipes belongs to airâĂŞwater data of Wongwises and Pipaththttakul (2006) and Das et al. (2002), air-kerosene data of Caetano et al. (1992) and steam-water data of Wurtz (1978). The void fraction data in rectangular pipe geometries is that of Marchaterre (1956), Marchaterre et al. (1960) and Sowinski and Dziubinski (2007). The correlation of Ishii (1977) for rectangular pipes is found to predict 41%, 63% and 84% of data points within ±5%, ±10% and ±15% error bands, respectively. In comparison to this, the proposed correlation predicts 49%, 68% and 86% of data points within the corresponding error bands. It appears that the slightly better accuracy of the Bhagwat and Ghajar (2014) correlation for ±5% over Ishii (1977) is because of the use of slightly higher value of $C_1 = 0.4$ compared to 0.35 used by Ishii (1977). It is also seen that Bhagwat and Ghajar (2014) tend to slightly under predict the data of air-sacchrose solution in 2.31 mm x 15 mm rectangular channel. However, majority of this data is for $\alpha \leq 0.25$ and hence an error of up to ±30% may be considered acceptable. For this data, Ishii (1977) predicts 69.4% and 81.6% of data points within ±20% and ±30% error bands, respectively. In comparison to this, Bhagwat and Ghajar (2014) predicts 63.9% and 97.2% of data points within ±20% and ±30% error bands, respectively. Due to lack of access to steam-water data, the proposed correlation could not be verified against the two phase flow data of steam-water at different pipe orientations. However, considering the performance of Bhagwat and Ghajar (2014) correlation at different pipe inclinations for other fluid combinations, it is likely to predict the void fraction in steam-water flows at different pipe orientations with a desired accuracy.

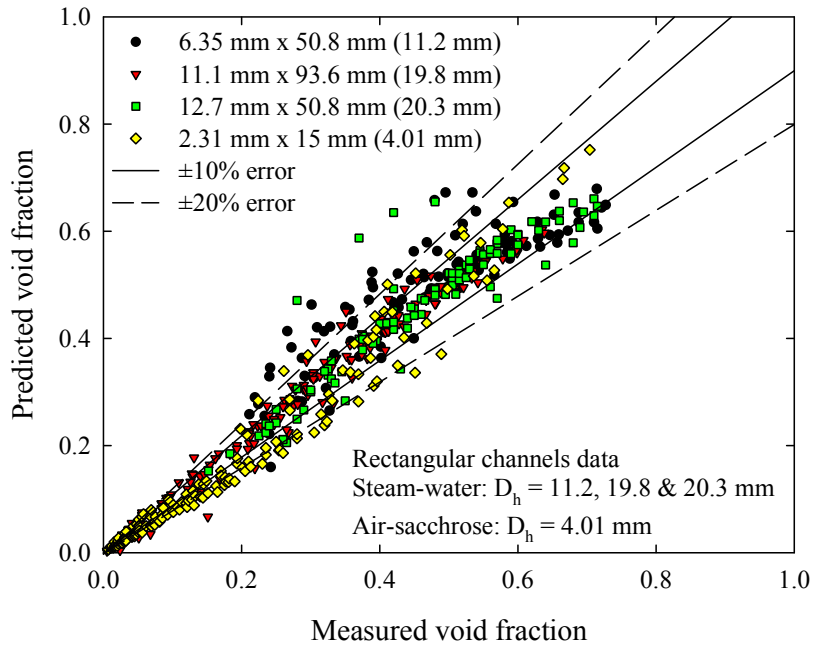

(a) Rectangular channel, $\theta = +90^o$ (steam-water), $\theta = 0^o$ (air-sacchrose)

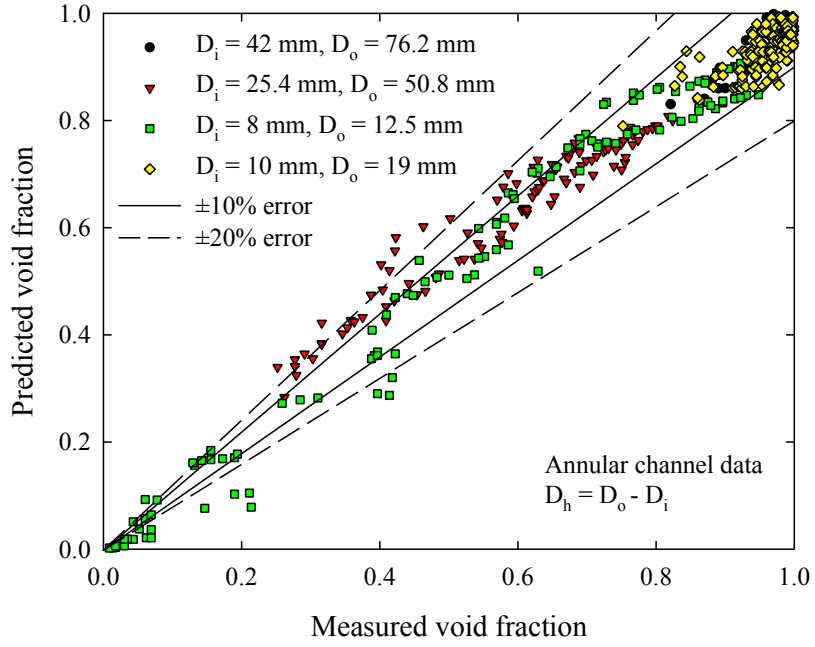

(b) Annular channel, $\theta = +30^o$, $+60^o$ and $+90^o$

Figure 5.14: Performance of Bhagwat and Ghajar (2014) correlation for non-circular pipe geometries.

Thus, form the tabulated comparisons and graphical illustrations made so far, it

is clear that the drift flux model based void fraction correlation proposed in this work i.e., the Bhagwat and Ghajar (2014) correlation is a robust correlation applicable for a wide range of two phase flow conditions. Moreover, Bhagwat and Ghajar (2014) correlation consistently performs better than existing flow pattern, fluid property and pipe orientation specific correlations available in the literature without making any reference to flow regime map. Based on the performance of different void fraction correlations, it is concluded that none of the existing correlations can accurately account for the two phase flow mechanism in downward pipe inclinations. Among all the correlations tested, Bhagwat and Ghajar (2014) exhibits comparatively good accuracy. Owing to its modular structure, Bhagwat and Ghajar (2014) offers enough scope for further modification of the distribution parameter and drift velocity expressions to gain better accuracy in downward pipe inclinations.

5.7 Chapter Summary

A flow pattern independent drift flux model based void fraction correlation is developed in this chapter. The correlation provides separate expressions for distribution parameter (C_o) and drift velocity (U_{GM}) as a function of several two phase flow variables that are known to influence void fraction. The general framework of the correlation is modular and offers enough flexibility for simplification and modification in case of specific two phase flow conditions Moreover, it is also illustrated that the void fraction correlation presented in this work works well for the limiting cases of two phase flow. The performance of this void fraction correlation is compared with other DFM and SFM based correlations available in the literature. It is found that the overall accuracy of the proposed void fraction correlation (Bhagwat and Ghajar (2014)) assessed against a comprehensive data bank consisting of a wide range of two phase flow conditions is better than all void fraction models available in the literature.

CHAPTER VI

MODELING OF TWO PHASE FRICTIONAL PRESSURE DROP

It is reported in Chapter II (Literature Review) that a plethora of two phase frictional pressure drop models exist in two phase flow literature. However, owing to their limited range of application (based on limited experimental database) correct selection of an appropriate correlation for a given two phase flow condition is quite a challenging task. To address this issue, the first part of this chapter presents a robust model to predict two phase frictional pressure drop that is applicable over a wide range of two phase flow conditions. The proposed correlation valid for micro to macro scale two phase flow is based on a consolidated data base of 9623 data points (horizontal and upward inclined two phase flow) amassed from 60 data sources in the two phase flow literature and consists of air-water, air-oil, refrigerants and other miscellaneous fluid combinations such as air-glycerin and air-kerosene. The proposed correlation is valid for non-stratified two phase flow patterns and the two phase flow region not affected by the phenomenon of flow reversal. The performance of the proposed correlation is validated against this data bank using statistical parameters and its accuracy is compared against selective top performing correlations available in the two phase flow literature. In the second part of this chapter, the concept of triangular relationship applicable to axisymmetric annular flow is studied and its validity is checked against the pressure drop data in vertical upward and downward two phase flow.

6.1 Databank Description

The consolidated database used for the development of a frictional pressure drop correlation is collected from 60 sources in the two phase flow literature and consists of 9623 data points with data in horizontal (7074 data points), vertical upward (935 data points) and upward pipe inclinations (1614 data points). The data in horizontal pipe orientation consists of 7074 data points with 4222 data points for refrigerants (circular and non-circular pipe geometries), 2053 data points for air-water fluid combination (circular and non-circular pipe geometries), 626 data points for air-oil fluid combination and 173 data points for air-kerosene and air-glycerin fluid combinations. The experimental data for the two phase flow of refrigerants consists of R12, R22, R123, R134a, R236fa, R245fa, R404A, R410A, R507, R32+R125, R290 (Propane), R1234yf, R422D and R717 (Ammonia), R744 (CO_2). The experimental data for refrigerants consists of both adiabatic (3104 data points) and evaporating (1118 data points) two phase flow and consists of pipe diameters in a range of 0.069 to 13.8 mm. For evaporating two phase flow, mean two phase flow quality (average of that at inlet and exit) reported by individual data sets is used for calculation of phase velocities. In case if the total component of the two phase pressure drop is reported then the frictional component is calculated by subtracting the accelerational component of the two phase pressure drop. The accelerational two phase pressure drop is calculated using separated flow model (see Eq. (2.10)) and is based on inlet and exit two phase flow quality and void fraction. The air-water data set in horizontal flow consists of a wide range of pipe diameters (0.5 to 152 mm) covering micro to macro scale two phase flow phenomenon. In comparison to the refrigerant data, the air-water data consists of lower system pressures ($P_{SYS} \leq 1$ MPa) and ambient system temperatures. Air-oil data consists of a wide range of oil viscosity ranging from 0.005 to 0.89 Pa-s and pipe diameters in a range of 23 to 78 mm. Both refrigerant and air-water data consists

of circular and non-circular (rectangular, annular) pipe geometries. The aspect ratio (width over height) of rectangular channels is in a range of 1 to 56. Very few of the existing two phase flow models are found to be based on the experimental data base consisting of mass flux in a range of $0 < G \leq 100$ kg/m^{2}s. In the present study, 1162 data points (16% of th data bank) satisfy the condition of $0 < G \leq 100$ kg/m^{2}s.

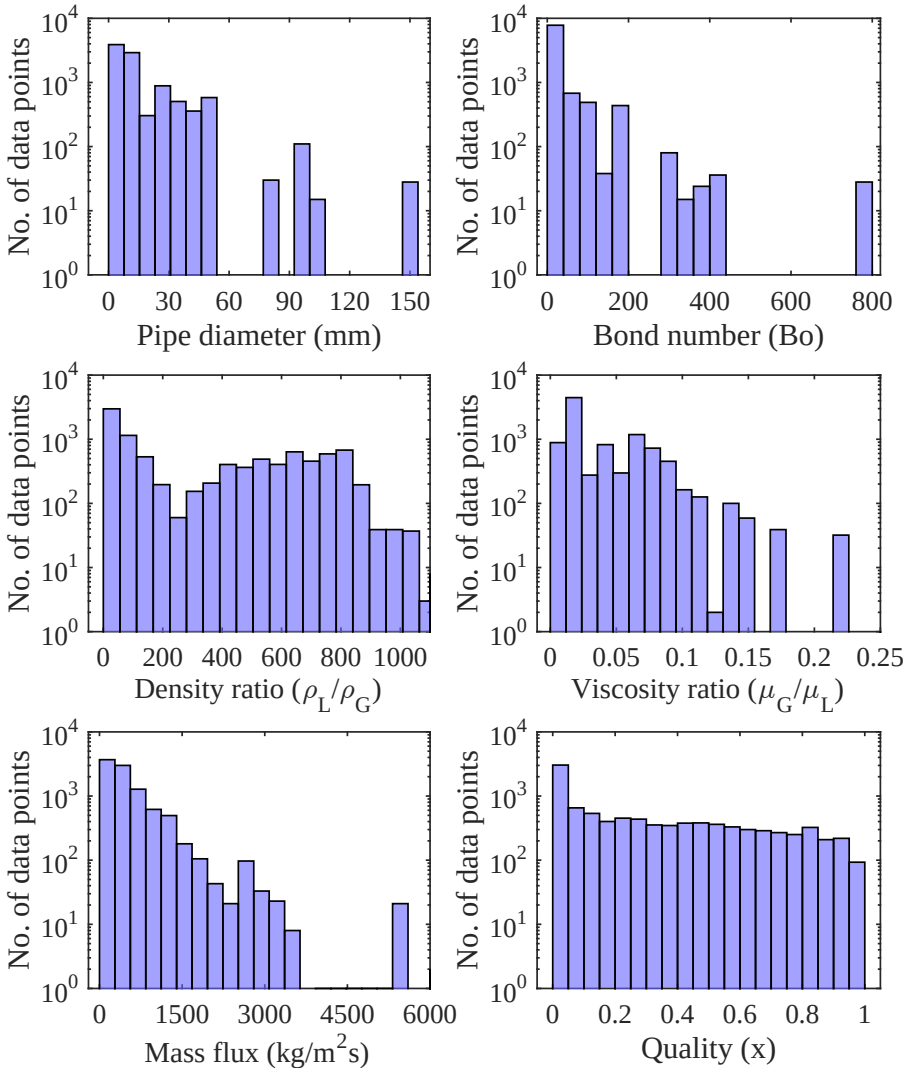

Figure 6.1: Distribution of experimental data bank (9623 data points) used for development of the proposed correlation.

The experimental data in vertical upward two phase flow consists of that measured at OSU (307 data points) and 11 data sources available in the literature. This

dataset consists of pipe diameters in a range of 9.5 to 50 mm, mass flux in a range of 5 to 3250 kg/m^{2}s and two phase flow quality in a range of 0.0001 to 0.93. The vertical upward two phase flow data consists of air-water, air-glycerin, air-kersoene, helium-water and Freon 12 vapor-water fluid combinations. The data for upward inclined two phase flow consists of the data measured at OSU (1152 data points air-water fluid combination, $D = 12.5$ mm) as well as the data from Beggs (1972) (190 data points, air-water fluid combination $D = 25.4$ mm) and Mukherjee (1979) (271 data points, air-kerosene fluid combination, $D = 38.1$ mm).

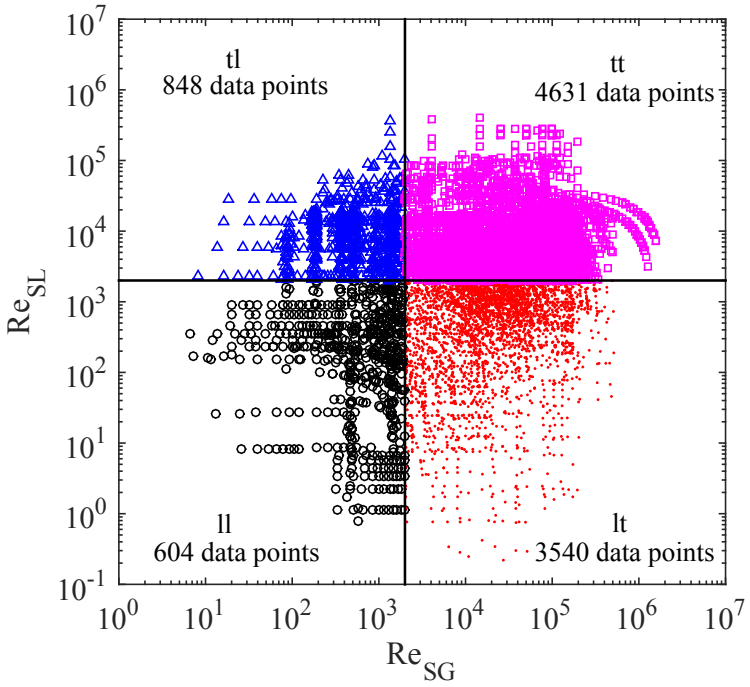

Figure 6.2: Distribution of experimental data in different flow regimes.

The distribution of experimental data at varying flow conditions used for the correlation development in the present study is shown in Figure 6.1. The distribution of hydraulic pipe diameter is such that it occupies micro to macro scale two phase flow ($0.069 \leq D_h \leq 152$ mm) that corresponds to a wide range of Bond numbers (0.0015 to 800). It is seen that the two phase flow quality is fairly distributed over the entire range ($0 < x < 1$) and hence is expected to occupy the entire range of flow patterns typically observed in gas-liquid two phase flow. The experimental data

is also observed to be distributed over a wide range of two phase mixture mass flux. The experimental data base also consists of a wide range of density ratio (ρ_L/ρ_G). The low values of density ratio correspond to high system pressure data such as that for refrigerants (typically for CO_2, propane, ammonia and refrigerants at higher saturation temperature) while high density ratio data consist of air-water, air-glycerin fluid combinations. In addition to the density ratio, a wide range of viscosity ratio (μ_G/μ_L) is also observed. The lower and higher values of (μ_G/μ_L) typically correspond to the air-oil and refrigerants two phase flow data, respectively. Additionally, the distribution of experimental data for four different cases of laminar-laminar (ll), laminar-turbulent (lt), turbulent-laminar (tl) and turbulent-turbulent (tt) two phase flow is shown in Fig. 6.2. From experience it can be said that the laminar-laminar and turbulent-laminar flow regions typically consist slug/plug and bubbly/bubbly-slug flow patterns, respectively. Whereas, the laminar-turbulent and turbulent-turbulent flow regions may consist of wavy slug (intermittent) and annular flow patterns. A brief summary of the range of different two phase flow parameters considered in this work is reported in Table 6.1. Some of the data sources that represent a majority of this data are listed in Appendix.

Table 6.1: Range of experimental data used for the validation of proposed correlation.

Parameter	Range
Hydraulic pipe diameter (mm)	0.069 - 152
Mass flux (kg/m^{2}s)	5 - 6980
Quality	0.00012 - 0.99
Density ratio (ρ_L/ρ_G)	5 - 920
Viscosity ratio (μ_L/μ_G)	10 - 5000
Surface tension (N/m)	0.0019 - 0.075
Pipe orientation (θ)	$0^o \leq \theta \leq +90^o$
Bond number (Bo)	0.0015 - 800
Liquid only Reynolds number (Re_{LO})	1 - 2.85×10^5
Gas only Reynolds number (Re_{GO})	1800 - 1.5×10^7
Viscosity number ($N_{\mu L}$)	0.0008 - 4
Lockhart-Martinelli parameter (X)	0.0018 - 780
Gas volumetric flow fraction (β)	0.005 - 0.99

6.2 Proposed Correlation for Two Phase Frictional Multiplier

A preliminary analysis of the existing two phase pressure drop correlations against the experimental database reported in the previous section showed the Muller-Steinhagen and Heck (1986) and Kim and Mudawar (2012) correlations to perform relatively better than other existing two phase flow models. The proposed correlation to predict the frictional component of the two phase pressure drop is in the form of two phase frictional multiplier (Φ_{LO}^2) and is essentially a modification of Muller-Steinhagen and Heck (1986) correlation. The correlation of Muller-Steinhagen and Heck (1986) is chosen over Kim and Mudawar (2012) since it is more modular in nature and offers more flexibility for the modification. Moreover, Muller-Steinhagen and Heck (1986) yields two phase fricitonal multiplier as a continuous function of two phase flow quality whereas, Kim and Mudawar (2012) shows a discontinuity at the threshold value of single phase Reynolds number that separates laminar flow from turbulent flow. The two phase frictional multiplier Φ_{LO}^2 is the normalized two phase frictional pressure drop based on the assumption that only liquid phase flows through the pipe at an equivalent mass flux as that of the two phase flow mixture. The correlation for Φ_{LO}^2 proposed by Muller-Steinhagen and Heck (1986) is essentially an interpolation between the pressure drop due to the flow of single phase liquid and single phase gas as shown in Eq. (6.1).

$$\left(\frac{dP}{dL}\right) = \left\{\left(\frac{dP}{dL}\right)_{LO} + 2\left[\left(\frac{dP}{dL}\right)_{GO} - \left(\frac{dP}{dL}\right)_{LO}\right]x\right\}(1-x)^{1/3} + \left(\frac{dP}{dL}\right)_{GO} x^3 \quad (6.1)$$

It is based on the assumption that the two phase frictional pressure drop increases linearly with increase in the two phase flow quality approximately up to 0.85 and then decreases to pressure drop due to single phase flow of gas as quality approaches

unity. The exponent of '1/3' and '3' are the empirical constants based on the experimental data base used by Muller-Steinhagen and Heck (1986). The modified form of Muller-Steinhagen and Heck (1986) correlation i.e., the proposed model is expressed in simplified form as shown in Eq. (6.2) where Y is represented by Eq. (6.3). The single phase friction factor for gas (f_{GO}) based on Re_{GO} and liquid (f_{LO}) based on Re_{LO} are calculated using correlation of Churchill (1977) given by Eqs. (6.4) and (6.5). Fanning friction factor correlation of Churchill (1977) is valid for both laminar as well as turbulent flow regimes and accounts for roughness ratio (ϵ/D). In case of rectangular pipe geometry, single phase friction factor for each phase in laminar flow regime is calculated using correlation reported by Shah and London (1978) (see Eq. (6.6)) where $\lambda \geq 1$ is the aspect ratio (width to height ratio) of the rectangular pipe geometry. Note that in case of $\lambda < 1$, Eq. (6.6) is still valid however, the power of aspect ratio (λ) should be changed to a negative value.

$$\Phi_{LO}^2 = \left(\left[(1-x)^{1/3}\left(1 + B_1 x(Y^2-1)\right)\right] + B_2 Y^2 x^3\right)\left(1 + B_3(1-x)^2\right) \tag{6.2}$$

$$Y = \sqrt{\frac{(dP/dL)_{GO}}{(dP/dL)_{LO}}} = \sqrt{\frac{f_{GO}}{f_{LO}}\frac{\rho_L}{\rho_G}} \tag{6.3}$$

For laminar, turbulent flow in circular pipes & turbulent flow in rectangular pipes:

$$f_{jO} = 2\left[\left(\frac{8}{Re_{jO}}\right)^{12} + \frac{1}{(a+b)^{1.5}}\right]^{1/12} \tag{6.4}$$

$$a = \left(2.457 \ln\left[\frac{1}{(7/Re_{jO})^{0.9} + (0.27\epsilon/D)}\right]\right)^{16} \quad \text{and} \quad b = \left(\frac{37530}{Re_{jO}}\right)^{16} \tag{6.5}$$

For laminar flow in rectangular pipes:

$$f_{jO} = \frac{24\left(1 - 1.3553\lambda^1 + 1.9467\lambda^2 - 1.7012\lambda^3 + 0.956\lambda^4 - 0.2537\lambda^5\right)}{Re_{jO}} \tag{6.6}$$

Using the physical from of Muller-Steinhagen and Heck (1986) correlation, the proposed modification to their correlation is introduced in form of parameters B_1 (multiplying factor to the term $Y^2 - 1$), B_2 (multiplying factor to the term Y^2) and B_3 which are modeled as variables as shown in Eqs. (6.7), (6.8) and (6.9), respectively. Simulated trends of original Muller-Steinhagen and Heck (1986) correlation reveals that the parameters B_1 and B_2 control slope of Φ_{LO}^2 vs. x for lower and higher values of quality, respectively. Whereas, parameter B_3 simply acts as a multiplier to Φ_{LO}^2 that modifies the overall value of two phase pressure drop as a function of pipe orientation. As expressed by Eq. (6.7), the parameter B_1 is modeled as a function of pipe diameter (D), fluid properties (ρ_L, ρ_G, μ_L and σ) and the two phase flow quality (x). The effect of these two phase flow variables on B_1 and hence Φ_{LO}^2 is accounted in form of non-dimensional numbers such as Bond number (Bo) and Viscosity number ($N_{\mu L}$). The non-dimensional numbers Bo and $N_{\mu L}$ are expressed by Eqs. (6.14) and (6.15), respectively. The variables Π_1, Π_2 and Π_3 used in parameter B_1 are expressed by Eqs. (6.10), (6.11) and (6.12), respectively. Parameter B_2 is modeled as a function of the density ratio (ρ_G/ρ_L) and is found to vary in a range of 0.5 to 1.0. As shown in Eq. (6.9), parameter B_3 is modeled as a function of pipe orientation such that its value varies in a range of 0 to 0.3. Based on the experimental data, the two different equations (of the form $y = ax^b + c$) are chosen for near horizontal and steeper pipe inclinations in the upward direction. Note that there is a good agreement (within 1%) between the extrapolated values of B_3 for two cases of $0^o \leq \theta \leq +20^o$ ($B_3 = 0.299$) and $+20^o < \theta \leq +90^o$ ($B_3 = 0.297$). The term $(1 - x)^2$ used in conjunction of B_3 ensures that the effect of C_3 on the predicted Φ_{LO}^2 is weighted such that it gradually decreases with increase in the two phase flow quality or alternatively as the flow patterns become inertia driven in nature and hence relatively insensitive

to the change in the pipe orientation.

$$B_1 = [0.85 + 1.703\,(1 - \exp(-6.25\,\xi \times Bo))] \times \Pi_1\Pi_2\Pi_3 \tag{6.7}$$

$$B_2 = 1 - \sqrt{\rho_G/\rho_L} \tag{6.8}$$

$$B_3 = \begin{cases} -0.3(1+\sin\theta)^{-16.25} + 0.3 & : 0^o \leq \theta \leq +20^o \\ -0.012(1+\sin\theta)^{4.1} + 0.34 & : +20^o < \theta + 90^o \end{cases} \tag{6.9}$$

$$\Pi_1 = \Big(1 + 2.65\left[1 - \exp(-1.677 N_{\mu L})\right]\Big) \tag{6.10}$$

$$\Pi_2 = \begin{cases} 0.55 & : \xi \leq 1.0,\ Bo \geq 1 \\ 1 & : \xi > 1.0,\ Bo < 1 \end{cases} \tag{6.11}$$

$$\Pi_3 = \left[1 + 0.005\left(\frac{1-x}{x}\right)\right]^{0.5} \tag{6.12}$$

$$\xi = 2.5\sqrt{\frac{\rho_L}{\rho_{ref}}}\left(\frac{\mu_G}{\mu_L}\right)^{0.25} \tag{6.13}$$

$$Bo = \frac{g(\rho_L - \rho_G)(D_h/2)^2}{\sigma} \tag{6.14}$$

$$N_{\mu L} = \frac{\mu_L}{\left[\rho_L \sigma \sqrt{\dfrac{\sigma}{g(\rho_L - \rho_G)}}\right]^{0.5}} \tag{6.15}$$

Getting back to parameter B_1, let's look at its physical significance and need for including parameters Π_1, Π_2 and Π_3. The parameter B_1 is modeled as a variable such that it is sensitive to the increase in Bond number in the vicinity of $Bo \approx 1$ ($0.7 < Bo < 1.3$) and thereafter follows a saturation trend. Note that this threshold value of Bo after which saturated trend ensues is subject to a small change with

variation in property group ξ. The inclusion of Bond number accounts for the balance between body and surface tension forces on the two phase frictional multiplier. Chen et al. (2001) reported that for small diameter pipes, effect of surface tension on two phase flow is more significant compared to the effect of gravity. Accordingly, for $Bo < 1$ the surface tension effects are prominent in comparison to the body forces whereas for $Bo > 1$ the effect of surface tension on the two phase flow is inconsequential. The variation of B_1 as a function of Bo for $\xi = 1.0$ is illustrated in Fig. 6.3. The experimental data presented in this figure is taken from the data bank for the two phase flow of refrigerants reported in Table 6.1 such that the corresponding value of B_1 for a fixed Bo gave minimum mean relative deviation. In particular, refrigerant data is chosen for plotting B_1 vs. Bo since it showed a large variation in Bo.

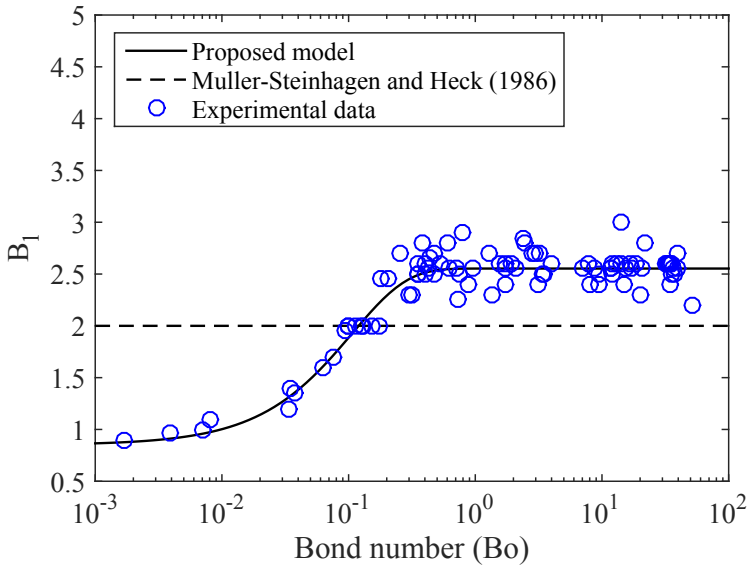

Figure 6.3: Variation of B_1 as a function of Bond number.

The data bank generated in this study shows that the condition of $Bo < 1$ corresponds to the pipe diameters in a range of 0.069 - 4.5 mm and consists of refrigerants (1822 data points) and well as air-water (645 data points) fluid combinations. According to the observations of Kandlikar (2002), approximately this range of pipe

diameter ($0 < D \leq 3$ mm) represents the micro to mini scale two phase flow phenomenon. The variable B_1 as a function of Bo increases the value of Φ_{LO}^2 with increase in the pipe diameter (due to increase in the gas-liquid interfacial area). Recently, Li and Wu (2010) and Venkatesan et al. (2011) also analyzed the two phase frictional pressure drop as a function of Bo and concluded that the Chisholm (1973) parameter C used in Lockhart and Martinelli (1949) correlation could be modeled as an increasing function of Bond number for $Bo \leq 1$. Two phase flow literature also reports the work of Chen et al. (2001), Hwang and Kim (2006) and Zhang et al. (2010) that models the two phase frictional multiplier as a function of Bo. Note that the Bond number defined in the present work uses pipe radius ($D/2$) as a length scale rather than the pipe diameter used by other correlations in two phase flow literature. The use of pipe radius or pipe diameter as a length scale is a matter of choice for a non-dimensional number. Based on the experimental data, it is found that the use of pipe radius instead of pipe diameter in the definition of Bond number extends the range of pipe diameters to the upper limit of 4.5 mm (close enough to the upper limit of mini channels diameter $\approx$ 3 mm suggested by Kandlikar (2002)) that could be classified in terms of $Bo \leq 1$. Regardless of the choice of length scale in definition of Bo, the important consideration here is that for micro to mini scale two phase flow, the two phase frictional pressure drop depends on the Bond number. It must also be mentioned that the physical form of the Bond number is comparable to that of Laplace number (La) and the Confinement number (N_{conf}) typically used in models developed for boiling two phase flows in miniaturized systems.

Variable B_1 also accounts for the effect of liquid dynamic viscosity through parameter Π_1 which is modeled as a function of Viscosity number ($N_{\mu L}$). Increase in liquid phase viscosity increases the shear in the liquid phase and hence increases the two phase frictional multiplier and consequently the two phase pressure drop. Based

on the experimental data used in this work, a correction factor to account for the effect of liquid viscosity on Φ_{LO}^2 is introduced such that its effect is significant approximately for $N_{\mu L} \geq 0.03$ and for $N_{\mu L} < 0.03, \Pi_1 \approx 1$. This threshold value of 0.03 is chosen based on the experimental data reported in Table 6.1. Similar type of threshold value ($N_{\mu L} = 0.06$), however in context of annular flow and liquid entrainment is provided by Ishii and Grolmes (1975), to identify the influence of liquid phase dynamic viscosity on two phase flow.

The parameter Π_2 switches between a constant value of 0.55 and 1.0 for two different cases based on Bo and ξ as shown in Eq. (6.11). A preliminary analysis of the experimental data showed that in comparison to liquid refrigerant and its vapor; data for air-water, air-oil, air-kerosene and air-glycerin fluid combinations is over predicted (parallel shift) while using Eq. (6.7). To reduce the magnitude of this over prediction, use of multiplying factor less than unity (0.55 in this case) is found to give the best fit. Using the property group of ξ defined by Eq. (6.13), these fluid combinations could be separated from the refrigerant data. Note that ρ_{ref} used in definition of ξ is reference value of the density equal to the density of liquid water taken as 1000 kg/m^3. Distribution of experimental data as a function of ξ for different fluid combinations is shown in Fig. 6.4. About 75% of the data for these fluids combinations (non-refrigerants) consists of $Bo > 1$ where the value of B_1 is in the vicinity of 2.55 (without using Π_1 and Π_3) where as for 25% of data with $Bo < 1$, parameter B_1 is in a range of 1 to 2.55. The use of multiplying factor $\Pi = 0.55$ is deemed necessary only for the case of $Bo > 1$. For $Bo < 1$ even if $\xi < 1$, use of multiplying factor is not required since for such a case, two phase flow is influenced by the surface tension force rather than the body force characterized by the fluid density and acceleration due to gravity. A comparison between measured and predicted values of two phase pressure drop show that for $Bo < 1$ use of $\Pi_2 = 0.55$ would predict only 34% of data points within $\pm 30\%$ error bands instead of 67% of

data points with $\Pi_2 = 1.0$. Similarly, for $Bo > 1$ use of $\Pi_2 = 1.0$ would predict only 31% of data points within ±30% error bands instead of 83% of data points with $\Pi_2 = 0.55$. Thus, the use of Π_2 in case of $\xi < 1$ is justified only for $Bo > 1$.

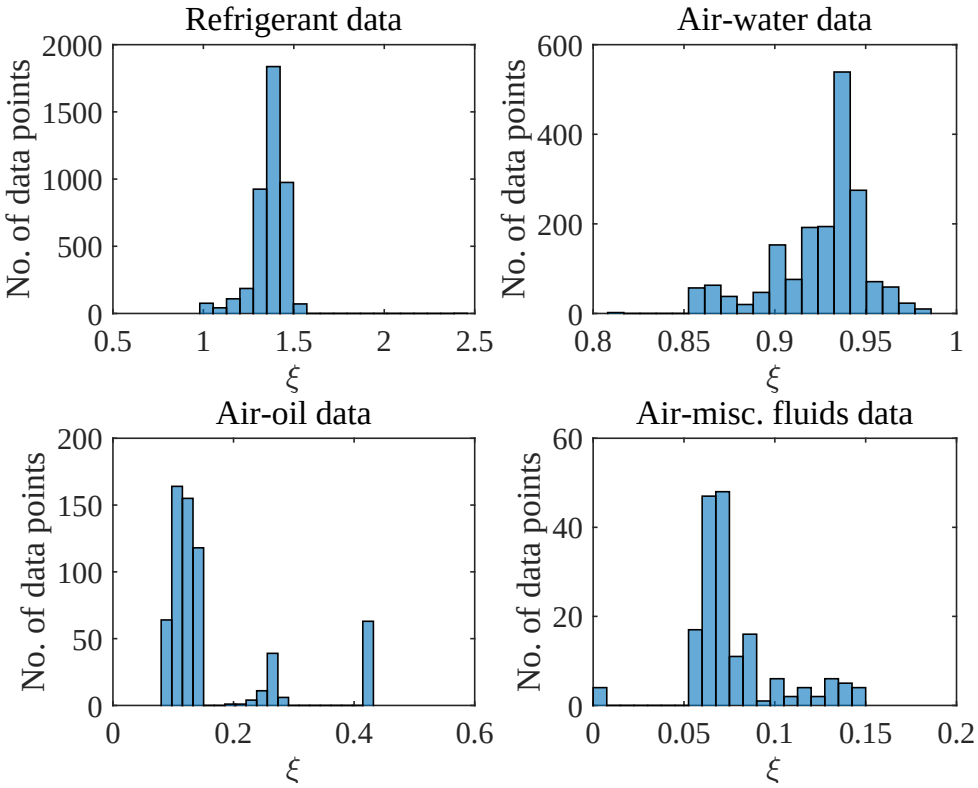

Figure 6.4: Distribution of pressure drop data for varying ξ values.

Finally, the variable Π_3 as a function of two phase flow quality (x) is modeled such that for small values of x, $\Pi_3 > 1$ whereas for $x \to 1$, $\Pi_3 \cong 1$. The small values of x typically correspond to bubbly and slug flow patterns with liquid and gas phase in laminar-laminar or turbulent-laminar flow regimes. Thus, the predicted values of two phase pressure drop are sensitive to Π_3 only in these flow regimes without affecting the predicted data in laminar-turbulent and turbulent-turbulent flow regimes. With the use of Π_3, the proposed correlation can predict 74% of data points within ±30% error bands whereas without considering Π_3, the proposed correlation can predict only 63% of data points within ±30% error bands. Note that these parameters Π_1, Π_2 and Π_3 are non-dimensional and have a physical form such that for the two phase flow of

refrigerants where usually $N_{\mu L} << 1$, $\xi > 1$ we get $\Pi_1 = 1$ and $\Pi_2 = 1$. Moreover, two phase flow of refrigerants consists of high system pressures with a high ratio of gas to liquid phase density (ρ_G/ρ_L) and hence results into relatively higher values of two phase flow quality such that $\Pi_3 \approx 1$. Thus, for two phase flow of refrigerants, the parameter B_1 can be modeled as a function of Bo and ξ as described by Eq. (6.7).

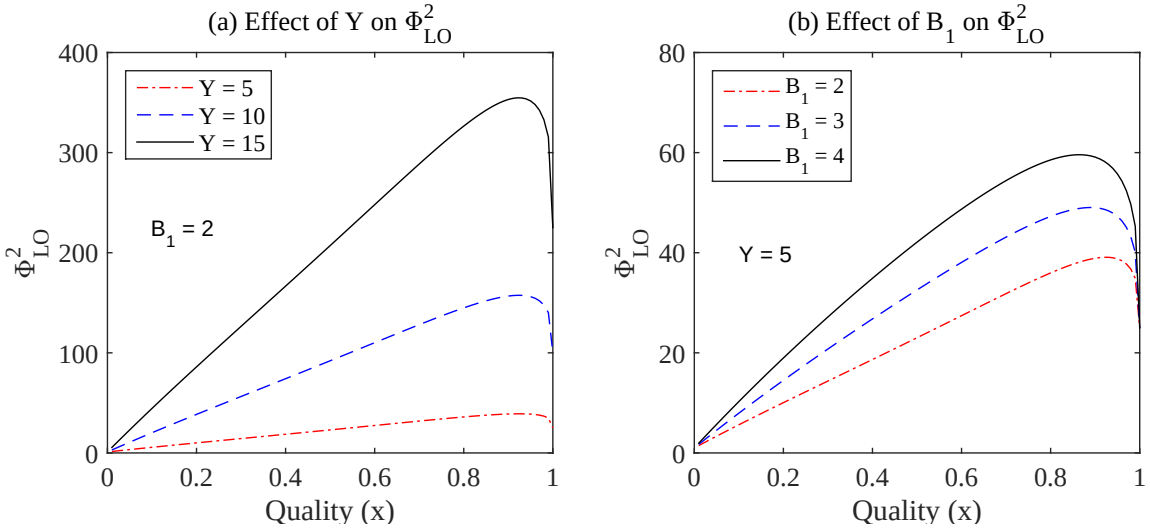

Figure 6.5: Variation of Φ^2_{LO} as a function of quality (x) for different values of Y.

The simulated trends of the two phase frictional multiplier (Φ^2_{LO}) defined by Eq. (6.2) is shown in Fig. 6.5. It is evident that Φ^2_{LO} increases with increase in the Y for fixed B_1 and the slope (sensitivity) of Φ^2_{LO} as a function of quality (x) depends on the magnitude of Y. Similarly, for a fixed value of Y, Φ^2_{LO} increases with increase in B_1. From the definition of Y it is clear that the lower values of Y may correspond to the high system pressures (higher values of ρ_G) or high liquid to gas viscosity ratio (embedded in the definition of f_{LO} and f_{GO}) whereas the opposite is true for higher values of Y. Based on the experimental data base it is found that for high ratios of (ρ_G/ρ_L) and (μ_L/μ_G), Y value is approximately in a range of $1 < Y < 5$ whereas for the opposite case, Y value is typically in a range of $5 < Y < 15$. For a fluid with higher liquid dynamic viscosity $(Y < 5)$, Φ^2_{LO} should sharply increase with increase in two phase flow quality. As mentioned earlier, this is achieved through a multiplying

factor Π_1 that increases the value of C_1 as a function of $N_{\mu L}$ and hence Φ_{LO}^2 and consequently the two phase frictional pressure drop. What follows is the validation of the proposed correlation against a range of experimental data (listed in Table 6.1) and two phase flow models available in the literature.

6.3 Performance Assessment of the Proposed Correlation

The performance of the proposed correlation is assessed against the experimental data bank summarized in Table 6.1 and the pressure drop correlations available in the two phase flow literature (reported in Chapter II). A preliminary analysis of the two phase pressure drop correlations showed that in general, compared to the homogeneous flow models, the correlations based on the separated flow model possess a better prediction capability over a wide range of pipe diameters. Thus, most of the correlations considered here for the purpose of comparison are based on the separated flow models. Nevertheless, acknowledging the fact that the homogeneous flow models tend to approximate the two phase flow in miniature systems, some of the top performing homogeneous flow model based correlations such as Beattie and Whalley (1982), Ciccihitti et al. (1960), Dukler et al. (1964), McAdams et al. (1942) and Shannak (2008) are also used to validate the accuracy of the proposed correlation. These correlations based on homogeneous flow models are also used for a comparison purpose in the recent modeling work of Xu and Fang (2012) and Kim and Mudawar (2012). Based on the accuracy of these correlations for horizontal two phase flow, and considering the recommendations of recent studies such as Xu and Fang (2012) and Kim and Mudawar (2012), following correlations of Muller-Steinhagen and Heck (1986), Lockhart and Martinelli (1949), Chisholm (1973), Friedel (1979), Chen et al. (2001), Li and Wu (2010), Lee and Lee (2001), Hwang and Kim (2006), Sun and Mishima (2009), Mishima and Hibiki (1996), Kim and Mudawar (2012) are used to

evaluate and compare the performance of the proposed correlation. Although, these correlations are not developed for the wide range of data listed in Table 6.1, the accuracy of these correlations is tested against the entire data set to check their perform outside the range of their application. The physical form of these correlations is reported in Chapter II. The performance of the proposed model and other two phase flow correlations is evaluated based on the statistical parameters such as mean relative deviation (MRD) and mean absolute relative deviation (MARD) defined by Eqs. (6.16) and (6.17). Note that achieving a low value of MRD or MARD is not the absolute measure to gauge the accuracy of any correlation since these parameters (MRD and MARD) are strongly influenced by the number of data points and distribution of the error. It is also important that these correlations be able to predict maximum number of data points within certain error bands. Accordingly, the accuracy of these correlations is also compared based on the percentage of data points predicted within $\pm 30\%$ (N_{30}) and $\pm 50\%$ (N_{50}) error bands. Considering the practical difficulty in modeling of two phase pressure drop (as a function of several two phase flow variables), use of higher error bands up to $\pm 50\%$ in the prediction of two phase pressure drop is considered as acceptable and has become a norm in the two phase flow literature. To check the goodness of the proposed correlation, its outcome is compared against the entire dataset arranged in different forms that may correspond to several different two phase flow conditions.

$$\text{MRD} = \frac{1}{N}\sum_{1}^{N}\frac{(dP/dL)_{\text{exp}} - (dP/dL)_{\text{pred}}}{(dP/dL)_{\text{exp}}} \times 100 \tag{6.16}$$

$$\text{MARD} = \frac{1}{N}\sum_{1}^{N}\frac{|(dP/dL)_{\text{exp}} - (dP/dL)_{\text{pred}}|}{(dP/dL)_{\text{exp}}} \times 100 \tag{6.17}$$

6.3.1 Performance Assessment of Frictional Pressure Drop Models in Horizontal Two Phase Flow

For different flow conditions in horizontal two phase flow, the comparison of the performance of the proposed correlation against the experimental data and other two phase flow models is presented below in Tables 6.2 to 6.5. Note that these correlations are arranged in order of their physical form i.e., those based on Φ_{LO}^2, Φ_L^2 and homogeneous flow models. To check the accuracy of different correlations for inertia driven vs. non inertia driven flows, the entire range of experimentally measured data is divided in terms of Lockhart-Martinelli parameter such that for $X < 1$ two phase flow can be considered to be inertia driven such that $(dP/dL)_G > (dP/dL)_L$ while the opposite is true for $X > 1$. Table 6.2 shows that for both $X \leq 1$ and $X > 1$, the proposed correlation gives best accuracy and predicts more than 70% and 90% of data points within $\pm 30\%$ (N_{30}) and $\pm 50\%$ (N_{50}) error bands, respectively. Compared to all other correlations, Muller-Steinhagen and Heck (1986) and Kim and Mudawar (2012) could be considered among top three performing correlations. Overall, the homogeneous flow models are found to perform slightly better for $X > 1$ (non-inertia driven region). Among all homogeneous flow models, Shannak (2008) is found to be relatively good performing correlation.

Since the parameter B_1 is modeled as a function of Bond number it is also of interest to see how the proposed correlation performs for the two cases of $Bo \leq 1$ and $Bo > 1$ such that the condition of $Bo \leq 1$ corresponds to mini and micro scale two phase flow (with dominant surface tension forces) while the condition of $Bo > 1$ corresponds to macro scale two phase flow (with dominant body forces). As mentioned earlier, pipe diameters in a range of 0.069 to 4.5 mm (for both refrigerants and air-water fluid combination) satisfied the condition of $Bo \leq 1$. As shown in Table 6.3, for the case of $Bo \leq 1$,the proposed correlation predicts the two phase pressure drop with

Table 6.2: Performance analysis of two phase pressure drop correlations for different ranges of Lockhart-Martinelli parameter (horizontal flow, 7074 data points).

Lockhart-Martinelli parameter	$0.001 < X \leq 1$				$1 < X < 1000$			
	(4913 data points)				(2161 data points)			
Correlation	(1)	(2)	N_{30}	N_{50}	(1)	(2)	N_{30}	N_{50}
Proposed correlation	-3	24	73	93	5	24	73	92
Muller-Steinhagen and Heck (1986)	3	27	63	88	13	27	65	89
Chisholm (1973)	-30	49	59	70	-23	48	55	78
Friedel (1979)	-93	112	42	63	-102	108	39	58
Chen et al. (2001)	-42	66	47	68	-56	79	35	52
Xu and Fang (2012)	-91	112	51	70	-116	137	55	66
Lockhart and Martinelli (1949)	-25	47	50	70	-28	48	58	70
Sun and Mishima (2009)	23	31	57	83	19	28	60	86
Mishima and Hibiki (1996)	13	42	53	77	19	43	56	78
Li and Wu (2010)	35	52	34	53	30	46	36	56
Lee and Lee (2001)	-40	60	49	67	-22	65	37	60
Kim and Mudawar (2012)	-1	28	68	86	-6	29	64	84
Beattie and Whalley (1982)	34	38	46	74	-18	46.5	52	69
Ciccihitti et al. (1960)	-59	98	47	76	-269	288	46	69
Dukler et al. (1964)	41	43	33	68	30	33	44	84
McAdams et al. (1942)	34	40	41	68	28	45	48	69
Shannak (2008)	19	33	57	81	6	36	55	78

(1) = MRD, (2) = MARD.

MRD of 3.8%, MARD of 24% and is capable of predicting 69% and 92% of data points within ±30% (N_{30}) and ±50% (N_{50}) error bands, respectively. Similar performance is given by Kim and Mudawar (2012) correlation that is essentially developed for small diameter pipes ($D \leq 6.2$ mm). Correlation of Li and Wu (2010) is developed for small diameter pipes in terms of Bond number (for $Bo \leq 11$) however, their correlation predicts only 50% of data within ±30% error bands and has a relatively higher MARD of 36.8%. Among homogeneous flow models, correlation of Shannak (2008) is found to be the best performing correlation that predicts 64% and 89% of data points within ±30% and ±50% error bands, respectively. For the case of $Bo > 1$, proposed correlation gives the highest accuracy by predicting 75% and 93% of the data points within ±30% and ±50% error bands, respectively. Among models

based on Φ_L^2 methods, Kim and Mudawar (2012) is consistently the best performing correlation with a MRD of -7% and MARD of 30%. For $Bo > 1$, a drop in accuracy of Kim and Mudawar (2012) is anticipated since most of the data (3330 data points) in this range consists of pipe diameters greater than 6.5 mm and the Kim and Mudawar (2012) correlation is developed for pipe diameters only up to 6.2 mm. Yet, their correlation gives better accuracy than other correlations based on Φ_L^2 method.

Table 6.3: Performance analysis of two phase pressure drop correlations for different ranges of Bond number.

Bond number range	$Bo \leq 1$				$Bo > 1$			
	(2467 data points)				(4607 data points)			
Correlation	(1)	(2)	N_{30}	N_{50}	(1)	(2)	N_{30}	N_{50}
Proposed correlation	3.8	24	69	92	-3	24	75	93
Muller-Steinhagen and Heck (1986)	5	26	64	84	8	27	64	91
Chisholm (1973)	-32	52	45	66	-25	44	54	78
Friedel (1979)	-59	80	37	58	-63	90	49	68
Chen et al. (2001)	-34	49	46	68	-63	82	41	57
Xu and Fang (2012)	-107	181	27	47	-2	28	66	87
Lockhart and Martinelli (1949)	-31	53	45	62	-25	45	58	79
Sun and Mishima (2009)	20	29	57	83	21	31	53	88
Mishima and Hibiki (1996)	18	32.8	48	80	-33	45	56	78
Li and Wu (2010)	-4	36.8	50	77	53	57	27	43
Lee and Lee (2001)	-19	52	37	59	-46	69	38	59
Kim and Mudawar (2012)	7	25	69	90	-7	30	66	88
Beattie and Whalley (1982)	24	35	45	79	13	43	39	69
Ciccihitti et al. (1960)	-50	86	48	74	-168	199	45	69
Dukler et al. (1964)	39	41	48	71	27	39	41	75
McAdams et al. (1942)	24	38	49	74	28	43	43	63
Shannak (2008)	4	28	64	89	21	37	51	78

(1) = MRD, (2) = MARD.

A quick comparison between the proposed correlation, Muller-Steinhagen and Heck (1986) and Kim and Mudawar (2012) for two different cases of $Bo \leq 1$ and $Bo > 1$ is shown in Fig. 6.6. For $Bo = 0.002$, the proposed model yields parameter $B_1 \approxeq 1$ compared to $B_1 = 2$ given by Muller-Steinhagen and Heck (1986). Consequently, Muller-Steinhagen and Heck (1986) over predicts the two phase pressure drop data.

For the second case of $Bo = 50$, the proposed model yields parameter $B_1 = 2.55$ compared to $B_1 = 2$ given by Muller-Steinhagen and Heck (1986) and as a result their correlation is found to under predict the two phase pressure drop. Since, the Kim and Mudawar (2012) correlation is developed for small diameter pipes, it predicts the two phase pressure drop data correctly for $Bo \leq 1$ ($D = 0.5$ mm) however, tend to loose its accuracy for $Bo = 50$ ($D = 14$ mm). A careful observation in Fig. 6.6 (a) shows a sharp change in the trend predicted by Kim and Mudawar (2012) correlation. It appears that this shift is due to multiple (two) solutions for C value (Chisholm parameter) predicted by their correlation for the threshold value of $Re_{SL} = 2000$ and $Re_{SG} = 2000$. Thus there appears to be a lack of continuity in the trends of Kim and Mudawar (2012) correlation for a smooth variation in single phase Reynolds number from laminar to turbulent.

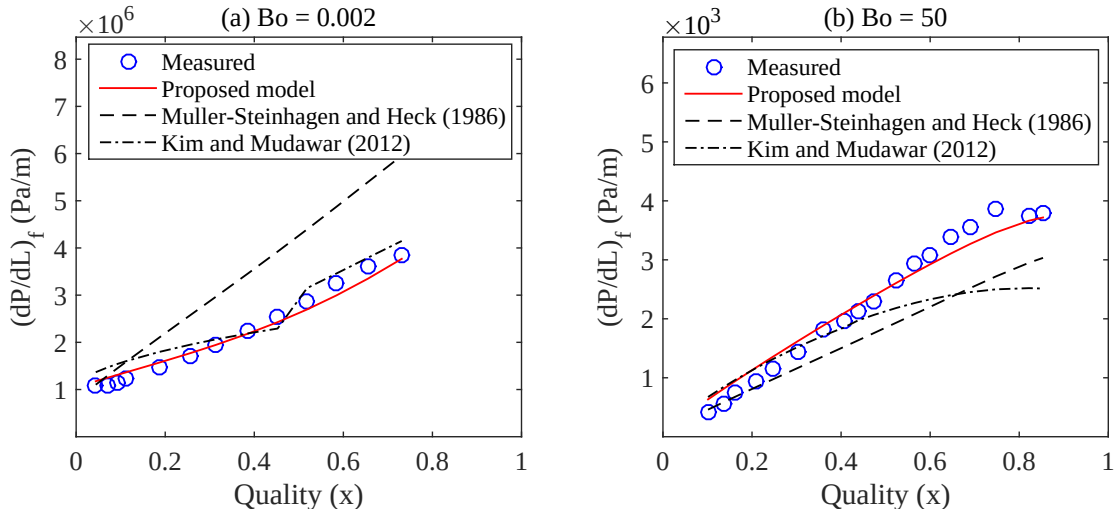

Figure 6.6: Comparison between two phase flow models for different values of Bond numbers at $G = 500$ kg/m^{2}s.

Another important consideration to validate the accuracy of the proposed correlation is to check its performance separately for circular (6052 data points) and non-circular (1022 data points) pipe geometries. With the exception of the data of Wongwises and Pipathttakul (2006) (annular geometry), all the data in non-circular

pipe geometries belonged to rectangular channels. As reported in Table 6.4, for circular channels, proposed correlation gives the best accuracy with a MRD of 2% and predicts 71% and 92% of data points within ±30% (N_{30}) and ±50% (N_{50}) error bands, respectively. In comparison to this, Muller-Steinhagen and Heck (1986) correlation can predict only 62% of data within ±30% error bands with MRD of 11%. Among the correlations based on Φ_L^2 method, Kim and Mudawar (2012) correlation gives the best accuracy with a small MRD of -1%. For non-circular pipe geometries, Kim and Mudawar (2012) gives the best accuracy by predicting 80% of data points within ±30% error bands. In comparison to this the proposed correlation predicts 75% of data within ±30% error bands. However, for a more relaxed criterion of ±50% error bands, the accuracy of the two correlations is comparable. Interestingly, albeit, Lee and Lee (2001) correlation is developed for narrow rectangular channels, it is not among the top performing correlations for the non-circular pipe geometries. Their correlation predicts only 67% of data points within ±30% error bands. This is possibly because their correlation is based on a very limited range of experimental data and hence cannot accommodate a wide variation in pipe geometries and fluid properties.

The performance of the proposed as well as other two phase flow correlations is also assessed against the experimental data categorized in terms of property group ξ defined by Eq. (6.13). As mentioned earlier, data corresponding to $\xi \leq 1$ consists of air-water, air-oil, air-glycerin and air-kerosene fluid combinations whereas the condition of $\xi > 1$ consists of refrigerant two phase flow data. As shown in Table 6.5, for $\xi \leq 1$, the proposed correlation gives best accuracy with a MRD of 3% and predicts 79% and 94% of data points within ±30% and ±50% error bands, respectively. In comparison to this, Muller-Steinhagen and Heck (1986) and Kim and Mudawar (2012) can only predict 64% and 63% of data points, respectively within ±30% error bands. Note that Kim and Mudawar (2012) correlation is developed for small diameter pipes ($D \leq 6.2$ mm) and hence is not expected to give very good accuracy for $\xi \leq 1$ since

Table 6.4: Performance analysis of two phase pressure drop correlations for different pipe geometries.

Pipe geometry	Circular				Non-circular			
	(6052 data points)				(1022 data points)			
Correlation	(1)	(2)	N_{30}	N_{50}	(1)	(2)	N_{30}	N_{50}
Proposed correlation	2	24	71	92	-7	22	75	94
Muller-Steinhagen and Heck (1986)	11	27	62	89	-19	27	68	84
Chisholm (1973)	-21	43	54	75	-79	85	30	47
Friedel (1979)	-112	120	43	63	-191	190	16	31
Chen et al. (2001)	-56	75	41	58	-43	46	47	64
Xu and Fang (2012)	-46	67	59	78	-660	660	10	27
Lockhart and Martinelli (1949)	-23	47	53	72	-44	54	43	62
Sun and Mishima (2009)	24	32	50	82	10	22	75	94
Mishima and Hibiki (1996)	-17	44.5	51	73	-1	27	70	90
Li and Wu (2010)	42	51	34	53	-19	41	50	71
Lee and Lee (2001)	37	65	37	58	-15	41	67	84
Kim and Mudawar (2012)	-1	29	64	86	-11	20	80	93
Beattie and Whalley (1982)	18	41	39	70	-99	113	55	93
Ciccihitti et al. (1960)	-129	163	45	72	15	29	52	63
Dukler et al. (1964)	39	41	28	66	29	32	40	92
McAdams et al. (1942)	34	44	33	63	19	29	54	95
Shannak (2008)	17	35	46	77	-1	27	72	89

(1) = MRD, (2) = MARD.

a majority of the data satisfying this condition consists of large diameter pipes. For $\xi \leq 1$ and $D > 6.2$ mm, Kim and Mudawar (2012) is found to consistently over predict two phase frictional pressure drop. Predictions of the proposed correlation for different values of ξ and different density ratios for a constant mass flux ($G = 300$ kg/m^{2}s) and fixed pipe diameter ($D = 1$ mm) is shown in Fig. 6.7. For the entire range of two phase flow quality, the proposed correlation correctly predicts the two phase frictional pressure drop regardless of the variation of phase density ratio or alternatively the system pressure.

Finally, for the refrigerant two phase flow, the accuracy of the proposed correlation is also validated against the adiabatic (3104 data points) and evaporating (1118 data points) two phase flow conditions. Table 6.6 reports that for adiabatic two phase

Table 6.5: Performance analysis of two phase pressure drop correlations for different values of ξ.

Range of ξ	$\xi \leq 1$				$\xi > 1$			
	(2852 data points)				(4222 data points)			
Correlation	(1)	(2)	N_{30}	N_{50}	(1)	(2)	N_{30}	N_{50}
Proposed correlation	3	22	79	94	-2	26	69	91
Muller-Steinhagen and Heck (1986)	-1	28	64	88	11	27	63	88
Chisholm (1973)	-26	47	58	75	-32	50	46	68
Friedel (1979)	-244	246	24	40	-42	55	49	70
Chen et al. (2001)	-92	111	28	43	-29	43	52	70
Xu and Fang (2012)	-101	116	49	64	-158	176	54	72
Lockhart and Martinelli (1949)	-1	29	63	83	-42	60	44	61
Sun and Mishima (2009)	23	30	63	83	20	32	53	82
Mishima and Hibiki (1996)	-20	39	60	80	-11	44	49	73
Li and Wu (2010)	42	50	38	57	27	49	28	48
Lee and Lee (2001)	2	48	40	70	-59	71	37	54
Kim and Mudawar (2012)	-11	29	63	81	3	27	66	89
Beattie and Whalley (1982)	-7	39	56	78	35	40	31	69
Ciccihitti et al. (1960)	-327	334	38	50	12	35	52	84
Dukler et al. (1964)	28	31	48	88	44	46	17	58
McAdams et al. (1942)	20	40	52	73	40	42	24	65
Shannak (2008)	3	35	58	79	23	33	47	80

(1) = MRD, (2) = MARD.

flow, the proposed correlation predicts 91% of data points within ±50% error bands with a MRD of -1% and MARD of 26%. For evaporating two phase flow, Xu and Fang (2012) exhibits best performance with a MRD of 4% and predicts 74% and 96% of data points within ±30% and ±50% error bands, respectively. Whereas, the proposed correlation predicts 71% and 95% of data points within ±30% and ±50% error bands, respectively. The slightly better accuracy of Xu and Fang (2012) correlation is anticipated since it is developed exclusively for evaporating two phase flow whereas drop in accuracy of Kim and Mudawar (2012) correlation is possibly because it is developed only for adiabatic and condensing two phase flows. To validate the performance of the proposed correlation, its accuracy is further compared against 2651 data points for adiabatic two phase flow of refrigerants and air-water fluid combinations used by

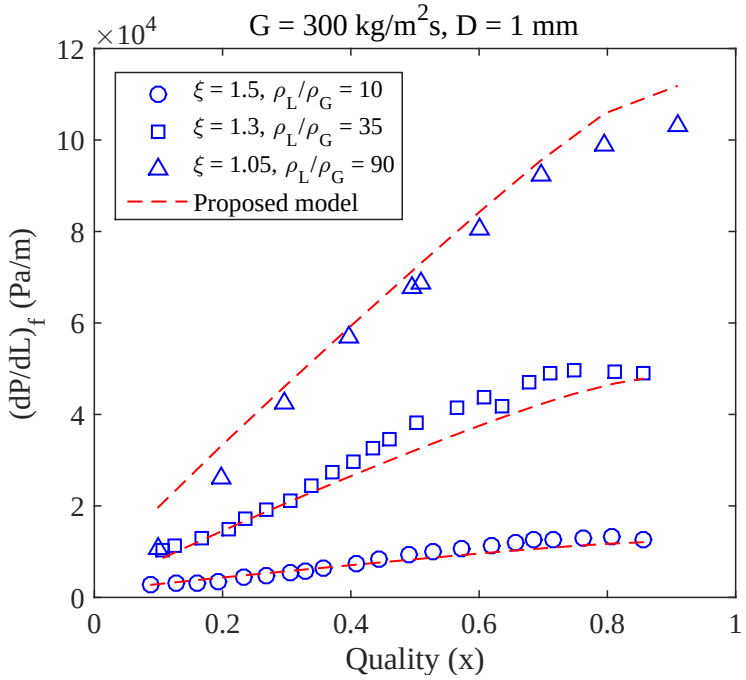

Figure 6.7: Prediction of the proposed correlation against different phase density ratios.

Kim and Mudawar (2012). For these similar data points (obtained from same data sources), the proposed correlation gives comparable performance (73% and 92% of data points within ±30% and ±50% error bands with a MRD of -5% and MARD of 26%) as that of Kim and Mudawar (2012) (74% and 91% of data points within ±30% and ±50% error bands with a MRD of -4% and MARD of 24%). Thus, it appears that drop in accuracy of Kim and Mudawar (2012) correlation occurs for two phase flow in large diameter pipes and evaporating two phase flow.

6.3.2 Performance Assessment of Frictional Pressure Drop Models in Upward Inclined Two Phase Flow

This section presents the performance assessment of two phase pressure drop models against the experimental data in vertical upward (935 data points) and upward inclined (1614 data points) two phase flow. The experimental data in vertical upward

Table 6.6: Performance analysis of two phase pressure drop correlations for adiabatic and evaporating two phase flow of refrigerants.

Type of two phase flow	Adiabatic				Evaporating			
	(3104 data points)				(1118 data points)			
Correlation	(1)	(2)	N_{30}	N_{50}	(1)	(2)	N_{30}	N_{50}
Proposed correlation	-1	26	69	91	4	22	71	95
Muller-Steinhagen and Heck (1986)	7	27	65	87	23	27	56	93
Chisholm (1973)	-34	52	44	66	-25	42	50	73
Friedel (1979)	-53	65	48	69	-15	29	65	84
Chen et al. (2001)	-35	48	54	74	-11	28	70	87
Xu and Fang (2012)	-120	132	47	64	4	21	74	96
Lockhart and Martinelli (1949)	-50	65	43	59	-22	46	47	67
Sun and Mishima (2009)	15	30	58	83	34	36	59	76
Mishima and Hibiki (1996)	-6	43	49	74	-24	43	48	72
Li and Wu (2010)	14	45	36	59	64	65	6	16
Lee and Lee (2001)	-58	71	36	53	-60	72	40	57
Kim and Mudawar (2012)	5.6	27	67	89	13	27	60	90
Beattie and Whalley (1982)	31	38	36	74	45	46	27	55
Ciccihitti et al. (1960)	7	37	53	83	27	31	48	87
Dukler et al. (1964)	41	43	22	64	52	52	25	49
McAdams et al. (1942)	37	40	29	70	48	48	23	50
Shannak (2008)	16	30	54	85	39	40	58	76

(1) = MRD, (2) = MARD.

two phase flow consists of the data measured at Two Phase Flow Lab, OSU as well as the data collected form the two phase flow literature. Note that the data considered for correlation development as well as performance assessment consists of the data not influenced by flow reversal phenomenon during the churn-annular flow transition and data that exhibits decreasing trends of two phase pressure drop with increase in gas flow rates. The region affected by flow reversal and characterized by decreasing trends of two phase pressure drop is identified using expression in terms of non-dimensional superficial phase velocities (see Chapter IV). According to this criterion (Eq. 4.28 and $Fr_{SG} < 1$), 207 data points in vertical and 269 data points in upward pipe inclinations were recognized as the data affected by flow reversal and hence are not considered in this work. For non-horizontal pipe inclinations, the proposed

correlation first predicts the two phase pressure drop that would occur in horizontal flow and then uses a multiplying factor of the form $(1 + B_3(1 - x)^2)$ to correct it for the effect of pipe orientation. The maximum effect (based on the best fit and overall data for each orientation) of pipe orientation on two phase frictional pressure drop is found to be up to 30% and hence the correction factor varies between 1 and 1.3 for upward pipe inclinations.

Table 6.7: Performance analysis of two phase pressure drop correlations for different ranges of Lockhart-Martinelli parameter (vertical upward flow 935 data points).

Lockhart-Martinelli parameter	$0.001 < X \leq 1$				$1 < X < 200$			
	(548 data points)				(387 data points)			
Correlation	(1)	(2)	N_{30}	N_{50}	(1)	(2)	N_{30}	N_{50}
Proposed correlation	9	23	80	95	-4	26	73	94
Muller-Steinhagen and Heck (1986)	-8	19	81	94	14	23	70	93
Chisholm (1973)	-26	33	66	79	3	26	71	83
Friedel (1979)	-40	44	53	68	-44	54	37	59
Chen et al. (2001)	-60	68	32	51	-62	71	21	39
Xu and Fang (2012)	-23	29	64	89	-2	23	74	89
Lockhart and Martinelli (1949)	26	40	39	74	1	25	69	89
Sun and Mishima (2009)	39	43	31	64	28	30	54	86
Mishima and Hibiki (1996)	8	27	70	92	-8	28	67	86
Li and Wu (2010)	64	64	8	23	59	61	27	41
Lee and Lee (2001)	22	41	44	85	-30	46	55	71
Kim and Mudawar (2012)	-2	21	85	91	-12	28	65	88
Beattie and Whalley (1982)	31	36	30	89	8	23	76	93
Ciccihitti et al. (1960)	-33	6	51	82	-2	26	70	86
Dukler et al. (1964)	38	41	37	80	25	28	56	91
McAdams et al. (1942)	20	28	54	92	7	23	72	93
Shannak (2008)	12	28	55	93	-2	25	71	86

(1) = MRD, (2) = MARD.

Unlike the horizontal two phase flow data with wide range of two phase flow conditions, the data in vertical and upward inclined two phase flow mostly consists of air-water fluid combinations and large diameter circular pipes such that $Bo > 1$. Hence, its difficult to make comparisons between two phase pressure drop correlations for different two phase flow conditions based on Bond number, pipe geometry or fluid

physical property group (ξ). Nevertheless, similar to the earlier comparisons, the performance of the proposed correlation in vertical upward pipe inclination is checked against the data categorized in terms of two ranges of X parameter representing the relative magnitudes of single phase pressure drop of liquid and gas phase. From Table 6.7 it is found that for vertical upward flow and $X \leq 1$, Kim and Mudawar (2012) correlation predicts 85% and 91% of data points within ±30% (N_{30}) and ±50% (N_{50}) error bands, respectively. Whereas, the proposed correlation predicts 80% and 95% of data points within ±30% and ±50% error bands, respectively. Muller-Steinhagen and Heck (1986) is also found to give comparable performance. Among homogeneous flow model based correlations, a significant improvement in the prediction accuracy is observed for a more relaxed error criterion of ±50%. For the case of $X > 1$ proposed correlation has a MRD of -4% and predicts 73% of data points within ±30% error bands. Similarly, Muller-Steinhagen and Heck (1986), Chisholm (1973), Xu and Fang (2012), Beattie and Whalley (1982), Ciccihitti et al. (1960), McAdams et al. (1942) and Shannak (2008) are found to predict 70% or more data points within ±30% error bands. Note that the accuracy of Kim and Mudawar (2012) deteriorates for $X > 1$. For air-water data in horizontal flow (large diameter pipes greater than 6.5 mm), Kim and Mudawar (2012) is found to over predict the two phase frictional pressure drop. As such, their correlation possibly predicts the data in vertical pipe correctly since the frictional pressure drop in vertical upward flow is found to be about 10 tp 15% greater than that in horizontal flow.

For the case of upward pipe inclinations, Table 6.8 reports that with $X \leq 1$, proposed correlation predicts 70% and 84% of data points within ±30% (N_{30}) and ±50% (N_{50}) error bands, respectively. Note that although Beattie and Whalley (1982) is found to be the best performing correlation for upward pipe inclinations ($X \leq 1$), their correlation under performs in horizontal and vertical upward two phase flow. In

Table 6.8: Performance analysis of two phase pressure drop correlations for different ranges of Lockhart-Martinelli parameter (upward inclined flow 1614 data points, $0^o > \theta > +90^o$).

Lockhart-Martinelli parameter	$0.01 < X \leq 1$				$1 < X < 300$			
	(416 data points)				(1198 data points)			
Correlation	(1)	(2)	N_{30}	N_{50}	(1)	(2)	N_{30}	N_{50}
Proposed correlation	-10	28	70	84	17	36	73	84
Muller-Steinhagen and Heck (1986)	-23	32	60	76	36	42	47	82
Chisholm (1973)	-98	102	24	47	22	45	63	83
Friedel (1979)	-67	73	26	48	-9	58	52	73
Chen et al. (2001)	-65	77	18	34	-18	66	26	50
Xu and Fang (2012)	-42	51	40	65	23	36	72	82
Lockhart and Martinelli (1949)	-16	39	62	78	21	40	60	79
Sun and Mishima (2009)	15	38	45	85	43	48	25	72
Mishima and Hibiki (1996)	-34	44	58	74	13	39	72	82
Li and Wu (2010)	70	71	3	25	70	71	4	19
Lee and Lee (2001)	-13	47	55	77	-4	46	56	72
Kim and Mudawar (2012)	-30	41	59	75	14	35	74	83
Beattie and Whalley (1982)	11	27	71	89	31	40	61	84
Ciccihitti et al. (1960)	-60	66	26	50	22	38	66	83
Dukler et al. (1964)	25	34	45	87	44	88	34	77
McAdams et al. (1942)	-1	26	74	86	30	39	63	84
Shannak (2008)	-18	31	66	80	22	38	68	84

(1) = MRD, (2) = MARD.

comparison to the horizontal and vertical upward pipe inclinations, Kim and Mudawar (2012) correlation predicts only 59% of data points within ±30% error bands with a MRD of -30%. For the case of $X > 1$, the proposed correlation as well as Xu and Fang (2012) and Kim and Mudawar (2012) give comparable performance by predicting more than 70% and 80% of data points within ±30% and ±50% error bands, respectively. Considering the entire data set of 9623 data points, 5877 and 3746 data points satisfy the condition $X \leq 1$ and $X > 1$, respectively. For the case of $X \leq 1$, the proposed correlation can predict 74% and 93% of data points within ±30% and ±50% error bands, respectively. In comparison to this, Muller-Steinhagen and Heck (1986) predicts 64% and 88% of data points while Kim and Mudawar (2012) predicts 65% and 86% of data points within ±30% and ±50% error bands, respectively. For the

second case of $X > 1$, the proposed correlation predicts 74%, 90%, Muller-Steinhagen and Heck (1986) predicts 60%, 87% and Kim and Mudawar (2012) predicts 69%, 85% of data points within ±30% and ±50% error bands, respectively.

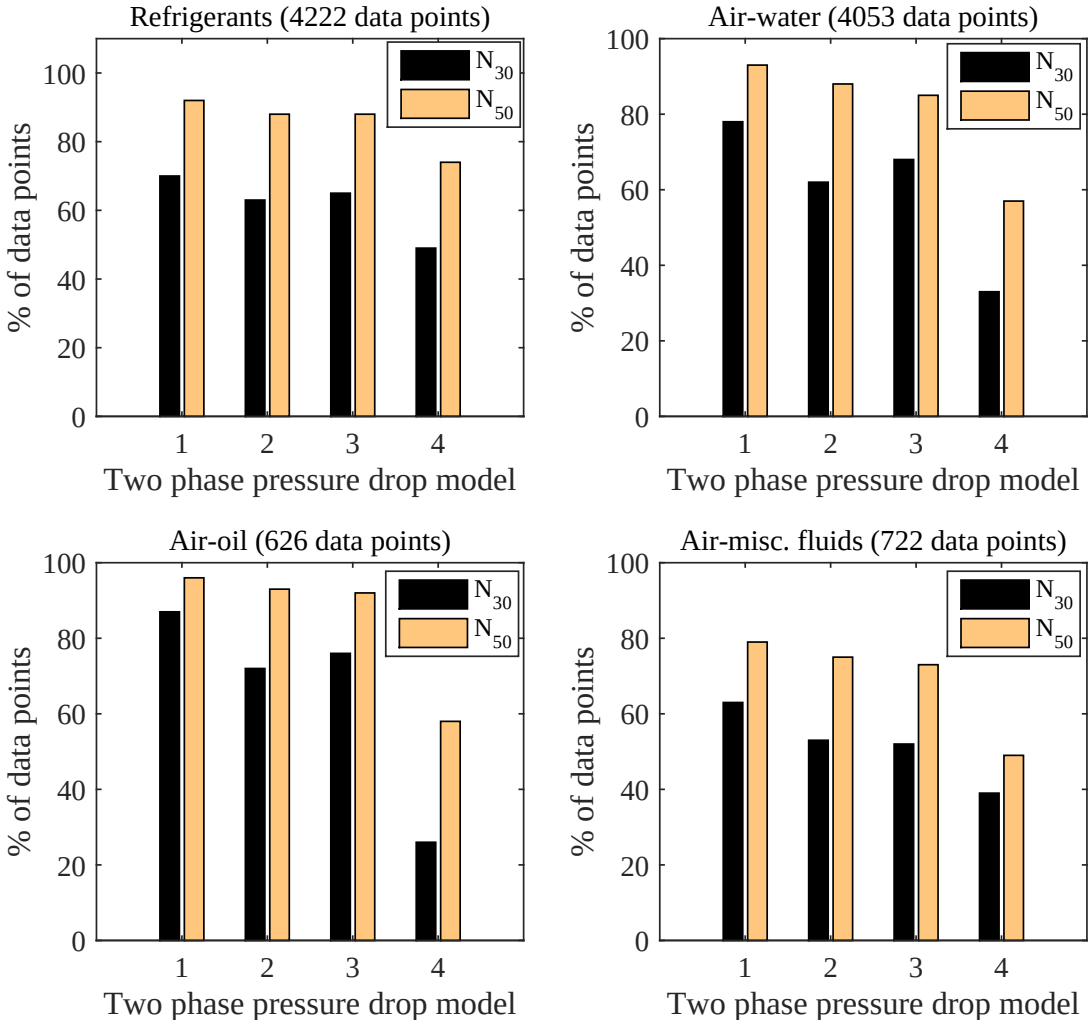

Figure 6.8: Comparison between two phase pressure drop correlations for different fluid combinations ((1) Proposed model, (2) Muller-Steinhagen and Heck (1986), (3) Kim and Mudawar (2012), (4) Shannak (2008)).

Fig. 6.8 shows the performance of proposed correlation and its comparison (based on percentage of data predicted within ±30% and ±50% error bands) against Muller-Steinhagen and Heck (1986), Kim and Mudawar (2012) and Shannak (2008) correlations for different fluid combinations. Clearly, for each fluid combination, the proposed model predicts highest number of data points within each criterion. Specifically,

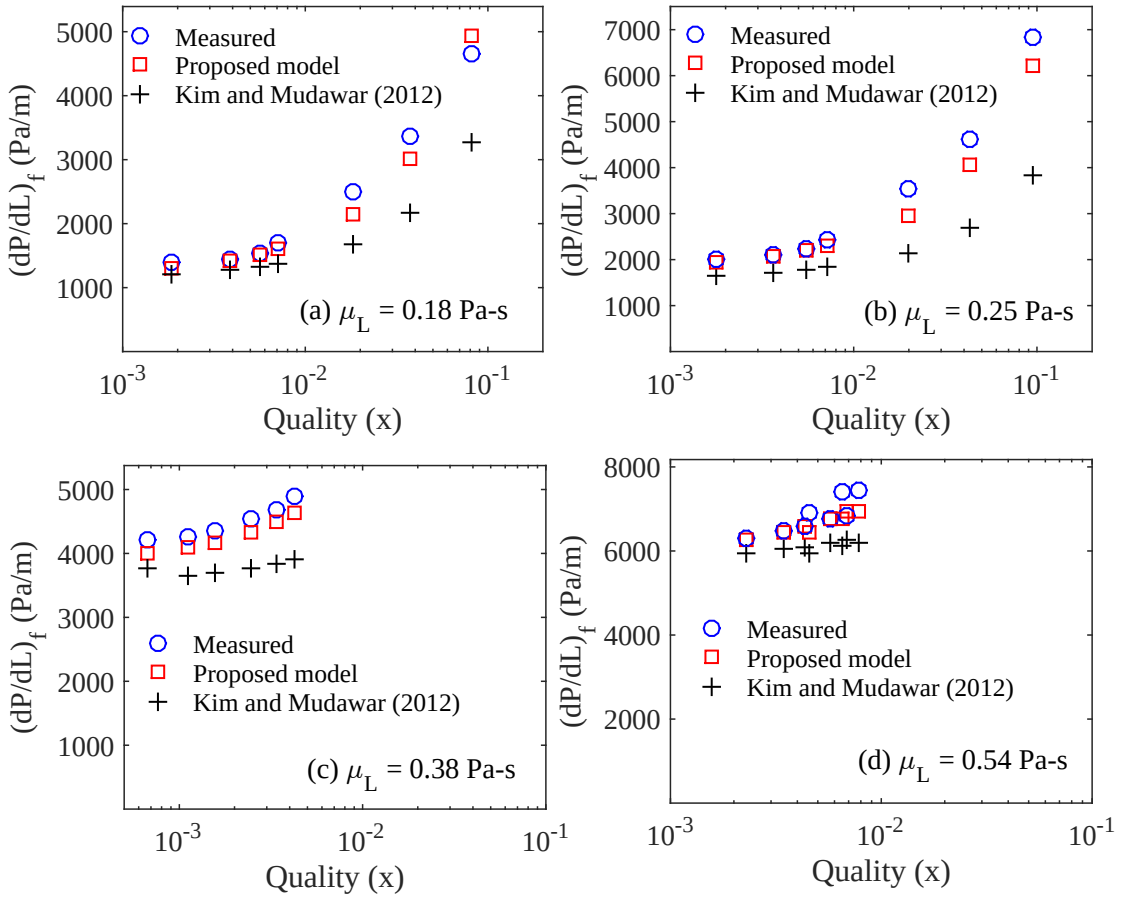

Figure 6.9: Comparison between proposed model and Kim and Mudawar (2012) correlation for liquid with high viscosity.

for air-water and air-oil data, the proposed correlation shows remarkable performance by predicting 78% and 87% of data points, respectively within ±30% error bands. For these fluid combinations, the proposed correlation has a mean relative deviation of 4.3% and 6.7%, respectively. For two phase flow of refrigerants, proposed model performs slightly better (70% of data points predicted within ±30% error bands) than Kim and Mudawar (2012) correlation (67% of data points predicted within ±30% error bands). The prediction of the proposed correlation for two phase flow refrigerants is further improved (75% of data points predicted within ±30% error bands) in case of the experimental dataset (482 data points) by Ong and Thome (2011) is omitted from the refrigerants data base. In particular, the experimental data of Ong and

Thome (2011) showed a strong departure from the majority of comparable data from other sources.

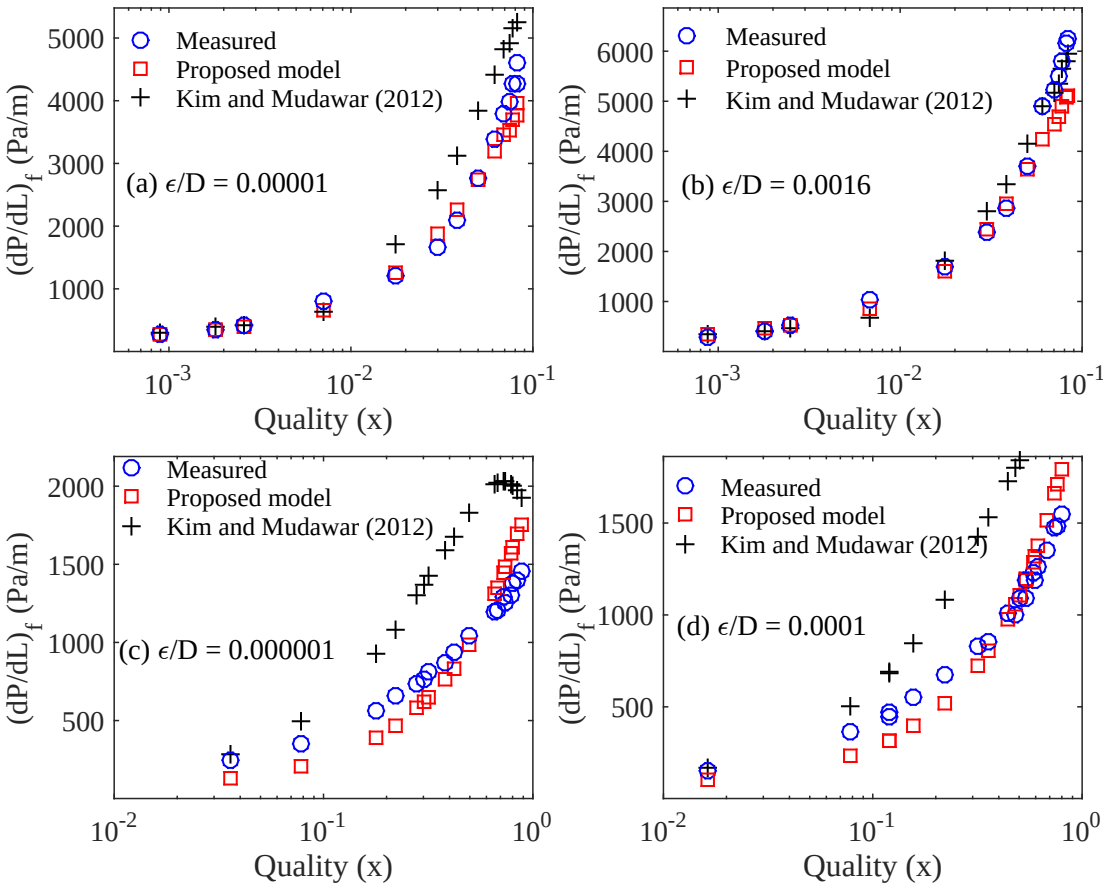

Figure 6.10: Comparison between proposed and Kim and Mudawar (2012) correlation for different roughness ratios (a) and (b): data measured at OSU, (c) and (d): data measured by Shannak (2008).

The comparison between proposed model and Kim and Mudawar (2012) correlation for varying liquid phase dynamic viscosity is shown in Fig. 6.9. Clearly, due to inclusion of Viscosity number ($N_{\mu L}$), the proposed correlation can very well predict trends of two phase pressure drop as a function of two phase flow quality for highly viscous liquid phase. For air-oil and other fluid combinations, more experimental data is needed to further validate the accuracy of proposed and other correlations available in the two phase flow literature. It is also of interest to make a comparison between

the proposed model and Kim and Mudawar (2012) correlation for the predicted frictional pressure drop in smooth and rough pipes. Comparisons in Fig. 6.10 show the proposed model to correctly mimic the trend of two phase frictional pressure drop vs. quality for different roughness ratios (ϵ/D). Kim and Mudawar (2012) is based on the single phase friction factor equation in smooth pipes and tends to over predict the two phase frictional pressure drop in smooth pipes. Obviously, for rough pipes, it predicts the data better since the frictional pressure drop in rough pipe depending upon the flow regime and pipe diameter is up to 30% higher than that in smooth pipes. In Fig. 6.10 data used in (a) and (b) is collected at OSU for air-water two phase flow in 12.5 mm I.D. pipe while that in (c) and (d) is reported by Shannak (2008) for air-water two phase flow in 52 mm I.D. pipe.

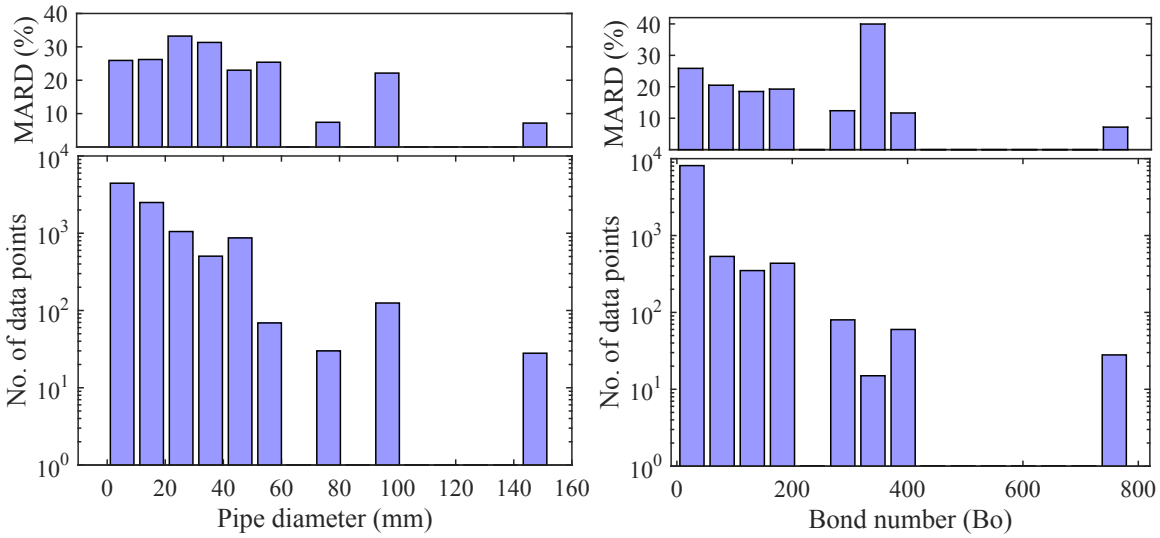

Figure 6.11: Mean absolute relative deviation of the proposed correlation for the distribution of data over a range of pipe diameters and Bond number.

Achieving a minimum MRD and MARD and predicting maximum percentage of data points within ±30% and ±50% error bands for a wide range of data set is not the only definitive approach to ascertain the accurate prediction of any model. Thus, it is also crucial to check the performance of proposed correlation for the distribution of data over a wide range of two phase flow conditions. Fig. 6.11 shows the mean relative

deviation (MARD) of the proposed correlation against the distribution of data over a wide range of pipe diameters and Bond numbers. Clearly, with the exception of pipe diameters in a range of 20 to 40 mm, the MARD for each range of pipe diameter is less than 30%.

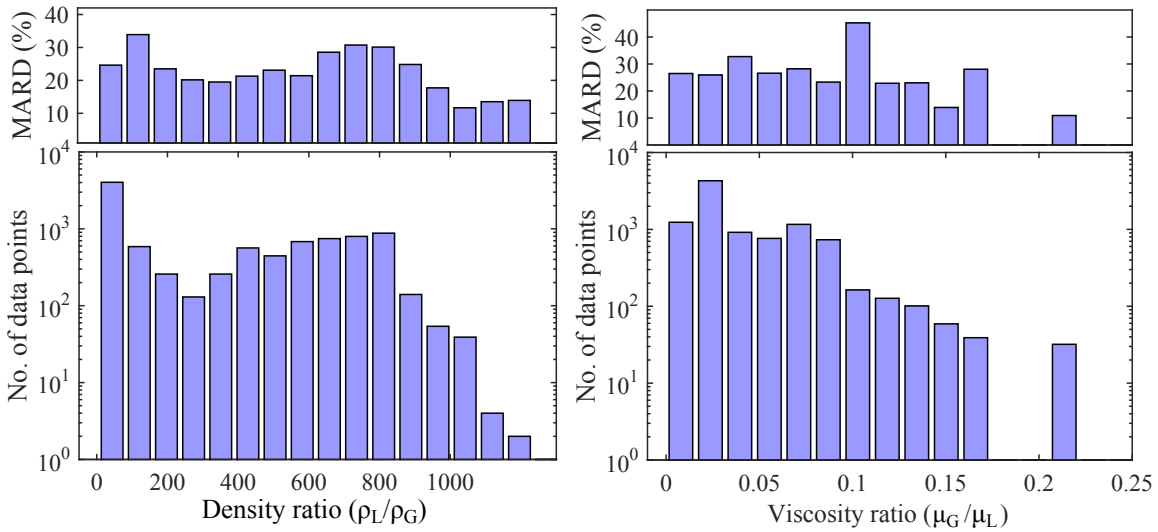

Figure 6.12: Mean absolute relative deviation of the proposed correlation for the distribution of data over a range of phase density and viscosity ratios.

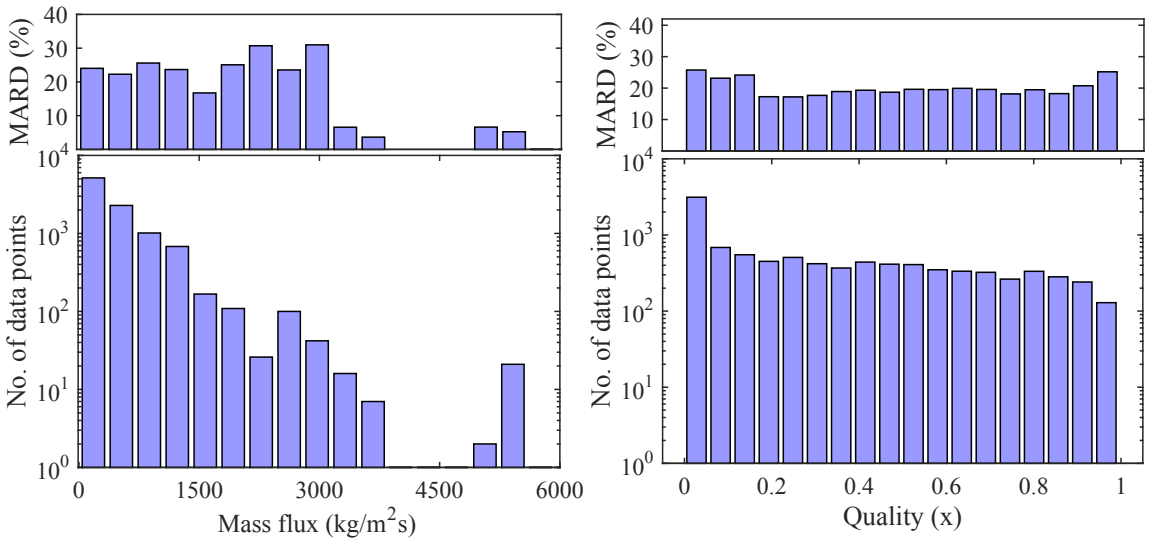

Figure 6.13: Mean absolute relative deviation of the proposed correlation for the distribution of data over a range of two phase mass flux and quality.

For a wide range of Bond numbers, with the exception of $Bo \approx 350$ the MARD

of the predicted two phase frictional pressure drop by the proposed correlation is less than 30%. Note that the condition $Bo \approx 350$ represents approximately 20 data points and hence slightly higher values of MARD do not affect the overall performance of the proposed correlation. Fig. 6.12 shows the MARD of the proposed correlation against the distribution of data over a wide range of phase density and viscosity ratios. With the exception of $(\mu_G/\mu_L) \approx 0.1$, the proposed correlation has a MARD of less than 30%. A close observation of the experimental data shows that this viscosity ratio corresponds to specific case of the two phase flow of air-water through annular pipe geometry. None of the correlations considered in this work are found to accurately predict two phase pressure drop data in annular pipe geometry reported by Wongwises and Pipaththttakul (2006). The MARD of proposed correlation for a wide range of two phase mixture mass flux and two phase flow quality is depicted in Fig. 6.13. For two phase mass flux greater than 3500 kg/m^{2}s, the MARD of predicted pressure drop using proposed correlation is less than 10%. Whereas, for the entire range of two phase flow quality ($0 < x < 1$), the proposed correlation consistently predicts the two phase pressure drop data with MARD less than 30%. These trends confirm that the proposed model can correctly predict two phase frictional pressure drop over a wide range of two phase flow conditions.

In addition to all these different forms of two phase flow conditions, it is also worthwhile to check the goodness of the proposed correlation for different cases of single phase flow regimes (laminar/turbulent). Fig. 6.14 shows the prediction of proposed correlation against the measured data for different combinations of single phase flow regimes. For laminar-laminar ($Re_{SL} \leq 2000$, $Re_{SG} \leq 2000$), laminar-turbulent ($Re_{SL} \leq 2000$, $Re_{SG} > 2000$) and turbulent-turbulent ($Re_{SL} > 2000$, $Re_{SG} > 2000$) flow regimes, the proposed correlation successfully predicts more than 70% and 90% of data points within ±30% and ±50% error bands, respectively. For the laminar-turbulent and turbulent-turbulent cases, MRD is less than 4% and MARD

is 25% or less. Accuracy of the proposed correlation slightly drops down for the case of turbulent-laminar flow ($Re_{SL} > 2000$, $Re_{SG} \leq 2000$). A careful observation of the experimental data shows that a majority of data in this flow regime belongs to the slug/churn (intermittent flow) transition in upward inclined two phase flow where the pressure drop increases suddenly due to slug breakup resulting into vigorous mixing and chaotic two phase flow behavior. Consequently, all two phase flow models under predict the frictional pressure drop for this case.

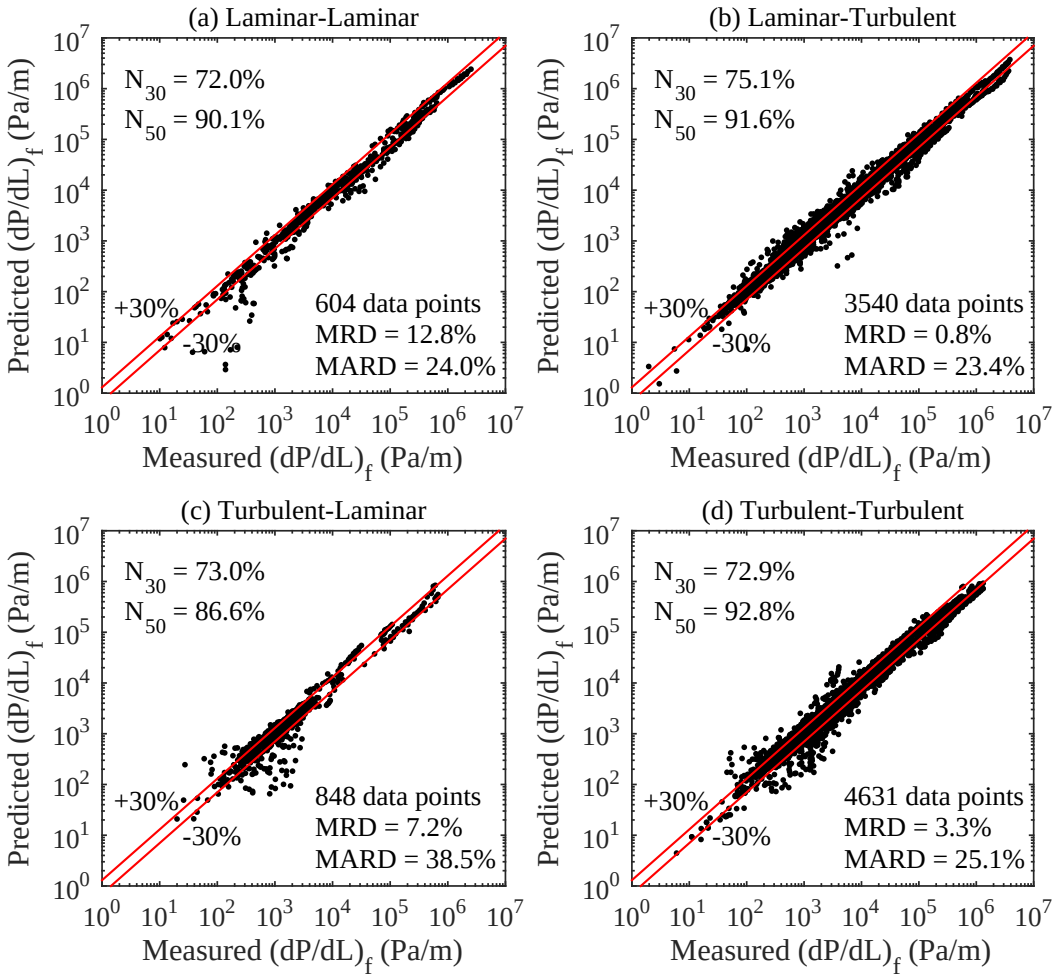

Figure 6.14: Prediction of the proposed correlation against the entire data for different single phase flow regimes (all data, 9623 data points).

Figs. 6.15 and 6.16 show the performance of Muller-Steinhagen and Heck (1986) and Kim and Mudawar (2012) correlations for different combinations of single phase

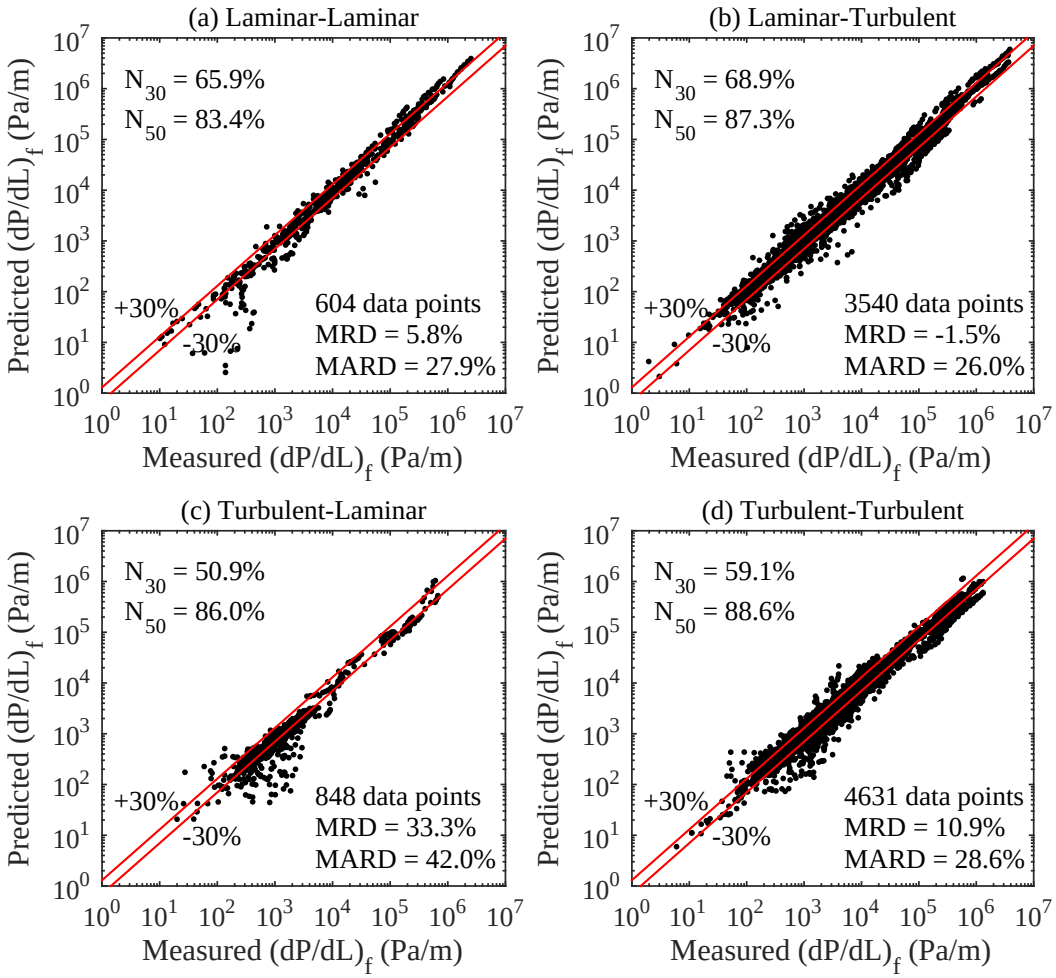

Figure 6.15: Prediction of Muller-Steinhagen and Heck (1986) correlation against the entire data for different single phase flow regimes (all data, 9623 data points).

flow regimes. Similar to the proposed correlation, accuracy of Muller-Steinhagen and Heck (1986) and Kim and Mudawar (2012) is found to deteriorate for the case of turbulent-laminar flow. Considering the overall accuracy in terms of N_{30}, N_{50}, MRD and MARD, the proposed correlation performs consistently better than Muller-Steinhagen and Heck (1986) and Kim and Mudawar (2012) for all four cases of single phase flow regimes. Compared to Muller-Steinhagen and Heck (1986), Kim and Mudawar (2012) has a better accuracy (in terms of N_{30} and N_{50}) over all four cases of single phase flow. In particular, accuracy of Muller-Steinhagen and Heck (1986) correlation drops down in turbulent-laminar and turbulent-turbulent two phase flow regimes. In these flow regimes, their correlation predicts less than 60% of data points

within ±30% error bands. In comparison to the proposed correlation, Kim and Mudawar (2012) also shows a drop in its accuracy for turbulent-turbulent flow regime. Finally, the performance of the proposed correlation over the entire data (9623 data points) consisting of horizontal, vertical and upward pipe inclinations is presented graphically in Fig. 6.17. For the consolidated data bank, proposed correlation predicts 74% and 92% of data within ±30% and ±50% error bands with a MRD of 3.3% and MARD of 25.4%. In comparison to this, Muller-Steinhagen and Heck (1986) correlation predicts 63% and 87% of data points within ±30% and ±50% error bands with a MRD of 8.9% and MARD of 28.6%. Whereas, the correlation of Kim and Mudawar (2012) can predict the entire data set with 67% and 86% of data points within ±30% and ±50% error bands a MRD of 2.4% and MARD of 28.4%.

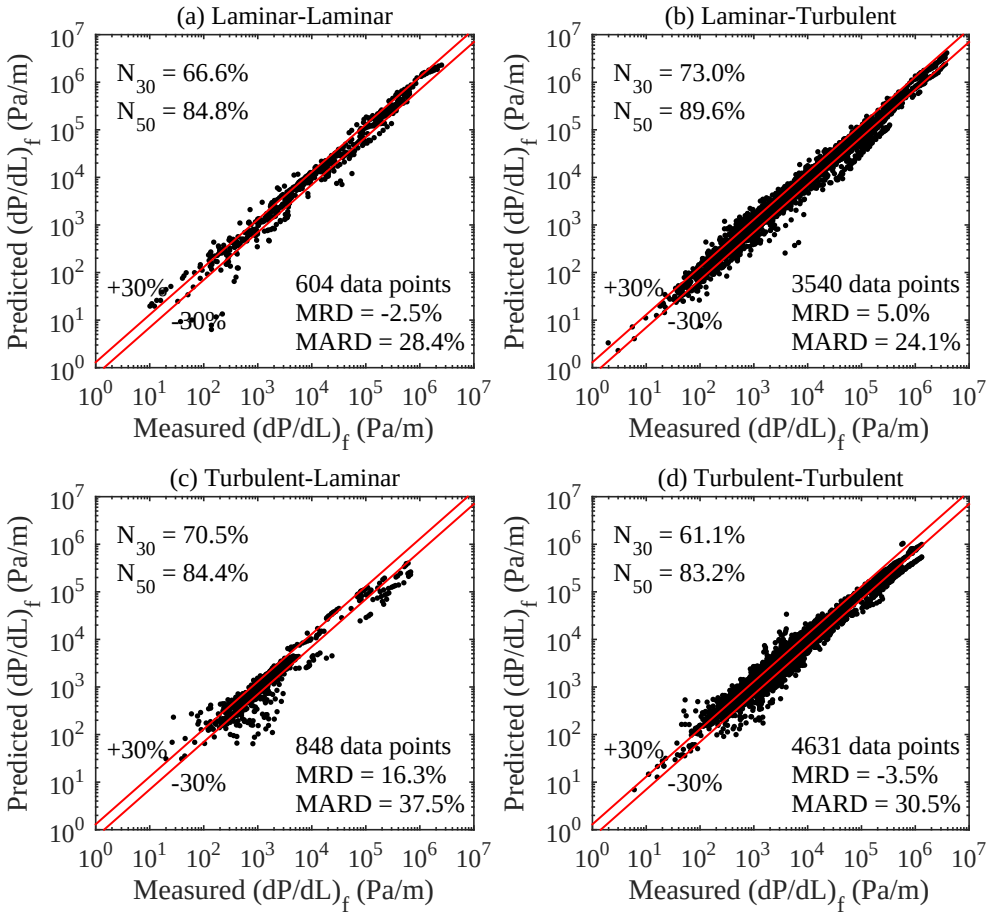

Figure 6.16: Prediction of Kim and Mudawar (2012) correlation against the entire data for different single phase flow regimes (all data, 9623 data points).

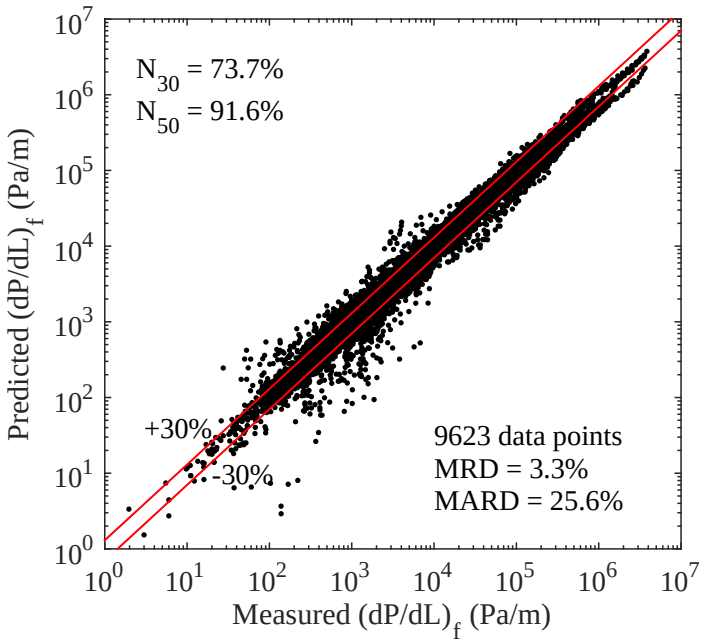

Figure 6.17: Performance of the proposed correlation against entire data (9623 data points).

6.4 Triangular Relationship for Annular Flow

Triangular relationship in annular flow in essence is a relationship between three principal dependent system parameters i.e., pressure gradient $(dP/dL)_f$, liquid film thickness (δ) and the liquid film flow rate $(\dot{m}_{LF})$ such that if any of these two variables are known then the third unknown variable can be calculated from their interrelationships. Although, the triangular relationship forms a basis for different correlations developed for annular flow, these dependent variables that form a triangular relationship cannot be practically calculated from system independent parameters such as phase flow rates, fluid properties and pipe geometry and hence require close form solutions. As shown in Fig. 6.18, the closure relations required to form the triangular relationship for annular flow are usually in form of equations for liquid entrainment fraction (E) and the interfacial friction factor (f_i) embedded in the equation to solve for two phase frictional multiplier and hence the two phase pressure drop. In order

to solve for the triangular relationship, following simplifying assumptions need to be made that reduce the number of equations and empirical relationships required to solve for the two phase pressure drop.

1. Liquid film thickness is very small compared to the pipe diameter such that $\delta << D$ and that the liquid film is uniformly distributed over the pipe circumference.

2. Shear stress in the liquid film is constant and approximately equal to the wall shear stress such that at the gas liquid interface, $\tau_i \approx \tau_w$.

3. Gravitational and accelerational effects on the gas core and liquid film are negligible (compared to the frictional pressure drop).

4. Annular flow is axisymmetric and is at equilibrium i.e., the liquid film thickness is uniform around the pipe circumference and the film thickness, liquid entrainment fraction does not change significantly over the pipe length.

A detailed description of the triangular relationship in annular flow is given by Hewitt and Hall-Taylor (1970) and Collier and Thome (1996).

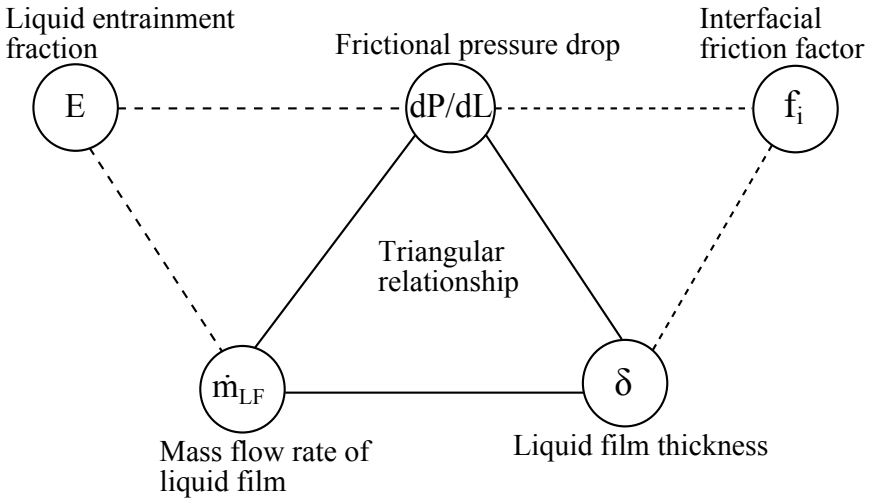

Figure 6.18: Triangular relationship in annular flow.

A review of two phase flow literature shows that all these assumptions are valid for annular flow at low liquid and high gas flow rates. With these assumptions, the momentum balance (see Chapter II) leads to Eq. (6.18). This two phase frictional pressure drop is expressed in terms of actual velocity of the liquid flowing in form of liquid film (in contact with the pipe wall) and that the liquid entrainment is negligible. Using the definition of two phase frictional multiplier (Φ_L^2), Eq. (6.18) could also be expressed as Eq. (6.19).

$$\left(\frac{dP}{dL}\right)_f = \frac{4\tau_w}{D} = \frac{2f_{TP}\rho_L U_L^2}{D} \tag{6.18}$$

$$\Phi_L^2 = \frac{(dP/dL)_f}{(dP/dL)_L} = \frac{1}{(1-\alpha)^2}\left(\frac{f_{TP}}{f_L}\right) \tag{6.19}$$

Hewitt and Hall-Taylor (1970) have reported that using a concept of equivalent diameter (diameter of different pipe geometries that give similar pressure drop) and definition of void fraction under no liquid entrainment, the Reynolds number of liquid flowing in form of film is identical to the Reynolds number of liquid phase flowing alone through the pipe. This implies that based on identical Reynolds number defined by Eq. (6.20), the friction factors of liquid flowing in form of film and that alone through the pipe must be identical i.e., $f_{TP} = f_L$. This relationship however does not acknowledge existence of liquid entrainment fraction which in practical cases may not be ignored. To account for the liquid entrainment fraction, Turner and Wallis (1965) have proposed use of a similar relationship in which the single phase pressure drop for total liquid flow is replaced by the single phase pressure drop for that part of the liquid flow which flows in form of film. Using this consideration, the two phase frictional multiplier given by Eq. (6.19) can be re-casted in form of Eq. (6.21).

$$\frac{\rho_L U_L 4\delta}{\mu_L} = \frac{\rho_L U_{SL} D}{\mu_L} \tag{6.20}$$

$$\Phi_{LF}^2 = \frac{(dP/dL)_f}{(dP/dL)_{LF}} = \frac{1}{(1-\alpha)_{LF}^2} \tag{6.21}$$

The frictional pressure drop due to flow of liquid phase in form of film can be calculated from Eq. (6.22) where the liquid film friction factor (f_{LF}) can be calculated using appropriate single phase friction factor correlation based on liquid film Reynolds number defined using liquid entrainment fraction such that $Re_{LF} = Re_{SL}(1-E)$.

$$\left(\frac{dP}{dL}\right)_{LF} = \frac{2f_{LF}\rho_L(U_{SL}(1-E))^2}{D} = \frac{2f_{LF}(G(1-x)(1-E))^2}{D\rho_L} \tag{6.22}$$

Eq. (6.22) can be regarded as an empirical correlation for determination of void fraction in the presence of liquid entrainment process however, its implementation also require knowledge of two phase frictional pressure drop. For a known value of void fraction and liquid entrainment fraction, Eq. (6.21) may not predict the correct magnitude of two phase frictional pressure drop due to lack of information on the interfacial roughness and hence the interfacial shear stress. To address this issue, one more closure relationship is required that links the interfacial friction/roughness to the liquid flow rate or any other previously calculated variables such as void fraction or liquid entrainment fraction. This relationship could be obtained by considering yet another form of the two phase frictional multiplier in form of Φ_G^2. Using assumptions 1 to 4, a momentum balance equation on the gas core results into Eq. (6.23). Using Eq. (6.23), the two phase frictional multiplier assuming only gas phase flowing through pipe can be expressed in form of Eq. (6.24) where the interfacial shear stress and the gas phase shear stress are expressed by Eqs. (6.25) and (6.26), respectively.

$$\left(\frac{dP}{dL}\right)_f = \frac{4\tau_i}{(D-2\delta)} \tag{6.23}$$

$$\Phi_G^2 = \frac{(dP/dL)_f}{(dP/dL)_G} = \frac{4\tau_i/(D-2\delta)}{4\tau_G/D} \tag{6.24}$$

Table 6.9: Different forms of gas-liquid interface velocity and associated interfacial friction factor and form of gas density suggested by Wallis (1968).

Form	U_i	f_i	ρ_G	Φ_G^2
I	U_{SG}	$f_G[1+90(1-\alpha)]$	ρ_G	$\frac{1+90(1-\alpha)}{\sqrt{\alpha}}$
II	U_G	$f_G[1+75(1-\alpha)]$	ρ_G	$\frac{1+75(1-\alpha)}{\alpha^{5/2}}$
III	U_c	$f_{Gc}[1+90(1-\alpha)]$	ρ_c	$[1+90(1-\alpha)]\frac{\rho_c}{\rho_G}\frac{f_{Gc}}{f_G}\frac{U_c^2}{U_{SG}^2}$

$$\tau_i = f_i\left(\frac{\rho_G U_i^2}{2}\right) \tag{6.25}$$

$$\tau_G = f_G\left(\frac{\rho_G U_{SG}^2}{2}\right) \tag{6.26}$$

Two phase flow literature reports several different forms of the velocity at gas-liquid interface. Some of these forms include substitution of the interface velocity with superficial gas velocity (U_{SG}), actual gas velocity (U_G), gas core velocity (based on core cross sectional area), difference between actual velocities of gas and liquid phase ($U_G - U_L$) etc. Note that the interfacial friction factor is related to the velocity at the gas-liquid interface and hence a different representation of U_i would require appropriate correlation for f_i. In a series of publications Wallis (1962), Wallis (1968), Wallis (1969) suggested three different representations for U_i and f_i as listed in Table 6.9. The core velocity U_c is based on the mass flow rate of gas phase + mass flow rate of liquid droplets in the gas core, f_{Gc} is based on the Reynolds number of gas core while ρ_c is the density of the gas core weighted by the liquid entrainment fraction.

Considering the flow behavior of annular flow pattern, a better approximation to represent the velocity of the gas liquid interface appears to be the difference between mean actual gas velocity and the mean velocity of the liquid phase flowing in form of film such that $U_i = U_G - U_{LF}$. Moreover, the gas density can be expressed in form of gas core density (as a function of liquid entrainment fraction). For the limiting

case of void fraction approaching unity ($\alpha \rightarrow 1$), we have $U_G >> U_{LF}$ and thus $U_i \rightarrow U_G \approx U_{SG}$. Also, at very low liquid flow rates ($\alpha \rightarrow 1$), $E \rightarrow 0$ and $\rho_c \approx \rho_G$. These conditions are similar to first two conditions of U_i and ρ_G given by Wallis (1968) listed in Table 6.9. Using suggested form of U_i, Eq. (6.24) is restructured as Eq. (6.27) where $D/(D-2\delta)$ could be expressed in terms of void fraction using the definition of cross-sectional averaged void fraction under the condition of negligible liquid entrainment.

$$\Phi_G^2 = \frac{f_i}{f_G}\frac{\rho_c}{\rho_G}\left(\frac{U_G - U_{LF}}{U_{SG}}\right)^2 \frac{D}{D-2\delta} \tag{6.27}$$

Moreover, an assumption of a smooth gas-liquid interface leads to $f_i \approx f_G$. Thus, for such a simplified two phase flow situation, Eq. (6.27) is a function of void fraction only. Note that these simplifying assumptions in particular the condition of $f_i \approx f_G$ is an unrealistic assumption for annular flow and the predicted value of two phase frictional multiplier may deviate by several order of magnitudes from the actual conditions. Thus, for practical application, the ratio f_i/f_G in Eq. (6.27) can be replaced with some empirical correlation available in the two phase flow literature. As mentioned earlier, use of a particular empirical correlation for f_i depends on the form of gas-liquid interface velocity, use of a $U_i = U_G - U_{LF}$ would require a modified form of f_i compared to that listed in Table 6.9. Use of the existing f_i listed in Table 6.9 would render an over prediction of two phase frictional pressure drop. Thus, for the correct prediction of two phase pressure drop, interfacial friction factor of the form $f_i = f_G \times [1 + 50(1-\alpha)\alpha]$ is recommended for use. The definition of actual phase velocity and the velocity of liquid in form of film yields $U_G = U_{SG}/\alpha$, $U_L = U_{SL} \times (1-E)/(1-\alpha)$ and Eq. (6.27) could be expressed in form of Eq. (6.28). The algorithm to solve for triangular relationship is shown in Fig 6.19.

$$\Phi_G^2 = \frac{[1 + 50\alpha(1-\alpha)]}{\alpha^{5/2}}\frac{\rho_c}{\rho_G}\left[1 - \frac{\rho_G}{\rho_L}\left(\frac{1-x}{x}\right)\left(\frac{\alpha}{1-\alpha}\right)(1-E)\right]^2 \tag{6.28}$$

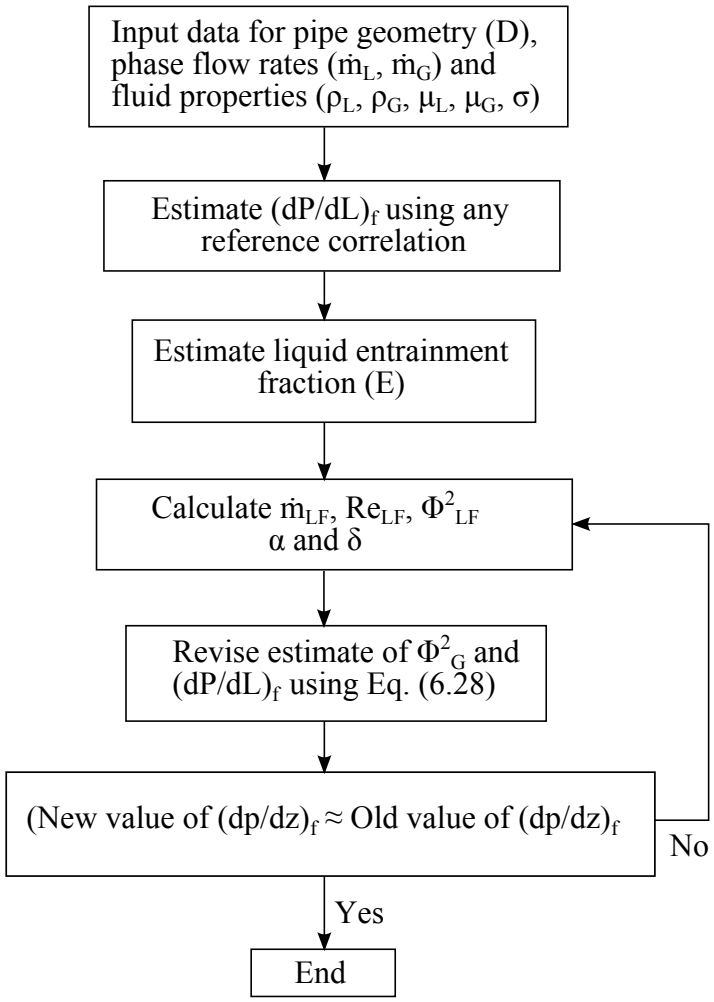

Figure 6.19: Algorithm to solve for triangular relationship in annular flow.

The amount of liquid entrainment fraction required to solve for the triangular relationship is determined using the correlation of Cioncolini and Thome (2012b) given by Eqs. (6.29) to (6.33). Their correlation is a two step method, predictive step (Eqs. (6.29) and (6.30)) that gives initial estimate of the liquid entrainment fraction as a function of gas core Weber number based on the gas density while the corrector step recalculates E (Eq. (6.33)) based on the core Weber number (Eq. (6.32)) core density (Eq. (6.31)) calculated from the E value in the predictor step.

$$We_c = \frac{\rho_G U_{SG}^2 D}{\sigma} \tag{6.29}$$

$$E_p = (1 + 280 \times We_c^{-0.8395})^{-2.209} \tag{6.30}$$

$$\rho_c = \frac{x + E_p(1-x)}{x/\rho_G + E_p(1-x)/\rho_L} \tag{6.31}$$

$$We_c = \frac{\rho_c U_{SG}^2 D}{\sigma} \tag{6.32}$$

$$E = (1 + 280 \times We_c^{-0.8395})^{-2.209} \tag{6.33}$$

As mentioned earlier, the triangular relationship is valid only for annular two phase flow and is based on the assumptions that the liquid film is uniformly distributed across the pipe cross section i.e., the flow is axisymmetric and that the liquid film thickness is very small compared to the pipe diameter. Moreover, it is also assumed that the interfacial shear stress is approximately equal to the wall shear stress. As such, the application of this method should be restricted only to the subregion of annular flow pattern where the conditions of $\delta << D$ and $\tau_i \approx \tau_w$ hold valid. In general, two phase literature reports the existence of annular flow for $\alpha \geq 0.75$. At the onset of annular flow ($\alpha \approxeq 0.75$), the liquid film thickness is considerable and the assumption of $\tau_i \approx \tau_w$ may not be valid. With increase in gas flow rate, the void fraction increases and reduces the liquid film thickness. Based on the experimental data it is found that for void fraction below 0.8, the predictions of triangular relationship (frictional pressure drop and void fraction) starts drifting and show deviation from the measured data. Thus, the application of the triangular relationship is recommended to be restricted to void fraction of $\alpha \geq 0.8$. As a thumb rule, a quick check to validate the application and outcome of the triangular relationship is to verify the condition of $\tau_i > \delta \rho_L g$. Fig. 6.20 shows that the ratio of $\tau_i / \delta \rho_L g$ decreases with decreasing void fraction. Considering the slope of this ratio as a function of void fraction, it is clear that for lower values of void fraction ($\alpha \approxeq 0.75$), $\tau_i \approx \delta \rho_L g$ and hence the application of triangular relationship is not valid.

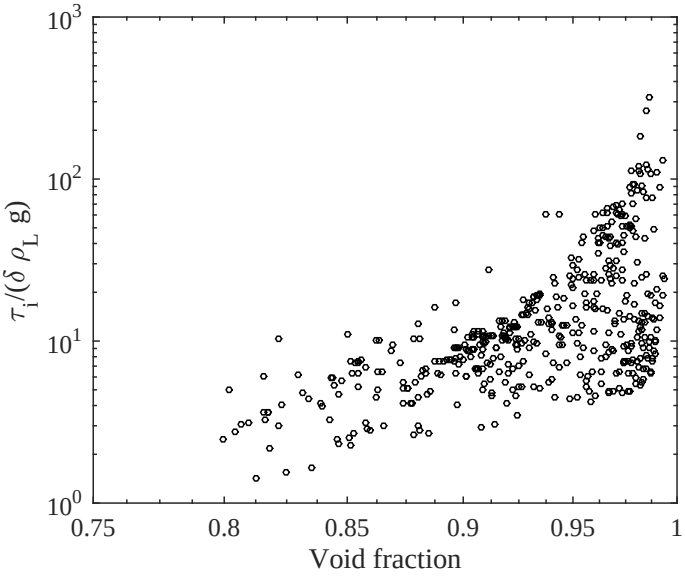

Figure 6.20: Ratio of τ_i to $\delta\rho_L g$ for varying void fraction based on 556 data points in vertical upward flow.

The comparison between measured and predicted values of two phase frictional pressure drop using triangular relationship is shown in Fig. 6.21. Out of 935 data points in vertical upward flow, 571 data points satisfied the criteria of $\alpha \geq 0.8$. The triangular relationship is found to reproduce the measured data with MRD of -3.2%, MARD of 22.2% and predicts about 82% and 91% of data points within ±30% and ±50% error bands, respectively. A comparison between the different forms of Φ_G^2 based on those suggested by Wallis (1968) and Eq. (6.28) is shown in Table 6.10. It is evident that as the approximation of gas-liquid interface velocity and the core density becomes more realistic, the accuracy of predicted frictional pressure drop increases progressively. In comparison to Eq. (6.28), use of the two phase frictional pressure drop multiplier (Eq. (6.2)) suggested in previous section gives a MRD of 10%, MARD of 22% and predicts 79% and 93% of data points within ±30% and ±50% error bands, respectively. Table 6.11 reports the prediction of Eq. (6.28) for different ranges of void fraction. The accuracy of triangular relationship is observed to increase with increase in the void fraction values. The drop in accuracy of triangular relationship with decrease in void fraction could be linked with its departure of the

assumption of $\tau_i > \delta\rho_L G$ as shown in Fig. 6.20. Although, there is no significant improvement in the accuracy of triangular relationship method (flow pattern specific) in comparison to the Eq. (6.2), use of triangular relationship over a narrow range of two phase flow conditions is useful since it gives supplementary information of void fraction and liquid film thickness.

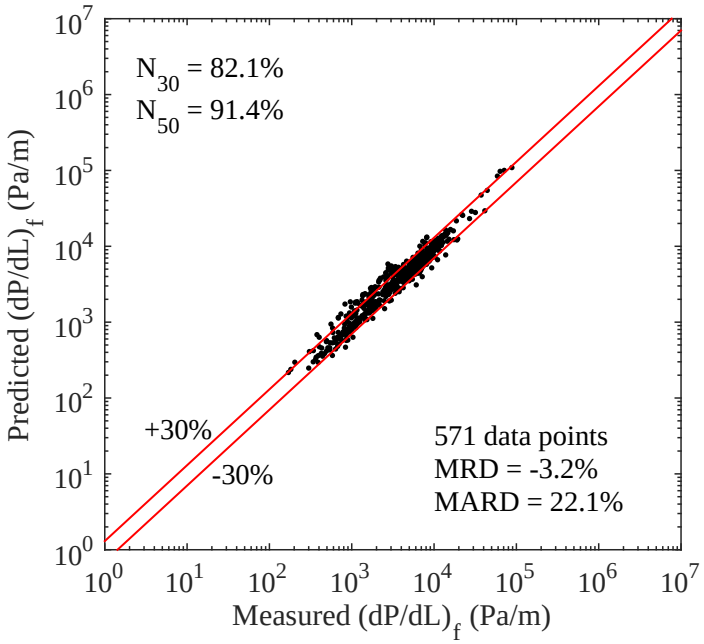

Figure 6.21: Comparison between measured and predicted two phase frictional pressure drop in vertical upward flow using triangular relationship.

Table 6.10: Comparison between the predictions of different forms of Wallis (1968) correlation (see Table 6.9) and the proposed modification for vertical upward flow (571 data points).

Form	MRD	MARD	N_{30}	N_{50}
I	-19	31	71	87
II	-20	26	73	86
III	-17	21	77	83
Eq. (6.28)	-3.2	22.2	82	91

The void fraction in annular flow obtained by solving for triangular relationship could be verified by comparing it against the flow pattern specific correlation of Cioncolini and Thome (2012a) developed exclusively for annular flow. As shown

Table 6.11: Performance of Eq. (6.28) for different ranges of void fraction in vertical upward flow (571 data points).

Void fraction	Data points	MRD	MARD	N_{30}	N_{50}
$0.8 \leq \alpha < 1$	63	-3.2	22	82	91
$0.85 \leq \alpha < 1$	87	-2.7	21	84	92
$0.9 \leq \alpha < 1$	246	-1.6	18	89	95
$0.95 \leq \alpha < 1$	175	-2.4	19	89	95

in Fig. 6.22, for void fraction in a range of $0.85 \leq \alpha < 1$, the predicted values of void fraction (using triangular relationship) are within $\pm 5\%$ of the values predicted by Cioncolini and Thome (2012a) correlation. For $\alpha < 0.85$, the predicted void fraction using triangular relationship starts deviating probably because the underlying assumptions of triangular relationship ($\delta << D$ and $\tau_i \approx \tau_w$) starts deviating from realistic two phase flow conditions. Fig. 6.23 shows the comparison between non-dimensional liquid film thickness (δ/D) calculated using triangular relationship and that calculated using the correlation of Berna et al. (2014) given by Eq. (6.34). Considering the experimental uncertainty in measurement of liquid film thickness (usually in microns/mm) and the fact that the liquid film thickness is a difficult quantity to measure (because of its spatial and temporal variation), its prediction within $\pm 50\%$ error bands is considered acceptable in the two phase flow literature.

$$\frac{\delta}{D} = 7.165 \times Re_{SL}^{0.48} Re_{SG}^{-1.07} \left(\frac{Fr_{SG}}{Fr_{SL}} \right)^{0.24} \tag{6.34}$$

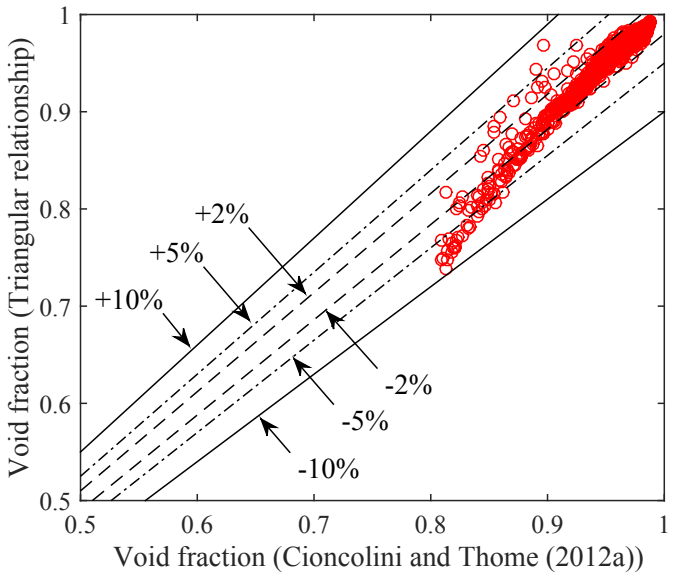

Figure 6.22: Comparison between void fraction predicted by triangular relationship and annular flow pattern specific correlation of Cioncolini and Thome (2012a).

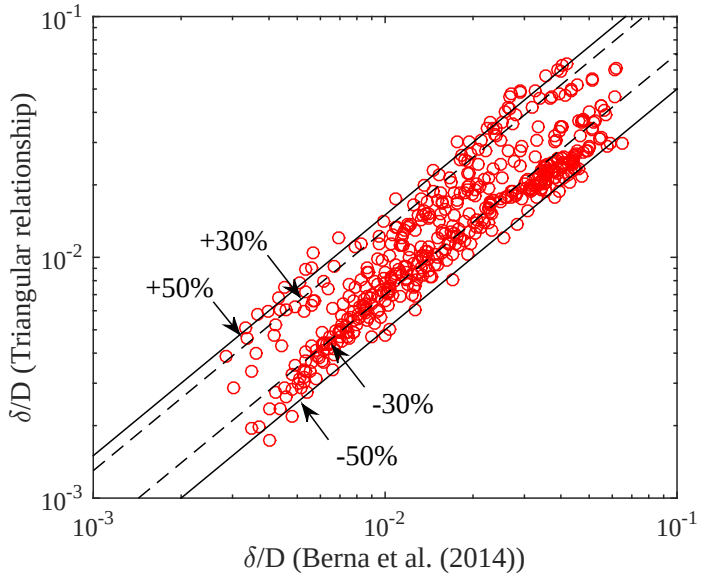

Figure 6.23: Comparison between non-dimensional liquid film thickness (δ/D) predicted by triangular relationship and annular flow pattern specific correlation of Berna et al. (2014).

The triangular relationship as mentioned earlier is applicable for axisymmetric annular flow and hence it is also of interest to check the validity of this concept for vertical downward annular flow. Experimental data used for vertical downward flow

shows that use of Eq. (6.28) consistently under predicts the two phase frictional pressure drop. Experimental measurements conducted at OSU ($D = 12.7$ mm) and that of Oshinowo and Charles (1974) ($D = 25.4$ mm) and Lau et al. (1992) ($D = 9.1$ mm) show that the frictional pressure drop in vertical downward flow is greater than that in vertical upward flow. Also, for similar mass flow rates, experiments carried out at OSU and by Oshinowo et al. (1984) exhibit enhanced two phase heat transfer in vertical upward flow (smaller liquid film thickness) compared to that in vertical downward flow. Considering the physical structure of annular flow pattern in these orientations it can be inferred that the film thickness in vertical downward flow is greater than that in vertical upward flow. Unfortunately, two phase flow literature does not report direct measurements of film thickness in upward and downward vertical flow at similar phase mass flow rates. Thus, it is clear that the wall shear stress and hence the interfacial shear stress in vertical downward flow (due to higher frictional pressure drop) would be greater than that in vertical upward flow. As such, to correctly predict the two phase frictional pressure drop, the ratio f_i/f_G in vertical downward flow would be greater than that in vertical upward flow. Based on the experimental data consisting of $12.5 \leq D \leq 45$ mm and air-water, air-kerosene and air-glycerin+water fluid combinations, the interfacial to gas friction factor ratio modeled as $f_i/f_G = 1 + 80\alpha(1-\alpha)$ is found to give the best fit. Note that for vertical downward flow, the triangular relationship algorithm given in Fig. 6.19 remains unchanged. The prediction of two phase frictional pressure drop using triangular relationship based on 200 data points for vertical downward flow (by using $f_i/f_G = 1+80\alpha(1-\alpha)$) is presented in Fig 6.24. It is found that use of $f_i/f_G = 1 + 50\alpha(1-\alpha)$ recommended for vertical upward flow would predict only 69% of data points within $\pm 30\%$ error bands.

It is important to reiterate that the triangular relationship discussed in this section is valid only for axisymmetric annular flow at equilibrium. As such, this re-

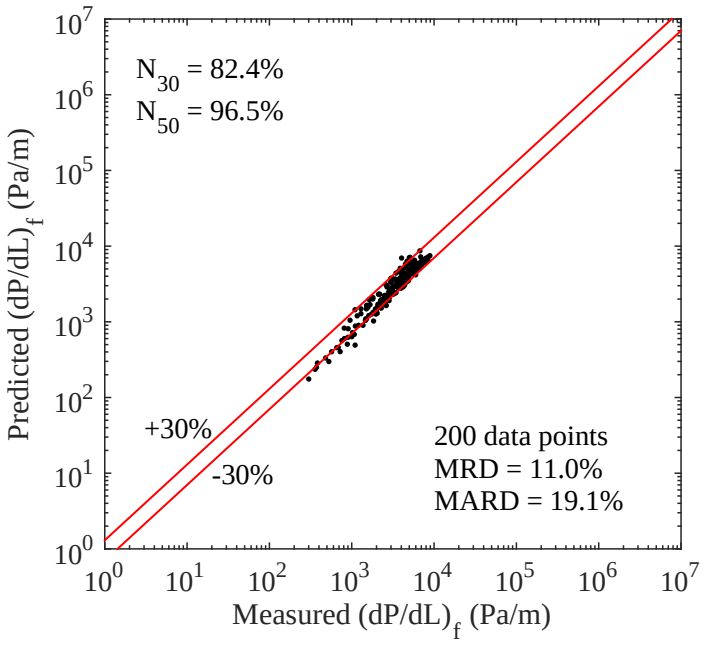

Figure 6.24: Comparison between measured and predicted two phase frictional pressure drop in vertical downward flow using triangular relationship.

lationship may not be used for horizontal and inclined two phase flow systems. For these pipe orientations, the circumferential liquid film distribution is asymmetric and hence for similar mass flow rates, resultant wall shear stress (or alternatively the interfacial shear stress) would be different for non-vertical (non-axisymmetric) annular flow. Moreover, the values of liquid film thickness predicted by triangular relationship in non-vertical pipe orientations are of no practical meaning and significance since in reality, δ at pipe bottom is much thicker compared to that at the pipe top wall. The two phase frictional pressure drop is based on δ (as a function of void fraction) which neither truly represents the bottom wall nor the top wall film thickness. The triangular relationship for vertical two phase flow analyzed in this work is validated for $D \geq 9$ mm. Unfortunately, due to lack of experimental data, the validity of this method could not be confirmed for smaller pipe diameters. For mini-micro channels, the condition of $\delta << D$ would be violated and triangular relationship may not yield accurate predictions. Thus, more experimental data is required to verify the goodness of this method at mini-micro scale two phase annular flow. It is also worthwhile to

highlight that the final converged values obtained using triangular relationship depend upon the closure relationships for liquid entrainment fraction (E), interfacial friction factor (f_i) which eventually control the resultant values of two phase frictional multiplier (Φ_G^2), void fraction (α) and film thickness (δ). There is no unanimity over the use of a particular set of closure equations and hence use of different set of equations may yield slightly different solutions of the triangular relationship. Following solved example gives a better idea of step by step approach required to solve the triangular relationship.

Example problem: Consider the vertical upward two phase flow of air-water mixture in 15.8 mm I.D. smooth pipe. At near atmospheric pressure, the two phase mixture flows with a quality (x) and mass flux (G) of 0.2 and 210 kg/m^{2}s, respectively. The physical properties of air and water are as follows: $\rho_G = 1.3$ kg/m^3, $\rho_L = 998$ kg/m^3, $\mu_G = 18.25 \times 10^{-6}$, $\mu_L = 0.001$ Pa-s and $\sigma = 0.072$ N/m. Using triangular relationship for annular flow, determine the two phase frictional pressure drop, void fraction and liquid film thickness. Assume that the axisymmetric annular flow pattern at equilibrium exists in the pipe.

Solution: The solution to this problem follows the calculation algorithm in Fig. 6.19.

(1) **Make initial estimate of two phase pressure drop:** Calculate gas and liquid phase Reynolds number and single phase friction factors.

$$Re_{SG} = \frac{GxD}{\mu_G} = \frac{210 \times 0.2 \times 0.0158}{18.25 \times 10^{-6}} = 36361 \Rightarrow \ f_G = 0.00572$$

$$Re_{SL} = \frac{G(1-x)D}{\mu_L} = \frac{210 \times (1-0.2) \times 0.0158}{0.001} = 2654 \Rightarrow \ f_L = 0.011$$

Calculate the frictional pressure drop for gas and liquid phase assuming each phase flowing along through the pipe.

$$\left(\frac{dP}{dL}\right)_G = \frac{2f_G(Gx)^2}{D\rho_G} = \frac{2 \times 0.00572(210 \times 0.2)^2}{0.0158 \times 1.3} = 982 \text{ Pa/m}$$

$$\left(\frac{dP}{dL}\right)_L = \frac{2f_L(G(1-x))^2}{D\rho_L} = \frac{2 \times 0.011(210(1-0.2))^2}{0.0158 \times 998} = 39.4 \text{ Pa/m}$$

The Lockhart and Martinelli (1949) parameter (X) and the two phase frictional multiplier (Φ_G^2) are determined. For turbulent-turbulent flow regime of gas and liquid flow use $C = 20$.

$$X = \sqrt{\frac{(dP/dL)_L}{(dP/dL)_G}} = \sqrt{\frac{39.4}{982}} = 0.2$$

$$\Phi_G^2 = 1 + CX + X^2 = 1 + 20 \times 0.2 + 0.2^2 = 5.04$$

Now, the two phase frictional pressure drop is calculated as,

$$\left(\frac{dP}{dL}\right)_f = \Phi_G^2 \times \left(\frac{dP}{dL}\right)_G = 5.04 \times 982 = 4957.3 \text{ Pa/m}$$

(2) **Estimate liquid entrainment fraction (E):** Liquid entrainment fraction is estimated using Cioncolini and Thome (2012b) correlation. First estimate the gas core Weber number using gas phase density and predict the initial estimate of liquid entrainment fraction. The superficial gas velocity required in determination of We_c is calculated as $U_{SG} = Gx/\rho_G = 32.3$ m/s. Then find the gas core density using initial estimate of E and recalculate Weber number and liquid entrainment fraction in corrector step.

$$We_c = \frac{\rho_G U_{SG}^2 D}{\sigma} = \frac{1.3 \times 32.3^2 \times 0.0158}{0.072} = 297.8$$

$$E = (1 + 280 \times We_c^{-0.8395})^{-2.209} = (1 + 280 \times 297.8^{-0.8395})^{-2.209} = 0.069$$

$$\rho_c = \frac{x + E(1-x)}{x/\rho_G + E(1-x)/\rho_L} = \frac{0.2 + 0.069(1-0.2)}{0.2/1.3 + 0.069(1-0.2)/998} = 1.66 \text{ kg/m}^3$$

$$We_c = \frac{\rho_c U_{SG}^2 D}{\sigma} = \frac{1.66 \times 32.2^2 \times 0.0158}{0.072} = 380.3$$

$$E = (1 + 280 \times We_c^{-0.8395})^{-2.209} = (1 + 280 \times 380.3^{-0.8395})^{-2.209} = 0.094$$

The updated value of core density (ρ_c) based on entrainment in corrector step is $\rho_c = 1.79$ kg/m^3. Based on the predicted liquid entrainment fraction ($E = 0.094$), the liquid film flow rate is calculated as $\dot{m}_{LF} = G(1-x)(1-E) \times A = 210(1-0.2)(1-0.094)\pi/4 \times D^2 = 0.03$ kg/s.

(3) **Get first estimate of void fraction and liquid film thickness:** To determine the void fraction and liquid film thickness, first calculate the two phase frictional multiplier (Φ_{LF}^2) based on liquid film flow rate. To determine Φ_{LF}^2 first find f_{LF} based on $Re_{LF} = Re_{SL}(1-E) = 2654 \times (1-0.094) = 2404$. The corresponding liquid film friction factor is $f_{LF} = 0.0113$.

$$\left(\frac{dP}{dL}\right)_{LF} = \frac{2f_{LF}(G(1-x)(1-E))^2}{D\rho_L} = \frac{2 \times 0.0113(210(1-0.2)(1-0.094))^2}{0.0158 \times 998} = 33.12 \text{ Pa/m}$$

$$\Phi_{LF}^2 = \frac{(dP/dL)_f}{(dP/dL)_{LF}} = \frac{4957.3}{33.12} = 149.7$$

$$\Phi_{LF}^2 = \frac{1}{(1-\alpha)^2} = 149.7 \Rightarrow \alpha = 0.918 \text{ and } \delta = 0.323 \text{ mm}$$

(4) **Update the value of two phase pressure drop:** Use Eq. (6.28) to calculate revised estimate of two phase frictional multiplier and compare it with initial

estimated value of $(dP/dL)_f = 4957.3$ Pa/m.

$$\Phi_G^2 = \frac{[1+50\alpha(1-\alpha)]}{\alpha^{5/2}}\frac{\rho_c}{\rho_G}\left[1-\frac{\rho_G}{\rho_L}\left(\frac{1-x}{x}\right)\left(\frac{\alpha}{1-\alpha}\right)(1-E)\right]^2$$
$$= \frac{1+50\times 0.918(1-0.918)}{0.918^{5/2}}\times\frac{1.79}{1.3}\left[1-\frac{1.3}{998}\left(\frac{1-0.2}{0.2}\right)\left(\frac{0.918}{1-0.918}\right)(1-0.094)\right]^2$$
$$= 7.264$$

Now, the updated value of two phase frictional pressure drop is calculated as,

$$\left(\frac{dP}{dL}\right)_f = \Phi_G^2 \times \left(\frac{dP}{dL}\right)_G = 7133 \text{ Pa/m}$$

(5) **Repeat steps (3) and (4) to get consistent values of α, δ and $(dP/dL)_f$:** Since the new value of Φ_G^2 and frictional pressure drop is greater than the initial estimate, recalculate Φ_{LF}^2 to obtain new estimates of δ and Φ_G^2. After 10 iterations, consistent values of void fraction, liquid film thickness and two phase frictional pressure drop are obtained. The final values of parameters obtained by solving for triangular relationship are:

Void fraction $(\alpha) = 0.927$

Liquid film thickness $(\delta) = 0.287$ mm $\rightarrow \delta/D = 0.018$

Liquid mass flow rates $(\dot{m}_{LF}) = 0.03$ kg/s

Two phase frictional pressure drop $(dP/dL)_f = 6295$ Pa/m.

The outcome of triangular relationship can be compared against the measured data and/or the empirical correlations developed exclusively for annular two phase flow. For similar flow conditions reported by Chiang (1986), the measured value of two phase frictional pressure drop is 6730 Pa/m. Using the correlation of Cioncolini and Thome (2012a) (see Chapter II), void fraction for given annular two phase flow conditions is found to be 0.935 whereas the non-dimensional liquid film thickness found using the correlation of Berna et al. (2014) (Eq. (6.34)) is $\delta/D = 0.0146$.

Note that the void fraction and pressure drop obtained using triangular relationship is within 1% and 6.5% of the measured values, respectively. Also, the predicted value of non-dimensional liquid film thickness (δ/D) using triangular relationship is within 23% of that predicted by Berna et al. (2014).

6.5 Chapter Summary

A separated flow model based correlation to predict the two phase frictional multiplier (Φ^2_{LO}) and hence the frictional component of the two phase pressure drop is proposed in this chapter. The proposed correlation adequately considers the effect of several two phase flow variables such as pipe diameter, fluid properties and the pipe orientation on two phase frictional pressure drop. The performance validation of this correlation against a comprehensive data bank consisting of 9623 data points distributed over a wide range of two phase flow conditions and the two phase flow models available in the literature confirms the robustness and accuracy of the proposed correlation. Based on the range of experimental data and the imposed limitation on this correlation, the proposed correlation is valid for horizontal, vertical upward and the entire range of upward pipe inclinations and should be used only for non-stratified flow patterns and the two phase flow region not affected by the phenomenon of flow reversal. Additionally, an annular flow pattern specific method based on triangular relationship between frictional pressure drop, liquid film thickness and liquid film flow rate is studied and its validity is analyzed against the data in vertical upward and downward annular flow. Using appropriate modeling approximation for gas-liquid interface velocity and interfacial friction factor, the triangular relationship is found to be valid for the range of $0.8 \leq \alpha < 1$ in both vertical upward and downward two phase flow.

CHAPTER VII

CONCLUSIONS AND RECOMMENDATIONS

One of the main objectives of this study was to experimentally investigate and understand the effect of pipe orientation on the structure and transition between two phase flow patterns, void fraction and two phase pressure drop. In addition to these experimental measurements, this study also aimed at developing robust models for the prediction of void fraction and two phase pressure drop applicable for a wide range of two phase flow conditions. A total of 2970 data points for flow visualization, void fraction and two phase pressure drop were measured in a 0.5" I.D. polycarbonate (smooth) and stainless steel (rough) pipes oriented at 0^o, $\pm 5^o$, $\pm 10^o$, $\pm 20^o$, $\pm 30^o$, $\pm 45^o$, $\pm 60^o$, $\pm 75^o$ and $\pm 90^o$ using air-water fluid combination. Following is a brief summary of the experimental accomplishments, key observations and modeling results that address the specific objectives of this work documented in Chapter I.

7.1 Summary and Conclusions

Flow Patterns and Flow Pattern Maps

1. The physical structure of the buoyancy driven flow patterns such as bubbly and slug flow is sensitive to the change in pipe orientation. For bubbly flow, the size, shape and distribution of bubbles across the pipe cross section depend on the the gas and liquid flow rates. Whereas in slug flow, its length and frequency

is a function of gas and liquid flow rates. The physical appearance of gas slug and its motion along the pipe axis is strongly governed by the pipe orientation.

2. Physical structure of stratified and annular flow patterns and transition boundary between them is virtually unaffected by the change in pipe orientation.

3. Stratified flow appears only in horizontal and downward pipe inclinations. Transition between slug-stratified and intermittent-stratified is significantly affected by the change in downward pipe inclination. Transition from stratified to slug and intermittent flows occur at higher liquid flow rates with increasing downward pipe inclination and then thereafter decreases towards lower liquid flow rates as the pipe is inclined towards vertical downward orientation.

4. Transient (unsteady) flow patterns exists at moderate liquid flow rates and very low gas flow rates typically during the stratified-slug transition in downward pipe inclinations. No fixed flow pattern exists at these flow rates and hence this transient region should be avoided for all practical purposes.

5. To correctly identify and separate the stratified flow from non-stratified flow, an empirical model using non-dimensional coordinates is developed and validated for horizontal and downward pipe inclinations. This model is validated against a comprehensive data bank is found to emulate the trends of Taitel and Dukler (1976) mechanistic model and an empirical model of Crawford et al. (1985).

Void Fraction

1. Void fraction is found to be affected by the change in pipe orientation, phase flow rates, fluid properties and pipe diameter. Effect of pipe orientation and phase flow rates on the void fraction is significant for low values of gas and

liquid flow rates. Pipe orientation and phase flow rates have first order effect on the void fraction. Effect of pipe diameter and fluid properties on void fraction is secondary however, this effect must be considered for modeling purpose.

2. Compared to upward inclined flows, void fraction is more sensitive to the change in downward pipe inclinations essentially due to change in the flow pattern. For stratified and annular flow patterns, void fraction remains virtually independent of the change in phase flow rates and pipe orientation. At very high liquid flow rates and low gas flow rates, effect of pipe orientation on the void fraction is little and is mainly because of the existence of bubbly and slug flow patterns at different pipe orientations.

3. For upward inclined flows at low gas and liquid flow rates, an inflection point in the void fraction trend is observed for $\theta \approx +30^o$. For downward pipe inclinations, an inflection point in void fraction trend is observed at $\theta \approx -60^o$ for low gas and intermediate liquid flow rates. The inflection point in upward pipe inclinations is essentially due to a difference in the relative magnitudes of the buoyancy and gravity forces that influences the bubble motion and hence the void fraction. Whereas, in downward pipe inclinations, inflection point is a consequence of the change in flow pattern from stratified to slug flow.

4. A flow pattern independent drift flux model based void fraction correlation is developed for a wide range of two phase flow conditions. This correlation provides expressions for distribution parameter and drift velocity as a function of several two phase flow variables that are known to affect the void fraction.

5. The proposed model published as Bhagwat and Ghajar (2014) correlation is applicable for micro to macro scale two phase flow of air-water, air-oil, steam-water, refrigerants and several other fluid combinations. This correlation is

shown to be valid for a range of system pressures, mass flux and circular and non-circular pipe geometries.

6. Bhagwat and Ghajar (2014) correlation needs further modification for improved accuracy for the case of $\alpha \geq \beta$ in downward pipe inclinations. This condition also corresponds to buoyancy dominated stratified and slug flow patterns in downward pipe inclinations.

Two Phase Pressure Drop

1. The relative contribution of hydrostatic, accelerational and frictional components of pressure drop to the total two phase pressure drop depends upon the flow patterns, pipe diameter and pipe orientation. Two phase frictional pressure drop in intermittent and annular flow patterns is sensitive to the change in gas and liquid flow rates whereas, in slug and stratified flow patterns it is relatively insensitive to the change in gas and liquid flow rates.

2. Total two phase pressure drop is found to be sensitive to the change in pipe orientation. At low gas and liquid flow rates, total two phase pressure drop increases with increase in upward pipe inclination up to $+75^o$ and then drops down further till the vertical upward orientation is attained. The two phase hydrostatic pressure drop is sensitive to the change in pipe orientation since it directly depends on void fraction as a function of pipe orientation.

3. Two phase frictional pressure drop is very sensitive to the change in gas and liquid phase flow rates for intermittent and annular flow regimes whereas for slug and stratified flow patterns, two phase frictional pressure drop is relatively insensitive to the increases in gas flow rate and essentially depends on change in liquid flow rate.

4. It is observed that two phase frictional pressure drop in rough pipe (stainless steel) is up to 40% higher than that in smooth (polycarbonate) pipe and could be even higher depending on roughness ratio ϵ/D . The effect of pipe surface roughness on frictional pressure drop is considerable in intermittent and annular flow regimes.

5. A peculiar phenomenon observed in upward inclined two phase flow is the reversal of liquid film identified in terms of pressure drop minimum regions. For steeper upward pipe inclinations, two pressure drop minimum regions are observed that occur approximately during the transition from slug to churn (intermittent) and then during the transition from churn (intermittent) to annular flow regime. Dimensionless gas and liquid flow rates corresponding to the pressure drop minimum regions as a function of pipe orientation are identified.

6. A flow pattern independent frictional pressure drop correlation based on a separated flow model is developed for micro to macro scale two phase flow in horizontal and upward pipe inclinations. The correlation is based on a comprehensive data set consisting of 9623 data points and is validated for two phase flow of refrigerants, air-water, air-oil, air-glycerin and air-kerosene fluid combinations. The accuracy of the proposed correlation is found to be consistently better than all other existing two phase flow models.

7. An annular flow pattern specific method of triangular relationship is studied and is used to predict frictional pressure drop, void fraction and liquid film thickness in vertical axisymmetric annular flow. An empirical form of the interfacial friction factor valid for $0.8 \leq \alpha < 1$ in vertical upward and downward pipe orientation is suggested.

7.2 Recommendations for Future Work

Based on the experimental and modeling work carried out in this study, certain limitations and shortcomings in the current state of knowledge in the field of two phase flow are identified. Based on these shortcomings, following recommendations are made to enhance further understanding and improve modeling accuracy of gas-liquid two phase flow under specific flow conditions.

1. Experimentally investigate the existence and span of stratified flow in small diameter ($D < 12.5$ mm) downward inclined pipes. Modify Bhagwat and Ghajar (2015) model if required.

2. Experimentally measure void fraction and pressure drop for varying pipe diameters and fluid properties in downward inclined pipes. Use this data to further enhance the understanding of the two phase flow behavior in downward inclined systems. Flow visualization in these experiments would also be useful in revealing the effect of pipe diameter and fluid properties on occurrence and span of transient (unsteady) behavior of two phase flow in downward inclined systems.

3. Investigate mechanistic modeling technique and closure relationships of Taitel and Dukler (1976) and its derivative forms to model void fraction and pressure drop in downward inclined stratified flow. Explore the possibility of developing stratified flow pattern specific correlations to predict void fraction and pressure drop using separated flow modeling approach.

4. Investigate the validity of triangular relationship for vertical axisymmetric two phase flow in non-circular (rectangular and annular) pipe geometries and various fluid combinations.

REFERENCES

Abduvayat, P., Manabe, R., Arihara, N., 2003. Effects of Pressure and Pipe Diameter on Gas-Liquid Two-Phase Flow Behavior in Pipelines. SPE Annual Technical Conference SPE 84229.

Adams, D.C., Burr, J., Hrnjak, P., Newell, T., 2006. Void Fraction of CO_2 and Ammonia in Multiport Aluminium Microchannel Tubes. International Refrigeration and Air-Conditioning Conference, Purdue University Paper 741, 1–7.

Akers, W.W., Deans, A., Crossee, O.K., 1959. Condensing Heat Transfer Within Horizontal Tubes. Chemical Engineering Progress 55, 171–176.

Ashwood, A.C., 2010. Characterization of the Macroscopic and Microscopic Mechanics in Vertical and Horizontal Annular Flow. Ph.D. Thesis. University of Wisconsin.

Awad, M.M., Muzychka, Y.S., 2004. A simple Two Phase Frictional Multiplier Calculation Method. International Pipeline Conference 1, 475–483.

Awad, M.M., Muzychka, Y.S., 2008. Effective Property Models for Homogeneous Two-Phase Flows. Experimental Thermal and Fluid Science 33, 106–113.

Azzopardi, B.J., 1986. Disturbance Wave Frequencies, Velocities and Spacing in Vertical Annular Two Phase Flow. Nuclear Engineering and Design 92, 121–133.

Bankoff, S.G., 1960. A Variable Density Single Fluid Model for Two Phase Flow with Particular Reference to Steam-Water Flow. Journal of Heat Transfer 11, 165–172.

Barbosa, J.R., Hewitt, G.F., Konig, G., Richardson, S.M., 2002. Liquid Entrainment, Droplet Concentration and Pressure Gradient at the Onset of Annular Flow in a Vertical Pipe. International Journal of Multiphase Flow 28, 943–961.

Barcozy, C.J., 1966. A Systematic Correlation for Two Phase Pressure Drop. Chemical Engineering Progress 62, 232–249.

Barnea, D., 1987. A Unified Model for Predicting Flow Pattern Transitions for The Whole Range of Pipe Inclinations. International Journal of Multiphase Flow 13, 1–12.

Barnea, D., Luninski, Y., Taitel, Y., 1983. Flow Pattern in Horizontal and Vertical Two Phase Flow in Small Diameter Pipes. Canadian Journal of Chemical Engineering 61, 617–620.

Barnea, D., Shoham, O., Taitel, Y., 1982. Flow Pattern Transition for Downward Inclined Two Phase Flow: Horizontal to Vertical. Chemical Engineering Science 37, 735–740.

Beattie, D.R.H., Whalley, P.B., 1982. A Simple Two-Phase Frictional Pressure Drop Calculation Method. International Journal of Multiphase Flow: Brief Communication 8, 83–87.

Beggs, H.D., 1972. An Experimental Study of Two Phase Flow in Inclined Pipes. Ph.D. Thesis. University of Tulsa.

Belt, R.J., Westende, V., Portela, L.M., 2009. Prediciton of the Interfacial Shear Stress in Vertical Annular Flow. International Journal of Multiphase Flow 35, 689–697.

Bendiksen, K.H., 1984. An Experimental Investigation of the Motion of Long Bubbles in Inclined Tubes. International Journal of Multiphase Flow 10, 467–483.

Benjamin, T.B., 1968. Gravity Currents and Related Phenomenon. Journal of Fluid Mechanics 31, 209–248.

Berna, C., Escriva, A., Cobo-Munzo, J.L., Herranz, L.E., 2014. Review of Droplet Entrainment in Annular Flow: Interfacial Waves and Onset of Entrainment. Progress in Nuclear Energy 74, 14–43.

Bhagwat, S.M., Ghajar, A.J., 2012. Similarities and Differences in the Flow Patterns and Void Fraction in Vertical Upward and Downward Two Phase Flow. Experimental Thermal and Fluid Science 39, 213–227.

Bhagwat, S.M., Ghajar, A.J., 2014. A Flow Pattern Independent Drift Flux Model Based Void Fraction Correlation for a Wide Range of Gas-Liquid Two Phase Flow. International Journal of Multiphase Flow 59, 186–205.

Bhagwat, S.M., Ghajar, A.J., 2015. An Empirical Model to Predict the Transition between Stratified and Non-Stratified Gas-Liquid Two Phase Flow in Horizontal and Downward Inclined Pipes. Heat Transfer Engineering 36, 1489–1498.

Bhagwat, S.M., Mollamahmutoglu, M., Ghajar, A.J., 2012a. Experimental Investigation and Empirical Analysis of Non-Boiling Gas-Liquid Two Phase Heat Transfer in Vertical Downward Pipe Orientation. Proceedings of ASME 2012 Summer Heat Transfer Conference 2, 349–359.

Bhagwat, S.M., Mollamahmutoglu, M., Ghajar, A.J., 2012b. Experimental Investigation and Performance Evaluation of Isothermal Frictional Two Phase Pressure Drop Correlations in Vertical Downward Gas-Liquid Two Phase Flow. Proceedings of ASME 2012 Summer Heat Transfer Conference 2, 337–348.

Blasius, H., 1913. Das Anhlichkeitsgesetz bei Reibungsvorgangen in Flussikeiten. Gebiete Ingenieurw 134.

Bonnecaze, R.H., Erskine, Greskovich, E.J., 1971. Holdup and Pressure Drop for Two Phase Slug Flow in Inclined Pipelines. AIChE 17, 1109–1113.

Bowers, C.D., Hrnjak, P.S., 2010. Determinaiton of Void Fraction in Separated Two Phase Flows Using Optical Techiniques. International Refrigeration and Air-Conditioning Conference, Purdue University , 2293 – 2302.

Caetano, E.F., Shoham, O., Brill, J.P., 1992. Upward Vertical Two Phase Flow Through an Annulus- Part 2. Modeling Bubbly, Slug and Annular Flow. Journal of Energy Resources Technology 114, 14–30.

Chen, I.Y., Yang, K.S., Chang, Y.J., Wang, C.C., 2001. Two Phase Presure Drop of Air-Water and R-410a in Small Horizontal Tubes. International Journal of Multiphase Flow 27, 1293–1299.

Chen, J.J., 1986. A Further Examination of Void Fraction in Annular Two-phase Flow. International Journal of Heat and Mass Transfer 29, 4269–4272.

Chen, N.H., 1979. An Explicit Equation for Friciton Factor in Pipes. Industrial Engineering Fundamentals 18, 296–297.

Cheng, L., Ribastski, G., Thome, J.R., 2008. Two Phase Flow Patterns and Flow Pattern Maps: Fundamental and Applications. Applied Mechanics Reviews 61, 1–28.

Chexal, B., Lellouche, G., Horowitz, J., Healzer, J., 1992. A Void Fraction Correlation for Generalized Applications. Progress in Nuclear Energy 27, 255–295.

Chiang, R., 1986. Study of Liquid Entrainment Rates in Annular Two Phase Flow through Smooth and Rifled Tubes. Ph.D. Thesis. Lehigh University.

Chisholm, D., 1967. A Therotical Basis for the Lockhart-Martinelli Correlation for Two Phase Flow. International Journal of Heat and Mass Transfer 10, 1767–1778.

Chisholm, D., 1973. Pressure Gradients Due to the Friction During the Flow of Evaporating Two Phase Mixtures in Smooth Tubes and Channels. International Journal of Heat and Mass Transfer 16, 347–358.

Choi, J., Pereyra, E., Sarica, C., Park, C., Kang, J.M., 2012. An Efficient Drift Flux Closure Relationship to Estimate Liquid Holdups of Gas-Liquid Two Phase Flow in Pipes. Energies 5, 5294–5306.

Churchill, S.W., 1977. Friction Factor Equation Spans all Fluid- Flow Regimes. Chemical Engineering 7, 91–92.

Ciccihitti, A., Lombardi, C., Silvestri, M., Soldaini, R., Zavatarelli, G., 1960. Two-Phase Cooling Experiments: Pressure Drop, Heat Transfer and Burnout Measurments. Energ. Nucl. 7, 407–429.

Cioncolini, A., Thome, J.R., 2012a. Void Fraction Prediction in Annular Two Phase Flow. International Journal of Multiphase Flow 43, 72–84.

Cioncolini, A., Thome, J.R., 2012b. Entrained Liquid Fraction Prediction in Adiabatic and Evaporating Annular Two Phase Flow. Nuclear Engineering and Design 243, 200–213.

Cioncolini, A., Thome, J.R., Lombardi, C., 2009. Unified Macro to Microscale Method to Predict Two Phase Fricitonal Pressure Drop of Annular Fows. International Journal of Multiphase Flow 35, 1138–1148.

Clark, N.N., Flemmer, R.L., 1985. Predicting the Holdup in Two Phase Bubble Upflow and Downflow Using the Zuber and Findlay Drift Flux Model. AIChE 31, 500–503.

Colebrook, C.F., 1939. Turbulent Flow in Pipes, with Particular Reference to the Transition between the Smooth and Rough Pipe Laws. Journal of Institute of Civil Engineering 11, 1938–1939.

Collier, J.G., Thome, J.R., 1996. Convective Boiling and Condensation. Oxford Science Publications. Third edition.

Colombo, L.P.M., Lucchini, A., Muzzio, A., 2012. Flow Patterns, Heat Transfer and Pressure Drop for Evaporation and Condensation of R134a in MicroFin Tubes. International Journal of Refrigeration 35, 2150–2165.

Cook, W., 2008. An Experimental Apparatus for Measurement of Pressure Drop and Void Fraction and Non-Boiling Two Phase Heat Transfer and Flow Visualization in Pipes for all Inclinations. M.S. Thesis. Oklahoma State University.

Crawford, T.J., Weinberger, C.B., Weisman, J., 1985. Two Phase Flow Patterns and Void Fractions in Downward Flow Part I: Steady State Flow Patterns. International Journal of Multiphase Flow 11, 761–782.

Das, G., Das, P.K., Purohit, N.K., Mitra, A.K., 2002. Liquid Holdup in Concentric Annuli during Cocurrent Gas-Liquid Upflow. The Canadian Journal of Chemical Engineering 80, 153–157.

Davidson, W.F., Hardie, P.H., Humphreys, C.G.R., Markson, A.A., Mumford, A.R., Ravese, T., 1943. Studies of Heat Transmission through Boiler Tubing at Pressures from 500-3300 lbs. Trans. of ASME 65, 553–591.

Dix, G.E., 1971. Vapor Void Fractions for Forced Convection with Subcooled Boiling at Low Flow Rates. Report NEDO-10491. General Electric Co.

Dukler, A.E., Hubbard, M.G., 1975. A Model for Gas-Liquid Slug Flow in Horizontal and Near Horizontal Tubes. Industrial and Engineering Chemistry Fundamentals 14, 337–347.

Dukler, A.E., Wicks, M., Cleveland, R.G., 1964. Frictional Pressure Drop in Two Phase Flow: A Comparison of Existing Correlations for Pressure Loss and Holdup. AIChE 10, 38–43.

Dumitrescu, D.T., 1943. Stromung an einer luftblase im senkrechten rohr. Z. angew. Match Mech , 139–149.

Fang, X.D., Xu, Y., Zhou, Z.R., 2011. New Correlations of Single Phase Friciton Factor for Turbulent Pipe Flow and Evaluation of Existing Single Phase Friciton Factor Correlations. Nuclear Engineering and Design 241, 897–902.

Fourar, M., Boris, S., 1995. Experimental Study of Air Water Two Phase Flow Through a Fracture. International Journal of Multiphase Flow 4, 621–637.

Franca, H., Lahey, R.T., 1992. The Use of Drift Flux Techniques for the Analysis of Horizontal Two Phase Flows. International Journal of Multiphase Flow 18, 787–801.

Friedel, L., 1979. Improved Friction Pressure Drop Correlation for Horizontal and Vertical Two Phase Pipe Flow. European Two Phase Flow Group Meeting Paper 18, 485–492.

Friedel, L., 1985. Two-Phase Frictional Pressure Drop Correlation for Vertical Downflow. German Chemical Engineering 8, 32–40.

Fukano, T., Furukawa, T., 1998. Prediction of the Effects of Liquid Viscosity on Interfacial Shear Stress and Frictional Pressure Drop in Vertical Upward Gas-Liquid Annular Flow. International Journal of Multiphase Flow 24, 587–603.

Garcia, F., Garcia, R., Padrino, J.C., Mata, C., Trallero, J.L., Joseph, D.D., 2003. Power Law and Composite Power Law Friciton Factor Correlations for Laminar Turbulent Gas Liquid Flow in Horizontal Pipe Lines. International Journal of Multiphase Flow 29, 1605–1624.

Ghajar, A.J., Bhagwat, S.M., 2013. Effect of Void Fraction and Two-Phase Dynamic Viscosity Models on Prediction of Hydrostatic and Frictional Pressure Drop in Vertical Upward Gas-Liquid Two Phase Flow. Heat Transfer Engineering 34, 1044–1059.

Ghajar, A.J., Bhagwat, S.M., 2014. Non-Boiling Gas-Liquid Two Phase Flow Phenomenon in Near Horizontal, Upward and Downward Inclined Pipe Orientations.

International Journal of Mechanical, Aerospace, Industrial and Mechatronics Engineering 8, 1039–1053.

Gibson, J., 1981. Effect of Liquid Properties, Inclination and Pipeline Geometry on Flow Patterns in Cocurrent Liquid-Gas Flow. M.S. Thesis. University of Cincinnati.

Goda, H., Hibiki, T., Kim, S., Ishii, M., Uhle, J., 2003. Drift Flux Model for Downward Two Phase Flow. International Journal of Heat and Mass Transfer 46, 4835–4844.

Godbole, P.V., Tang, C.C., Ghajar, A.J., 2011. Comparison of Void Fraction Correlations for Different Flow Patterns in Upward Vertical Two Phase Flow. Heat Transfer Engineering 32, 843–860.

Gokcal, B., 2008. An Experimental and Therotical Investigation of Slug Flow for High Oil Viscosity in Horizontal Pipes. Ph.D. Thesis. University of Tulsa.

Gokcal, B., Al-Sarkhi, A., Sarica, C., 2009. Effects of High Oil Viscosity on Drift Velocity for Horizontal and Upward Inclined Pipes. SPE Proj Fac. & Const. 4, 32–40.

Gomez, L., Shoham, O., Schmidt, Z., Choshki, R., Northug, T., 2000. Unified Mechanistic Model for Steady State Two Phase Flow: Horizontal to Upward Vertical Flow. Society of Petroleum Engineers 5, 339–350.

Gronnerud, R., 1979. Investigation of Liquid Holdup, Flow Resistance and Heat Transfer in Circulation Type of Evaporators, Part IV: Two Phase Flow Resistance in Boiling Refrigerants. Annexe 1972-1, Bull. de l'Inst. Froid .

Guo, T., Jeong, H.J., 2014. Experimental Study on Flooding and Flow Reversal in Small Diameter Tubes with Various Inclinations and Horizontal Lengths. International Journal of Refrigeration 38, 290–298.

Han, H., Zhu, Z., Gabriel, K.S., 2006. A Study on the Effect of Gas Flow Rate on the Wave Characteristics in Two Phase Gas-Liquid Annular Flow. Nuclear Engineering and Design 236, 2580–2588.

Hazuku, T., Takamasa, T., Matsumoto, Y., 2008. Experimental Study on Axial Development of Liquid Film in Vertical Upward Annular Two Phase Flow. International Journal of Multiphase Flow 34, 111–127.

Hewitt, G., Lacey, P.M.C., Nicholls, B., 1965. Transitions in Film Flow in Vertical Tube. Proceedings of Two Phase Flow Symposium, Exeter. Paper B4 2.

Hewitt, G.F., Hall-Taylor, N.S., 1970. Annular Two Phase Flow. Pergamon Press. First edition.

Hewitt, G.F., Martin, C.J., Wilkes, N.S., 1985. Experimental and Modeling Studies of Churn-Annular Flow in the Region Between Flow Reversal and the Pressure Drop Minimum. Physicochemical Hydrodynamics 6, 69–86.

Hewitt, G.F., Roberts, D.N., 1969. Studies of Two Phase Flow Patterns by Simultaneous X-Ray and Flash Photography. Technical Report AERE-M 2159. Atomic Energy Research Establishment.

Hibiki, T., Ishii, M., 2003. One-Dimensional Drift Flux Model and Constitutive Equations for Relative Motion between Phases in Various Two-Phase Flow Regimes. International Journal of Heat and Mass Transfer 46, 4935–4948.

Hill, A.V., 1910. The Possible Effects of the Aggregation of the Molecules of Hemoglobulin on its Dissociation Curves. Journal of Physiology 40, 4–7.

Hills, J.H., 1976. The Operation of a Bubble Column at High Throughputs Part 1: Gas Holdup Measurements. The Chemical Engineering Journal 12, 89–99.

Hlaing, N.D., Sirivat, A., Siemanond, K., Wilkes, J.O., 2007. Vertical Two Phase Flow Regimes and Pressure Gradients: Effect of Viscosity. Experimental Thermal and Fluid Science 31, 567–577.

Hwang, Y.W., Kim, M.S., 2006. The Pressure Drop in Microtubes and the Correlation Development. International Journal of Heat and Mass Transfer 49, 1804–1812.

Ishii, M., 1977. One Dimensional Drift Flux Model and Constitutive Equations for Relative Motion Between Phases in Various Two Phase Flow Regimes. Argonne National Laboratory , 77–47.

Ishii, M., Grolmes, M.A., 1975. Inception Criteria for Droplet Entrainment in Two Phase Cocurrent Film Flow. AIChE Journal 21, 308–318.

Jeyachandra, B.C., 2011. Effect of Pipe Inclinaiton on Flow Characteristics of High Viscosity Oil Gas Two Phase Flow. Ph.D. Thesis. University of Tulsa.

Jung, D.S., Radermacher, R., 1989. Prediction of Pressure Drop during Horizontal Annular Flow Boiling of Pure and Mixed Refrigerants. International Journal of Heat and Mass Transfer 32, 2435–2446.

Kajero, O.T., Azzopardi, B.J., Abdulkareem, L., 2012. Experimental Investigation of the Effect of Liquid Viscosity on Slug Flow in Small Diameter Bubble Column. European Physical Journal Web of Conference 25, 1037–1061.

Kaji, M., Azzopardi, B.J., 2010. The Effect of Pipe Diameter on the Structure of Gas-Liquid Flow in Vertical Pipes. International Journal of Multiphase Flow 36, 303–313.

Kandlikar, S.G., 2002. Fundamental Issues Related to Flow Boiling in Minichannels and Microchannels. Experimental Thermal and Fluid Science 26, 389–407.

Kang, C., Jepson, W, P., Wang, H., 2002. Flow Regime Transitions in Large Diameter Inclined Multiphase PipeLines. NACE, International Annual Conference and Exposition, Denver, CO Paper No. 02243.

Kataoka, I., Ishii, M., 1987. Drift Flux Model for Large Diameter Pipe and New Correlation for Pool Void Fraction. International Journal of Heat and Mass Transfer 30, 1927–1939.

Keinath, B., 2012. Void Fraction, Pressure Drop and Heat Transfer in High Pressure Condensing Flows through Microchannels. Ph.D. Thesis. Georgia Institute of Technology.

Kim, S.M., Mudawar, I., 2012. Universal Approach to Predicting Two Phase Frictional Pressure Drop for Adiabatic and Condensing Mini/Micro Channel Flows. Internation Journal of Heat and Mass Transfer 22, 3246–3261.

Kline, S.J., McClintock, F.A., 1953. Describing Uncertainities in Single Sample Experiments. Mechanical Engineering 1, 3–8.

Kokal, S.L., Stanislav, J.F., 1989a. An Experimental Study of Two Phase Flow in Slightly Inclined Pipes I: Flow Patterns. Chemical Engineering Science 44, 665–679.

Kokal, S.L., Stanislav, J.F., 1989b. An Experimental Study of Two Phase Flow in Slightly Inclined Pipes II: Liquid Holdup and Pressure Drop. Chemical Engineering Science 44, 681–693.

Lau, V., Jiang, Y., Rezkallah, K.S., 1992. Pressure Drop during Upward and Downward Two Phase Gas-Liquid Flow in a Vertical Tube. FED-Multiphase Flow in Wells and Pipelines 144, 81–87.

Lau, V., Rezkallah, K.S., 1995. New Data on Water-Air Hydrodynamics in Vertical Upward and Downward Tubes. Canadian Nuclear Assosciation Annual Conference , 1–16.

Laurinat, J.E., 1982. Studies of the Effect of the Pipe Size on Horizontal Annular Two Phase Flow. Ph.D. Thesis. University of Illinois, Urbana Champaign.

Lee, J.H., Lee, S.Y., 2001. Pressure Drop Correlations for Two Phase Flow Within Horizontal Rectangular Channels with Small Heights. International Journal of Multiphase Flow 27, 783–796.

Li, W., Wu, Z., 2010. A General Correlation for Adiabatic Two Phase Pressure Drop in Mini/Micro Channels. International Journal of Heat and Mass Transfer 53, 2732–2739.

Lim, T.W., 2005. Flow Pattern and Pressure Drop of Pure Refrigerants and Their Mixtures in Horizontal Tube. Journal of Mechanical Science and Technology 19, 2289–2295.

Lim, T.W., Fujita, Y., 2002. Flow Pattern and Pressure Drop in Flow Boiling of Pure Refrigerants and Their Mixture in Horizontal Tube. Memoirs of the Faculty of Engineering, Kyushu University 62, 41–54.

Lin, S., Kwok, C.C.K., Li, R.Y., Chen, Z.H., Chen, Z.Y., 1991. Local Frictional Pressure Drop during Vaporization of R12 Through Capillary Tubes. International Journal of Multiphase Flow 17, 95–102.

Lips, S., Meyer, J.P., 2012a. Effect of Gravity Forces on Heat Transfer and Pressure Drop During Condensation of R134a. Microgravity, Science and Technology 24, 157–164.

Lips, S., Meyer, J.P., 2012b. Experimental Study of Convective Condensation in an Inclined Smooth Tube Part I: Inclination Effect on Flow Patterns and Heat Transfer Coefficient. International Journal of Heat and Mass Transfer 55, 395–404.

Lips, S., Meyer, J.P., 2012c. Experimental Study of Convective Condensation in an Inclined Smooth Tube. Part II: Inclination Effect on Pressure Drop and Void Fraction. International Journal of Heat and Mass Transfer 55, 405–412.

Lockhart, R.W., Martinelli, R.C., 1949. Proposed Correlation of Data for Isothermal Two Phase, Two Component Flow in Pipes. Chemical Engineering Progress 45, 39–48.

Lombardi, C., Carsana, C.G., 1992. A Dimensionless Pressure Drop Correlation for Two Phase Mixtures Flowing Upflow in Vertical Ducts Covering Wide Parameter Ranges. Heat and Technology 10, 125–141.

Mandhane, J.M., Gregory, G.A., Aziz, K., 1974. A Flow Pattern Map for Gas-Liquid Flow in Horizontal Pipes. International Journal of Multiphase Flow 1, 537–553.

Mao, Z.S., Dukler, A.E., 1993. The Myth of Churn Flow. International Journal of Multiphase Flow 19, 377–383.

Marchaterre, J.F., 1956. The Effect of Pressure on Boiling Density in Multiple Rectangular Channels. Report ANL-5522. Argonne National Labs.

Marchaterre, J.F., Petrick, M., Lottes, P.A., Weatherland, R.J., Flinn, W.S., 1960. Natural and Forced Circulation Boiling Studies. Report ANL-5735. Argonne National Labs.

Martinelli, R.C., Nelson, D.B., 1948. Prediction of Pressure Drop During Forced Circulation Boiling of Water. Trans. of ASME 90, 695–702.

McAdams, W.H., Woods, W.K., Heroman, L.V., 1942. Vaporization Inside Horizontal Tubes - II Benzene Oil Mixtures. Trans. of ASME 64, 193–200.

Milan, M., Borhani, N., Thome, J.R., 2014. A New Type of Flow Structure in Co-Current Adiabatic Vertically Downward Air-Water Flow: Membrane Flow. International Journal of Multiphase Flow 58, 246–256.

Mishima, K., Hibiki, T., 1996. Some Characteristics of Air-Water Two Phase Flow in Small Diameter Vertical Tubes. International Journal of Multiphase Flow 22, 703–712.

Mukherjee, H., 1979. An Experimental Study of Inclined Two Phase Flow. Ph.D. Thesis. University of Tulsa.

Muller-Steinhagen, H., Heck, K., 1986. A Simple Friction Pressure Drop Correlation for Two-Phase Flow in Pipes. Chemical Engineering Process 20, 297–308.

Nassos, G.P., Bankoff, S.G., 1967. Slip Velocity Ratios in an Air-Water System Under Steady-State and Transient Conditions. Chemical Engineering Science 22, 661–668.

Nedderman, R.M., Shearer, C.J., 1963. The Motion and Frequency of Large Disturbance Waves in Annular Two Phase Flow of Air-Water Mixtures. Chemical Engineering Science 18, 661–670.

Nguyen, V.T., 1975. Two Phase Gas-Liquid Cocurrent Flow : An Investigation of Holdup, Pressure Drop and Flow Patterns in a Pipe at Various Inclinations. Ph.D. Thesis. University of Auckland, New Zeland.

Nicholson, M.K., Aziz, K., Gregory, G.A., 1978. Intermittent Two Phase Flow in Horizontal Pipes: Predictive Models. Canadian Journal of Chemical Engineering 56, 653–663.

Nicklin, D.J., Wilkes, J.O., Davidson, J.F., 1962. Two Phase Flow in Vertical Tubes. Institute of Chemical Engineers 40, 61–68.

Oliemans, R.V.A., Pots, B.F.M., Trompe, N., 1986. Modeling of Annular Dispersed Two Phase Flow in Vertical Pipes. International Journal of Multiphase Flow 12, 711–732.

Ong, C.L., Thome, J.R., 2011. Experimental Adiabatic Two Phase Pressure Drops of R134a, R236fa and R245fa in Small Horizontal Circular Channels , in: Proceedings of the ASME/JSME 2011 8th Thermal Engineering Joint Conference.

Oshinowo, O., 1971. Two Phase Flow in a Vertical Tube Coil. Ph.D. Thesis. University of Toronto, Canada.

Oshinowo, O., Betts, R.C., Charles, M.E., 1984. Heat Transfer in Co-current Vertical Two-Phase Flow. Canadian Journal of Chemical Engineering 62, 194–199.

Oshinowo, T., Charles, M.E., 1974. Vertical Two Phase Flow Part II: Holdup and Pressure Drop. Canadian Journal of Chemical Engineering 52, 438–448.

Owen, D.G., 1986. An Experimental and Therotical Analysis of Equlibrium Annular Flow. Ph.D. Thesis. University of Birmingham, UK.

Owens, W.L., 1961. Two Phase Pressure Gradients. ASME International Development of Heat Transfer 2, 363–368.

Permoli, A., Francesco, D., Prima, A., 1971. A Dimensionless Correlation for Determining Density of Two Phase Mixtures. La Termotecnica 25, 17–26.

Petukhov, B.S., 1970. Heat Transfer and Friction in Turbulent Pipe Flow with Variable Physical Properties. Advances in Heat Transfer 6, 503–564.

Quiben, J.M., Thome, J.R., 2007. Flow Pattern based Two Phase Frictional Presure Drop Model for Horizontal Tubes. Part I: Diabatic and Adiabatic Experimental Study. International Journal of Heat and Fluid Flow 28, 1049–1059.

Rouhani, S.Z., Axelsson, E., 1970. Calculation of Void Volume Fraction in the Subcooled and Quality Boiling Regions. International Journal of Heat and Mass Transfer 13, 383–393.

Sacks, P.S., 1975. Measured Characteristics of Adiabatic and Condensing Single Component Two Phase Flow of Refrigerant in a 0.377 inch Diameter Horizontal Tube. ASME Winter Annual Meeting, Houston, TX 75 WA/HT-24, 1–12.

Sawant, P., Ishii, M., Hazuku, T., Takamasa, T., Mori, M., 2008. Properties of Disturbance Waves in Vertical Annular Two-Phase Flow. Nuclear Engineering and Design .

Schubring, D., 2009. Behaviour Interrelationships in Annular Flow. Ph.D. Thesis. University of Wisconsin.

Shah, R.K., London, A.L., 1978. Laminar Flow Forced Convection in Ducts: A Source Book for Compact Heat Exchanger Analytical Data. Academic Press, New York.

Shannak, B.A., 2008. Frictional Pressure Drop of Gas Liquid Two-Phase Flow in Pipes. Nuclear Engineering and Design 238, 3277–3284.

Shedd, T.A., 2010. Void Fraction and Pressure Drop Measurements for Refrigerant R410a flows in Small Diameter Tubes. Technical Report AHRTI 20110-01.

Shipley, D.G., 1982. Two Phase Flow in Large Diameter Pipes. Chemical Engineering Science 39, 163–165.

Shoham, O., 1982. Flow Pattern Transitions and Characterization in Gas-Liquid Two Phase Flow in Inclined Pipes. Ph.D. Thesis. Tel-Aviv University.

Smith, S.L., 1969. Void Fraction in Two Phase Flow: A Correlation Based on an Equal Velocity Head Model. Institute of Mechanical Engineers 184, Part 1, 647–657.

Souza, A.L., Pimenta, M.M., 1995. Prediction of Pressure Drop During Horizontal Two Phase Flow of Pure and Mixed Refrigerants. ASME Cavitation and Multiphase Flow Symposium 210, 161–171.

Sowinski, J., Dziubinski, M., 2007. The Effect of Liquid Phase Viscosity on the Void Fraction in a Two Phase Gas-Liquid Flow in Narrow Minichannels. Proceedings of European Congress of Chemical Engineering ECCE-6.

Spedding, P.L., Che, J.J.J., Nguyen, N.T., 1982. Pressure Drop in Two Phase Gas-Liquid Flow in Inclined Pipes. International Journal of Multiphase Flow 8, 407–431.

Spedding, P.L., Watterson, J.k., Raghunatham, S.R., Ferguson, M.E.G., 1998. Two Phase Cocurrent Flow in Inclined Pipes. Internation Journal of Heat and Mass Transfer 41, 4205 – 4228.

Spedding, P.L., Woods, G.S., Raghunathan, S.R., Watterson, J.k., 2000. Flow Pattern, Holdup and Pressure Drop in Vertical and Near vertical Two and Three Phase Upflow. Institution of Chemical Engineers, Trans. of IChemE 78, 404–418.

Sujumnong, M., 1997. Heat Transfer, Pressure Drop and Void Fraction in Two Phase Two Component Flow in Vertical Tube. Ph.D. Thesis. University of Manitoba, Canada.

Sun, K., Duffey, R., Peng, C., 1981. The Prediction of Two Phase Mixture Level and Hydrodynamically Controlled Dryout under Low Flow Conditions. International Journal of Multiphase Flow 7, 521–543.

Sun, L., Mishima, K., 2009. Evaluation Analysis of Prediction Methods for Two Phase Flow Pressure Drop in Mini Channels. International Journal of Multiphase Flow 35, 47–54.

Taitel, Y., Dukler, A.E., 1976. A Model for Predicting Flow Regime Transitions in Horizontal and Near Horizontal Gas-Liquid Flow. AIChE 22, 47–55.

Taylor Hall, N.S., Hewitt, G.F., Lacey, P.M.C., 1963. The Motion and Frequency of Large Disturbance Waves in Annular Two Phase Flow. Chemical Engineering Science 18, 537–552.

Thom, J.R.S., 1964. Prediction of Pressure Drop During Forced Circulation Boiling of Water. International Journal of Heat and Mass Transfer 7, 709–724.

Thome, J.R., 2006. Engineering Data Book III, Chapter 17: Void Fractions in Two Phase Flow. Wolverine Tube Inc.

Tran, T.N., 1998. Pressure Drop and Heat Transfer Study of Two Phase Flow in Small Channels. Ph.D. Thesis. Texas Tech University.

Tran, T.N., Chu, Y.C., Wambsganss, M.W., France, D.M., 2000. Two Phase Pressure Drop of Refrigerants during Flow Boiling in Small Channels: An Experimental Investigation and Correlation Development. International Journal of Multiphase Flow 26, 1739–1754.

Turner, J.M., Wallis, G.B., 1965. The Separate Cylinders Model of Two Phase flow. Technical Report Report No. NYO-3114-6. Thayer's School of Engineering, Dartmouth College.

Usui, K., Sato, K., 1989. Vertically Downward Two Phase Flow: (I) Void Distribution and Average Void Fraction. Journal of Nuclear Science and Technology 26, 670–680.

Venkatesan, M., Das, S.K., Balakrishnan, A.R., 2011. Effect of Diameter on Two Phase Pressure Drop in Narrow Tubes. Experimental Thermal And Fluid Science 35, 531–541.

Wallis, G.B., 1962. The Onset of Droplet Entrainment in Annular Gas-Liquid Flow. General Electric Report No. 62, GL 127.

Wallis, G.B., 1968. Vertical Annular Flow: I, A Simple Theory, in: Annual Meeting of the AIChE, Tampa, Florida.

Wallis, G.B., 1969. One Dimensional Two Phase Flow. McGraw-Hill.

Wang, C.C., Chiang, C.S., Lin, S.P., Lu, D.C., 1997. Visual Obervation of Two Phase Flow Pattern of R22, R134-a and R407C in a 6.5 mm Smooth Tube. Experimental Thermal and Fluid Science 15, 395–405.

Wang, C.C., Chiang, S.K., Chang, Y.J., Chung, T.W., 2001. Two Phase Flow Resistance of Refrigerants R22, R410A and R407C in Small Diameter Tubes. Institution of Chemical Engineers, Trans. of IChemE 79, 553–560.

Weber, M.E., 1981. Drift in Intermittent Two Phase Flow in Horizontal Pipes. Canadian Journal of Chemical Engineering 59, 398–399.

Weisman, J., Kang, S.Y., 1981. Flow Pattern Transitions in Vertical and Upward Inclined Lines. International Journal of Multiphase Flow 7, 271–291.

Wisman, R., 1975. Analytical Pressure Drop Correlation for Adiabtic Vertical Two-Phase Flow. Applied Science Research 30, 367–380.

Woldesemayat, M.A., Ghajar, A.J., 2007. Comparison of Void Fraction Correlations for Different Flow Patterns in Horizontal and Upward Inclined Pipes. International Journal of Multiphase Flow 33, 347–370.

Wolf, A., Jayanti, S., Hewitt, G.F., 2001. Flow Development in Vertical Annular Flow. Chemical Engineering Science 56, 3221–3235.

Wongs-ngam, J., Nualboonrueng, T., Wongwises, S., 2004. Performance of Smooth and Micro-finned Tubes in High Mass Flux Region of R-134a during Condensation. Heat and Mass Transfer 40, 425–435.

Wongwises, S., Pipathttakul, M., 2006. Flow Pattern, Pressure Drop and Void Fraction of Gas-Liquid Two Phase Flow in an Inclined Narrow Annular Channel. Experimental Thermal and Fluid Science 30, 345–354.

Wurtz, J., 1978. An Experimental and Therotical Investigation of Annular Steam-Water Flow in Tubes and Annuli at 30 and 90 bar. Technical Report. Riso National Laboratory, Report No. 372.

Xu, Y., Fang, X., 2012. A New Correlaiton of Two Phase Frictional Pressure Drop for Evaporating Two Phase Flow in Pipes. International Journal of Refrigeration 35, 2039–2050.

Xu, Y., Fang, X., 2014. Correlations of Void Fraction for Two Phase Refrigerant Flow in Pipes. Applied Thermal Engineering 64, 242–251.

Yamazaki, Y., Yamaguchi, K., 1979. Characteristics of Cocurrent Two Phase Downflow in Tubes- Flow Pattern, Void Fraction and Pressure Drop. Journal of Nuclear Science and Technology 16, 245–255.

Yashar, D.A., Wilson, M.J., Kopke, H.R., Graham, D.M., Chato, J.C., Newell, T.A., 2001. An Investigation of Refrigerant Void Fraction in Horizontal, MicroFin Tubes. HVAC&R Research 7, 67–82.

Yijun, J., Rezkallah, K., 1993. A Study on Void Fraction in Vertical Co-Current Upward and Downward Two-Phase Gas-Liquid Flow - I: Experimental Results. Chemical Engineering Communication 126, 221–243.

Yoon, S.H., Cho, E.S., Hwang, Y.W., Kim, M.S., Min, K., Kim, Y., 2004. Characteristics of Evaporative Heat Transfer and Pressure Drop of Carbon Dioxide and Correlation Development. International Journal of Refrigeration 27, 111–119.

Zhang, W., Hibiki, T., Mishima, K., 2010. Correlations of Two Phase Frictional

Pressure Drop and Void Fraction in Mini-Channel. Heat and Mass Transfer 53, 433–465.

Zivi, S.M., 1964. Estimation of Steady State Steam Void Fraction by Means of the Principle of Minimum Entropy Production. Trans. of ASME, Journal of Heat Transfer 86, 247–252.

Zuber, N., Findlay, J., 1965. Average Volume Concentration in Two Phase Systems. ASME Journal of Heat Transfer 87, 453–468.

APPENDIX

The two phase flow data bank used in this work consists of 19,848 data points with 10,225 and 9623 data points for void fraction and two phase pressure drop, respectively. This data bank consists of several different fluid combinations and is generated from around 130 sources available in the two phase flow literature. Some of these data points are acquired from theses/dissertations presented in tabular form while others are digitized from the technical papers/reports using Get Data Graph Digitizer software version 2.26. The experimental two phase flow measurements carried out at following list of research labs/universities represent a majority of the data used in this work. Distribution of the void fraction and pressure drop data bank for different two phase flow variables are reported in Chapters V and VI. More details of the data bank distribution and the corresponding publications/authors can be obtained from Dr. Afshin Ghajar at Oklahoma State University.

Void Fraction Databank

Air-Oil Data

1. Imperial College of Science, Technology and Medicine, London, UK. (Dr. Hewitt and co-workers).
2. University of Tulsa, OK (TUFPP Research Group).
3. University of Calgary, Canada.

Air-Water Data

1. Oklahoma State University, OK (Two phase flow lab, Dr. Ghajar and co-workers).
2. University of Manitoba, Canada (Dr. Sims and co-workers).
3. University of Toronto, Canada (Dr. Charles and co-workers).
4. University of Saskatchewan, Canada (Dr. Rezkallah and co-workers).
5. University of Tulsa, OK (TUFPP Research Group).
6. University of Technology, Thonburi, Thailand (Fluid Mechanics, Thermal Engineering and Multiphase Flow Research Lab, Dr. Wongwises and co-workers).
7. Purdue University, IN (Dr. Ishii and co-workers).
8. University of Illinois, Urbana Champaign, IL (Dr. Hanratty and co-workers).
9. University of Nottingham, UK (Dr. Azzopardi and co-workers).
10. The QueenâĂŹs University of Belfast, UK (Dr. Spedding and co-workers).
11. University of Amsterdam, Netherlands (Dr. Hamersma and co-workers).
12. University of Tel-Aviv, Israel (Dr. Barnea and co-workers).
13. CISE (Center Information Studies and Experiences, Italy)

Refrigerant Data

1. Georgia Institute of Technology, GA (Sustainable Thermal Systems Laboratory, Dr. Garimella and co-workers).
2. University of Illinois, Urbana Champaign, IL (Air Conditioning and Refrigeration Center, Dr. Harnjak and co-workers).
3. University of Wisconsin, Madison (Multiphase Visualization and Analysis Laboratory, Dr. Shedd and co-workers).
4. University of Pretoria, South Africa (Thermofluids Research Group, Dr. Josua Meyer and co-workers).

5. University of Technology, Thonburi, Thailand (Fluid Mechanics, Thermal Engineering and Multiphase Flow Research Lab, Dr. Wongwises and co-workers).

6. Swiss Federal Institute of Technology, Switzerland (Heat and Mass Transfer Laboratory, Dr. Thome and co-workers).

Steam-Water Data

1. Riso National Laboratory, Denmark.

2. Argonne National Laboratory.

3. CISE (Center Information Studies and Experiences, Italy)

4. Japan Atomic Energy Agency.

5. Aktiebolaget Atomenrgi, Stockholm, Sweden (Dr. Rouhani, Dr. Becker and co-workers).

Miscellaneous Fluid Combinations

1. University of Tulsa, OK (TUFPP Research Group).

2. University of Manitoba, Canada.

3. University of Toronto, Canada.

4. Technical University of Lodz, Poland.

5. CISE (Center Information Studies and Experiences, Italy)

Pressure Drop Data Bank

Air-Oil Data

1. University of Tulsa, OK (TUFPP Research Group).
2. University of Calgary, Canada.
3. Imperial College of Science, Technology and Medicine, London, UK. (Dr. Hewitt and co-workers).
4. Universita degli Studi di Brescia, Italy (Dr. Farsetti and co-workers).

Air-Water Data

1. Oklahoma State University, OK (Two Phase Flow Lab, Dr. Ghajar and co-workers).
2. University of Tulsa, OK (TUFPP Research Group).
3. University of Toronto, Canada (Dr. Charles and co-workers).
4. University of Manitoba, Canada (Dr. Sims and co-workers).
5. University of Illinois, Urbana Champaign, IL (Dr. Hanratty and co-workers).
6. The QueenâĂŹs University of Belfast, UK (Dr. Spedding and co-workers).
7. University of Houston, TX (Dr. Dukler and co-workers).
8. University of Saskatchewan, Canada (Dr. Gabriel and co-workers).
9. Delft University of Technology, Netherlands (Multiscale Physics Laboratory).
10. University of Amsterdam, Netherlands (Dr. Hamersma and co-workers).
11. University of Wisconsin, Madison (Multiphase Visualization and Analysis Laboratory, Dr. Shedd and co-workers).
12. University of Sydney, Australia (Dr. Fletcher and co-workers).
13. Al-Balqa Applied University, Jordan (Dr. Shannak).
14. Koszalin University of Technology, Poland (Dr. Dutkowski and co-workers).

15. University of Technology, Thonburi, Thailand (Fluid Mechanics, Thermal Engineering and Multiphase Flow Research Lab, Dr. Wongwises and co-workers).

16. Argonne National Laboratory.

Refrigerant Data

1. Georgia Institute of Technology (Sustainable Thermal Systems Laboratory, Dr. Garimella and co-workers).

2. University of Illinois, Urbana Champaign, IL. (Air Conditioning and refrigeration Center).

3. University of Wisconsin, Madison (Multiphase Visualization and Analysis Laboratory, Dr. Shedd and co-workers).

4. Swiss Federal Institute of Technology, (Heat and Mass Transfer Laboratory, Dr. Thome and co-workers).

5. University de Lyon, France (Heat Exchangers Laboratory).

6. Universita degli Studi di Napoli, Italy.

7. Universita degli Studi di Padova, Italy.

8. Royal Institute of Technology, Sweden (Division of Applied Thermodynamics and Refrigeration, Dr. Palm and co-workers).

9. CERN (European Organization for Nuclear Research, Switzerland).

10. Argonne National Laboratory.

VITA

SWANAND MADHAV BHAGWAT

Candidate for the Degree of

Doctor of Philosophy

Thesis: EXPERIMENTAL MEASUREMENTS AND MODELING OF VOID FRACTION AND PRESSURE DROP IN UPWARD AND DOWNWARD INCLINED NON-BOILING GAS-LIQUID TWO PHASE FLOW

Major Field: MECHANICAL AND AEROSPACE ENGINEERING

Biographical:

Personal Data: Born in Akola (India) on May 2, 1986, the son of Madhuri and Madhav Bhagwat.

Education:

Completed the requirements for the Doctor of Philosophy in Mechanical Engineering at Oklahoma State University, Stillwater, Oklahoma in July, 2015.

Completed the requirements for the Master of Science in Mechanical and Aerospace Engineering from Oklahoma State University, Stillwater, Oklahoma, USA in May 2011.

Completed the requirements for the Bachelor of Engineering Degree in Mechanical Engineering from Amravati University, India in July 2008.

Experience: Graduate Teaching/Research Assistant in Mechanical and Aerospace Engineering, Oklahoma State University, Stillwater from 2009 to 2015.

Professional Memberships: American Society of Mechanical Engineers (ASME).